

**STRENGTH AND DURABILITY PROPERTIES OF
LOW-CALCIUM FLY ASH BASED GEOPOLYMER CONCRETE**

A Thesis

**Submitted in fulfilment of the requirement
for the award of the degree of**

**DOCTOR OF PHILOSOPHY
IN
CIVIL ENGINEERING**

SUBMITTED BY

**ANKUR MEHTA
(Registration No.: 951202005)**

UNDER THE GUIDANCE OF

**Dr. RAFAT SIDDIQUE
Senior Professor, CED
Thapar University, Patiala**

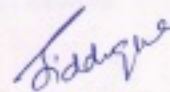


**DEPARTMENT OF CIVIL ENGINEERING
THAPAR UNIVERSITY
PATIALA-147004**

2017

CERTIFICATE

Certify that the thesis entitled "**Strength and Durability Properties of Low-Calcium Fly Ash Based Geopolymer Concrete**" which is submitted by Arkur Mehta, in fulfilment of the requirements for the award of degree of Doctor of Philosophy in Department of Civil Engineering, Thapar University, Patiala is a record of candidate's own original and independent research work carried out by him under my supervision and guidance. The matter embodied in this thesis has not been submitted in part or full to any other University or Institute for the award of any degree.



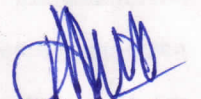
(Dr. Rafat Siddique)

Senior Professor
Department of Civil Engineering
Thapar University
Patiala, Punjab
India

DECLARATION

I, hereby declare that the research work presented in this thesis titled “**Strength and Durability Properties of Low-Calcium Fly Ash Based Geopolymer Concrete**” submitted for the award of the degree of Doctor of Philosophy in the department of Civil Engineering, Thapar University, Patiala is an authenticated record of my own research work carried out under the supervision of Dr. Rafat Siddique, Senior Professor, Department of Civil Engineering, Thapar University, Patiala and refers other researcher`s work are duly listed in the reference section.

The matter presented in this thesis has not previously been submitted in part or full to any other University or Institution for award of any degree in India or abroad.



(Ankur Mehta)

ACKNOWLEDGEMENT

- First of all I thank the almighty whose blessings have enabled me to accomplish this research work.
- I would like to express my gratitude to my supervisor Dr. Rafat Siddique, Senior Professor, Department of Civil Engineering, Thapar University, Patiala, India for his invaluable guidance, moral support and encouragement during the entire period of this research which cannot adequately be expressed in words in this acknowledgement.
- I would like to extend my acknowledgement to my advisory committee members Dr. Prem Pal Bansal, Dr. Kulvir Singh and Dr. Gurbir Kaur for their valuable suggestions and feedbacks. Also, the inputs provided by Dr. Naveen Kwatra, Head, Department of Civil Engineering, Thapar University, his interest and critical appraisal at every stage of this research are invaluable.
- The help and support provided by technical staff Sh. Ram Sumiran during the entire research period is greatly appreciated.
- I also acknowledge the support of SAI Laboratory, Thapar University for SEM/EDS and XRD analysis.
- Special thanks to my father Er. R.K Mehta for his constant support and guidance, mother Mrs. Seema Mehta, wife Er. Neha Mehta, brother Ar. Akshat Mehta and son Arnav for their patience and understanding during the whole research program.


(Ankur Mehta)

LIST OF PUBLICATIONS

1. Mehta, A., and Siddique, R., “An overview of geopolymers derived from industrial by-products-Review.” *Construction and Building Materials (Elsevier)*; Vol. 127, September 2016; pp.:183-198 (IF: 3.169).
2. Mehta, A., and Siddique, R., “Strength, permeability and micro-structural characteristics of low-calcium fly ash based geopolymers.” *Construction and Building Materials (Elsevier)*; Vol. 141, March 2017; pp.:325-334 (IF: 3.169).
3. Mehta, A., and Siddique, R., “Sulfuric acid resistance of fly ash based geopolymer concrete.” *Construction and Building Materials (Elsevier)*; Vol. 146, April 2017; pp.: 136-143 (IF: 3.169).
4. Mehta, A., and Siddique, R., “Properties of low-calcium fly ash based geopolymer concrete incorporating OPC as partial replacement of fly ash.” *Construction and Building Materials (Elsevier)*; Vol. 150, June 2017; pp.: 792-807 (IF: 3.169).

ABSTRACT

With the fast growing infrastructure development, the demand of cement is bound to increase. But in producing 1 tonne of cement, around 1 tonne of carbon dioxide is released. For the changing environment, green house gases such as carbon dioxide, carbon monoxide, etc have been considered as responsible which also enhance the most hazardous environmental problem of global warming. This clearly reflects the inability of cement concrete to fit in the contemporary picture of sustainable development. On the other hand, various industrial by-products such as fly ash, metakaolin, slags, etc have prompted their use as supplementary cementitious material due to their cement like physical and chemical properties. Geopolymer technology utilizes these industrial by-products having high silica and alumina in the production of binders by polymerization reaction. The reaction is activated by hydroxides and silicates of alkalis such as sodium or potassium.

The present research work involves the development of low-calcium fly ash based geopolymer concrete. Control geopolymer concrete with 3-day compressive strength of 41.3MPa was developed with fly ash content of 310 kg/m³, alkali solution-to-fly ash ratio of 0.55, sodium silicate-to-sodium hydroxide ratio of 2.5, total aggregate content of 70%, molarity of sodium hydroxide as 10M, fine aggregates-to-total aggregates ratio of 0.35 and temperature curing at 80 °C for 24 hours. Further, additional geopolymer concretes were made by partially replacing fly ash with Ordinary Portland cement (OPC) (5-30%). Workability properties such as slump and compaction factor, strength properties such as compressive strength and split tensile strength, and durability properties such as water absorption, porosity sorptivity, chloride permeability and resistance to sulphuric acid solution were performed up to the age of 365 days. For reference, conventional cement concrete of similar 28-day compressive strength was also developed and properties were evaluated.

Workability test results showed decrease in slump and compaction factor with the increase of OPC content in geopolymer concrete. The decrease in trend was found to be linear as high value of coefficient of determination was obtained. Compressive strength and split tensile strength increased with the increase in OPC up to 20%, and beyond that they decreased. The maximum compressive and split tensile strength of 66.81 and 5.35 MPa, respectively was obtained for geopolymer concrete with 20% OPC at 365 days. Also, for geopolymer concrete

mixtures, high 3-day compressive strength and split tensile strength was obtained of around 92-98% and 91-95% of their 28-day values, respectively. For reference, 3-day values of compressive strength and split tensile strength for conventional cement concrete were found to be 38 and 55% of their 28-day values, respectively. Microstructural analysis of geopolymer concrete mixtures with inclusion of OPC as partial replacement of fly ash showed the coexistence of additional calcium based compounds (calcium-silicate hydrate and calcium alumino-silicate hydrate) with polymerization product (sodium-alumino-silicate hydrates).

Water absorption, porosity and sorptivity decreased with the increase in OPC up to 20%, and beyond that they increased. The minimum values of water absorption, porosity and sorptivity were observed to be 1.1%, 6.1% and $2.54\mu\text{mm/s}^{1/2}$, respectively for geopolymer concrete mixture with 20% OPC at 365 days. Also, with the increase in OPC content up to 20%, reduction in chloride permeability in terms of total charge passed was observed. Beyond 20% OPC, the total charge passed values increased slightly. With reference to permeability range as specified in ASTM C1202, geopolymer concrete with OPC content from 10-30% exhibited the chloride permeability of “very low” category at all ages.

The geopolymer concrete mixtures with OPC ranging from 0-30% showed better sulphuric acid resistance in comparison to conventional cement concrete at all ages. Also, with the increase in OPC in geopolymer concrete, the loss of compressive strength for sulphuric acid exposed geopolymer concrete decreased with the increase in OPC content up to 10%, and beyond that, it increased i.e. maximum compressive strength after sulphuric acid exposure was retained by geopolymer concrete with 10% OPC.

TABLE OF CONTENTS

	Page No.
<i>Title</i>	
<i>Certificate</i>	i
<i>Declaration</i>	ii
<i>Acknowledgement</i>	iii
<i>List of Publications</i>	iv
<i>Abstract</i>	v
<i>Table of Contents</i>	vii
<i>List of Tables</i>	xi
<i>List of Figures</i>	xiii
<i>Abbreviations</i>	xviii
<i>List of Units</i>	xx
CHAPTER 1 INTRODUCTION	1
1.1 GENERAL	1
1.2 GEOPOLYMERS	3
1.2.1 Structure of Geopolymers	4
1.2.2 Constituents of Geopolymers	6
1.2.2.1 Source Materials	6
1.2.2.2 Alkali-Activating Solution	14
1.2.3 Curing Parameters for Geopolymers	15
1.3 ADVANTAGES OF GEOPOLYMERS	16
1.4 GEOPOLYMERS IN CONSTRUCTION APPLICATIONS	17
1.5 LIMITATIONS AND CHALLENGES FOR FIELD APPLICATIONS	22
1.6 SIGNIFICANCE OF RESEARCH	23
1.7 GAPS IN RESEARCH AREA	24
1.8 OBJECTIVE AND SCOPE OF RESEARCH WORK	24
1.9 METHODOLOGY	25

1.10	OVERVIEW OF THESIS	25
CHAPTER 2 REVIEW OF LITERATURE		27
2.1	USE OF INDUSTRIAL BY-PRODUCTS (IBP) IN GEOPOLYMERS	27
2.1.1	General	27
2.1.2	Synthesis of Geopolymers using Industrial By-Products (IBP)	27
2.2	FRESH PROPERTIES OF GEOPOLYMERS CONTAINING IBP	31
2.2.1	Fly Ash based Geopolymers	32
2.2.2	IBP (other than fly ash) based Geopolymers	34
2.3	STRENGTH PROPERTIES OF GEOPOLYMERS CONTAINING IBP	34
2.3.1	Fly Ash based Geopolymers	35
2.3.2	IBP (other than fly ash) based Geopolymers	39
2.4	DURABILITY PROPERTIES OF GEOPOLYMERS CONTAINING IBP	44
2.4.1	Fly Ash based Geopolymers	45
2.4.2	IBP (other than fly ash) based Geopolymers	46
2.5	GEOPOLYMERS AT ELEVATED TEMPERATURES	47
CHAPTER 3 EXPERIMENTAL PROGRAM		50
3.1	INTRODUCTION	50
3.2	MATERIAL CHARACTERIZATION	51
3.2.1	Fly ash	51
3.2.2	Ordinary Portland cement (OPC)	52
3.2.2.1	Consistency	53
3.2.2.2	Setting Times	53
3.2.2.3	Compressive Strength	53
3.2.3	Aggregates	55
3.2.3.1	Coarse Aggregates	56
3.2.3.2	Fine Aggregates	57
3.2.4	Alkali-Activating Solution	59
3.2.5	Super plasticizer	59
3.3	MIXTURE DESIGN	60
3.3.1	Fly Ash Based Geopolymer Concrete (GPC)	60
3.3.2	Conventional Cement Concrete (CCC)	63
3.4	CASTING AND CURING OF SPECIMENS	64

3.5	TEST METHODS FOR EVALUATION OF PROPERTIES	65
3.5.1	Workability Properties of Geopolymer Concrete	65
3.5.1.1	Slump	65
3.5.1.2	Compaction factor	67
3.5.2	Strength Properties of Geopolymer Concrete	68
3.5.2.1	Compressive Strength	68
3.5.2.2	Split Tensile Strength	69
3.5.3	Durability Properties of Geopolymer Concrete	70
3.5.3.1	Water Absorption and Porosity	70
3.5.3.2	Sorptivity	71
3.5.3.3	Rapid Chloride Permeability	73
3.5.3.4	Sulphuric Acid Resistance	74
3.5.4	Microstructure Properties of Geopolymer Concrete	75
3.5.4.1	SEM/EDS Analysis	75
3.5.4.2	XRD Analysis	77
CHAPTER 4 RESULTS AND DISCUSSIONS		79
4.1	WORKABILITY PROPERTIES OF GEOPOLYMER CONCRETE	79
4.1.1	Slump	79
4.1.2	Compaction Factor	80
4.2	STRENGTH PROPERTIES OF GEOPOLYMER CONCRETE	81
4.2.1	Compressive Strength	81
4.2.2	Split Tensile Strength	84
4.2.3	Microstructure Properties of Geopolymer Concrete	87
4.2.3.1	Geopolymer concrete mixture with 0% OPC	87
4.2.3.2	Geopolymer concrete mixture with 10% OPC	94
4.2.3.3	Geopolymer concrete mixture with 20% OPC	100
4.2.3.4	Geopolymer concrete mixture with 30% OPC	106
4.3	DURABILITY PROPERTIES OF GEOPOLYMER CONCRETE	112
4.3.1	Water Absorption and Porosity	113
4.3.2	Sorptivity	116
4.3.3	Rapid Chloride Permeability	118
4.3.4	Sulphuric Acid Resistance	120
4.3.4.1	Change in Mass	121

4.3.4.2	Change in Compressive Strength	122
4.3.4.3	Microstructure properties of sulphuric acid exposed geopolymer concrete	123
4.4	COST-BENEFIT ANALYSIS	131
4.5	QUALITY CONTROL REQUIREMENTS FOR FIELD APPLICATIONS	133
CHAPTER 5 CONCLUSIONS		135
5.1	DEVELOPMENT OF GEOPOLYMER CONCRETE	135
5.2	WORKABILITY PROPERTIES OF GEOPOLYMER CONCRETE	135
5.2.1	Slump	136
5.2.2	Compaction Factor	136
5.3	STRENGTH PROPERTIES OF GEOPOLYMER CONCRETE	136
5.3.1	Compressive Strength	136
5.3.2	Split Tensile Strength	137
5.3.3	Microstructure	137
5.4	DURABILITY PROPERTIES OF GEOPOLYMER CONCRETE	137
5.4.1	Water Absorption and Porosity	138
5.4.2	Sorptivity	138
5.4.3	Rapid Chloride Permeability	138
5.4.4	Sulphuric Acid Resistance	139
5.5	RECOMMENDATIONS	139
5.6	SUGGESTIONS FOR FUTURE STUDY	139
REFERENCES		141

LIST OF TABLES

<i>TABLE NUMBER</i>	<i>TITLE</i>	<i>PAGE NUMBER</i>
CHAPTER 1 INTRODUCTION		
1.1	Physical properties of fly ash	8
1.2	Chemical composition of fly ash	8
1.3	Physical properties of ground granulated blast furnace slag	10
1.4	Chemical composition of ground granulated blast furnace slag	10
1.5	Physical properties of metakaolin	12
1.6	Chemical composition of metakaolin	12
1.7	Physical properties of rice husk ash	13
1.8	Chemical composition of rice husk ash	13
1.9	Applications of geopolymers based on Si/Al ratio (Davidovits, 1991)	16
CHAPTER 3 EXPERIMENTAL PROGRAM		
3.1	Chemical composition of fly ash particles (present study)	52
3.2	Physical properties of OPC (present study)	54
3.3	Chemical composition of OPC particles (present study)	55
3.4	Physical test results of coarse aggregates (present study)	57
3.5	Sieve analysis results of coarse aggregates (present study)	57
3.6	Physical test results of fine aggregates (present study)	58
3.7	Sieve analysis of fine aggregates (present study)	59
3.8	Physical properties of sodium hydroxide (supplied by the manufacturer)	59
3.9	Parameters considered for the development of GPC	60
3.10	1 st group of Trial mixtures designed by Taguchi method	61
3.11	2 nd group of Trial mixtures designed by Taguchi method	62

3.12	3 rd group of trial mixtures for 3-day compressive strength of 41.1 MPa	63
3.13	Mixture proportions of fly ash based GPC	63
3.14	Mixture proportions of CCC	64
3.15	Chloride ion penetrability based on total charge passed (ASTM 1202-15)	74

CHAPTER 4 RESULTS AND DISCUSSIONS

4.1	Permeability category of GPC as per ASTM C1202	120
4.2	Design mixture adopted for the present study	131
4.3	Cost comparison of F100C0 and CCC	132
4.4	Cost comparison of F80C20 and CCC (60)	132

LIST OF FIGURES

<i>FIGURE NUMBER</i>	<i>TITLE</i>	<i>PAGE NO.</i>
CHAPTER 1 INTRODUCTION		
1.1	Types of geopolymer structures with Si-Al ratio as a) 1, b) 2 & c) 3 (Davidovits, 1991)	5
1.2	Mechanism of geopolymers (Xu and Van Deventer, 2000)	5
1.3	Mechanism of geopolymers (Weng and Sagoe-Crentsil, 2007)	6
1.4	Structure model of geopolymer with low silica-alumina ratio (Davidovits, 2002)	6
1.5	Scanning electron microscope micrographs of fly ash (Chindaprasirt et al., 2011)	9
1.6	Scanning electron microscope micrographs of blast furnace slag (Aguilar et al., 2010)	11
1.7	Scanning electron microscope micrographs of metakaolin (He et al., 2012)	12
1.8	Scanning electron microscope micrographs of rice husk ash (Kusbiantoro et al., 2012)	14
1.9	Placing of pavement using geopolymer concrete (Aldred and Day, 2012)	18
1.10	Pre-cast geopolymer retaining wall for private residence (Aldred and Day, 2012)	18
1.11	Water tanks cast with blended concrete (left) and geopolymer concrete (right) (Aldred and Day, 2012)	19
1.12	Boat ramp constructed with geopolymer concrete (Aldred and Day, 2012)	20
1.13	Installation of pre-fabricated geopolymer concrete bridge at Murrarie (Aldred and Day, 2012)	20

1.14	Composite girder and geopolymer concrete Deck Bridge in Brisbane (Aldred and Day, 2012)	21
1.15	Geopolymer concrete floor beam (left) and rendered view of proposed building (right) (Aldred and Day, 2012)	22
1.16	Phases of research	26
CHAPTER 3 EXPERIMENTAL PROGRAM		
3.1	Schematic diagram of experimental program	50
3.2	SEM/EDS analysis of fly ash particles (present study)	51
3.3	XRD analysis of fly ash particles (present study)	52
3.4	SEM/EDS analysis of OPC particles (present study)	54
3.5	XRD analysis of OPC particles (present study)	55
3.6	Making of concrete in a pan mixture	65
3.7	Experimental set up for measuring workability by using slump cone	66
3.8	General types of slump (Koehler and Fowler, 2003)	66
3.9	Experimental set up for measuring workability by using compaction factor	67
3.10	Experimental set up for measuring compressive strength	69
3.11	Experimental set up for measuring split tensile strength	70
3.12	Experimental set up for measuring sorptivity of concrete	72
3.13	Experimental set up for measuring chloride permeability of concrete	73
3.14	The Vacuum Pump, desiccators, and container with de-aerated water (Singh, 2012)	74
3.15	Experimental setup for Scanning Electron Micrograph	76
3.16	Basic layout of X-ray diffractometers (Jumate and Manea, 2011)	77
3.17	Experimental setup for XRD analysis	78
CHAPTER 4 RESULTS AND DISCUSSIONS		
4.1	Effect of adding OPC on slump of GPC	80
4.2	Effect of adding OPC on compaction factor of GPC	81
4.3	Compressive strength of GPC versus OPC content	82

4.4	Effect of OPC inclusion on compressive strength of GPC	83
4.5	Split tensile strength of GPC versus OPC content	86
4.6	Effect of OPC inclusion on split tensile strength of GPC	86
4.7	SEM/EDS analysis of GPC with 0% OPC at 3 days	89
4.8	XRD analysis of GPC with 0% OPC at 3 days	89
4.9	SEM/EDS analysis of GPC with 0% OPC at 7 days	90
4.10	XRD analysis of GPC with 0% OPC at 7 days	90
4.11	SEM/EDS analysis of GPC with 0% OPC at 28 days	91
4.12	XRD analysis of GPC with 0% OPC at 28 days	91
4.13	SEM/EDS analysis of GPC with 0% OPC at 90 days	92
4.14	XRD analysis of GPC with 0% OPC at 90 days	92
4.15	SEM/EDS analysis of GPC with 0% OPC at 365 days	93
4.16	XRD analysis of GPC with 0% OPC at 365 days	93
4.17	SEM/EDS analysis of GPC with 10% OPC at 3 days	95
4.18	XRD analysis of GPC with 10% OPC at 3 days	95
4.19	SEM/EDS analysis of GPC with 10% OPC at 7 days	96
4.20	XRD analysis of GPC with 10% OPC at 7 days	96
4.21	SEM/EDS analysis of GPC with 10% OPC at 28 days	97
4.22	XRD analysis of GPC with 10% OPC at 28 days	97
4.23	SEM/EDS analysis of GPC with 10% OPC at 90 days	98
4.24	XRD analysis of GPC with 10% OPC at 90 days	98
4.25	SEM/EDS analysis of GPC with 10% OPC at 365 days	99
4.26	XRD analysis of GPC with 10% OPC at 365 days	99
4.27	SEM/EDS analysis of GPC with 20% OPC at 3 days	101
4.28	XRD analysis of GPC with 20% OPC at 3 days	101
4.29	SEM/EDS analysis of GPC with 20% OPC at 7 days	102
4.30	XRD analysis of GPC with 20% OPC at 7 days	102
4.31	SEM/EDS analysis of GPC with 20% OPC at 28 days	103
4.32	XRD analysis of GPC with 20% OPC at 28 days	103
4.33	SEM/EDS analysis of GPC with 20% OPC at 90 days	104
4.34	XRD analysis of GPC with 20% OPC at 90 days	104
4.35	SEM/EDS analysis of GPC with 20% OPC at 365 days	105
4.36	XRD analysis of GPC with 20% OPC at 365 days	105

4.37	SEM/EDS analysis of GPC with 30% OPC at 3 days	107
4.38	XRD analysis of GPC with 30% OPC at 3 days	107
4.39	SEM/EDS analysis of GPC with 30% OPC at 7 days	108
4.40	XRD analysis of GPC with 30% OPC at 7 days	108
4.41	SEM/EDS analysis of GPC with 30% OPC at 28 days	109
4.42	XRD analysis of GPC with 30% OPC at 28 days	109
4.43	SEM/EDS analysis of GPC with 30% OPC at 90 days	110
4.44	XRD analysis of GPC with 30% OPC at 90 days	110
4.45	SEM/EDS analysis of GPC with 30% OPC at 365 days	111
4.46	XRD analysis of GPC with 30% OPC at 365 days	111
4.47	Water absorption of GPC versus OPC content	114
4.48	Effect of OPC inclusion on water absorption of GPC	114
4.49	Porosity of GPC versus OPC content	115
4.50	Effect of OPC inclusion on porosity of GPC	116
4.51	Sorptivity of GPC versus OPC content	117
4.52	Effect of OPC inclusion on sorptivity of GPC	118
4.53	Effect of OPC on chloride ion penetration in GPC	119
4.54	Change in mass of sulphuric acid exposed GPC	121
4.55	Change in compressive strength of sulphuric acid exposed GPC	123
4.56	SEM micrograph of sulphuric acid exposed GPC with 0% OPC at 365 days	124
4.57	SEM micrograph of sulphuric acid exposed GPC with 10% OPC at 365 days	126
4.58	SEM micrograph of sulphuric acid exposed GPC with 20% OPC at 365 days	126
4.59	SEM micrograph of sulphuric acid exposed GPC with 30% OPC at 365 days	127
4.60	EDS results of sulphuric acid exposed GPC with 0, 10, 20 & 30% OPC at 365 days	127
4.61	XRD analysis of GPC with 0% OPC exposed to sulphuric acid for 365 days	129
4.62	XRD analysis of GPC with 10% OPC exposed to sulphuric acid for 365 days	129

4.63	XRD analysis of GPC with 20% OPC exposed to sulphuric acid for 365 days	130
4.64	XRD analysis of GPC with 30% OPC exposed to sulphuric acid for 365 days	130

ABBREVIATIONS

<i>Abbreviations</i>		<i>Word (s)</i>
A	-	Albite
ACI	-	American Concrete Institute
An	-	Anorthite
Anh	-	Anhydrite
ASTM	-	American Society for Testing and Materials
B	-	Bavenite
BIS	-	Bureau of Indian Standards
C	-	Calcite
CASH	-	Calcium-Alumino-Silicate Hydrate
CCC	-	Conventional Cement Concrete
CSH	-	Calcium-Silicate Hydrate
CTM	-	Compression Testing Machine
EDS	-	Energy Dispersive X-ray spectroscopy
FA	-	Fly Ash
FTIR	-	Fourier Transformation Infrared Spectroscopy
GGBS	-	Ground Granulated Blast furnace Slag
GPC	-	Geopolymer Concrete
IBP	-	Industrial By-Products
IPCC	-	Intergovernmental Panel Climate Change
ITZ	-	Interfacial Transition Zone
LOI	-	Loss on Ignition
M	-	Mullite

MIP	-	Mercury Intrusion Porosity
MIRHA	-	Microwave Incinerated Rich Husk Ash
N	-	Nepheline
NASH	-	Sodium-Alumino-Silicate Hydrate
NMR	-	Nuclear Magnetic Resonance
OPC	-	Ordinary Portland Cement
P	-	Portlandite
PFA	-	Pulverized Fuel Ash
POFA	-	Palm Oil Fuel Ash
Q	-	Quartz
RCPT	-	Rapid Chloride Permeability Test
RHA	-	Rice Husk Ash
SCGC	-	Self-Compaction Geopolymer Concrete
SCM	-	Supplementary Cementitious Materials
SEM	-	Scanning Electron Micrograph
SP	-	Super Plasticizer
T	-	Tamarugite
TGA	-	Thermo Gravimetric Analysis
VI	-	Volume Intrusion
XRD	-	X-Ray Diffraction
XRF	-	X-Ray Fluorescence

LIST OF UNITS

<i>Units</i>		<i>Word (s)</i>
°C	-	Degree Celsius
%	-	Percentage
µm	-	Micrometer
C	-	Coulombs
cm	-	Centimetre
g	-	Gram
h	-	Hour
kg	-	Kilogram
kg/m ³	-	Kilogram per cubic meter
kN	-	Kilo Newton
kV	-	Kilo Volt
l	-	Litre
m	-	Meter
m/s	-	Meter per second
m ² /kg	-	Square meter per kilogram
mg	-	Milligram
min	-	Minute
ml	-	Millilitre
mm	-	Millimetre
MPa	-	Mega Pascal
N	-	Newton

N/mm^2	-	Newton per square metre
rpm	-	Revolutions per minute
s	-	Second
V	-	Volt
θ	-	Theta

-

CHAPTER-1

INTRODUCTION

This chapter presents the general introduction and background about the concept of geopolymers. It also includes the mechanism of geopolymers followed by its advantages and limitations. The significance and objectives of this research are also presented.

1.1 GENERAL

Concrete is the largest consumer of natural resources and is being used only second to water globally (Mehta, 2002). The increase in demand of concrete directly increases the demand for Portland cement as well. For the production of over 14 billion tons of concrete globally, around 2.8 billion tons of cement is produced per year (Cembureau, 2007). Also, the emission of gasses like carbon dioxide by industrial sector causes the most hazardous problem of global warming which further increases with the growing use of Portland cement. It has been reported that producing one ton of Portland cement, approximately one ton of carbon dioxide is released (McCaffrey, 2002; Davidovits, 1994a). The United Nations Intergovernmental Panel Climate Change (IPCC) also considered the carbon dioxide emissions as a significant factor for the change in climate (IPCC, 2007). This clearly reflects the impact of global warming in near future and therefore, it becomes essential to find alternative cementitious materials that can very well satisfy the need for construction materials with least contribution to global warming and help in making a sustainable environment. The other sources of harmful gasses are from various industries which release waste and by-products that also create disposal problems as well. These industrial by-products with the cement-like physical and chemical properties, such as fly ash, silica fume, steel slag, palm oil, fuel ash etc (Palomo et al., 1999) have prompted their use in concrete production as supplementary cementitious materials (SCMs).

Enormous efforts have been observed from various publications towards the utilization of these SCMs for the production of binders as an alternative to Portland cement which may reduce the carbon emissions significantly (Topcu et al., 2014). Aggarwal et al. (2007) utilized bottom ash as partial replacement of aggregates and reported improvement in strength properties of concrete. Mishra et al. (1994) incorporated the use of industrial by-products such

as blast furnace slag, fly ash, and silica fume in concrete and observed the decrease in chloride permeability. Smarzewski and Barnat-Hunek (2016) studied the influence of adding waste foundry sand and observed the improvement in salt crystallization and freezing-thawing resistance of concrete. Khatib et al. (2014) concluded the improvement in compressive strength when cement was replaced by metakaolin up to 10%, and beyond that the strength reduced. Netinger et al. (2015) reported the utilization of steel slag as replacement of aggregates in improving the post-fire properties of concrete. It was observed that slag in the lower temperature range (up to 400 °C) improved the performance of concrete by increasing the residual compressive strength up to 16%. Ng et al. (2015) utilized the blended mixture of silica fume and aerogel for the production of ultra high-performance mortar. It was observed to reduce the thermal conductivity by a high factor of 5 which can reduce requirements for insulation materials and hence slimmer concrete sections can be used.

To reduce the consumption of cement, efforts have also been made to utilize construction wastes in new construction applications. Recycled aggregates were utilized by Prince and Singh (2014) for increasing the bond strength between the deformed steel bars and concrete. Rao et al. (2007) also utilized the recycled aggregates in the production of concrete and reported that recycled aggregates can be used for making normal structural concrete with the addition of condensed silica fume and fly ash. Gayarre et al. (2014) reported the decrease in density of the concrete when optimized by using recycled aggregates which resulted in a decrease in its compressive strength. However, they suggested the provision of adequate curing process that can protect the concrete from the climate effects significantly and help in achieving the reasonable compressive strengths.

Tripathy and Barai (2006) studied the compressive strength of mortar, made with crushed stone dust as cement replacement, under different curing regimes. They concluded that comparable or better compressive strength was obtained with the cement replacement up to 40% than control mortar mixture. Milicevic et al. (2015) prepared the precast concrete floor blocks by adding crushed clay brick and roof tiles as aggregates. They reported that the use of 50% fine and 75% coarse crushed brick and tile aggregates satisfied the mechanical and thermal properties required for the concrete blocks.

To eliminate the use of higher cement content for the production of high strength concrete, some studies have also made the use of steel fibers in improving the strength characteristics.

For instance, Bhargava et al. (2006) reported the increase in compressive strength with the addition of steel fibers of different aspect ratios blended together in the concrete. This high strength fiber reinforced concrete also found to have better ductility in comparison to the concrete optimized by high cement content. Madan et al. (2007) also studied the effect of adding steel fibers as replacement of web reinforcement in the deep beams and concluded better crack control and deformation characteristic of beams.

The use of industrial by-products as SCMs in concrete applications is found to be beneficial, however; these wastes can only be used as partial replacement of OPC (Chalee et al., 2010, Krammart and Tangtermsirikul, 2004) and cannot totally replace it. In this context, geopolymer technology has enticed the researchers all across the globe as an alternative to cement binder. It was originally coined by Glikhovskiy (Glukhovskiy, 1959) and further developed by Davidovits (Davidovits, 1991) as a binder material. It is a technology that involves the production of binders by polymerization reactions of aluminosilicates with alkaline solutions, which can be used effectively in concrete applications. As the source materials for alumina and silica are of geological origin and also the reaction mechanism is polymerization process, Davidovits termed this technology as Geopolymers. This technology if used as an alternative to conventional concrete, can reduce the carbon dioxide emissions by about 80% (Davidovits, 1994b; Gartner, 2004).

1.2 GEOPOLYMERS

The mechanism of geopolymers involves the production of binders by polymerization reaction which takes place in the presence of high temperature. The critical feature of the polymerization reaction is that water is required only to facilitate adequate workability and does not affect the polymerization mechanism. Instead, it is expelled from the reaction at the time of curing. On the other hand, in case of conventional concrete, hydration products such as calcium silicate and calcium hydroxide are formed with the reaction of alkalis with water. With the course of time, the calcium hydroxide evaporates which results in the formation of voids in the matrix. These voids allow the percolation of external harmful ions and cause deterioration. Whereas, in case of geopolymers, due to polymerization, comparatively lesser voids are formed that also have a positive influence on the mechanical properties and also renders it more resistant to heat, water ingress, alkali-aggregate reactivity and other types of chemical attack.

1.2.1 Structure of Geopolymers

Alumino-silicate gel is formed by the polymerization reaction of silica and alumina with an alkali-activating solution. This gel holds the loose aggregates and yields three-dimensional amorphous to crystalline polymeric structures having strong Si-O-Al bonds. The mechanism depends on the type of source materials containing silica and alumina, and the alkaline activators. Different studies have proposed different approaches for the geopolymer formation. Davidovits (1991) explained three types of three-dimensional amorphous to crystalline alumina-silicate geopolymer structures depending upon the ratio of silica to alumina as shown in Fig. 1.1.

When the ratio of silica to alumina is 1:1, orthosialates are formed which reacts with an alkali-activating solution to form poly (sialate) type (Si-O-Al-O-) geopolymers, whereas when silica to alumina ratio is 2:1, orthosialate-siloxo is formed which further reacts to form poly (sialate-siloxo) type (Si-O-Al-O-Si-O-) geopolymers. Similarly when silica to alumina ratio is 3:1, ortho-sialate and di-siloxonate are initially formed which further undergo polymerization to form poly (sialate-disiloxo) type (Si-O-Al-O-Si-O-Si-O-) geopolymers.

Xu and Van Deventer (2000) described the geopolymer mechanism, as shown in Fig. 1.2, in three steps i.e. formation of precursor ions by the dissolution of alumina and silica from the source materials, the formation of monomers from the condensation of precursor ions, and polymerization of monomers to form three-dimensional polymeric structures.

Similarly, Weng and Sagoe-Crentsil (2007) also explained the mechanism of geopolymer formation as a 3-step procedure; dissolution, hydrolysis and condensation with the formation of poly (sialate) geopolymer structure for low silica to alumina ratio, as shown in Fig. 1.3.

The three-dimensional tightly packed poly-crystalline structure model of geopolymers is also explained by Davidovits (2002) as shown in Fig. 1.4.

1.2.2 Constituents of Geopolymers

1.2.2.1 Source Materials

Geopolymers require two types of materials, firstly the source material having alumina and silica, and secondly, the alkali-activating solution that can initiate the polymerization reaction.

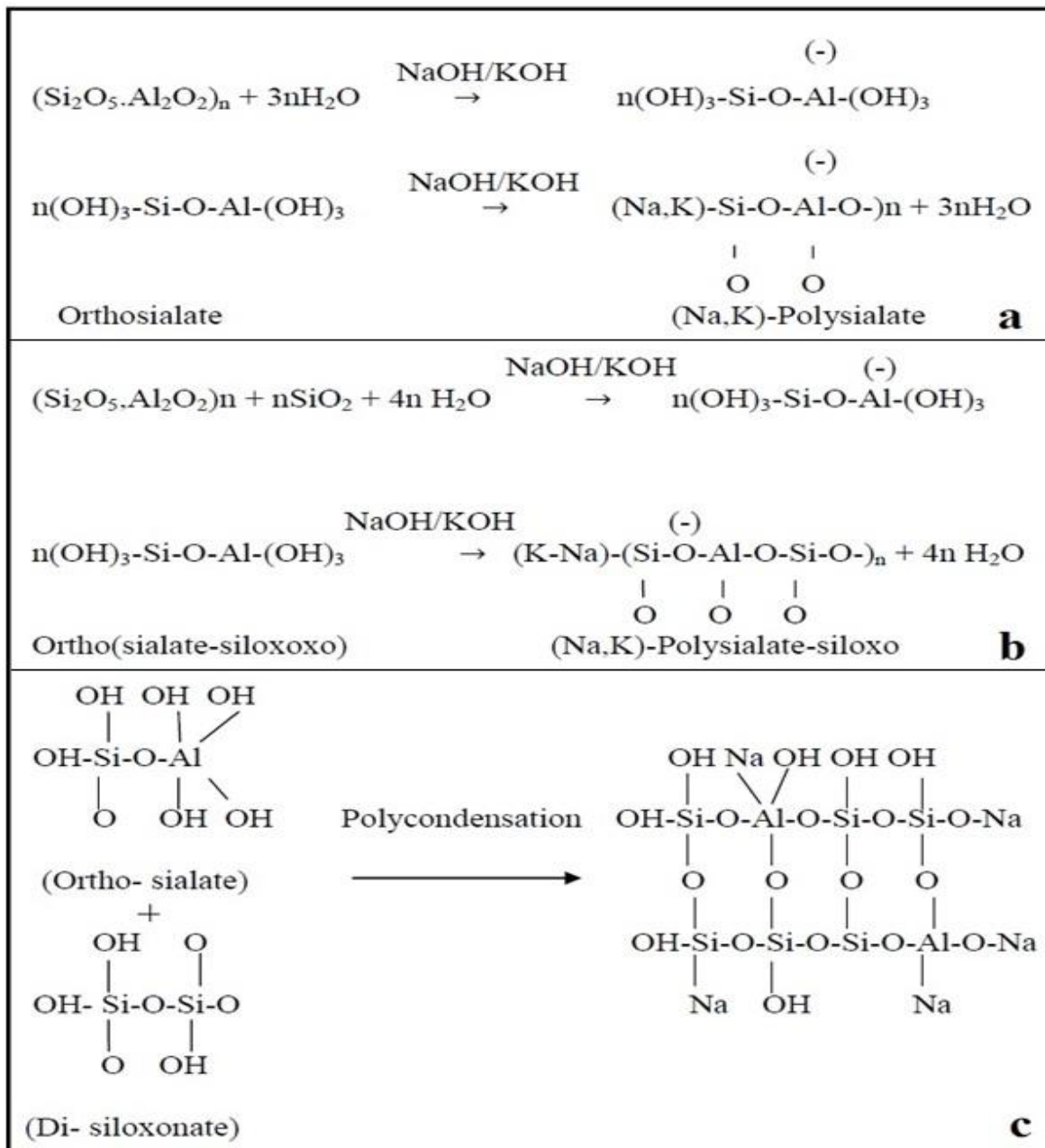


Fig.1.1: Types of geopolymer structures with Si-Al ratio as a) 1, b) 2 and c) 3 (Davidovits, 1991)

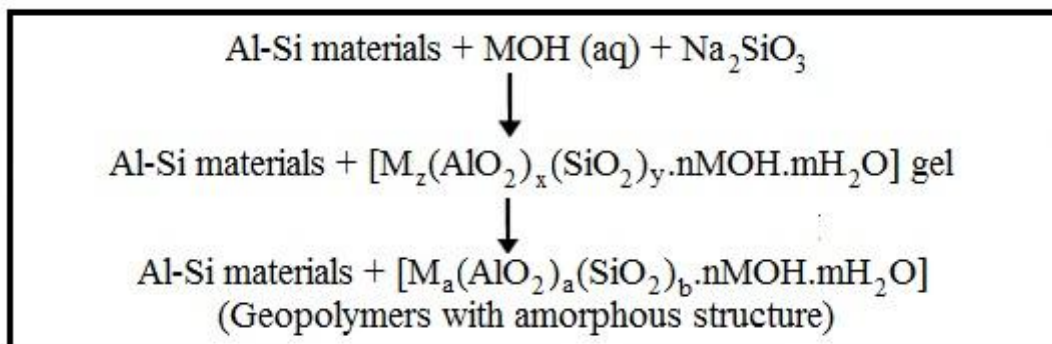


Fig.1.2: Mechanism of geopolymers (Xu and Van Deventer, 2000)

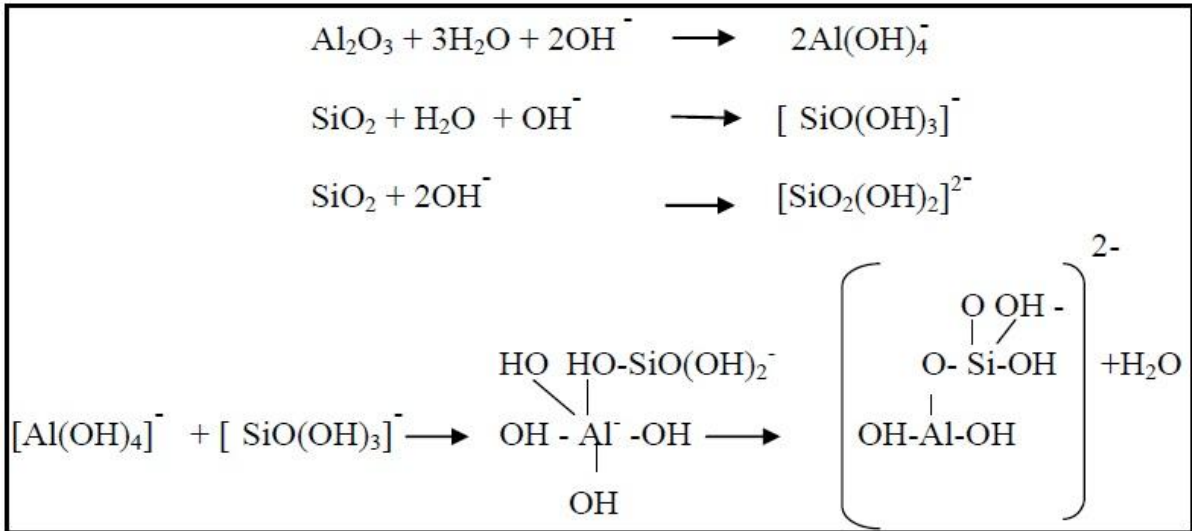


Fig.1.3: Mechanism of geopolymers (Weng and Sagoe-Crentsil, 2007)

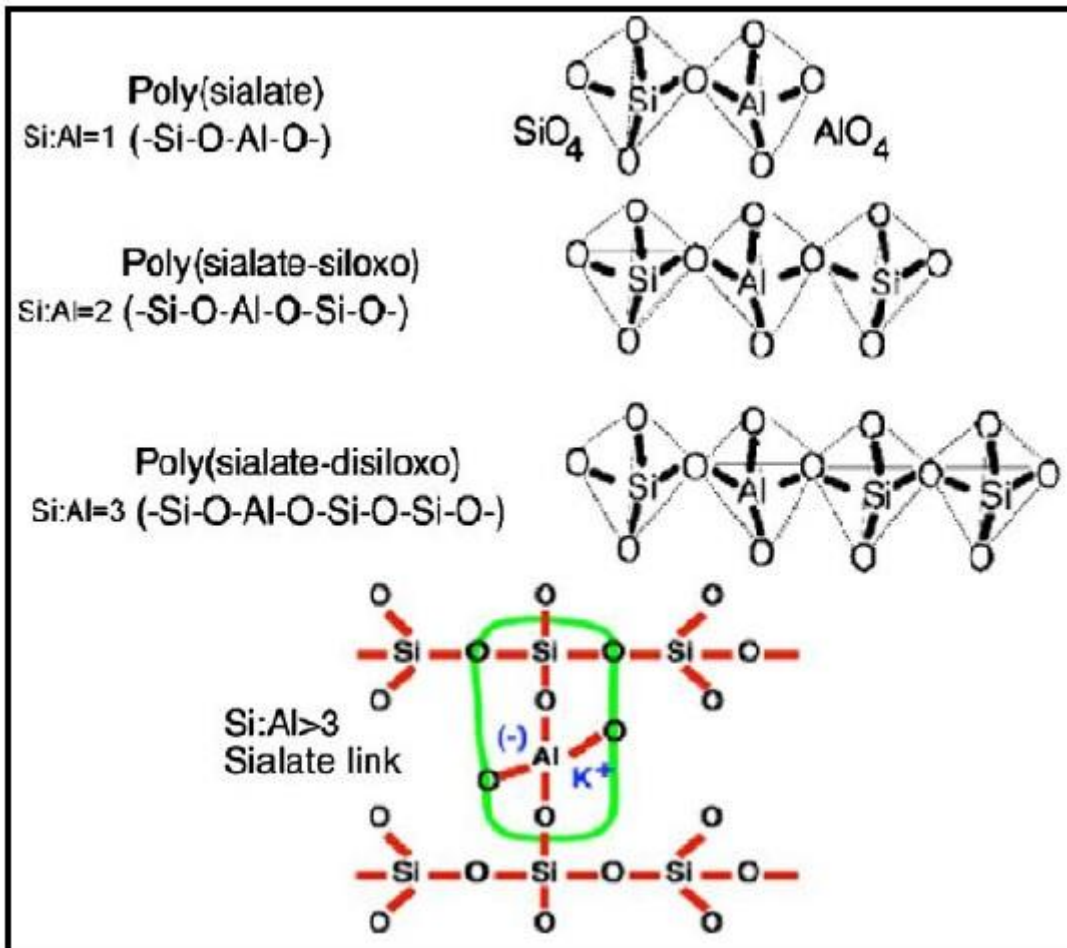


Fig.1.4: Structure model of geopolymers with low silica-alumina ratio (Davidovits, 2002)

Silica and alumina can be considered as that of geological origin which can be obtained from natural minerals such as kaolinite, clays, etc (Barbosa et al., 2000; Yang et al., 2010);

however, it can also be obtained from industrial by-products such as fly ash, metakaolin, blast furnace slag, etc (Kourti et al., 2011; Wongpa et al., 2010; He et al., 2013) which can be liberated by alkaline solutions. The choice may depend upon various factors such as cost, availability or any specific type of application. It has also been observed in the previous study (Barbosa et al., 2000) that the geopolymers having source materials with high-calcium such as slag, Class-C fly ash, etc yield higher compressive strength in comparison with low-calcium such as clay, mine tailing, etc. However, some studies (Xu and Van Deventer, 2002) conclude the improvement in compressive strength by using the combination of calcined and non-calcined materials as source material. The degree of polymerization depends on how much the source material is amorphous and also on its fineness. Most of the studies so far have been more confined to use fly ash as source material but other SCMs such as ground granulated blast furnace slag, metakaolin, rice husk ash, etc have also shown potentials to be used as source material in the synthesis of geopolymers. Also, the finer size of fly ash yields higher reactivity than other materials of similar fineness. Fernandez-Jimnez and Palomo (2003) investigated various types of fly ash to be used as source material in geopolymers and concluded that low-calcium fly ash is more beneficial with particle size less than 45μ , loss on ignition (LOI) less than 5%, iron oxide content less than 10% and reactive silica in between 40-50%. Other studies (Van Jaarsveld et al., 2003) suggested the use of high-calcium fly ash due to the formation of additional calcium-based hydrated compounds which increase the compressive strength significantly.

- **Fly Ash**

Fly ash is an industrial by-product collected by electrostatic precipitators and scrubber systems when coal is burnt to produce heat in thermal power stations. It is a powdery material with very fine particle size ranging from $0.5-100\mu\text{m}$. Most of the fly ash particles are spherical in shape and light tan in color. It consists mainly of silica oxide (SiO_2) in the round and smooth amorphous form as well as in crystalline form. The chemical composition of fly ash depends mainly on the type of burnt coal. The sub-bituminous coal yields fly ash with high calcium content whereas bituminous coal yields fly ash with high iron content. The fly ash obtained from different sources shows a large variation in their chemical composition. Depending on the amount of calcium, silica, alumina and iron, ASTM C618 classified the fly ash into three categories: Class N fly ash, Class F fly ash and Class C fly ash. Class F fly ash corresponds to the low-calcium fly ash obtained by combustion of bituminous coal or anthracite and consists mainly of alumino-silicate glass that exhibits pozzolanic

characteristics. On the other hand, Class C refers to high-calcium fly ash formed by combustion of lignite or sub-bituminous coal which contains more than 20% calcium oxide and shows cementitious properties. Due to serious implications of landfill problems of fly ash, it is being used in various applications. One such effective utilization of fly ash is the use in concrete production which can improve its mechanical and durability properties significantly. Fly ash is released from thermal power plants in such large amount that in spite of its utilization in research and development sectors as well as in government or non-government sectors, only 50% of the total have been able to be utilized. It has been used in larger proportions as supplementary cementitious material (SCM) in concrete production and in new technologies such as geopolymer binders. The physical and chemical properties of fly ash particles are shown in Tables 1.1 and 1.2, respectively.

Table 1.1: Physical properties of fly ash

<i>Physical properties</i>	<i>Chindaprasirt et al. (2011)</i>	<i>Junaid et al. (2015)</i>	<i>Abdulkareem et al. (2014)</i>	<i>Temuujin et al. (2010)</i>	<i>Sachan and Sahu (2013)</i>	<i>Nazari and Sanjayan (2015)</i>
Specific gravity	2.38	2.1	-	2.12	1.16	2.04
Average particle size (μm)	16	16	15.5	14.4	-	15
Blaine fineness (cm^2/g)	3900	-	4630	-	3000	6590

Table 1.2: Chemical composition of fly ash

<i>Chemical composition (%)</i>	<i>Sachan and Sahu (2013)</i>	<i>Kong et al. (2007)</i>	<i>Liu et al. (2012)</i>	<i>Mobili et al. (2016)</i>	<i>Castel and Foster (2015)</i>	<i>Kong and Sanjayan (2010)</i>	<i>Olivia and Nikraz (2012)</i>
SiO ₂	57.1	48.8	53.31	44	66.56	48.8	50.50
Al ₂ O ₃	23.83	27	26.43	29.1	22.47	27	26.57
Fe ₂ O ₃	6.86	10.2	7.53	6	3.54	10.2	13.77
CaO	3.34	6.2	4.46	5.5	1.64	6.2	2.13
Na ₂ O	-	0.37	1.15	0.4	0.58	0.37	0.45
MgO	0.56	1.4	2.45	1.5	0.65	1.4	1.54
K ₂ O	-	0.85	0.9	1.1	1.75	0.85	0.77
SO ₃	0.54	0.22	0.9	1.1	0.10	0.22	0.41
LOI	5.2	1.7	4	0	1.66	1.7	0.60

Chindaprasirt et al. (2011) studied the micrograph of fly ash particles of three types of fineness; a) coarse fly ash (CFA), b) medium fly ash (MFA), and c) fine fly ash (FFA) with

particle sizes; 200, 50 and 20 μm , respectively as shown in Fig.1.5. The most of the particles were found to be spherical in shape. It reacts with the unwanted cement hydration product calcium hydroxide ($\text{Ca}(\text{OH})_2$) and produces additional C-S-H which improves the microstructure of concrete significantly. It also fills the pores between the cement particles and improves the durability properties due to improved microstructure.

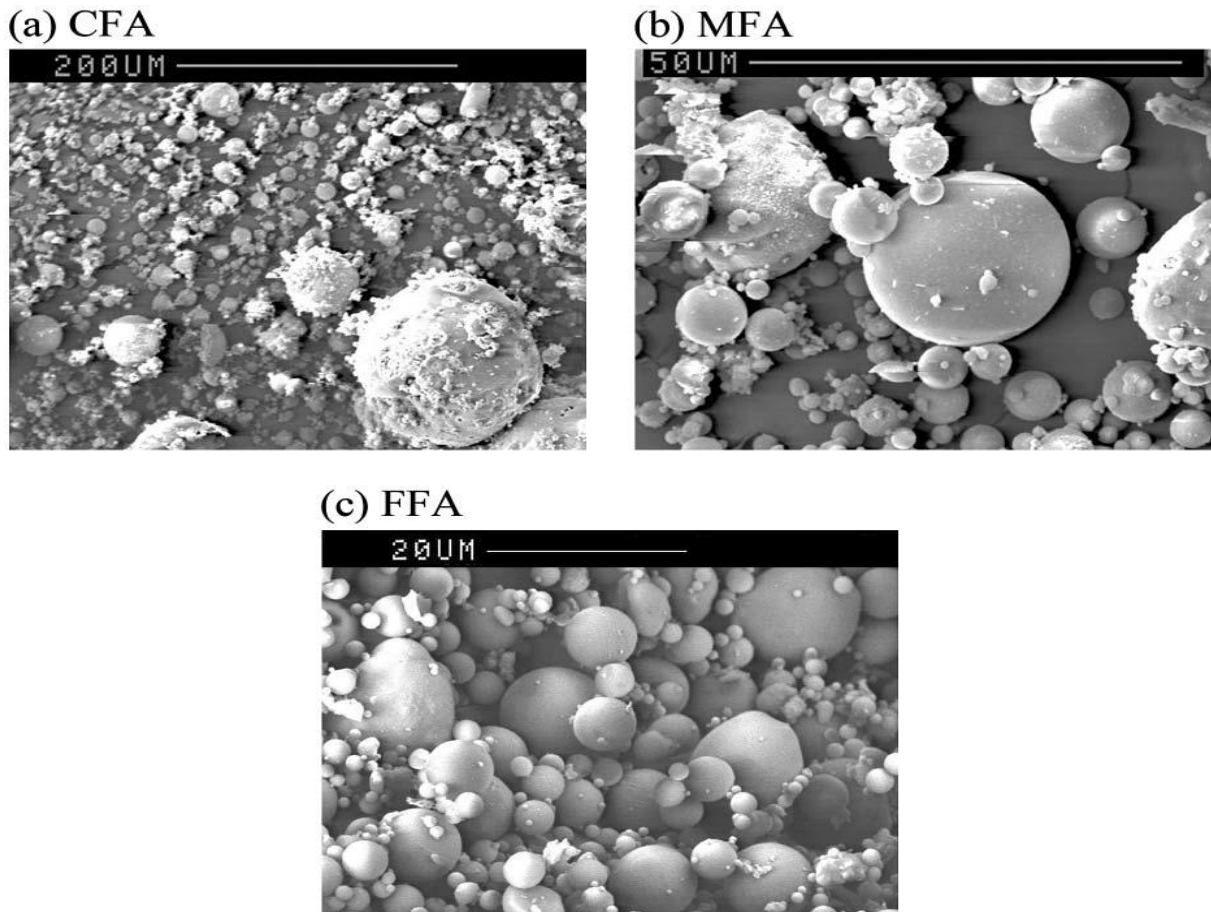


Fig.1.5: Scanning electron microscope micrographs of fly ashes (Chindaprasirt et al., 2011)

- **Ground Granulated Blast Furnace Slag**

Ground Granulated Blast furnace Slag (GGBS) is an industrial by-product from the iron manufacturing industries. It is a powdery material with near white color. When it is used in concrete applications, it imparts a lighter and brighter color to concrete with the smooth surface finish. The chemical composition of GGBS comprises mainly the oxides of calcium, silica, and alumina. The shape and size of its particles are dependent on the types of grinding techniques such as an airflow mill, ball mill, a vibro-mill or steel balls as grinding medium. Ball mill processing produces the widest particle size whereas an airflow mill

produces the narrowest. Regarding the shape, vibro-mill produces the spherical shape particles with smooth surface whereas an airflow mill produces edges type.

A large amount of blast furnace slag is being produced for which its disposal has become the major challenge to deal with. The waste landfill can be associated with a number of environmental hazards which does not fit in the contemporary picture of the sustainable development. Also, with the tremendous growth in iron and steel industries, the production of blast furnace slag is bound to increase which possess a high environment threat. It has been widely used in cement and concrete applications over several years due to its cementing properties.

The physical and chemical properties of blast furnace slags are shown in Tables 1.3 and 1.4, respectively. It can be seen that the average particle size ranges from 13-17 μm . The silica content ranges from 32-36% whereas the alumina content ranges from 11-20%. Aguilar et al. (2010) studied the microstructure of ground granulated blast furnace slag, as shown in Fig.1.6 and found to be finer in size.

Table 1.3: Physical properties of ground granulated blast furnace slag

<i>Physical properties</i>	<i>Bernal et al. (2012)</i>	<i>Tasong et al. (1999)</i>	<i>Wan et al. (2004)</i>	<i>Aguilar et al. (2010)</i>	<i>Sagawa et al. (2011)</i>	<i>Nagendra et al. (2016)</i>	<i>Thakur et al. (2016)</i>
Average particle size (μm)	15	14.78	13.69	14.26	16.34	17.36	13.38
Blaine fineness (cm^2/g)	3990	4500	5100	5333	4070	4160	3020

Table 1.4: Chemical composition of ground granulated blast furnace slag

<i>Chemical composition (%)</i>	<i>Bernal et al. (2012)</i>	<i>Tasong et al. (1999)</i>	<i>Aguilar et al. (2010)</i>	<i>Nagendra et al. (2016)</i>	<i>Thakur et al. (2016)</i>	<i>Yuksel et al. (2011)</i>
SiO ₂	32.29	35.34	33.8	33.77	34.72	35.10
Al ₂ O ₃	16.25	11.59	11.5	13.24	19.11	17.54
Fe ₂ O ₃	2.35	0.34	0.6	0.65	0.5	0.70
CaO	42.25	41.99	38.3	33.77	35.27	37.80
Na ₂ O	-	-	0.5	-	0.16	-
MgO	2.87	8.04	9.0	8.46	8.46	5.50
K ₂ O	-	-	0.9	-	0.58	-
SO ₃	-	0.23	3.4	2.23	0.18	0.70
LOI	1.91	-	-	-	-	1.08

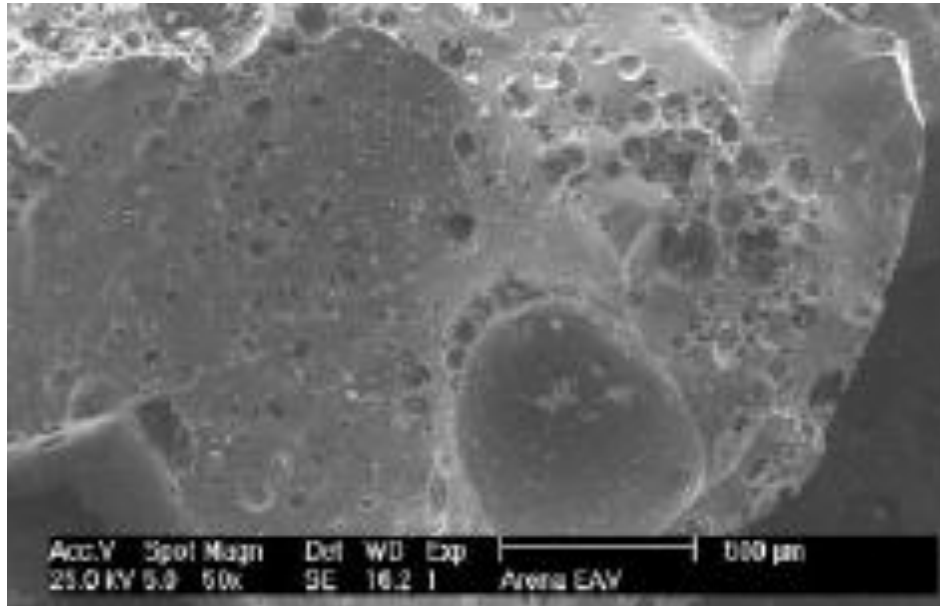


Fig.1.6: Scanning electron microscope micrographs of blast furnace slag (Aguilar et al., 2010)

Due to its slightly bigger size particles, it is dried and grounded to the cement size particles. It can be used as an addition or partial replacement to cement in the concrete proportion depending on the requirement of particular concrete applications.

- **Metakaolin**

Metakaolin is produced by the calcination of kaolin clay at very high temperatures of around 500-800°C. Kaolin is a material of geological origin which is used in the manufacture of porcelain. Kaolinite is the mineralogical term of kaolin consisting of hydrated aluminium-di-silicate. Prefix “meta” in metakaolin refers to the change in kaolin caused by dehydroxylation due to immense heat over a period of time. After the stage of dehydroxylation, a crystal two-dimensional structure is obtained which is known as metakaolin. Immense care is required during its production as excess heat after it is produced, will burn the material and form mullite which is dead burnt inactive material. The mean particle size of metakaolin is 3μm and its 99.9% particles are finer than 16μm. The chemical composition of metakaolin comprises mainly oxides of alumina and silica with very low calcium content. The physical and chemical compositions of metakaolin, as reported in various studies, are shown in Tables 1.5 and 1.6, respectively.

It can be observed that the silica content of metakaolin ranges from 43-56% whereas alumina content ranges from 37-52%. Also, He et al. (2012) showed the micrograph of metakaolin, as

shown in Fig.1.7. It has been widely used in concrete applications due to its very high pozzolanic reactivity. It reacts with calcium hydroxide (Ca(OH)_2) and produces calcium silicate hydrate (CSH) as well as alumina containing phases. It can be used in concrete applications to provide high strength and improve the high surface finish. It can also be used in the production of lightweight concrete and precast concrete for various architectural, industrial, and structural purposes.

Table 1.5: Physical properties of metakaolin

Physical properties	Bernal et al. (2012)	Kong and Sanjayan (2007)	He et al. (2012)	Kouamo et al. (2012)	Rovnanik (2010)	Yip et al. (2008)
Average particle size (μm)	12.2	12	4.5	9.95	4.80	1.89
Blaine fineness (cm^2/g)	178	234	-	205	131	125

Table 1.6: Chemical composition of metakaolin

Chemical composition (%)	Cachim et al. (2010)	Bernal et al. (2012)	Kong and Sanjayan (2007)	Cwirzen et al. (2014)	Pacheco-Torgal et al. (2011)	Cyr et al. (2014)	Ferraz et al. (2014)
SiO_2	59.90	50.72	55.9	54.8	50.75	67.1	65.34
Al_2O_3	32.29	44.63	37.2	40.4	43.48	26.8	28.13
Fe_2O_3	1.28	-	1.7	0.8	2.45	2.6	0.98
CaO	0.04	2.69	0.11	0.1	-	1.1	0.06
Na_2O	0.24	-	0.27	0.1	0.04	0.01	-
MgO	0.17	-	0.24	0.4	0.11	0.1	0.08
K_2O	2.83	-	0.18	2.7	-	0.1	3.8
SO_3	-	-	0.02	-	-	0	-
LOI	2.8	1.02	0.8	1.1	-	0.8	1.46

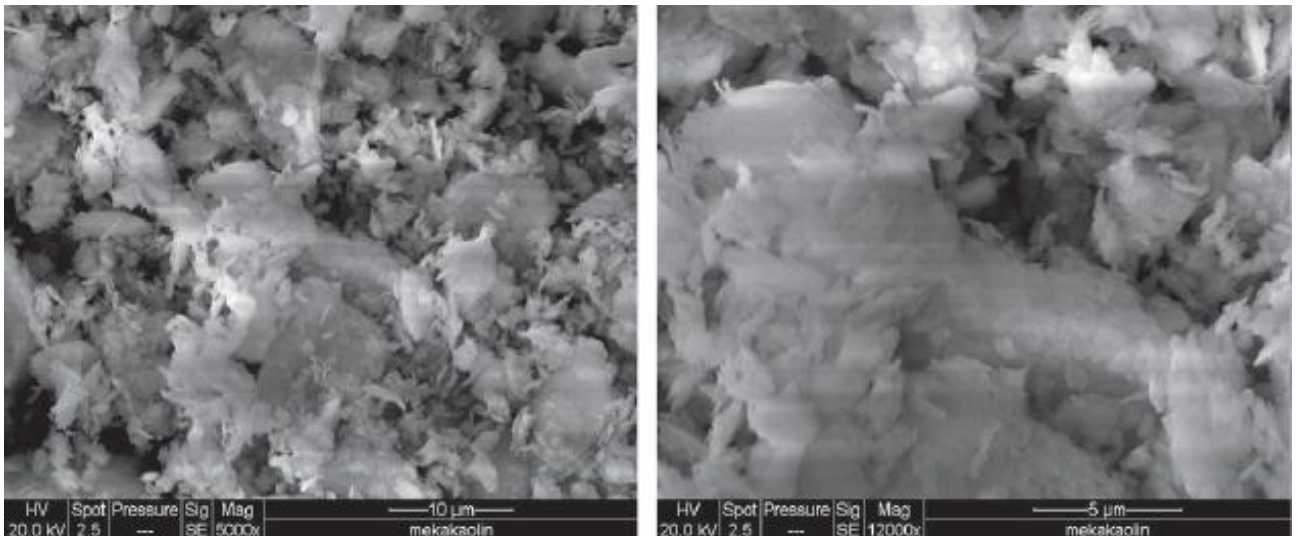


Fig.1.7: Scanning electron microscope micrographs of metakaolin (He et al., 2012)

- **Rice Husk Ash**

Rice Husk Ash (RHA) is generated by burning rice husk, which is an agricultural by-product. Rice husk consists of cellulose (50%), silica (15-20%), and lignin (25-30%). When it is subjected to burning, cellulose and lignite are removed. The particle size is largely dependent on burning temperature and its environment, therefore to produce high-quality RHA, fair control on burning conditions is required. It has been estimated from the studies that around 20% of the rice weight constitutes rice husk and when it is burnt; around 25% of RHA is generated. The physical appearance of completely burnt RHA is grey to white while that of partially burnt RHA is blackish in color. The physical and chemical properties of rice husk ash, as reported in various studies, are shown in Tables 1.7 and 1.8, respectively.

Table 1.7: Physical properties of rice husk ash

<i>Physical properties</i>	<i>Bohlooli et al. (2012)</i>	<i>He et al. (2012)</i>	<i>Kusbiantoro et al. (2012)</i>	<i>Mehta (1992)</i>	<i>Feng et al. (2004)</i>	<i>Bui et al. (2005)</i>
Average particle size (μm)	7	25	16.76	-	7.4	5
Blaine fineness (cm^2/g)	331	-	673	99% passing $45\mu\text{m}$	-	-

Table 1.8: Chemical composition of rice husk ash

<i>Chemical composition (%)</i>	<i>Bohlooli et al. (2012)</i>	<i>He et al. (2012)</i>	<i>Kusbiantoro et al. (2012)</i>	<i>Mehta (1992)</i>	<i>Bui et al. (2005)</i>
SiO ₂	81.4	91.5	89.34	87.2	86.98
Al ₂ O ₃	0.4	-	0.45	0.15	0.84
Fe ₂ O ₃	0.12	-	0.40	0.16	0.73
CaO	3.23	-	0.76	0.55	1.40
Na ₂ O	0.36	-	-	1.12	0.11
MgO	-	-	0.49	0.35	0.57
K ₂ O	-	2.3	4.98	3.68	2.46
SO ₃	0.85	-	0.90	0.24	-
C	-	6	-	-	-
LOI	3.55	-	-	8.55	5.14

The average particle size ranges from 5-25 μm and contains high silica content from 81-92%. Different forms of silica are produced depending on the temperature and duration of combustion of rice husk. For example, the combustion temperature upto 900°C and duration of less than 1 minute yield amorphous silica whereas at high combustion temperature of

around 1000 °C for more than 5 minutes, crystalline type silica is generated (Yeoh et al., 1979). Kusbiantoro et al. (2012) studied the microstructure properties of rice husk ash with the micrograph as shown in Fig.1.8. Also, Hwang and Wu (1989) reported the increase in silica content with the increase in combustion temperature of rice husk.



Fig.1.8: Scanning electron microscope micrographs of rice husk ash (Kusbiantoro et al., 2012)

1.2.2.2 Alkali-Activating Solution

The alkali-activating solution liberates alumina and silica from the source materials and form monomers which further reacts and undergoes polymerization. Therefore, the solution has an effective role to play in the mechanism which can alter the extent of polymerization by regulating the effective silica and alumina in the geopolymer system. The solution consists of soluble alkali metals normally sodium or potassium. The most common and generally used solution is the mixture of hydroxides and the silicates of sodium or potassium (Palomo et al., 1999; Barbosa et al., 2000; Xu and Van Deventer, 2000; Swanepoel and Strydom, 2002). However, some studies use only alkali hydroxides for the activation of alkalis (Teixeira-Pinto et al., 2002). The parameters that can influence the properties of geopolymers in term of alkali solution can be the molarity of alkali hydroxide, the ratio of silicates to hydroxides of alkalis, etc. Palomo et al. (1999) compared the combination of potassium hydroxide and potassium silicate, with sodium hydroxide and sodium silicate as alkali-activating solutions and studied their effect on the mechanical properties of geopolymer concrete. They concluded that mixture of sodium silicate and sodium hydroxide yielded better compressive

strength of geopolymer concrete. Motorwala et al. (2013) studied the effect of different molarities of sodium hydroxide solution and concluded the increase in compressive strength with the increase in molarity up to a certain limit. Xu and Van Deventer (2000) obtained the best strength results with the combination of sodium hydroxide and sodium silicate as an alkali-activating solution. They also reported higher dissolution of silica and alumina by sodium hydroxide solution in comparison to potassium hydroxide solution as an alkali-activation solution.

1.2.3 Curing Parameters for Geopolymers

For enhancing the polymerization reactions, high temperature is generally required which influences the properties of geopolymers significantly. There are various factors that influence the effective curing of the specimens such as curing temperature, curing period and delay time. Curing temperature refers to the temperature that is sustained inside the oven for the particular time period and curing duration refers to the time period for which the specimens are kept at a particular temperature; whereas, delay time refers to the time period between the casting and the moment they are kept inside the oven for curing. Chindaprasirt et al. (2011) investigated the effects of fly ash fineness and curing variables such as delay time, curing temperature and its duration on strength properties of geopolymer mortars. It was concluded that for the specimens with coarse fly ash, the delay time of 3 hours yielded maximum compressive strength whereas, for the specimens with medium fly ash, maximum results were observed with a delay time of 2 hours. On the other hand, the delay time of 1 hour produced the fine fly ash based geopolymer mortars with maximum compressive strength. Curing temperature was applied in the range of 30-90°C and curing duration in the range of 24-72 hours. Compressive strength was observed to increase with the increase in curing temperature up to 75°C and beyond that it decreased. Similarly, compressive strength increased with the increase in curing duration, however, the difference between the 48 hours and 72 hours curing was not significant, therefore, for economic considerations, 48 hours curing period was reported to be optimum. The overall study reported the maximum compressive strength results with heat curing at 75°C for 48 hours with delay time of 2 hours for medium fly ash. Similar effect of curing variables was also reported in other studies (Hardjito et al., 2008; Skavara et al., 2005; Winnefeld et al., 2010) as well. Van Jaarsveld et al. (2002) also reported the formation of cracks and other negative effects of curing at too high temperature. They concluded that physical properties can be influenced by the curing temperature significantly and it should be applied in the mild range. Palomo et al. (1999) also

reported the influence of curing temperature and its duration on mechanical properties of geopolymer mortars. High temperature curing with longer duration yielded better strength properties but upto a certain limit and beyond that it decreased.

1.3 ADVANTAGES OF GEOPOLYMERS

Geopolymers consume lesser energy and release much lower carbon dioxide than the conventional Portland cement concrete (Gartner, 2004). It has the potential of having an environmentally friendly binder with lowest greenhouse intensity in the production of cementitious materials (Spannagle, 2002). Some commercial geopolymer concrete based products with superior properties are also available. These can be used in various applications such as grouts, fiber reinforced sheets, massive concrete panels, bricks, ceramic tiles, floor surfaces, storage areas, runways, etc (Davidovits, 1994). Davidovits (1991) categorized the list of applications which depends on the chemical structure of geopolymers in terms of silica to alumina ratio, as shown in Table 1.9.

Table 1.9 Applications of geopolymers based on Si/Al ratio (Davidovits, 1991)

<i>Si/Al Ratio</i>	<i>Applications</i>
1	Bricks Ceramics Fire protection
2	Low CO ₂ cements and concretes Radioactive and toxic waste encapsulation
3	Fire protection fiberglass composite Foundry equipment Heat resistant composites, 200-1000 °C Tooling for aeronautics (titanium process)
4-19	Sealants for industries, 200-600 °C Tooling for aeronautics (SPF aluminum)
20-45	Fire resistant and heat resistant fiber composites

As a construction material, geopolymer concrete can provide a lot of benefits (Bakharev, 2005; Kong et al., 2007; Olivia, 2011) such as:

- In terms of contribution in reducing carbon emissions, geopolymer concrete emits only 78 kg/m³ of carbon dioxide in comparison to 248 kg/m³ from conventional cement based concrete construction.
- The source materials used for geopolymers are mainly of geological origins such as kaolin, clay or industrial by-products such as fly ash, bottom ash, rice husk ash, etc.

With the use of these waste products in producing the alternative binders to OPC, they alleviate the disposal problems as well.

- With the subsection of high-temperature curing, geopolymer concrete provides very high strength in relatively quick time in comparison to conventional concrete.
- Geopolymer is also found to exhibit excellent durability characteristics with low shrinkage and high fire resistance.

1.4 GEOPOLYMERS IN CONSTRUCTION APPLICATIONS

Depending on the chemical structure of geopolymers, they possess a wide range of applications in various industries like automobile, aerospace, foundries, metallurgies, plastic, and civil engineering industries. Due to their similar behavior to those of zeolites, they have a big potential to absorb toxic wastes (Comrie et al., 1988). GEOPOLYMITE 50, a product of Cordi-Geopolymere SA, produced by mixing aluminosilicates with alkali solutions, has been extensively used for waste containment. Geopolymer technology is advancing in various field applications especially in Australia and Europe. In Australia, this technology has been used for the production of railway sleepers, fire, and chemical resistant wall panels, protective coatings, repair materials, sewer pipelines as well as masonry units (Gourley and Johnson, 2005). Balaguru et al. (1999) reported the use of geopolymers as a coating on the pavement applications as well as to strengthen the conventional concrete structures. They concluded the high performance of geopolymer composites in terms of more resistance to fire, toxic chemicals and under ultra violet lights in comparison to organic polymers. The engineers from AECOM, Australia (Aldred and Day, (2012)) have reported the utilization of geopolymers in actual field applications as shown below in this section.

- **Pavements**

Two different geopolymer concrete grades of M25 and M40 were cast to develop 900×5.5 meters pavement, as shown in Fig.1.9. The major difference observed in the application of geopolymer concrete to that of conventional concrete was the absence of free available surface water even for the operations like screeding and trowelling. Therefore, to protect the surface against drying, the aliphatic based spray was used for the surface coating. Also, at the Port of Brisbane, geopolymer concrete bridge pavement slab of the M32 grade was cast in November 2010. This technology has also been used by local councils for the production of footpaths as well.



Fig.1.9: Placing of pavement using geopolymer concrete (Aldred and Day, 2012)

- **Retaining Wall**

A retaining wall of M40 geopolymer concrete was constructed at a private residence in Toowoomba to retain the earth of 3 meters, as shown in Fig.1.10. It contained 50 pre-cast geopolymer concrete panels of size 6×2.4 meters. They were cured in the ambient curing conditions at the casting yard before they were placed at the site.



Fig.1.10: Pre-cast geopolymer retaining wall for private residence (Aldred and Day, 2012)

- **Water Tanks**

Ahn and Kishi (2010) reported the autogenously healing behavior of geomaterials due to gel swelling mechanism. Based on these results, in March 2011, two water tanks were cast with M32 grade, one with blended cement of 80% OPC and 20% fly ash and the other purely with geopolymer concrete, as shown in Fig.1.11.



Fig.1.11: Water tanks cast with blended concrete (left) and geopolymer concrete (right) (Aldred and Day, 2012)

The maximum size of aggregates used was 10 mm. Self-healing behavior was shown by OPC based concrete due to calcium hydroxide deposition, whereas in comparison, geopolymer concrete tank exhibited relatively rapid healing of cracks.

- **Boat Ramps**

The boat ramp at Bundaberg was replaced by M40 grade precast geopolymer concrete reinforced with Glass Fiber Reinforced Polymer (GFRP), as shown in Fig.1.12. The project was awarded to Wagners Company by the Department of Maritime Safety. The pre-cast ramps were cast in Toowoomba while the approach slab was cast-in-situ for which batching was done with a transit time of 6.5 hours. To maintain the workability during casting, chemical activators were used.



Fig.1.12: Boat ramp constructed with geopolymer concrete (Aldred and Day, 2012)

- **Precast Bridge Decks**

The bridge at Murrarie pre-fabricated by Wagners Company, Toowoomba in 2009, was one of the earliest field applications of geopolymer concrete. The bridge structure was a precast composite structure made by fiberglass girders stitched by bridge deck of M40 grade geopolymer concrete, as shown in Fig.1.13.



Fig.1.13: Installation of pre-fabricated geopolymer concrete bridge at Murrarie (Aldred and Day, 2012)

Since then the bridge is sustaining its service life with the loading of continual agitator trucks and has been observed with no signs of distress as such. Another bridge was constructed with this technology as The Bundaleer Road Bridge, West Moggill, Brisbane in May 2012. This was also a precast composite structure of girders with M40 grade geopolymer concrete based deck, as shown in Fig.1.14. The project pertained to the Council of Brisbane city and I-cubed Pvt Ltd. The geopolymer concrete deck acted as the compression flange to the bridge in addition to a serviceable wearing deck.



Fig.1.14: Composite girder and geopolymer concrete Deck Bridge in Brisbane (Aldred and Day, 2012)

- **Precast Beams**

The geopolymer concrete was first ever applied to a multi-storeyed building where floor beams were precast and suspended to three floors. The client was the University of QLD and the Architect was Hassell group. Apart from the structural benefits, geopolymer concrete also had an aesthetical feature with an arch curved soffit. Thirty-three (in number) precast floor beams-slab elements were cast of two different sizes, 10.8×2.4 meters and 9.6×2.4 meters, from M40 grade geopolymer concrete and were placed with the help of cranes at the site. The precast panels and the rendered view of the proposed building are shown in Fig.1.15.



Fig.1.15: Geopolymer concrete floor beam (left) and rendered view of proposed building (right) (Aldred and Day, 2012)

1.5 LIMITATIONS AND CHALLENGES FOR FIELD APPLICATIONS

With the need of sustainable development across the globe, OPC concrete is being criticized due to its high energy intensive characteristics which have opened the gates for new promising technologies such as geopolymers. This technology has the potential not only to replace OPC in various applications but also solves the disposal problem of various industrial wastes as well. However, there are few constraints that did not allow geopolymers to have full faith in replacing OPC. It has been observed from various studies that for geopolymer concrete to achieve better or comparable properties to that of high strength conventional concrete, high-temperature curing is required which is not feasible especially for cast-in-situ applications (Ahmari et al., 2012). Another major limitation which is resisting its use in is the absence of any standard parameters for its mixture design. The design mixture of geopolymer concrete depends on the properties of its constituents such as source materials, alkali-activators, and aggregates, however, the source materials obtained from different sources does not possess similar properties. For example, the chemical constituents of fly ash obtained from one source do not comply with the chemical constituents of fly ash obtained from another source. Therefore, it requires a different dosage of alkali-activators and different curing variables each time for every source material. A proper criterion for the mixture

design to obtain a specific concrete grade is yet to be established. Olivia and Nikraz (2011) also reported some limitations of geopolymers such as:

- High-temperature curing is required to obtain high compressive strength which is not feasible in various field applications.
- To provide adequate workability, the use of admixtures becomes mandatory which can create the economic concern.
- Due to high alkalis in the geopolymer system, immense care is required to deal with the problems like alkali-silica reaction, efflorescence, etc which can hamper the aesthetic appearance of the structure.
- Due to the absence of any reference handbooks or standard code provisions related to the application of geopolymer concrete, proper workmanship is required with the sound knowledge of technical know-how of this technology.

Duxson et al. (2007) also reported the problem of impurity elements such as carbon, magnesium, iron, etc present in the source materials which may cause extra pathways during polymerization and alters the properties of geopolymers during its synthesis as well as in final properties. Van Jaarsveld et al. (2003) also reported the problem of variation in properties of source materials obtained from different sources that result in significant variation in strength properties.

1.6 SIGNIFICANCE OF RESEARCH

With ever increasing infrastructure development, the world is bound to use high energy-intensive Portland cement whose production accounts for about 7% of the total carbon dioxide emissions. Also, a lot of problems have been encountered in the recent years for the disposal of various industrial wastes and by-products. These wastes are generated from a wide spectrum of industries and their management poses many challenges to the industry. Geopolymer technology is enticing the researchers all across the globe as recent studies have shown their potential to be used as an alternative to the conventional OPC based concrete. Geopolymer concrete has shown to possess high strength characteristics, high resistance to external attack and low permeability. It utilizes the industrial by-products such as fly ash, bottom ash, rice husk ash, metakaolin, etc that are rich in silica and alumina and low-cost alkali solutions such as sodium silicate, sodium hydroxide, etc to undergo polymerization reactions. In this study, fly ash is used as source material and the mixture of sodium hydroxide and sodium silicate are used as alkali-activating solutions.

The novelty of this research is to report the results of fresh, strength and durability properties of low-calcium fly ash based geopolymer concrete incorporating additional calcium source (in the form of OPC). Also using Taguchi method of analysis, the optimum values of various parameters considered for the development of geopolymer concrete such as ratio of alkali solution to fly ash, ratio of sodium silicate to sodium hydroxide, molarity of sodium hydroxide, etc. would be reported based on maximum compressive strength.

1.7 GAPS IN RESEARCH AREA

Till date, the major thrust of investigations on geopolymer concrete has been confined to the comparison of its mechanical properties with the conventional concrete. They are found to possess better strength as well as durability properties. However, the limitation that is not instilling the confidence of engineers and architects is the requirement of high-temperature curing. Various precast applications of geopolymer concrete have been reported but no major work has been reported on cast-in-situ construction applications. The need of the time is to develop some mechanism that can eliminate the requirement of additional temperature curing. This can be done by including some additives with the source materials that may increase the effective temperature within the geopolymer system and provide the activation for the polymerization reaction. The inclusion of additional calcium in the geopolymer system might serve the purpose but before pointing directly to the self-cured characteristics, its effect on essential properties such as workability, strength and durability properties are monitored. Few studies have reported the positive effects of adding OPC on strength properties of geopolymers but with no significant implications. Also, very little investigation has been carried out so far on durability aspects of OPC blended geopolymers. Therefore, this research is proposed to study the effect of including additional calcium source (in the form of OPC) on workability, strength and durability properties of low-calcium fly ash based geopolymer concrete.

1.8 OBJECTIVES AND SCOPE OF RESEARCH WORK

The objectives of the proposed study are as under:-

1. Development of geopolymer concrete containing Ordinary Portland Cement as partial replacement of fly ash.
2. To study the workability and strength properties of geopolymer concrete containing OPC as partial replacement of fly ash.

3. To study the durability properties of geopolymer concrete containing OPC as partial replacement of fly ash.

1.9 METHODOLOGY

The research was conducted to study the influence of additional calcium content (in the form of OPC) in a low-calcium fly ash based geopolymer concrete. Different phases of research are shown in Fig.1.16. Physical and chemical properties of fly ash and ordinary Portland cement (OPC) were determined followed by physical tests on aggregates. Mixture design for geopolymer concrete as well as for conventional cement concrete was established by performing various trial mixtures. The specimens for different mixtures were cast and tested for various properties such as workability, strength and durability properties.

1.10 OVERVIEW OF THESIS

The proposed work is divided into the following five chapters:

- Chapter-1** Describes the background of this research related to the environmental problems associated with conventional concrete and the need for its alternatives, introduction to geopolymers, their advantages, limitations, applications, and also the objectives and scope of the present research work.
- Chapter-2** Summarizes the existing literature on source materials used for the synthesis of geopolymers, different curing methods, fresh, strength, and durability properties of geopolymers, microstructures of geopolymers, phase developments in geopolymers, fire resistance of geopolymers and their recent developments.
- Chapter-3** Describes the experimental program carried out to develop the mixture proportions, the mixing process, and the curing regime of geopolymer concrete. It also includes the procedure of test methods applied in this research work for characterization of materials and laboratory tests performed to evaluate the properties of geopolymer concrete mixtures.
- Chapter-4** Describes, in detail, the test results of workability, strength and durability properties of low-calcium fly ash based geopolymers incorporated by additional calcium source (in the form of OPC) as fly ash replacement. The microstructure analysis results in terms of Scanning Electron Micrograph (SEM), Energy Dispersive X-ray Spectroscopy (EDS) and X-Ray Diffraction

(XRD) are also presented. In addition, the relationship of compressive strength with split tensile strength, water absorption and total charge passed in Rapid chloride permeability test is also presented in this chapter.

Chapter-5 Covers the important conclusions drawn from the present study and also offers suggestions and recommendations for future research in the light of the findings of the present study.

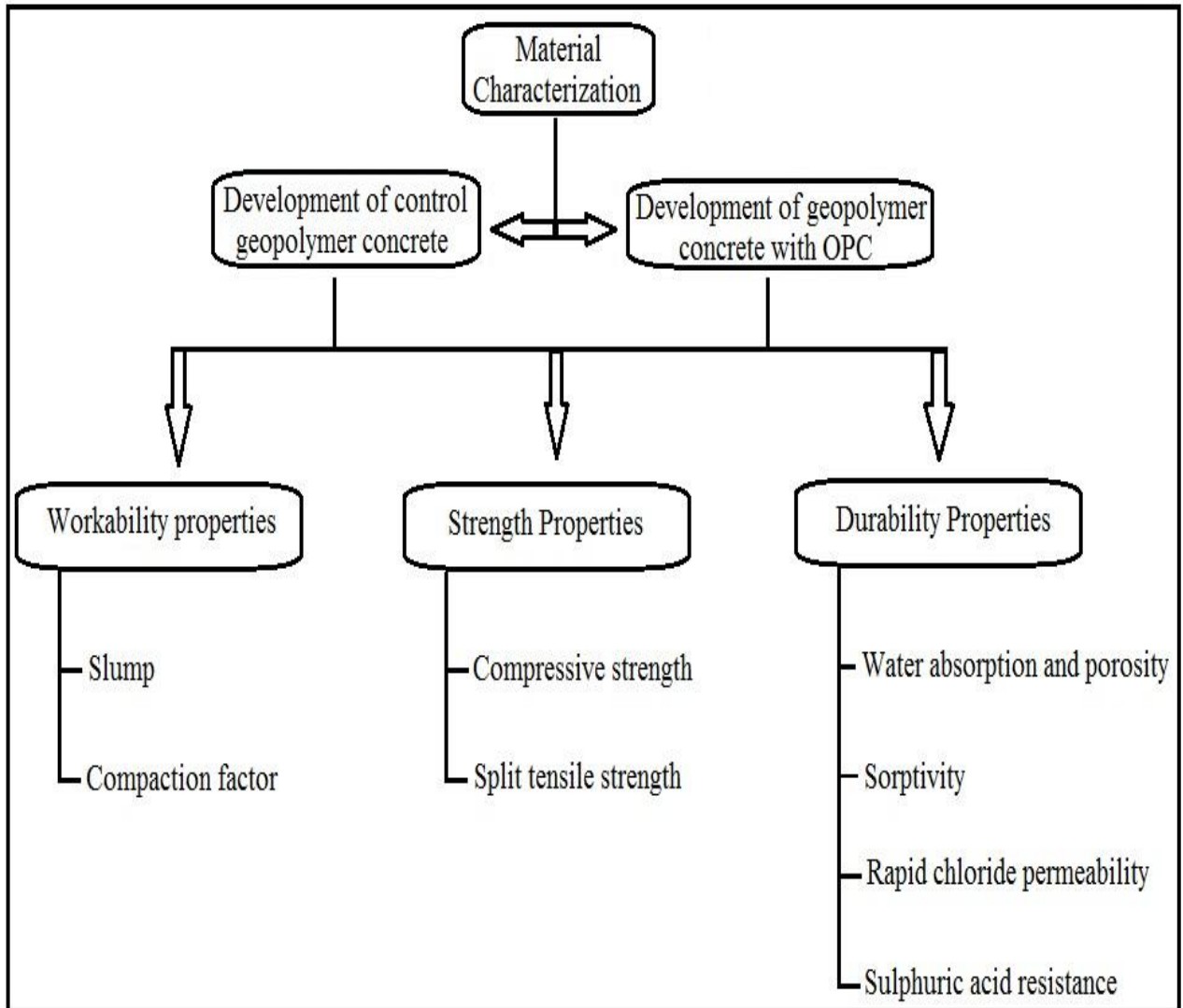


Fig.1.16: Phases of research

CHAPTER-2

REVIEW OF LITERATURE

This chapter presents the review of literature on the utilization of industrial by-products (IBP) such as fly ash, bottom ash, etc as source materials for the synthesis of geopolymer pastes, mortars and concrete. Also, the review of fresh, strength and durability properties of geopolymer pastes, mortars and concretes, and their behavior at elevated temperatures have also been presented.

2.1 USE OF INDUSTRIAL BY-PRODUCTS (IBP) IN GEOPOLYMERS

2.1.1 General

The mechanism of geopolymers includes three steps starting from the dissolution of silica and alumina from the source materials followed by coagulation and gelation of the dissolved materials which then further polymerizes to form 3-D networks of silica aluminates structures (Silva et al., 2007). The silica and alumina in the geopolymer system are supplied by the source materials; therefore, the potential of industrial by-products to be utilized as source material in geopolymers depends on its chemical composition. Various studies have synthesized the geopolymer pastes, mortars and concrete using industrial by-products (IBP) such as fly ash, blast furnace slag, volcanic ash, metakaolin, granulated blast furnace slag, granulated corex slag, etc. They have been used as alone or as a mixture of two or more by-products which can be termed as blended geopolymers. It has been observed from the previous studies that the properties of geopolymers synthesized by different IBP depend on various factors such as physical and chemical properties of the source material, curing regime, sodium hydroxide concentration, the ratio of sodium silicate to sodium hydroxide, etc. Maximum studies have used fly ash as source material due to its pozzolanic behavior and easy availability. The brief review of utilization of IBP in the synthesis of geopolymers is presented here.

2.1.2 Synthesis of Geopolymers using Industrial By-Products (IBP)

Chindaprasirt et al. (2007) used high-calcium fly ash as source material to investigate the properties of geopolymer mortars with different sodium hydroxide (NaOH) concentration.

Sodium hydroxide (NaOH) of three concentrations 10M, 15M and 20M, and sodium silicate with 15.32% Na₂O, 32.87% SiO₂ and 51.81% water, were used. Also, to control the workability Type F melamine formaldehyde superplasticizer (SP) with a minimum base water content of 5% by mass of the geopolymer paste was used. The mixing procedure started with the mixing of NaOH solution, base water and fly ash for 5 min in a pan mixer followed by addition of sand and further mixed for 5 min. This was followed by the addition of sodium silicate solution and extra water or SP (where adequate workability was not obtained) followed by the final mixing of another 5 min.

Kong et al. (2007) studied the effect of elevated temperatures on geopolymer mortars synthesized by metakaolin and fly ash at different proportions. Metakaolin used was a product of kaolin (china) clay calcined at 750°C with an average particle size of 38 µm and the fly ash was of Class F low-calcium. The fineness of the kaolin and fly ash was 100 and 89%, respectively passing through a 45 µm sieve. Alkaline activators consisted of Grade D sodium silicate solution (Na₂SiO₃) with specific gravity of 1.53 and modulus ratio (Ms) equal to 2 (where $M_s = \text{SiO}_2 / \text{Na}_2\text{O}$, Na₂O=14.7% and SiO₂=29.4%) and the hydroxide solution which was prepared to a concentration of 7M using potassium hydroxide (KOH) flakes of 90% purity and distilled water, were used. The alkali precursor (either metakaolin or fly ash) and alkali-activating solution were hand mixed for 10 min and a further 5 min in a mixer. The specimens were cast and sealed with a film to prevent moisture loss. The curing was done inside a laboratory oven for 24 h at 80°C.

Temuujin et al. (2010) studied the effect of varying levels of sand aggregates (10 to 50%) on various properties of geopolymer mortars. The fly ash and fine aggregates were collected from the local source available. The activating solution was prepared by mixing sodium silicate D-51 with a chemical composition of 14.7% Na₂O, 29.4% SiO₂ and 55.9% water by weight, and 14 M sodium hydroxide solution prepared from analytical grade sodium hydroxide pellets. The weighed components for the paste were mixed in a centrifuge mixer for 5 min followed by defoaming for 30 seconds. Extra water was added to the mixture for the aggregate content of 40 and 50% due to inadequate workability. The paste was then placed in cylindrical plastic molds which were cured at 70°C for 24 h. After curing, the moulds were removed from the oven and kept at ambient temperature for 3 days followed by de-moulding.

Kong and Sanjayan (2010) studied the effect of elevated temperature on geopolymer mortars synthesized by using Class F fly ash as a precursor. Alkaline activators consisted of sodium

silicate solution (Na_2SiO_3), with specific gravity of 1.53 and modulus ratio (M_s) equal to 2 (where $M_s = \text{SiO}_2/\text{Na}_2\text{O}$, $\text{Na}_2\text{O} = 14.7\%$ and $\text{SiO}_2 = 29.4\%$), and hydroxide solutions prepared by mixing 7M potassium hydroxide (KOH) flakes of 90% purity with distilled water. Two commercially available superplasticizers, Glenium 27, a carboxylic ether polymer with long lateral chains and the other, Rheobuild 1000, a sulfonated polymer-based superplasticizer, were used as an additive to some of the concretes to provide adequate workability. For making the paste, fly ash and alkali-activating solution were hand mixed for 10 min and further 5 min in a mixer. The mixture was then cast into molds and sealed with a cling film to avoid moisture loss. All specimens were cured undisturbed for 24h at room temperature before being subjected to high temperature curing at 80°C for 24h in a laboratory grade oven.

Chindaprasirt et al. (2011) synthesized the geopolymer mortars by using three types of fly ashes with different fineness i.e. coarse fly ash, medium fly ash and fine fly ash. A sodium silicate solution with a composition of 15.32% Na_2O , 32.87% SiO_2 and 51.81% water, and 10M sodium hydroxide solution (NaOH) were used as an alkali-activating solution. The mixture consisted of fly ash, sand, NaOH solution, sodium silicate solution and base water. The NaOH solution, fly ash and water were mixed for 5 min in a pan mixer and the sand was then added to the mixture with the sand to fly ash ratio of 2.75, followed by further mixing for another 5 min. The alkali-activating solution was then added with a final mixing of 5 min followed by the casting of specimens.

Joseph and Mathew (2012) utilized low-calcium Class F fly ash as source material, with 90% passing through the $45\mu\text{m}$ sieve for the synthesis of geopolymer concrete. The alkali solution was prepared by mixing 10M sodium hydroxide (NaOH) and sodium silicate (Na_2SiO_3) solution with 34.64% SiO_2 , 16.27% Na_2O and 49.09% water. The alkali solution was first prepared 24 h prior to its use to bring down its temperature to the ambient temperature and dry mixture was prepared with coarse and fine aggregates in saturated surface dry condition well mixed with fly ash in a pan mixture. To improve the workability, naphthalene based water reducing admixture with a dosage of 2% by weight of fly ash was used which was mixed separately with the alkali liquid and then added to the dry mixture mixed together for 5 min. Specimens were prepared and kept at room temperature for 60 min with further subjected to temperature curing in an electric oven with curing temperatures ranging from $60\text{-}120^\circ\text{C}$ and curing period of 6-72 h to calculate the optimum curing regime.

Kusbiantoro et al. (2012) investigated the properties of geopolymer concrete with Class F fly ash and microwave incinerated rice husk ash (MIRHA) blend as the source material. MIRHA was obtained from the incineration process of rice husk at 800°C incineration temperature grounded in a ball mill to increase its fineness. Alkali activators used were 8 M NaOH and Na₂SiO₃ with modular ratio Ms=2.0 (Na₂O: 14.73%, SiO₂: 29.75% and H₂O: 55.52%). Three different curing regimes were made, one as ambient temperature with the maximum temperature of 35±1 °C, second as external exposure with maximum temperature of 55±1 °C and third as oven curing with delay time of 1 hour and cure at temperature of 65 °C for 24 hours.

Ariffin et al. (2013) prepared geopolymer concrete specimens by using blended ash of pulverized fuel ash (PFA) and palm oil fuel ash (POFA) with the mean particle size of 45 µm. The commercial grade sodium hydroxide (NaOH) and sodium silicate (Na₂SiO₃) solutions were mixed as an alkali-activating solution. Local crushed granite sand as fine aggregates with a specific gravity of 2.62 and coarse aggregates with a specific gravity of 2.68 was used. In order to enhance the workability superplasticizer was added to the mixture and specimens were prepared with an alkaline solution to blended ash ratio of 0.4 and ratio of sodium silicate (Na₂SiO₃) to sodium hydroxide (NaOH) as 2.5. The blended ash and the aggregates were first to dry mixed in pan mixer for 5 min followed by the addition of alkali-activating solution which was further mixed for another 5 min. The superplasticizer was used to achieve the workability in between the slump range of 80-100mm. The casting was done and the specimens were covered using vacuum bagging film and subjected to room temperature (28 °C) for 28 days.

Chotetanorm et al. (2013) used different finenesses of bottom ash (BA) to synthesize geopolymer mortars and to study various properties. Three finenesses of BA were used: fine BA, medium BA and coarse BA (C), with corresponding median particle sizes of 16, 25 and 32 µm respectively. The alkaline activators used were sodium silicate solution (NS) with 13.8% Na₂O, 32.2% SiO₂ and 54.0% H₂O and 10M NaOH solution (NH). The mixing of BA and NH was done for 5 min followed by the addition of sand and NS with extra water (if required) with a final mixing of 5 min. The mortar mixtures were then cast into molds which were wrapped with the cling film to avoid moisture loss. They were left in the laboratory at 25 °C as delay time for one hour and then cured at 75 °C for 48 h.

Demie et al. (2013) used low-calcium fly ash as source material to synthesize self-compacting geopolymer concrete (SCGC). A combination of sodium silicate (Na_2SiO_3) with the composition of 55.52% water, 29.75% SiO_2 and 14.73% Na_2O , and 12 M sodium hydroxide (NaOH) were used as alkali solution which was prepared one hour prior to its use. The solids components of SCGC, i.e. the fly ash, fine and coarse aggregates, were dry mixed in the pan mixer for about 2.5 min followed by mixing the liquid part of the mixture separately, i.e. the sodium silicate solution, the sodium hydroxide solution, extra water and the SP which were premixed thoroughly before being added to the dry mixture.

Reddy et al. (2013) investigated the durability properties of geopolymer concrete synthesized by low-calcium fly ash. Combinations of sodium hydroxide (NaOH) and sodium silicate (Na_2SiO_3) were used as alkali activators which were prepared 24 h prior to use. Two different concentrations of sodium hydroxide, 8M and 14M were used, and polycarboxylate based Type F high-range water reducing superplasticizer in liquid form was used as an admixture. The casting was done and the specimens were heat-cured in an oven at 60 °C for 24h.

Pangdaeng et al. (2014) used high-calcium fly ash to synthesize geopolymer mortars and studied the effect of adding ordinary Portland cement (OPC) at different curing conditions. The Blaine finenesses of FA and OPC were 2460 and 3600 cm^2/g , respectively. The alkaline solutions were prepared by mixing 10M sodium hydroxide (NaOH) and sodium silicate (Na_2SiO_3) (15.32% Na_2O , 32.87% SiO_2 , and 51.81% H_2O). A dry mixture consisting of FA, OPC and sand were mixed followed by addition of alkali solution and further mixed for another 5 min inside the pan mixture. The fresh geopolymer mortars specimens were prepared and placed in 23 °C controlled room for a period of 24 h. They were then demoulded and put into different curing conditions; vapour-proof membrane curing (where samples were kept in a control room temperature of 23 °C), temperature curing (where samples were wrapped with a plastic membrane to prevent moisture loss), oven curing (where samples were cured at 40 °C for 24 h) and wet curing (where the samples were immersed in water in a 23 °C until their testing age).

2.2 FRESH PROPERTIES OF GEOPOLYMERS CONTAINING IBP

The presence of different IBP such as silica fume, fly ash, metakaolin, bottom ash, GGBS etc as source material in geopolymers due to their different physical, chemical and mineralogical composition exhibited different effects on fresh properties. Most of the studies have used fly

ash as the main source material and also blended with other waste materials as well. A few studies have also utilized other waste materials such as metakaolin, rice husk ash, etc as main source material.

Fresh properties determine the ease with which the concrete can be easily mixed, placed, and transported. The effect of adding various IBP on the fresh properties of geopolymer pastes, mortars and concrete are shown here in this section. This section has been categorized into fly ash based geopolymers, where the main source material is fly ash and the other as blended geopolymers where geopolymers are developed by utilizing industrial by-products other than fly ash.

2.2.1 Fly Ash based Geopolymers

Chindaprasirt et al. (2007) investigated various properties of geopolymer mortars developed from coarse lignite high-calcium fly ash. Flow tests were conducted with varying ratios of sodium silicate to sodium hydroxide (NaOH) and different concentrations of NaOH. For the specimens with inadequate workability, superplasticizer (SP) was added. For 10M NaOH specimens, the flow of geopolymer mortar decreased with an increase in the ratio of sodium silicate to NaOH, whereas for 15M NaOH specimens, the mixture was relatively thicker and slightly more water (3.4% by weight of fly ash) was added to produce mortar with similar flow pattern. For 20M NaOH specimens, the mixture was even thicker and to obtain similar flow, the extra water (6.8% by weight of fly ash) was added. It was concluded that the increase in the concentration of NaOH and the amount of sodium silicate solution increased the viscosity and decreased the workability of the solution. Therefore, to obtain the mixes with the suitable flow, extra water or SP was required.

Chindaprasirt et al. (2011) studied the effect of fly ash fineness on the workability of geopolymer mortars developed from classified high-calcium fly ash. The results showed that the flow of geopolymer mortars increased with an increase in fly ash fineness with the flow values being 125, 150 and 175% for specimens with coarse fly ash (CFA), medium fly ash (MFA) and fine fly ash (FFA) respectively. The increased flow was due to the particle shape and smooth surface of fine fly ash that had a dominant influence on the workability of geopolymer mortars which acted as ball bearings. It was concluded that fine fly ash increases the workability of fresh mortar or reduces the water requirement of mortar for the same flow.

Joseph and Mathew (2012) investigated the workability of fly ash based geopolymer concrete. The very high viscosity of geopolymer concrete was observed and no appreciable slump value was obtained even with the use of admixture. Compaction factor test was performed and it was observed that the compacting factor was higher for a higher ratio of alkali to fly ash.

Demie et al. (2013) studied the influence of different Superplasticizer (SP) dosage on the workability of fly ash based self-compacting geopolymer concrete (SCGC). For all mixtures, the ratio of sodium silicate to sodium hydroxide solution was kept as 2.5 and the ratio of fine aggregate to fly ash was kept as 2.125. A total of five mixtures; S1, S2, S3, S4 and S5 (with SP dosages 3, 4, 5, 6 and 7%) was prepared for the investigation. Different workability tests such as slump flow test, J-ring test, L-box test and V-funnel test were performed to evaluate the workability. The test results of the quantitative analysis and visual observations showed that mix samples S1, S2 and S3 with 3, 4 and 5% respectively failed to exhibit the required workability as per EFNARC limits of SCC, due to an insufficient amount of SP which made the mixes less workable. However, mix samples S4 and S5 with 6 and 7% SP attained the required values. The mixes with 6 and 7% SP improved the workability to the extent required for SCC by coating themselves with the binder particles and transferred them a highly negative charge so that they repel each other which in turn resulted in de-flocculation and dispersion of binder particle.

Nath and Sarker (2014) studied the effect of adding ground granulated blast furnace slag (GGBFS) as replacement of fly ash, on the workability of fly ash based geopolymers. Different blended geopolymer mixtures were prepared, S00 as control specimen with 100% fly ash, S10, S20 and S30 as fly ash replacement with 10, 20 and 30% respectively by GGBFS. The geopolymer specimens (concrete and mortar) were prepared and stored at a controlled temperature of 20-23°C leaving the top surface open and left in air until the testing age at 20-23°C. The workability of fresh geopolymer concrete specimens was tested by slump test and the flow was measured by flow table immediately after mixing. It was observed that both the slump as well as flow was influenced by the replacement of fly ash with GGBFS. Highest slump and flow values were achieved for the specimens with 0% GGBS which indicated the decrease in slump and flow values with the increase in fly ash replacement by GGBS.

Pangdaeng et al. (2014) investigated the workability of high-calcium fly ash geopolymer mortars. Fly ash (FA) was replaced with ordinary Portland cement (OPC) at 0, 5, 10 and 15% by weight of binders. The alkali-activating solution was prepared by mixing sodium hydroxide (NaOH) (10M) and sodium silicate (Na_2SiO_3) (15.32% Na_2O , 32.87% SiO_2 , and 51.81% water). Setting time of geopolymer pastes and flow tests on mortars was conducted and the results showed a reduction in their values with the addition of OPC resulted. This was attributed to the fact that the OPC contained a reasonably high calcium oxide (CaO) content which accelerated the setting and hardening of pastes (Chindaprasirt et al., 2012) due to extra nucleation sites for precipitation of dissolved species which increased its solidification rate and caused rapid hardening.

2.2.2 IBP (other than fly ash) based Geopolymers

Pacheco-Torgal et al. (2011) investigated the effect of various parameters such as sodium hydroxide concentration, superplasticizer content and metakaolin replacement by calcium hydroxide on the workability of alkali-activated metakaolin based geopolymer mortars. The results showed an increase in flow with the increase in superplasticizer content, higher metakaolin replacement and at lower sodium hydroxide concentration. Similar results were also obtained by Sathonsaowaphak et al. (2009). The highest flow was obtained at 10M sodium hydroxide concentration with 10% calcium hydroxide substitution and 3% superplasticizer dosage.

Nazari and Sanjayan (2015) used aluminum slag and gray cast iron slag as alumino-silicate source in the synthesis of geopolymers and determined the workability properties. In total four mixtures of slags were used as aluminum slag to gray cast iron slag in ratio 20:80, 30:70, 60:40 and 50:50. The mixtures were dry mixed for about 1 min in order to attain maximum possible homogeneity and cured at room temperature till the testing age. Workability of the freshly prepared geopolymer paste, as well as concrete specimens, was studied at different concentrations of sodium hydroxide (NaOH). It was observed that for both paste and concrete specimens, the slump was in the suitable range for various applications like roller compacted concrete or interlocking paving block productions.

2.3 STRENGTH PROPERTIES OF GEOPOLYMERS CONTAINING IBP

Strength properties determine the quality of concrete in terms of its load carrying capacity for which it is designed throughout its intended life. The properties of geopolymer pastes,

mortars and concrete synthesized from various IBP have been shown in this section. It has been observed that the majority of the reported literature have synthesized the geopolymers with fly ash as source material and very few studies have incorporated by-products other than fly ash. Therefore, this section is further sub-divided into two sections; first, the properties of geopolymers with fly ash as source material, and the second as properties of geopolymers synthesized by IBP other than fly ash.

2.3.1 Fly Ash based Geopolymers

Joseph and Mathew (2012) investigated the influence of various parameters such as aggregate content, the ratio of sodium silicate to sodium hydroxide, the ratio of alkali to fly ash and molarity of sodium hydroxide on compressive strength of fly ash based geopolymer concrete. The result showed 92.8 and 96.4% of the 28day strength on 3 and 7days whereas the ordinary concrete had a strength of 77.5 and 87.9% which clearly showed the high early age strength development of geopolymer concrete. It was also observed that the compressive strength of geopolymer concrete; increased with increase in total aggregate content up to a value of 70% and then it decreased, increased with increase in the ratio of fine aggregate to total aggregate for a value up to 0.35 and then it decreased, increased with the ratio of sodium silicate to sodium hydroxide up to a value of 2.5 and then it decreased and increased with the increase in alkali to fly ash ratio up to 0.55 and beyond that it decreased. The increase in compressive strength for all parameters was due to the change in microstructure and the decrease beyond the certain value was due to incompleteness of dissolution during the formation of geopolymer. The influence of molarity of NaOH on compressive strength of geopolymer concrete was also studied and it was observed that the compressive strength increased with the increase in molarity of NaOH up to value of 10 and beyond that the compressive strength decreased. This was attributed to the fact that although the concentration of NaOH solution used for synthesis had a positive influence on dissolution, hydrolysis and condensation reactions but excess alkali concentration hinders the condensation of the silicate species.

Kusbiantoro et al. (2012) investigated the effect of different curing regimes on compressive strength of geopolymer concrete with fly ash and rice husk ash (RHA) as blended source materials. Three curing regimes were considered; ambient temperature curing, external exposure curing and oven curing. Best test results were reported for the specimens cured in an oven due to the high dissolution of silica and alumina from the fly ash caused by polarization of hydroxide ions and the increase in pH of the solution which created, even

more dissolution of aluminosilicate. Also, RHA was included in the mixture as fly ash replacement (3 and 7%) and the specimens were subjected to oven curing. EDS analysis was performed on the specimens as well. It was observed that for 0% RHA, there was a decrease in Si/Al ratio from 3 to 28 days, whereas for specimens having RHA, increase in Si/Al ratio was observed from 3 to 28 days. The decrease in the ratio of 0% RHA specimens was due to a higher rate of dissolution of alumina than silica from the fly ash at early ages of polymerization (Pietersen et al., 1989). On the other hand for 7% RHA specimens, there was a contribution from RHA also for dissolution of silica accumulating the increase in Si/Al ratio. This increase in ratio further forms the Si-O networks during polymerization which resulted in a denser matrix with better bonding.

Demie et al. (2013) studied the influence of different Superplasticizer (SP) dosage on strength properties of fly ash based self-compacting geopolymer concrete (SCGC). The details of mixture proportioning and synthesis are already discussed in the previous section. The compressive strength results showed the highest compressive strength of 53.80 MPa for the specimen with 7% SP. Although the difference in 28 days compressive strength values for the specimens with 6% (51.52 MPa) and 7% (53.80 MPa) was not significant, therefore 6% SP dosage was suggested to be the optimum content due to economic considerations. It was concluded that SP was required in geopolymer concrete to improve not only workability but also to enhance the hardened compressive strength of SCGC. The Field Emission Scanning Electron Microscope (FESEM) analysis was also carried out to identify the inner microstructure of SCGC samples. It was observed that the polymerization reaction of 6% SP specimen was significantly enhanced with a big difference in interfacial transition zone (ITZ) width between the specimens with 3 and 6%. Also, the porosity of the ITZ and its width considerably decreased as compared to specimens with 3, 4 and 5% SP. Therefore the utilization 6% SP was found to be a more efficient way of densifying (refining) the ITZ, because it avoided many of the pores, disconnect the micro crack path and making its structure more homogenous in composition.

Patil and Allouche (2013) investigated the compressive strength of geopolymer concrete specimens synthesized by two types of Class F and Class C fly ash, obtained from different sources. It was concluded that high strength geopolymer concrete can be easily synthesized using Class C or Class F fly ash as compared to that of normal OPC concrete specimens with the maximum compressive strength of 103MPa.

Reddy et al. (2013) investigated the effect of different concentrations of sodium hydroxide on strength properties of low-calcium fly ash based geopolymer concrete in the marine environment. The results showed the increase in compressive strength with the increase in molarity of sodium hydroxide (NaOH), for example, the compressive strength of specimens with 8M and 14M NaOH was 29.7 and 56.2 MPa respectively. Also, with the development in age, the compressive strength at 28 days was increased to 39.9 and 60.2 MPa respectively. For comparison, compressive strength test for conventional OPC based concrete was also performed with 7 and 28 days strength values reported as 22 and 33 MPa respectively. It was also reported that around 93% of 28-day strength was obtained at 7 days for the specimens with 14M NaOH concentration. In addition, tensile strength tests were also performed and it was observed to be higher than conventional OPC concrete specimens. Most of the cylindrical specimens of geopolymer concrete did not exhibit complete destruction after failure, which also proved the toughness of the geopolymer matrix.

Adak et al. (2014) investigated the effect of adding nano silica on strength properties such as the compressive and flexural strength of fly ash based geopolymer mortars. Four different mixtures with different nano silica dosages (4, 6, 8 and 10%) were developed along with control mortar specimens of 100% fly ash geopolymer and normal OPC mortars. The specimens with 100% fly ash were cured at 60°C for 48 hours whereas specimens with nano silica were cured at room temperature only. The strength test showed best results of specimens with 6% nano silica in comparison to control as well as other mixtures. The microscopic analysis also confirmed the results as specimen with 6% nano silica found to have more transformation of amorphous compound to the crystalline compound making its microstructure even denser than other mixtures with less number of un-reacted particles.

Haq et al. (2014) compared the polymerization reaction of geopolymer concrete synthesized by using fly ash and bottom ash. Fourier Transformation Infrared Spectroscopy (FTIR) studies showed the proper bonding of geopolymers obtained by both ashes. It was indicated by the high level of vibrations for geopolymer concrete specimens in comparison to very small bands of around 1040-1080 cm^{-1} due to a small level of Si-O-Si vibrations. The extent of polymerization was also predicted from the height ratios and area ratios of the peaks of Si-O-Si vibrations. It was concluded from the results that the extent and degree of polymerization were higher in the case of fly ash as compared to bottom ash.

Nath and Sarker (2014) investigated the strength properties of fly ash based geopolymers by adding ground granulated blast furnace slag (GGBFS) as fly ash replacement. The mixture details were explained in the previous section where S00 was denoted as control specimen with 100% fly ash, S10, S20 and S30 as fly ash replacement with 10, 20 and 30% GGBFS respectively. It was observed from the compressive strength results that S00 specimen with no replacement reacted slowly but when GGBS was added in the mixture, there was a significant increase in the strength at 3 days as well as at 28 days. The mixtures with 10, 20 and 30% replacement by GGBS was observed to have 33, 74 and 110% higher strength respectively when compared to normal control geopolymer mixture with no replacement. In other words, it was concluded that for every 10% increment in fly ash replacement level with GGBS, there was an increase in 28 days strength of round 10 MPa.

Pangdaeng et al. (2014) carried out an experimental investigation to study the compressive strength of high-calcium fly ash based geopolymer mortars. Fly ash (FA) was replaced with ordinary Portland cement (OPC) at 0, 5, 10 and 15% by weight of binders. The compressive strength results showed an increase in value with the increase in OPC replacement level. This was attributed to the fact that the calcium elements reacted and formed additional C-S-H and C-A-S-H which coexisted with geopolymer products (Kroehong et al., 2011) and contributed to the strength development. The effect of curing parameters was also investigated as the specimens were exposed to three different curing regimes i.e. ambient curing (MC), water curing (WC) and temperature curing (TC), and their micrographs were observed by scanning electron microscopic (SEM) analysis. The noticeable difference was observed between the differently cured samples, for example FA-MC paste showed a large amount of non-reacted fly ash particles in the matrix which indicate the relatively low stage of polymerization. On the other hand, FA-TC and FA-WC paste matrices appeared denser than the FA-MC paste, whereas 10PC-TC and 10PC-WC pastes also appeared denser than the 10PC-MC paste. This confirmed that the high calcium fly ash polymerization was slow at room temperature and needed temperature curing to accelerate the strength development (Wongpa et al., 2010). The increases in the OPC content increased the calcium in the system and its reaction produced extra hydration products and liberated heat which also promoted the polymerization.

Torres-Carrasco and Puertas (2015) studied the influence of waste glass on the properties of fly ash based geopolymers. For this three alkaline activators were used i.e. 8M NaOH, 10M NaOH + 15% water glass and 10M NaOH solution. The dry mixture was prepared and mixed

with NaOH solution by the magnetic stirrer at 80 °C for 6h and further filtered . The paste samples were prepared and temperature cured at 85 °C for 20h. For the oven cured specimens, the compressive strength test was carried out at 1, 2, 7 and 28 days. The effect of high concentration of NaOH was denoted by the increase in compressive strength value for 10M NaOH in comparison to 8M NaOH. Also with the inclusion of water glass i.e. increase of SiO₂ content in the medium, the increase in strength values were observed at all ages. Further when waste glass was included in the medium at different dosages of 10, 15 and 25%, even higher compressive strength values were observed. The best results were obtained at 15%, whereas the reduction in strength beyond 15% was due to further increase in Si content which lowered the pH of solution. Also when 15% waste glass was used, the dissolved silica was essentially monomeric (Puertas and Torres-Carrasco, 2014), whereas when the content increased, the solution becomes saturated which hindered the full utilization of glass and thus hindered the higher degree of polymerization. Si MAS Nuclear Magnetic Resonance (NMR) analysis was also carried out on the virgin fly ash sample and was observed that Si atoms were very unevenly distributed. The geopolymer specimens were also tested and it was observed that various signals indicating Al₄, SiAl₃, Si₂Al₂, Si₃Al₁, Si₄ were detected and all being chabazite-Na-like structure. Also, when external silica source i.e. waste glass in this study was added, similar but more clearly defined signals were detected. It can also be clearly observed from this study that fly ash can be used effectively as source material for geopolymers.

2.3.2 IBP (other than fly ash) based Geopolymers

Aguilar et al. (2010) investigated the properties of light weight metakaolin-fly ash based geopolymer concrete. Three densities of geopolymer concrete; 1200, 900 and 600 kg/m³ were obtained by aeration of blast furnace slag lightweight aggregates in the ratio of binder : aggregate as 1:1 with the curing at 75 °C. The mechanical properties like compressive strength and flexural strength were observed. The results for concrete of density 1200 kg/m³ were found to be satisfactory with lower price and less environmental impact. Also as the curing temperature rises incrementally, the compressive and flexural strength were found to be developed at early ages. The Scanning Electron Microscopic (SEM) images of the geopolymer light weight concrete with blast furnace slag sand grains showed good bonding and dense microstructures of geopolymer pastes with a strong interfacial zone.

Rattanak et al. (2010) examined the effects of adding $\text{Al}(\text{OH})_3$ on the properties of rice husk ash (RHA) based geopolymers. FTIR analysis was carried out and Si-O bond was observed for the virgin RHA, whereas for the geopolymer samples, signals confirming to Si-Al-O bonds were observed which indicated that RHA can be used effectively for the development of geopolymers. Also with the addition of $\text{Al}(\text{OH})_3$ in the mixture, the intensity of peak depicting Si-Al-O bond increased considerably.

He et al. (2012) compared the compressive strength of two types of geopolymers; first by using metakaolin, and the other by a mixture of two wastes, fly ash and red mud, mixed in equal quantities. It was observed from the stress-strain curves that metakaolin based geopolymer (MK-GP) had higher compressive strength as well as higher stiffness than red mud and fly ash based geopolymer (RM-GP) at the low duration of curing. But with an increase in curing duration, the difference in stiffness of the two geopolymers was found to be smaller. In other words for RM-GP, with an increase in curing duration, the failure pattern found to be shifted from ductile to brittle, whereas for MK-GP, failure pattern was found to be brittle for all curing ages. Also, the strength values for MK-GP were stabilized at the age of 9 days which suggested its complete curing cycle of 9 days, whereas for RM-GP the complete curing was achieved in 21 days. Such behavior was also confirmed by XRD analysis of the samples which showed amorphous characteristics as indicated by broad hump for both samples (Li and Liu, 2007; Guo et al., 2010). These humps were more pronounced for MK-GP samples than RM-GP, which suggested a higher degree of polymerization for metakaolin-based geopolymers.

Kouamo et al. (2012) compared the strength properties of geopolymers synthesized by source materials; metakaolin and volcanic ash. The effect of adding alumina oxide (Al_2O_3) as replacement of source materials (0, 10, 20, 30 and 50%) was also investigated simultaneously. The mixtures were labeled as M0 to M4 for metakaolin and Z0 to Z4 for volcanic ash. For M0 and Z0 specimens the compressive strength results showed higher strength values for metakaolin because of more amorphous phase characteristics (as shown by XRD analysis) and finer average particle size for metakaolin. This was attributed to the fact that during polymerization the amorphous phases had higher dissolution characteristics and also the finer particles with more specific surface area reacted faster (Van Jaarsveld et al., 2003). For metakaolin-based geopolymers, the compressive strength was found to increase with an increase in alumina oxide content up to 20%, and beyond that it decreased which was also confirmed by the previous findings (Fletcher et al., 2005; Silva et al., 2007). On the other

hand for volcanic ash, with the increase in replacement levels up to 50%, the strength was found to be increased. This was attributed to the fact that in the case of volcanic ash based geopolymer the alumina oxide having smaller particle size becomes more reactive than volcanic ash and with an increase in its content the polymerization increased. Also, to check the bond characteristics, FTIR studies were performed on the virgin metakaolin as well as volcanic ash and also on the resultant geopolymer concrete formed by using these source materials. When the results of source materials were compared to those of their resulting geopolymers, the intensity of the bands ranged between 3225 to 3384 cm^{-1} , and 1392 to 1645 cm^{-1} , which represented higher stretching (-OH) and bending (H-O-H) for geopolymer concrete specimens. Also, the bands indicating Si-O-Si and Al-O-Si represented the higher degree of polymerization in all specimens of metakaolin-based geopolymers as compared to volcanic ash based geopolymers. This was due to the fact that in the case of volcanic ash based geopolymers, bands indicating O-C-O bonds were observed that confirmed the presence of sodium bicarbonate which further disrupts the polymerization process. It was concluded on basis of FTIR results that metakaolin-based geopolymers had better bond characteristics than volcanic ash based geopolymers.

Kusbiantoro et al. (2012) investigated the properties of geopolymer concrete with Class F fly ash and microwave incinerated rice husk ash (MIRHA) blended as the source materials. Three different curing regimes were studied; one as ambient temperature with the maximum temperature of 35+1°C, second as external exposure with a maximum temperature of 55+1°C, and third as oven curing with a delay time of 1 hour and curing at a temperature of 65°C for 24 hours. The specimens were subjected to compressive strength tests after 3, 7 and 28 curing days. It was observed that the increment of temperature from ambient and external exposure curing showed a trend of consistent strength development. The improvement in the compressive strength of MIRHA based geopolymer concrete was up to 22.34% higher than non-MIRHA based specimen in ambient curing whereas the inclusion of MIRHA in the external exposure curing regime had an adverse effect on strength of fly ash based geopolymer concrete. Also, increasing the curing temperature to 65°C improved the MIRHA based geopolymer concrete compressive strength. With 3% inclusion of MIRHA in fly ash based geopolymer system, 14.17% improvement in strength than non-MIRHA based specimen was observed, whereas 7% inclusion incremented the strength up to 19.41%.

The densification of geopolymer gel appears to be affected by several factors, such as the reactivity of source material, access to the elevating temperature, and alkali activation system used. Field emission scanning electron microscopy (FESEM) tests were also performed for microscopic analysis. Micrographs were studied for all the curing regimes which showed porous geopolymer matrix structure for ambient curing due to insufficient growth of geopolymer gel. This resulted in low capability to transfer external load within geopolymer concrete system and hence created a low strength geopolymer concrete specimen. For external curing regime, aluminosilicate gels produced from the reaction were dispersed and occupied the existing pre-water-filled voids but due to different dissolution rate between blended and unblended source material, different geopolymer matrix density was formed resulted in higher porosity which reduced the capability of geopolymer concrete system to sustain and distribute the external load properly. On the other hand, FESEM of oven cured specimen provided a clear vision on the appearance of geopolymer gel from gelation process and provided a suitable condition to accelerate the polymeric reaction.

Sata et al. (2012) investigated the compressive strength of lignite bottom ash based geopolymer mortars. The materials used for the study were Portland cement (OPC), fly ash (FA) and lignite bottom ash (BA) with three finenesses i.e. fine BA (FBA), medium BA (MBA) and coarse BA (CBA) with corresponding Blaine finenesses of 5300, 3400 and 2100 cm^2/g , respectively. The PC mortar consisted of only OPC as cementitious material whereas PFA40 and PFBA40 mixes consist of Portland cement with OPC replaced by FA and FBA at the dosage of 40% by weight. GFBA, GMBA, and GCBA were geopolymer mortars made from FBA, MBA and CBA, respectively. The specimens were cast and temperature cured at 75 °C for 48 h. The results showed that the compressive strength of cement mortars (PC, PFA40 and PFBA40) increased with the curing age in accordance with the strength development of Portland cement, however the strength development of geopolymer mortars (GFBA, GMBA and GCBA) increased at a lower rate. The development of compressive strength was also affected by the BA fineness as the use of FBA in geopolymer mortar yielded higher compressive strengths than the coarser ones. This was attributed to the fact that BA with high finenesses and high surface areas dissolved more silica and alumina (Sathonsaowaphak et al., 2009) and thus resulted in the increase in higher polymerization and compressive strength.

Ahmari and Zhang (2013) investigated the properties of geopolymer pastes synthesized by adding cement kiln dust (CKD) in mine tailings (MT) as source materials. The specimens

were temperature cured for 7 days at 90°C and kept at room temperature for 6 hours before testing. Two different concentrations of NaOH were used, 10 and 15M. The results showed that for both concentrations of NaOH, the unconfined compressive strength (UCS) increases with increase in CKD content. The results were also affected by the concentration of NaOH as addition of 10% CKD resulted in 200 and 90% strength increase for 10M and 15M, respectively. The improvement in UCS by the addition of CKD was attributed due to the increase in alkalinity of the system by additional calcium content of CKD which helped in more dissolution of Si and Al in larger amount, secondly additional source of alumina-silicates by addition of CKD, which contributed higher geopolymerization, and thirdly due to dense micro structure and finer particles of CKD that filled the small pores making a relatively denser microstructure. From the XRD patterns, it was observed that calcium oxide (CaO) and calcium hydroxide (Ca(OH)₂), which were present in CKD powder originally, completely disappeared after the geopolymerization. Further the high peaks indicates higher calcium carbonate (CaCO₃) content which indicated that part of Ca reacted with air and yielded CaCO₃ and due to its low solubility in alkaline solutions, it helped in enhancement of durability as Ca(OH)₂ does not exist in the system.

Chotetanorm et al. (2013) studied the effects of bottom ash (BA) fineness with three types of fineness i.e. fine BA (F), medium BA (M) and coarse BA (C), on strength properties of geopolymer mortars. The mortar specimens were cast and cured at 75°C for 48 hours. It was observed that strength of geopolymer mortars was significantly affected by the fineness of BA. The 28-day strength was found to be highest for the fine BA in comparison to medium and coarse BA with the values 54.5, 48 and 40 MPa respectively.

He et al. (2013) studied the mechanical properties of geopolymer composites by incorporating industrial wastes such as red mud (RM) and rice husk ash (RHA). Various parameters such as curing duration, the ratio of RHA/RM, particle sizes and alkalinity were studied to investigate polymerization. It was observed that the time required for the complete curing for RM and RHA based geopolymers was found to be 35 days which was very high in comparison to other raw materials like fly ash, metakaolin, slag, etc. For metakaolin-based geopolymers, the curing time was reported to be 14 days (He et al., 2011) whereas for fly ash based geopolymers the curing time was reported as 28 days (Zhang et al., 2010). Also, the particle size of RHA is larger than other materials that cause a negative influence on the polymerization reaction (Ryu et al., 2013). Based on other test analysis also the authors concluded that it was very difficult to have a practical implementation of this kind of

geopolymer because of long curing duration, uncertainty in the extent of polymerization and variability in the composition of RHA and RM.

Nath and Kumar (2013) compared two types of iron making slags; granulated corex slag (GCS) and granulated blast furnace slag (GBFS), as fly ash replacement (10 to 50%) for the development of geopolymers. The strength tests were conducted and found to be better for GCS based geopolymer. The strength was found to increase with the increase in slag content for both cases due to the enhancement of C-S-H gel (Buchwald et al., 2007; Puertas and Fernandez-Jimenez, 2003). The results were also analyzed by FTIR, XRD and SEM analysis. From FTIR study it was observed that peak intensity was more for GCS based geopolymers due to more glassy and heterogeneous characteristics (Rees et al., 2007). The XRD pattern also showed better results for GCS based geopolymers where crystalline phases were seen to be transformed into other phases during polymerization. From the microstructure analysis, fully reacted dense matrix and presence of C-S-H, as well as A-S-H gel for GCS based geopolymers, was observed.

Nazari and Sanjayan (2015) studied the strength properties of geopolymers obtained by using aluminum slag and gray cast iron slag as aluminosilicate source. Four mixtures of slags were formed as aluminum slag to gray cast iron slag in ratio 20:80, 30:70, 60:40 and 50:50. The compressive strength of blended geopolymer specimens was also determined at different curing ages and the maximum value was observed at aSiO₂/Al₂O₃ ratio of 3. The increase in strength was also observed with the increase in NaOH concentration at all ages which was due to the easier dissolution of aluminum and silicon ions and resulted in more polymeric resultants. The results were also verified by the SEM analysis and it was observed that for specimens with 16M NaOH, slightly denser microstructure was obtained which resulted in slightly higher compressive strength values. Other studies have reported even higher strength values such as Collins and Sanjayan (1999) obtained values of 60 MPa with the use of alkali-activated slag while Wang et al. (2014) obtained strength of 80 MPa, which are way above the requirement of strength for concrete for residential purposes of 31 MPa as per ACI 318 and ACI 322.

2.4 DURABILITY PROPERTIES OF GEOPOLYMERS CONTAINING IBP

For assessing the serviceability of concrete structures, durability properties are of major concern. The properties such as permeability, sorptivity, resistance against acids, sulphates, etc can easily provide the information regarding the microstructure of concrete. The

durability properties of geopolymer pastes, mortars and concrete by using various IBP as source materials have been shown here in this section. Further, as fly ash has been used in the majority of the reported literature, therefore this section is further sub-divided into the durability properties of geopolymers when fly ash has been used as source material and the other where IBP other than fly ash have been used for the synthesis.

2.4.1 Fly Ash based Geopolymers

Chindaprasirt et al. (2011) studied the effect of fly ash fineness on shrinkage characteristics of geopolymer mortars developed from classified high-calcium fly ash. The drying shrinkage tests were performed on the specimens made with 1 h of delay time and 48 h of curing at 75 °C. The coarse fly ash (CFA), medium fly ash (MFA) and fine fly ash (FFA) geopolymer mortars showed a shrinkage strain of 25, 21 and 20×10^{-6} mm/mm after 1 day, and 60, 49 and 44×10^{-6} mm/mm after 7 days, respectively. However, after 14 days, expansion rather than shrinkage of the geopolymer mortars was observed. After 91 days, the expansions of the CFA, MFA and FFA mortars were 61, 29 and 1×10^{-6} mm/mm, respectively. The results suggested that the high-calcium fly ash based geopolymer mortars showed excellent volume stability with very little shrinkage, particularly when fine fly ash was used. The dimensional changes of fly ash based geopolymers were insignificant when compared to normal Portland cement or fly ash mortars.

Ahmari et al. (2012) studied the properties of fly ash based geopolymer bricks made by incorporating copper mine tailings as fly ash replacement. It was observed that for almost all types of applications, geopolymer bricks had adequate strength, abrasion resistance and water absorption as per ASTM requirements. However, conditions such as water content, sodium hydroxide (NaOH) content, curing temperature, etc should be properly selected as also mentioned in other studies (Zhang et al., 2011).

Adak et al. (2014) investigated the effect of adding nano silica on durability properties such as water absorption and chloride permeability of fly ash based geopolymer mortars. Four different mixtures with different nano silica dosages (4, 6, 8 and 10%) were developed along with control mortar specimens of 100% fly ash geopolymer and normal OPC mortars. The results showed that specimens with 6% nano silica have better durability properties than other specimens as less amount of charge was passed indicating less value of diffusion coefficient due to the presence of more crystalline compounds. Similar results were also obtained for

water absorption where specimen with 6% nano silica showed lesser water absorption making its pore structure more optimum (Khater et al., 2012).

Pangdaeng et al. (2014) studied porosity and water absorption properties of high-calcium fly ash geopolymer mortars. Ordinary Portland cement (OPC) was added as fly ash replacement at 0, 5, 10 and 15% by weight of binders. The results of porosities and water absorptions of mortars showed the decrease in values with the increase in OPC as fly ash replacement. This was due to the fact that the addition of OPC increased the hydration and the amount of C-S-H and C-A-S-H, which filled the pores and reduced porosity as well as water absorption and hence improved the density of the matrix.

2.4.2 IBP (other than fly ash) based Geopolymers

Ariffin et al. (2013) investigated the resistance of bottom ash based geopolymer (BAG) concrete against sulphuric acid. The specimens, after casting were exposed to 2% sulphuric acid immersion with pH of 1 up to 18 months. To study the effect, mass change and compressive strength at different ages were observed. After 18 months exposure, the results showed that mass loss for BAG was just 8% in comparison to the control OPC specimen with around 20% mass loss. The compressive strength results showed 35% strength loss whereas OPC specimen showed around 68% strength loss. The results hence showed around 50% more resistance to the sulphuric acid of bottom ash based geopolymers in comparison to normal OPC concrete. The exposed geopolymer specimens were also subjected to FTIR analysis and major bands were determined at 3465, 1645, 1425 and 1040 cm^{-1} . The band at 1040 cm^{-1} indicated the presence of N-A-S-H gel, derived from the solid precursor (Lee and Van Deventer, 2007; Shi et al., 2007). In general, in the case of material used as fly ash or slag, band identified the range of 950 and 1100 cm^{-1} can be categorized as C-A-S-H for slags and N-A-S-H for fly ash indicating highly siliceous gels.

Chotetanorm et al. (2013) investigated porosity and sulphate resistance of geopolymer mortars synthesized by using three type of bottom ash (BA) of different finenesses such as fine BA (F), medium BA (M) and coarse BA (C). For porosity, the intruded volume and pore size distribution tests were conducted by using Mercury Intrusion Porosity (MIP). The results showed that volume intrusion (VI) was dependent on the fineness of BA. For fine BA, the increase in VI was lower than medium and coarse BA which showed an increase in large pores with the increase in BA median particle size. The improvement in porosity was attributed to the fact that with the high specific surface area, there would be the easy

dissolution of silica, alumina and calcium which results in higher polymerization (Sathonsaowaphak et al., 2009) with fewer pores. To observe the sulphate resistance, mortar bars specimens were immersed in 10% sodium sulphate solution and tested for expansion and weight change until 360 days. The expansion and weight change were also found to be dependent on BA fineness and showed better results as the fineness increases. The expansion and weight gain through the XRD study were found to be related to the formation of ettringite and gypsum.

2.5 GEOPOLYMERS AT ELEVATED TEMPERATURES

Geopolymers have shown high resistance to deteriorations at elevated temperatures. Various studies have been carried out to observe their behavior at high temperatures. Some of them are listed here in this section.

Dombrowski et al. (2006) investigated the influence of adding calcium content on thermal properties of fly ash based geopolymers. Calcium hydroxide was included in the geopolymer system as fly ash replacement. It was observed that when fly ash was replaced by 8% calcium hydroxide, the thermal properties showed significant improvement at room temperature as well as at elevated temperatures. This was attributed to the increase in reaction hydrated products due to additional calcium in the geopolymer system which increased the density of the matrix and improved the strength.

Kong et al. (2007) compared the geopolymer paste specimens exposed to elevated temperatures synthesized by two source materials; fly ash and metakaolin. The specimens were prepared and subjected to an elevated temperature of 800 °C. It was observed that metakaolin based geopolymer paste exhibited surface micro-cracks of around 0.1-0.2 mm whereas no cracks were observed on the surface of fly ash based geopolymer pastes. In terms of compressive strength, its value decreased slightly after the temperature exposure for metakaolin based whereas the value increased for fly ash based geopolymer pastes. Thermo gravimetric analysis (TGA) was also carried out on the exposed specimens and it was observed that due to dehydration of chemically bounded water at high temperature, some modifications occurred in the chemical microstructure. Also, the moisture within the binders evaporates which caused surface cracking and internal damage in the microstructure.

Kong and Sanjayan (2008) investigated the effect of elevated temperatures on the behavior of fly ash based geopolymer pastes and concrete. The alkalisolution was prepared by mixing

sodium silicate and potassium hydroxide. The specimens were prepared and subjected to elevated temperatures of 800 °C. Various parameters were considered and it was observed that the most significant factor which affected the fire resistance was the ratio of fly ash to alkali. For temperature exposed geopolymer paste specimens, the compressive strength was found to increase, whereas it decreased in case of geopolymer concrete specimens. The decremented strength values were attributed to different values of thermal expansion of paste and aggregate that caused cracks and initiated deterioration.

Pan et al. (2009) investigated the change in the compressive strength of geopolymer mortar exposed to elevated temperature. Two types of fly ashes were used for the synthesis and specimens were prepared with the compressive strength ranging from 5-60 MPa. It was reported that the loss or gain in compressive strength of geopolymers depends on the strength of specimens before the exposure, for example, when specimens were exposed to 800 °C, loss in strength was observed for the specimens with original compressive strength greater than 16 MPa, whereas gain in strength was observed for the specimens with initial compressive strength less than 16 MPa. The strength gain was attributed to the cindering of the unreacted particles in the microstructure which undergo further polymerization, whereas stress loss was because the paste and aggregates were not thermally compatible. It was concluded that after the exposure to elevated temperature increase in ductility was exhibited for the specimens with lower initial strength, whereas low ductility was exhibited by the specimens with higher initial strength.

Kong and Sanjayan (2010) investigated the effect of various parameters such as size and type of aggregates, specimens size and super plasticizer addition on the fire resistance of fly ash based geopolymer paste, mortar and concrete. The size of specimens and aggregates were found to be almost significant factor which influences the geopolymer properties exposed to elevated temperature. With the addition of superplasticizer, a decrease in strength was observed which was dependent on the type and content of superplasticizers. The strength degradation was reported to be 26 and 41.5% for the geopolymer paste and concrete specimens exposed to an elevated temperature of 800 °C. The results for mortar specimens could not be observed.

Pan and Sanjayan (2010) evaluated the stress-strain behavior of fly ash based geopolymer pastes subjected to elevated temperatures from 23-680 °C. Sodium hydroxide and sodium silicate was used as alkali-activators. The increase in compressive strength was observed with

slight reduction in specimen size for the elevated temperature between 200-290 °C. On the contrary, strength values increased as well as specimens were expanded when elevated temperature range between 380-520 °C.

CHAPTER-3

EXPERIMENTAL PROGRAM

This chapter describes the details of an experimental investigation carried out in this research work for the characterization of materials, development of fly ash based geopolymer concrete with partial inclusion of OPC, and the tests methods adopted to evaluate the fresh, strength, durability and microstructure properties geopolymer concrete.

3.1 INTRODUCTION

An experimental investigation has been carried out to evaluate the effect of adding OPC on properties of fly ash based geopolymer concrete. It includes material characterization and development of geopolymer concrete by performing trial mixtures using Taguchi method. It also includes the details of tests procedure adopted to evaluate the workability, strength and durability properties of geopolymer concrete (GPC) as well as conventional cement concrete (CCC). The schematic diagram of experimental program is illustrated in Fig.3.1.

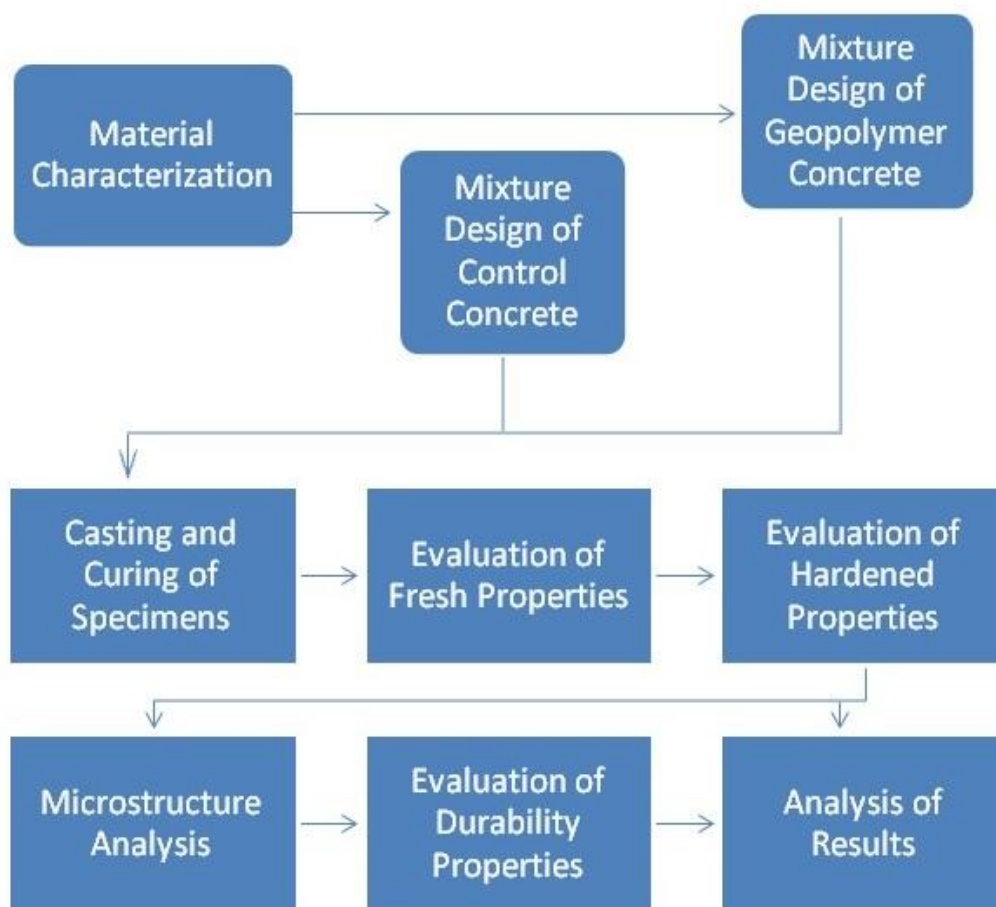


Fig.3.1: Schematic diagram of experimental program

3.2 MATERIAL CHARACTERIZATION

The materials used in this study were tested for their physical and chemical properties. The procedures followed to evaluate these properties have been listed here in this section.

3.2.1 Fly Ash

Fly ash used in this study was obtained from Rajiv Gandhi Thermal Power Plant, Hissar. The particles passing through 45 μ m sieve were used and were found to be greyish white in colour. Specific gravity was determined in accordance with BIS: 4031 (Part11)-1988. The weight of empty pycnometer, pycnometer with fly ash, pycnometer with dry fly ash and water, pycnometer with water was recorded, and specific gravity was calculated to be 2.31 (Mehta and Siddique, 2017). To observe the microstructure, scanning electron microscopy (SEM), energy dispersive X-ray spectroscopy (EDS) and X-ray diffraction (XRD) analysis were carried out as shown in Fig.3.2 and 3.3. The detailed procedures for conducting these microstructure tests have been explained later in the section 3.5.4. It was observed that most of the fly ash particles were spherical in shape. From EDS analysis, the calcium oxide content was found to be less than 5%, and the total oxides content of silica, alumina and iron was calculated to be greater than 70%, therefore in accordance with ASTM standards, fly ash used in this study was termed as low-calcium Class F fly ash. The chemical composition was also obtained by performing X-ray fluorescence (XRF) analysis, as shown in Table 3.1 and found to be in accordance with BIS: 3812-1981. The phases obtained in XRD study were identified through Xpert High Score Plus and Match software. Quartz and mullite were found to be the major phases present in fly ash particles.

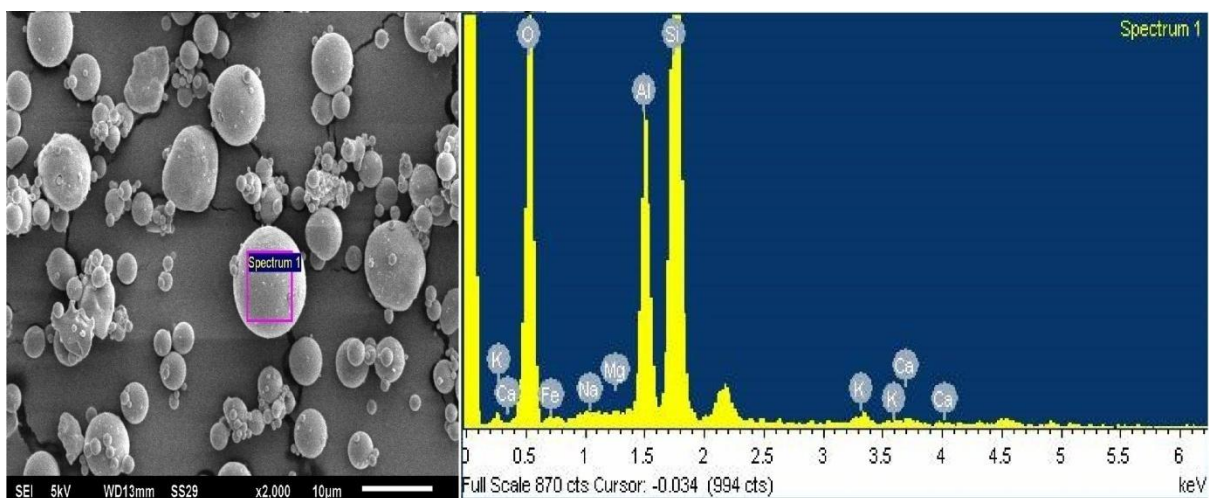


Fig.3.2: SEM/EDS analysis of fly ash particles (present study)

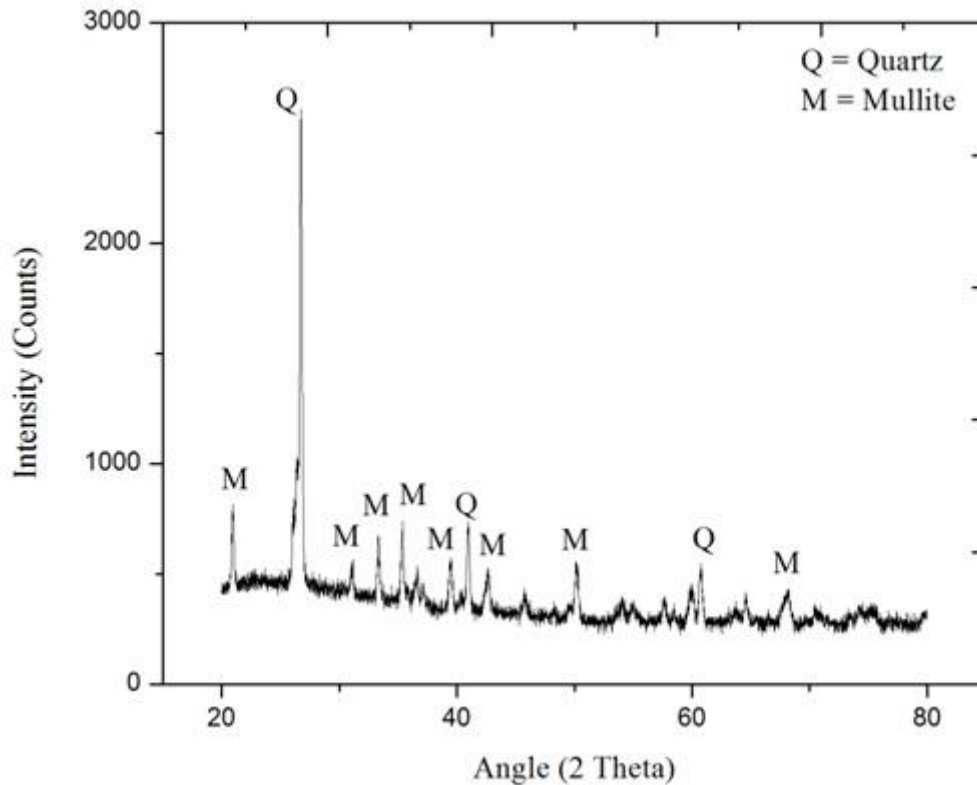


Fig.3.3: XRD analysis of fly ash particles (present study)

Table 3.1: Chemical composition of fly ash particles (present study)

<i>Chemical constituents in oxides form</i>	<i>Values obtained by XRF analysis (%)</i>
Silica Oxide (SiO ₂)	53.59
Aluminium oxide (Al ₂ O ₃)	28.46
Iron oxide (Fe ₂ O ₃)	8.71
Calcium oxide (CaO)	4.23
Sodium oxide (Na ₂ O)	0.58
Magnesium oxide (MgO)	1.84
Potassium oxide (K ₂ O)	1.63
Sulphur trioxide (SO ₃)	0.96

3.2.2 Ordinary Portland Cement (OPC)

Ordinary Portland cement (OPC) of 43 grade was used as an additional source of calcium in the low-calcium fly ash based GPC. Due to the presence of various standard parameters and code provisions that govern its physical and chemical properties, and also due to its easy availability, OPC was preferred over other materials as additional calcium sources. For reference, CCC mixture was also prepared by using the same source of OPC. The physical properties such as consistency, setting times and compressive strength of OPC particles were determined in accordance with BIS: 4031-1988.

3.2.2.1 Consistency

The standard consistency of cement was determined by using Vicat's apparatus and can be defined as the consistency which allows the Vicat's plunger to penetrate into the Vicat's mould up to 5 to 7 mm from the bottom, as explained in BIS: 4031 (Part 4)-1988. The procedure consisted of the formation of paste from 500 g of cement and assumed percentage value of consistency of water. The paste was prepared, filled and leveled in the Vicat's mould up to the top level. The prepared mould was placed below the Vicat's plunger arrangement which was lowered to touch the top surface followed by releasing and sinking into the mould immediately. The sinking value of plunger was measured from the marked perforations and various trial mixtures with different assumed consistencies were performed till the standard consistency was achieved.

3.2.2.2 Setting Times

The initial and final setting times of OPC were determined by using Vicat's apparatus as per BIS: 4031 (Part 5)-1988. After determining the standard consistency of OPC, the paste was prepared by using water content as 85% of the standard consistency value. The paste was prepared and filled in the Vicat's mould which was kept below the Vicat's needle arrangement after proper leveling. Initial setting time can be defined as the time period elapsed between the moments when water was added to OPC till the needle failed to pierce the above-mentioned value. The needle was allowed first to just touch the top surface and then to penetrate under the action of its own weight. This procedure was repeated till the needle failed to penetrate at 5 ± 0.5 mm from the bottom. For evaluating the final setting time, Vicat's needle was replaced by Vicat's annular arrangement. The basic concept of final setting time was related to the setting of cement which was indicated by the failure of an external object to mark any impression. The Vicat's annular arrangement was allowed to touch the surface of the paste again and again till the moment when it got failed to make any impression on the paste. The time elapsed between this moment and the moment when water was first added to the OPC was calculated as final setting time. At this moment it can be believed that OPC is finally set.

3.2.2.3 Compressive Strength

For evaluating the compressive strength, mortar cubes of size 70×70×70 mm were cast and tested as per BIS: 4031 (Part 6)-1988. OPC was mixed with sand in the ratio 1:3. To prepare

the mortar, 200 g of OPC was mixed with 600 g of sand followed by addition of water as $(P/4+3)$ percent of the total mass of OPC and sand, where, P denotes the standard consistency of water. The cubes were filled and compacted on the vibration machine for two minutes. After 24 hours, the mortar specimens were de-moulded and kept inside the water bath for curing at $27 \pm 1^\circ\text{C}$ till the testing age. The specimens were tested in the compression testing machine where load was applied gradually without any jerk. The strength was evaluated at 3, 7 and 28 days of curing.

The results obtained for the physical tests on OPC particles are shown in Table 3.2. It was observed that the values obtained for all the tests were within the specified limits as mentioned in BIS: 8112-1989. To observe the microstructure properties, SEM, EDS, and XRD analysis were carried out with the results as shown in Figs.3.4 and 3.5.

Table 3.2: Physical properties of OPC (present study)

<i>Physical property</i>	<i>Test value</i>	<i>Standard values (BIS: 8112-1989)</i>
Consistency (%)	32	-
Initial setting time (minutes)	89	>30
Final setting time (minutes)	373	<600
Fineness (m^2/kg)	307	>225
Compressive strength (3 days)	28.7	>23
Compressive strength (7 days)	37.9	>33
Compressive strength (28 days)	48.5	>43

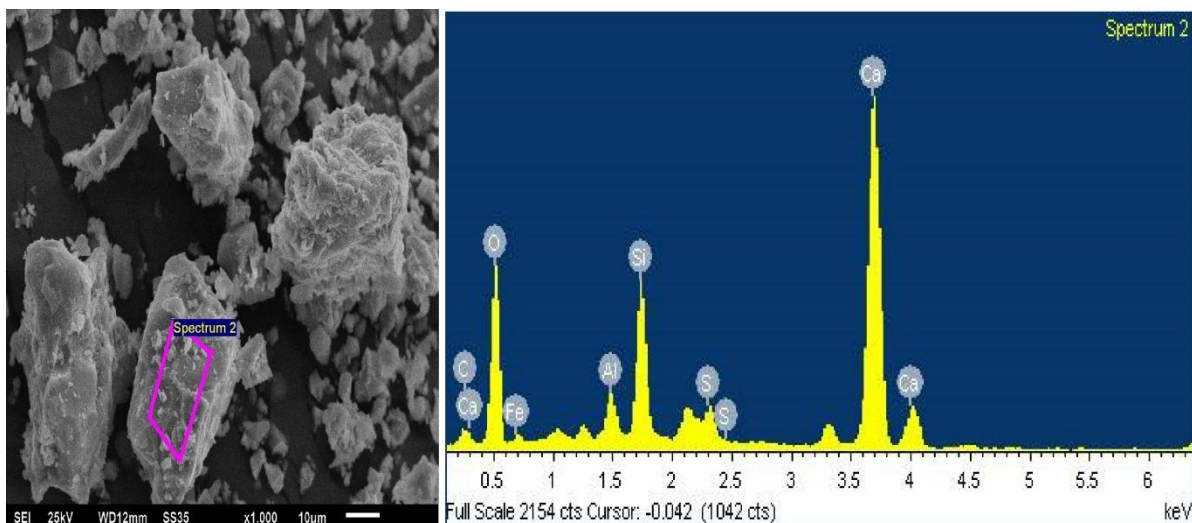


Fig.3.4: SEM/EDS analysis of OPC particles (present study)

The micrograph showed the presence of irregular shaped and bigger sized particles than fly ash, whereas, XRD analysis showed the presence of portlandite and calcite. These both

phases are associated with calcium compounds such as calcium hydroxides, calcium carbonates, etc. The chemical composition was also determined through XRF analysis as shown in Table 3.3. It was observed that the OPC particles had a high calcium content of around 63%.

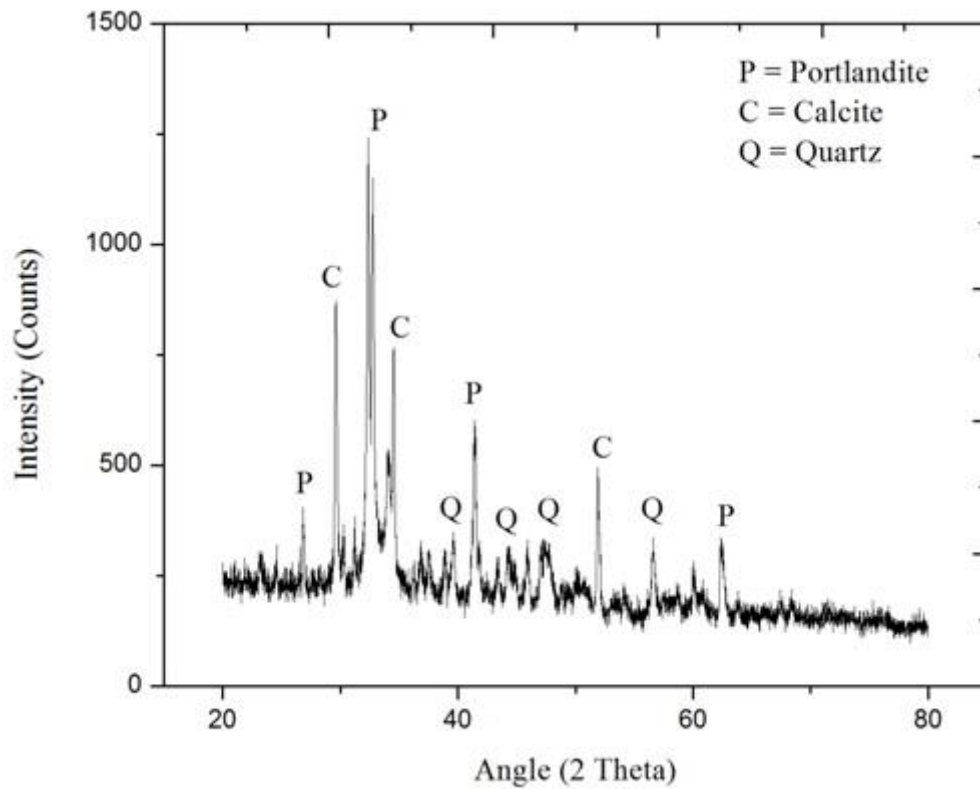


Fig.3.5: XRD analysis of OPC particles (present study)

Table 3.3: Chemical composition of OPC particles (present study)

<i>Chemical constituents in oxides form</i>	<i>Values obtained by XRF analysis (%)</i>
Calcium oxide (CaO)	62.76
Aluminium oxide (Al ₂ O ₃)	5.69
Silica Oxide (SiO ₂)	23.61
Iron oxide (Fe ₂ O ₃)	3.06
Magnesium oxide (MgO)	0.98
Potassium oxide (K ₂ O)	0.76
Sodium oxide (Na ₂ O)	0.28

3.2.3 Aggregates

The major volume of the concrete mixture is occupied by aggregates which provide a dimensional stability to the concrete. Generally, two size groups of aggregates are used; coarse aggregates with a particle size greater than 4.75 mm and fine aggregates with a

particle size less than 4.75 mm. Coarse aggregate contributes to the increase in crushing strength of concrete by making a solid hard mass, whereas fine aggregates refer to small angular or rounded grains which fill the voids between the coarse aggregate particles and considerably reduce the shrinkage properties of concrete. It also assists the cement paste in holding coarse aggregates in suspension as a binder which provides plasticity and thereby reducing the possibility of segregation between paste and aggregates. The cost of concrete is reduced significantly since they occupy about 80% of the total volume of concrete. So, it becomes extremely important that the aggregates should meet basic requirements for the concrete to be workable, strong, durable and economical.

3.2.3.1 Coarse Aggregates

The aggregate particles retained over 4.75 mm BIS sieve can be termed as coarse aggregates. Different types of coarse aggregates can be helpful in providing different characteristics, for example, crushed aggregates can improve strength properties due to their interlocking, whereas rounded aggregates can improve fresh properties by virtue of their lower internal friction. The coarse aggregates used in the present study were obtained from the local sources with the maximum size of 20 mm. They were washed thoroughly to remove dust and further subjected to oven dry for 24 hours so as to remove the excess moisture. The physical tests such as specific gravity and water absorption were performed on coarse aggregate particles in accordance with BIS: 2386 (Part 3)-1997. To perform the test, around 3000 g of coarse aggregate particles were submerged in water for around 24 hours which were further allowed to dry at room temperature. The dry aggregate with no surface moisture was weighed (as A). They were then placed in the wire basket filled with water and submerged weight was noted (as B). They were further subjected to the oven at 110 °C for about 24 hours and the oven dried weight was noted (as C). After the values A (weight of saturated surface dry aggregate in g), B (weight of saturated aggregate in water), and C (weight of oven dry aggregate) were known; specific gravity and water absorption were measured as:

$$\text{Specific gravity} = \frac{C}{(A - B)}$$

$$\text{Water absorption} = \frac{(A - C)}{C} \times 100$$

The physical tests and sieve analysis results of coarse aggregates mentioned above, as shown in Table 3.4 and 3.5, respectively were observed to be within the limits specified in BIS: 383-1970.

Table 3.4: Physical test results of coarse Aggregates (present study)

<i>Characteristics</i>	<i>Values</i>
Color	Grey
Shape	Angular
Maximum size	20 mm
Specific gravity (%)	2.65
Water absorption (%)	0.98

Table 3.5: Sieve analysis results of coarse aggregates(present study)

<i>Sieve passing through (mm)</i>	<i>Mass retained (g)</i>	<i>Mass retained (%)</i>	<i>Cumulative mass retained (%)</i>	<i>Cumulative mass passing (%)</i>	<i>BIS specifications (%) (BIS: 383-1970)</i>
80	0	0	0	100	-
40	0	0	0	100	100
20	111.5	3.72	3.72	96.28	85-100
10	2645.5	88.18	91.90	8.10	0-20
4.75	180	6	97.90	2.10	0-5
Pan	63	2.1	100	0	-
Coarse aggregates confirmed to BIS: 383-1970 Fineness modulus of coarse aggregates = 6.93 Weight of sample taken = 3000 g					

3.2.3.2 Fine Aggregates

The major significance of fine aggregates in the concrete mechanism is to provide uniformity and workability. It helps to have plasticity in the mixture so that to avoid the possibility of segregation between the paste and coarse aggregates. They may be classified as; natural sand obtained from natural disintegration of rocks, crushed stone sand obtained by crushing of hard stone, and crushed gravel sand which is produced by crushing of natural gravels. In the present study, river sand obtained from the local sources was used as fine aggregates. The physical tests such as specific gravity, water absorption and particle size distribution were performed on river sand in accordance with BIS: 2386 (Part 1)-1963. For this, around 500 g of sand was submerged in water in a tray for 24 hours where entrapped air was removed by gentle agitation. After 24 hours, the water was drained by decantation through filter paper. The sand was allowed to dry at the room temperature and weighed (as A) with no visible surface moisture. After drying at room temperature, the sand particles were filled in the pycnometer bottle filled completely with water. The bottle was locked and weighed (as B). The bottle was further emptied and re-filled with only water up to the same level and was again weighed (as C). On the other hand, the sand emptied from the pycnometer bottle was

placed inside an oven and dried at 110°C for 24 hours. The dried sand particles were allowed to cool at room temperature and again weighed (as D). After determining the values of A (weight of saturated surface dry sample), B (weight of pycnometer containing sample and water), C (weight of pycnometer filled with water) and D (weight of oven dried sample); specific gravity and water absorption values were obtained by the following expressions:

$$\text{Specific gravity} = \frac{D}{[A - (B - C)]}$$

$$\text{Water absorption} = \frac{(A - D)}{D} \times 100$$

To determine the fineness modulus of sand particles, 1000 g of sand particles were oven dried at 100°C for around 24 hours and allowed to cool at room temperature. Sieve analysis was performed on the oven dry sand particles for about 5 minutes with the sieves of different sizes placed in the order as 10, 4.75, 2.36, 1.18 mm, 600, 300, 150µm, and pan at bottom. The results of physical tests and sieve analysis performed on fine aggregates, as in Tables 3.6 and 3.7, were found to be satisfactory in accordance with BIS: 383-1970.

Table 3.6: Physical test results of fine aggregates (present study)

<i>Characteristics</i>	<i>Values</i>
Type	River sand
Water absorption (%)	1.04
Specific gravity (%)	2.64
Fineness modulus	2.55
Grading zone	Zone-II

Table 3.7: Sieve analysis of fine aggregates (present study)

<i>Sieve passing</i>	<i>Mass retained (g)</i>	<i>Mass retained (%)</i>	<i>Cumulative mass retained (%)</i>	<i>Cumulative mass passing (%)</i>	<i>BIS specifications (%) for Zone-II</i>
10 mm	0	0	0	0	100
4.75 mm	12	1.2	1.2	98.8	90-100
2.36 mm	53	5.3	6.5	93.5	75-100
1.18 mm	225	22.5	29.0	71.0	55-90
600 µm	157	15.7	44.7	55.3	35-59
300 µm	316	31.6	76.3	23.7	8-30
150 µm	208	20.8	97.1	2.90	0-10
Pan	29	2.9	100.0	0	-

Fine aggregates confirmed Zone-II as per BIS: 383-1970

Fineness modulus of coarse aggregates = 2.55

Weight of sample taken = 1000 g

3.2.4 Alkali-Activating Solution

In general, the alkali-activating solution consists of hydroxides and silicates of sodium or potassium which is required to liberate silica and alumina from the source material and undergo polymerization to form polymeric binders. In this study, the alkali-activating solution was prepared by mixing sodium silicate (Na_2SiO_3) and sodium hydroxide (NaOH) in the ratio optimized by the trial mixtures. Sodium hydroxide solution for the optimized molarity was prepared by mixing NaOH pellets obtained from Fischer Scientific Company with distilled water. The physical properties of NaOH were supplied by the manufacturer as shown in Table 3.8. Sodium silicate solution was procured from the local source which was obtained by mixing sodium oxide, silica oxide and water in an approximate ratio of 2:1:3 (information supplied by the manufacturer). Also, various studies (Kong and Sanjayan, 2008; Li and Liu, 2007) reported that the preparation of alkali solutions release a large amount of heat and so to bring down its temperature to the ambient condition, it should be left at room temperature for about 24 hours before mixing to the dry mixture. On the other hand, a few studies suggested that the alkali solutions should directly be mixed to the dry mixture (Wongpa et al., 2010; Bondar et al., 2011). In the present study, the alkali solution was mixed together 24 hours prior to its use so that the effect of any additional source of heat, other than curing temperature, could be eliminated.

Table 3.8: Physical properties of sodium hydroxide (supplied by the manufacturer)

<i>Characteristics</i>	<i>Value</i>
Boiling point (°C)	1390
Melting point (°C)	318
Formula weight	40
Color	White
pH	14
Density (g/mL)	2.13
Vapour pressure	1mmHg at 739 °C

3.2.5 Superplasticizer

Based on trial mixtures performed for the development of geopolymer concrete, superplasticizer was added to obtain adequate workability. High range water reducing superplasticizer, Sikament-610, was used at 2% by weight of fly ash. The chemical base of the superplasticizer used was modified naphthalene formaldehyde sulphonate with specific

gravity 1.225. The product data sheet provided by the manufacturer ensured its compliance with BIS: 9103-1999, ASTM C 494-99/99a Type F and G. It also ensured a substantial increase in workability and reduction of around 15% water in ideal conditions.

3.3 MIXTURE DESIGN

Low-calcium fly ash was used as source material for the development of control geopolymer concrete (with 100% FA) and further geopolymer mixtures were prepared with the inclusion of OPC as partial replacement of fly ash (5-30%). For reference, conventional cement concrete mixture of similar 28-day compressive strength was also prepared. The methods adopted for the mixture design of both types of concrete are presented here.

3.3.1 Fly Ash based Geopolymer Concrete (GPC)

Due to the absence of any reference standards for the mixture proportioning of geopolymer concrete, trial mixtures were performed to achieve the 3-day compressive strength of around 40 MPa by using Taguchi method.

For the development of GPC, various parameters were considered such as ratio of alkali solution-to-fly ash (0.45-0.75), ratio of sodium silicate-to-sodium hydroxide (2.0-2.75), molarity of sodium hydroxide (5-20M), total aggregate content (60-75%), ratio of fine aggregates-to-total aggregates (0.30-0.45) and curing temperature (60-90°C for constant duration of 24 hours), as shown in Table 3.9. Trial mixtures, designed by Taguchi method, were grouped into 3 groups of mixtures and optimum values were obtained based on maximum 3-day compressive strength.

Table 3.9: Parameters considered for the development of GPC

<i>Factors</i>	<i>Level 1</i>	<i>Level 2</i>	<i>Level 3</i>	<i>Level 4</i>
A: Ratio of sodium silicate to sodium hydroxide	2.00	2.25	2.50	2.75
B: Total aggregate content (%)	60	65	70	75
C: Ratio of alkali solution to fly ash	0.45	0.55	0.65	0.75
D: Molarity of sodium hydroxide (M)	5	10	15	20
E: Curing temperature (°C) (for constant duration of 24 hours)	60	70	80	90
F: Ratio of fine aggregates to total aggregates	0.30	0.35	0.40	0.45

1st group of 16 trial mixtures, as shown in Table 3.10, were prepared to determine the optimum values of sodium silicate-to-sodium hydroxide ratio, total aggregate content and

alkali solution-to-fly ash ratio, wherein other parameters such as molarity of sodium hydroxide (15M), curing temperature (70 °C for 24 hours), fine aggregates-to-total aggregates ratio (0.35), and fly ash content (350kg/m³) were assumed as constant based on the previous literature (Fernandez-Jimenez et al., 2006; Hardjito et al., 2004; Wongpa et al., 2010; Joseph and Mathew, 2012) which yielded good strength values with these values of parameters.

Table 3.10: 1st group of Trial mixtures designed by Taguchi method

<i>1st group of Trial Mixture</i>	<i>Combination</i>	<i>Factors</i>			<i>3-day compressive strength (MPa)</i>
		<i>A</i>	<i>B</i>	<i>C</i>	
T1	A1B1C1	2.00	60	0.45	42.6
T2	A1B2C2	2.00	65	0.55	43.7
T3	A1B3C3	2.00	70	0.65	43.5
T4	A1B4C4	2.00	75	0.75	42.9
T5	A2B1C4	2.25	60	0.75	43.2
T6	A2B2C1	2.25	65	0.45	43.6
T7	A2B3C2	2.25	70	0.55	44.5
T8	A2B4C3	2.25	75	0.65	43.8
T9	A3B1C3	2.50	60	0.65	45.9
T10	A3B2C4	2.50	65	0.75	46.3
T11	A3B3C2	2.50	70	0.55	47.4
T12	A3B4C1	2.50	75	0.45	46.8
T13	A4B1C4	2.75	60	0.75	44.9
T14	A4B2C3	2.75	65	0.65	45.7
T15	A4B3C2	2.75	70	0.55	46.3
T16	A4B4C1	2.75	75	0.45	45.3

Based on results from 1st group of trial mixtures, the optimum values of sodium silicate-to-sodium hydroxide ratio (2.5), total aggregate content (70%) and alkali solution-to-fly ash ratio (0.55) were obtained as maximum 3-day compressive strength was obtained for the T11 trial mixture. These values together with fly ash content of 350 kg/m³, were kept as constant for the 2nd group in which 16 trial mixtures were further prepared to find out the optimum values of other three parameters such as molarity of sodium hydroxide, curing temperature and fine aggregates-to-total aggregates ratio, as shown in Table 3.11. The results exhibited the optimum values of molarity of sodium hydroxide as 10M, curing temperature as 80 °C for 24 hours and fine aggregates-to-total aggregates ratio of 0.35 as maximum 3-day compressive strength was obtained for T23 trial mixture.

In the 3rd group of trial mixtures, based on results from 1st and 2nd group, the obtained optimum values of parameters were kept as constant i.e. alkali solution-to-fly ash ratio of 0.55, sodium silicate-to-sodium hydroxide ratio of 2.5, total aggregate content of 70%, molarity of sodium hydroxide as 10M, curing temperature as 80°C for 24 hours and fine aggregates-to-total aggregates ratio of 0.35, and different fly ash values were considered to obtain 3-day compressive strength of around 40MPa, as shown in Table 3.12.

The final design mixture for control GPC was obtained with fly ash content of 310 kg/m³, alkali solution-to-fly ash ratio of 0.55, sodium silicate-to-sodium hydroxide ratio of 2.5, total aggregate content of 70%, molarity of sodium hydroxide as 10M, fine aggregates-to-total aggregates ratio of 0.35, and temperature curing at 80°C for 24 hours.

Table 3.11: 2nd group of Trial mixtures designed by Taguchi method

2nd group of Trial Mixture	Combination	Factors			3-day compressive strength (MPa)
		D	E	F	
T17	D1E1F1	5	60	0.30	42.3
T18	D1E2F2	5	70	0.35	42.8
T19	D1E3F3	5	80	0.40	43.7
T20	D1E4F4	5	90	0.45	43.3
T21	D2E1F4	10	60	0.45	46.8
T22	D2E2F1	10	70	0.30	47.7
T23	D2E3F2	10	80	0.35	48.8
T24	D2E4F3	10	90	0.40	48.4
T25	D3E1F3	15	60	0.40	46.5
T26	D3E2F4	15	70	0.45	47.0
T27	D3E3F2	15	80	0.35	47.4
T28	D3E4F1	15	90	0.30	46.9
T29	D4E1F4	20	60	0.45	44.7
T30	D4E2F3	20	70	0.40	45.1
T31	D4E3F2	20	80	0.35	45.3
T32	D4E4F1	20	90	0.30	44.9

Further, to develop geopolymer concrete with Ordinary Portland cement (OPC) as partial replacement of fly ash, OPC was included in the control geopolymer concrete mixture at 5, 10, 15, 20, 25 and 30% as partial replacement of fly ash. The finally adopted mixture design for GPC was obtained as shown in Table 3.13. F100C0 denotes control GPC with 0% OPC, whereas F95C05, F90C10, F85C15, F80C20, F75C25 and F70C30 denote the geopolymer

concrete mixtures with different contents of OPC as 5, 10, 15, 20, 25 and 30%, respectively as partial replacement of fly ash.

Table 3.12: 3rd group of trial mixtures for 3-day compressive strength of 41.1 MPa

<i>Fly Ash (kg/m³)</i>	<i>Alkali solution (kg/m³)</i>	<i>Sodium silicate (kg/m³)</i>	<i>Sodium hydroxide (kg/m³)</i>	<i>Coarse aggregates (kg/m³)</i>	<i>Fine aggregates (kg/m³)</i>	<i>Super plasticizer (kg/m³)</i>	<i>Compressive strength (3 days)(MPa)</i>
280	154	110	44	1204	649	5.6	39.1
290	160	114	46	1204	649	5.8	39.7
300	165	118	47	1204	649	6.0	40.2
310	171	122	49	1204	649	6.2	41.1

Table 3.13: Mixture proportions of fly ash based GPC

<i>Mixture</i>	<i>Fly ash (kg/m³)</i>	<i>OPC (kg/m³)</i>	<i>Alkali-activating solution (kg/m³)</i>	<i>Coarse aggregates (kg/m³)</i>	<i>Fine aggregates (kg/m³)</i>	<i>Superplasticizer (kg/m³)</i>
F100C0	310.0	0	171	1204	649	6.2
F95C05	294.5	15.5	171	1204	649	6.2
F90C10	279.0	31.0	171	1204	649	6.2
F85C15	263.5	46.5	171	1204	649	6.2
F80C20	248.0	62.0	171	1204	649	6.2
F75C25	232.5	77.5	171	1204	649	6.2
F70C30	217.0	93.0	171	1204	649	6.2

3.3.2 Conventional Cement Concrete (CCC)

Conventional cement concrete (CCC) mixture was designed in accordance with the guidelines provided in BIS: 10262-2009. To perform the trial mixes, the compressive strength was considered as its quality index. The 28-day characteristic strength of around 40 MPa was targeted with adequate workability so that it can be properly mixed, compacted and placed. The stipulations for proportioning M40 OPC based concrete are given below:

Grade designation	: M40
Target compressive strength at 28 days	: 48.25 MPa
Type of cement	: OPC 43 grade
Workability	: 75 mm (slump)
Exposure condition	: Mild
Chemical admixture type	: Superplasticizer
Maximum size of aggregate	: 20 mm

For the mixture proportioning, physical tests were conducted on OPC, coarse aggregates and fine aggregates. The test data required for the mixture design, as calculated before, is given below:

Specific gravity of OPC	3.12
Specific gravity of coarse aggregates	2.65
Water absorption of coarse aggregates	0.98
Sieve analysis	Confirmed to BIS: 383-1970
Specific gravity of fine aggregates	2.64
Water absorption of fine aggregates	1.04
Zone as per BIS: 383-1970	Zone II
Specific gravity of superplasticizer (value provided by the manufacturer)	1.22

After performing various trial mixtures, the final mixture design was adopted as shown in Table 3.14.

Table 3.14: Mixture proportions of CCC

<i>Mixture</i>	<i>Water-cement ratio</i>	<i>OPC (kg/m³)</i>	<i>Fine aggregates (kg/m³)</i>	<i>Coarse aggregates (kg/m³)</i>	<i>Water (kg/m³)</i>	<i>Superplasticizer (kg/m³)</i>
CCC	0.40	410	667	1191	164	4.1

3.4 CASTING AND CURING OF SPECIMENS

The dry mixture was prepared by mixing fly ash, OPC, coarse and fine aggregates in a pan mixer for about five minutes until the uniform color was obtained, without any clusters. GPC was prepared by adding alkali-activating solution with superplasticizer to the dry mixture. The alkali-activating solution was prepared by mixing sodium hydroxide (NaOH) of molarity 10M and sodium silicate (Na₂SiO₃), 24 hours prior to its use as explained before in earlier section 3.2.4. The constituents were mixed in the pan mixer for about 15 minutes until a homogeneous concrete mixture was prepared, as shown in Fig.3.6. CCC was also prepared by mixing the dry mixture with water and superplasticizer. GPC and CCC were subjected to workability tests and further filled in the required steel moulds.

The moulds were oiled properly before the casting operation. Cube specimens of size 150×150×150 mm were cast to determine the compressive strength and 100×100×100 mm to determine sulphuric acid resistance. For determining the split tensile strength, cylindrical specimens of size 150×300 mm were cast. For the properties like water absorption and

porosity, sorptivity and rapid chloride permeability, parent cylindrical specimens of size 100×200 mm were cast from which discs of size 100×50 mm were cut for testing. The conventional concrete specimens were de-moulded after 24 hours of adding water to the concrete mixer and kept in the water curing tank till their testing age. On the other hand, curing procedure for geopolymer concrete was different. The geopolymer concrete specimens after casting were kept at room temperature for 1 hour as delay time and further placed in an oven at 80 °C for 24 hours with the top surface covered by steel plate. After oven curing, the specimens were de-moulded and covered with the cling film to avoid the moisture loss. The cling film covered specimens were kept at the room temperature until their testing age.



Fig.3.6: Making of concrete in a pan mixture

3.5 TEST METHODS FOR EVALUATION OF PROPERTIES

3.5.1 Workability Properties of Geopolymer Concrete

Fresh properties correspond to the workability of concrete which indicates the ease with which the concrete can be placed. Workability of geopolymer concrete mixtures was evaluated by slump and compaction factor test.

3.5.1.1 Slump

Slump test is the most extensively used test method for the evaluation of workability of fresh concrete. It is an inexpensive test and widely used in field applications around the globe. The

apparatus consists of a mould in the frustum of a cone shape with atop diameter as 100 mm, base diameter as 200 mm and height 300 mm as shown in Fig.3.7. To determine the slump, the concrete was filled in the mould in three layers with each layer was compacted by 25 strokes using a tamping rod.

Once the compacted concrete was filled, the slump cone mould was lifted upwards vertically and the change in height of fresh concrete was measured. In general, four types of height modifications are encountered, as shown in Fig.3.8. The most desirable shape for various applications is the true slump whereas; zero and collapsed slump are not desirable and are outside the range of this test method.



Fig.3.7: Experimental set up for measuring workability by using slump cone

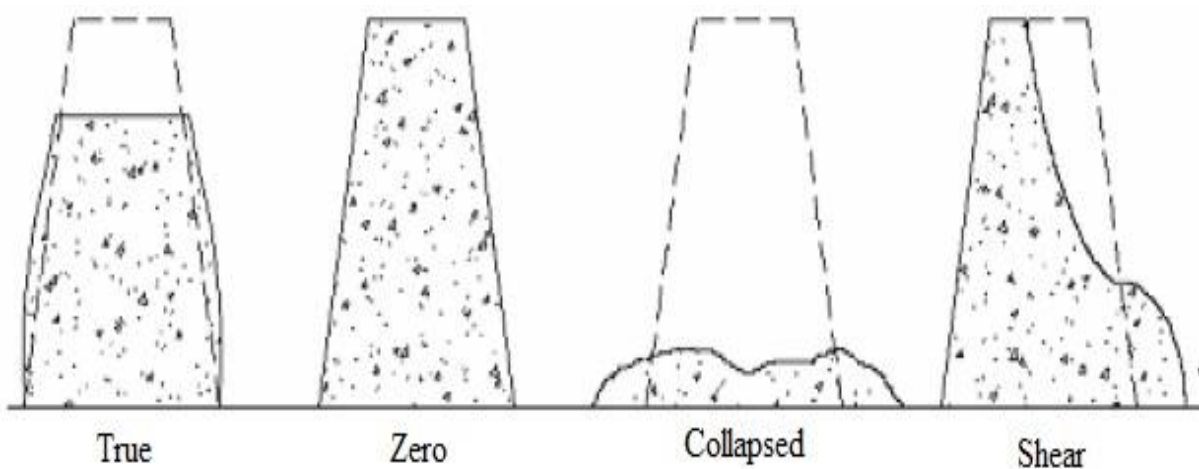


Fig.3.8: General types of slump (Koehler and Fowler, 2003)

3.5.1.2 Compaction Factor

The compaction factor apparatus consists of a rigid frame which supports a cylinder with two vertically aligned conical hoppers above it, as shown in Fig.3.9. When the concrete mixtures are expected to have low workability, this test method is more precise than slump cone test as such concrete may fail to provide any slump value. The volume of a cylinder is smaller than both the hoppers while the top hopper is slightly larger than the lower. In order to perform the test, the uncompacted concrete was first filled in the top hopper. The gate of the top hopper was opened and the concrete was allowed to drop freely into the lower hopper. A tamping rod was used to strike off the excess concrete. Once all of the concrete was fallen in the lower hopper, the door of the lower hopper was opened and all of the concrete was allowed to fall to the bottom cylinder. It again struck off by using the tamping rod and once all of the concrete was fallen to the cylinder, the mass of uncompacted concrete was recorded. In the same cylinder, the concrete was compacted by using rod and vibration and the mass of fully compacted concrete was recorded. The compaction factor of the concrete specimen was calculated as the ratio of the mass of fully compacted concrete to that of the mass of uncompacted concrete.



Fig.3.9: Experimental set up for measuring workability by using compaction factor

3.5.2 Strength Properties of Geopolymer Concrete

Hardened concrete refers to the state of concrete when it is set permanently and ready to withstand external loadings for which it is designed. The strength of the hardened concrete is an important aspect in judging the structural performance of concrete.

3.5.2.1 Compressive Strength

The compressive strength of concrete gives an idea about the quality of the concrete in the hardened state in terms of its load carrying ability. For testing the compressive strength of geopolymer concrete mixtures, cube specimens of size 150×150×150 mm were cast and tested in an axially loaded compression testing machine (CTM) of 3000 kN capacity. Geopolymer concrete specimens were temperature cured whereas conventional concrete specimens were cured in water, therefore before testing, the specimens were kept at room temperature for an hour to bring it to the ambient conditions. In general, the failure takes place in the vertical plane when any member is subjected to the compression loading setup. The conventional concrete specimens after being taken out from the curing tank were wiped with cloth for any traces of surface water and kept at room temperature for half an hour to remove the surface moisture. On the other hand, the cling film was removed from the geopolymer concrete specimens and was subjected to the loading. The load was applied axially without any jerk till the specimens were unable to sustain the further load, in accordance with BIS: 516-1959. The cube specimens were placed in the CTM in such a manner that was applied to the opposite sides of the cube as cast, as shown in Fig.3.10.

For each mixture, three specimens were tested and the results were reported as their average at the ages of 3, 7, 28, 90 and 365 days. The compressive strength was reported as the maximum load in the compression test divided by the total cross-sectional surface area of the cube specimen.

$$f_{ck} = \frac{P}{A}$$

Where,

f_{ck} = characteristic strength (N/mm²)

P = maximum load applied (in N), and

A = cross-sectional area of cube specimens (mm²)



Fig.3.10: Experimental set up for measuring compressive strength

3.5.2.2 Split Tensile Strength

Split tensile strength test was conducted on geopolymer concrete mixtures in accordance with BIS: 5816 - 1999. Cylindrical specimens of size 150×300 mm were cast and tested at the ages of 3, 7, 28, 90 and 365 days. The cylindrical specimen was placed in CTM with the major axis perpendicular to the axis of loading as shown in Fig.3.11. Three specimens were tested for each sample and the results were reported as their average. The load was applied gradually without any jerk continuously until the specimen breaks into two halves.

The maximum load taken by the specimen was recorded and split tensile strength was calculated from below:

$$f_{ct} = \frac{2P}{\pi lD}$$

Where,

P = Maximum load applied to the specimen (in N),

l = length of specimen (in mm), and

D = cross-sectional dimension of specimen (in mm)



Fig.3.11: Experimental set up for measuring split tensile strength

3.5.3 Durability Properties of Geopolymer Concrete

In order to judge the structural performance of concrete, durability is another very important aspect other than strength and serviceability. It gives an idea about the time period for which the concrete structure is serviceable and also the maintenance required by it to remain serviceable.

3.5.3.1 Water Absorption and Porosity

Water absorption of concrete can be defined as its ability to absorb the external fluid and fill the pore spaces in the concrete matrix whereas, porosity can be defined as the number of void spaces present in the concrete matrix. The movement of fluids in the concrete matrix takes place not only through porous media but also by diffusion and absorption. In general, effective porosity of a hardened concrete can be measured by its water absorption. These properties are the significant components of the microstructure of concrete matrix. Water

absorption and porosity tests were conducted on the hardened geopolymer and conventional concrete specimens. Discs of size 100×50 mm were cut from the cylindrical 100×200 mm specimens and tested in accordance with ASTM C 642-97 at the ages of 28, 90 and 365 days. The test procedure consisted of drying the specimens in an oven at 110°C for 24 hours. The specimens were allowed to cool at the room temperature and weighed. Thereafter, the specimens were immersed in water for 24 hours and again weighed. The process was repeated if the difference between the consecutive weight readings was less than 0.5%. After that the specimens were immersed in the boiling water for around 5 hours and allowed to cool at the room temperature and again weighed. At last, the weight of specimens in water was also recorded as submerged weight. From these recorded values of weight, porosity and water absorption were calculated by the following:

$$\text{Porosity(\%)} = \frac{(B - A)}{(A)} \times 100$$

$$\text{Water absorption (\%)} = \frac{(g_2 - g_1)}{(g_2)} \times 100$$

Where,

A = mass of oven dried sample in air (in g)

B = mass of saturated surface dry sample in air (in g), and

$$g_1 = \text{Dry bulk density} = \frac{A}{(C - D)} \times \rho$$

$$g_2 = \text{Apparent density} = \frac{A}{(A - D)} \times \rho$$

Where,

C = mass of saturated surface dry sample after boiling in air (in g),

D = mass of saturated sample in water (in g), and

ρ = density of water = 1 g/cm³

3.5.3.2 Sorptivity

Sorptivity tests were conducted on the geopolymer concrete mixtures at the ages of 28, 90 and 365 days, in accordance with ASTM C 1585-04. In general, sorptivity can be described as the ingress of fluids inside the concrete surface through the capillary action caused by its pore structure. Discs of size 100×50 mm were cut from the parent cylindrical 100×200 mm concrete specimens. The specimens were oven dried at a temperature of 50 ± 2°C before

testing. To measure the capillary suction, the specimens were sealed from the sides as well as from the top by using a plastic sheet and the initial mass of the specimens were recorded. The sealed specimens were kept in a tray with 2-5 mm depth immersed in water, as shown in Fig.3.12.

Soon after the immersion, the masses of the specimens were measured at 1, 5, 10, 20, 30 minutes, 1, 2, 3, 4, 5 and 6 hours by taking them out and wiping off the excess surface water.



Fig.3.12: Experimental set up for measuring sorptivity of concrete

The rate of sorptivity was calculated by the slope of linear regression analysis curve by using the following formula:

$$s = \frac{I}{\sqrt{t}}$$

Where,

s = rate of sorptivity (in mm/s),

t = time elapsed (in seconds), and

$$I = \frac{m_t}{\frac{a}{d}}$$

Where,

m_t = average increase in mass (in g),

a = exposed surface area of the specimen (in mm^2), and
 d = density of water (in g/mm^3)

3.5.3.3 Rapid Chloride Permeability

Permeability refers to the ability of the concrete to resist harmful external ions or chemicals that may damage the concrete bonding and result in its deterioration. A highly permeable concrete refers to the large voids and pore spaces in the matrix which increases the ingress of external ions and hampers the durability of concrete structures. Chloride ions can affect the durability of concrete significantly as they can corrode the inside steel reinforcement which may also result in complete deterioration of RCC. Rapid chloride permeability tests were conducted on geopolymer concrete mixtures at the ages of 28, 90 and 365 days in accordance with ASTM C1202-97. The test method consists of determining electrical conductance, as shown in Fig.3.13 from which estimation of chloride permeability can be done as shown in Table 3.15 (ASTM C1202-97). The concrete discs of size 100×50 mm were cut and placed inside the moulds whose one end was immersed in sodium chloride (NaCl) solution and other was immersed in sodium hydroxide (NaOH) solution for 6 hours. A constant voltage of 60V DC was maintained throughout the test. The samples before keeping into the moulds were placed inside the vacuum desiccator bowl for 3 hours. No air was allowed to penetrate inside the bowl and specimens were fully submerged in the aerated water for 18 hours as shown in Fig.3.14. The temperature of the specimen was maintained at $20\text{-}25^\circ\text{C}$ at the time the test was initiated (when the power supply was turned on).

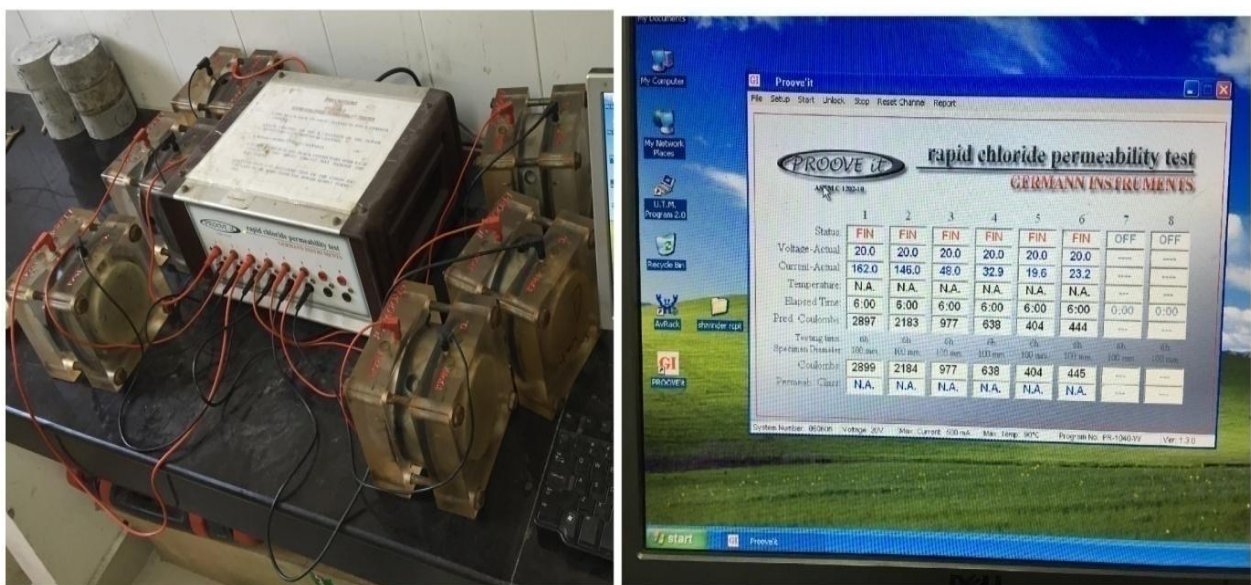


Fig.3.13:Experimental set up for measuring chloride permeability of concrete

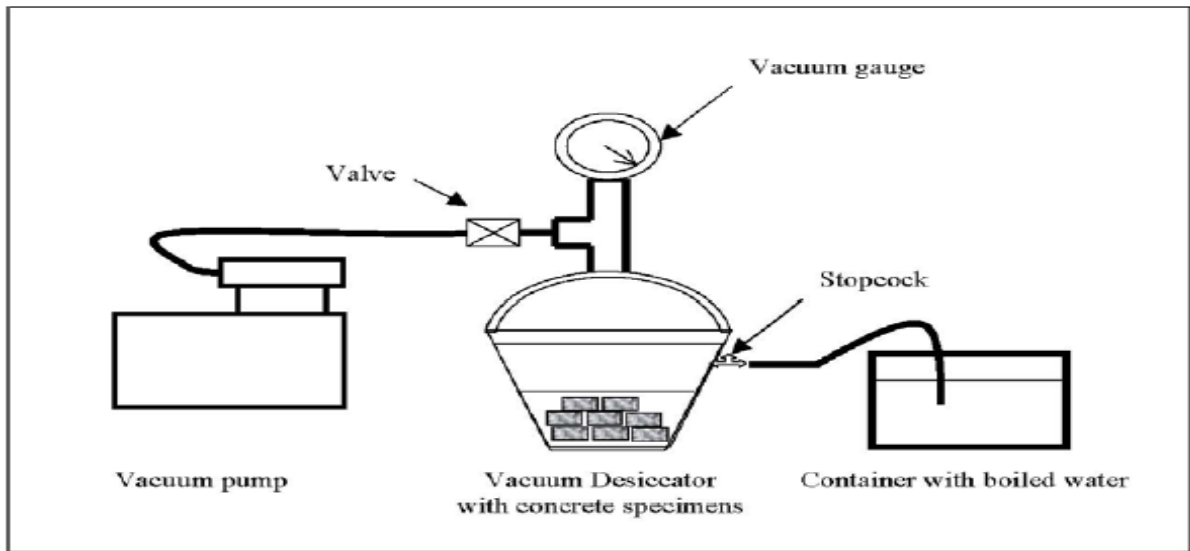


Fig.3.14: The Vacuum Pump, desiccators, and container with de-aerated water (Singh, 2012)

Table 3.15: Chloride ion penetrability based on total charge passed (ASTM 1202-15)

<i>Charge passed (coulombs)</i>	<i>Permeability category</i>
>4000	High
2000-4000	Moderate
1000-2000	Low
100-1000	Very low
<100	Negligible

3.5.3.4 Sulphuric Acid Resistance

The sulphuric acid resistance of geopolymer concrete mixtures was evaluated as per procedure adopted by Ariffin et al. (2013). The reason for choosing sulphuric acid over any other acid is due to its practical utilization as concrete members are often subjected to sulphuric acid in various applications like mining, sewage and food processing industries. It was observed from the previous studies (Hardjito et al., 2004; Kong and Sanjayan, 2008) that geopolymer concrete exhibit very less strength development after 28 days, therefore the de-moulded specimens after curing were wrapped with the cling film and kept at room temperature for 28 days with the expectation that the specimens obtained the bulk of its strength at 28 days. On the other hand, conventional concrete specimens were subjected to water curing up to 28 days. After 28 days, the specimens were immersed in 2% sulphuric acid solution with pH 1.0 up to 365 days. The pH of the acid solution was monitored using pH meter and in order to maintain the constant pH, concentrated sulphuric acid at desired concentrations were repeatedly added throughout the testing age. The deterioration of the

exposed specimens was measured in terms of change in mass and change in compressive strength at 28, 90 and 365 days, and was determined as per formulas given below:

$$\text{Change in Mass (\%)} = \frac{(M2 - M1)}{M1} \times 100$$

$$\text{Change in compressive strength (\%)} = \frac{(S2 - S1)}{S1} \times 100$$

Where,

M1 = Mass of specimens before immersion,

M2 = Mass of specimen after immersion at the testing age,

S1 = Average compressive strength of specimens at 28 days, and

S2 = Average compressive strength of specimens at the testing age

The microstructure of exposed specimens was also examined for the maximum deterioration by microscopic analysis such as SEM, EDS and XRD analysis.

3.5.4 Microstructure Properties of Geopolymer Concrete

After the destructive tests of hardened concrete, the residues of specimens were further subjected to microstructure analysis. Scanning electron microscopy (SEM) and energy dispersive spectroscopy (EDS) analysis were performed to observe the microstructure and chemical constituents whereas, for phase identifications, X-ray diffraction (XRD) test was conducted.

3.5.4.1 SEM/EDS Analysis

The scanning electron microscopy (SEM) is an electron microscope which uses a focussed electron beam to scan a sample by generating images. Various signals are formed after the interaction of these electrons with the atoms of the sample which provides the information about the compositional and topographic analysis of the sample. The electron beam in a typical SEM is emitted from an electron gun that is fitted to a tungsten filament (as a cathode) and due to its highest melting point; it gets electrically heated for the emission of electrons. The samples in SEM can generally be scanned at high resolutions, even better than 1 nanometer. The general mechanism of SEM analysis is the detection of secondary electrons that are emitted by the atoms of the sample due to the excitation caused by the electron beam. These secondary electrons are detected by a special detector which depends on the topography of samples. This detector after detecting the secondary electrons displays an image showing the topography of the surface of the sample. The SEM apparatus is also

equipped with an energy dispersive spectroscopy (EDS) arrangement as shown in Fig.3.15. In this system, the X-rays with an appropriate trajectory are emitted by the sample and collected by a biased disc of SiLi (silicon-lithium) diode. It is a small diameter disc which is cooled by liquid nitrogen. These X-rays are detectable as a voltage created by the electron-hole pairs in the diode. These voltage pulses are quantified and described as a function of energy (in Kev) as a spectrum of counts. At the particular region of interest, these peaks are identified as the chemical elements.

For the concrete samples, these electrons scan its microstructure and identify useful information about the hydration of cement paste, bonding with aggregates, microcracks and pores, and interfacial transitional zone (ITZ). These factors generally govern the essential properties such as mechanical and durability properties of concrete. In this study, SEM and EDS analysis were performed on fly ash and OPC particles for their characterization, as well as on geopolymer concrete specimens.



Fig.3.15: Experimental setup for Scanning Electron Micrograph

When geopolymer concrete specimens were tested for compressive strength, the fractured pieces were collected and mounted on SEM stub, where microstructure analysis was performed using secondary electron (SE) mode. To make the concrete powder samples electrically conductive, they were coated with a thin layer of gold before placing on the stem.

Images were produced by the detectors at high resolutions and useful identifications were inferred.

3.5.4.3 XRD Analysis

X-ray diffraction (XRD) is a technique used to determine the phases in the sample. Diffraction is a term used to describe a physical phenomenon in which electromagnetic waves avoid the obstacles in its path. This phenomenon can also be applied in the field of material science where electromagnetic waves such as X-rays are applied to material atoms and diffraction is produced as a reflection at particular angles. It works on the principle that all the crystalline phases have their diffraction image. For the analysis, diffractometers are placed in accordance to Bragg-Brentano system in which the sample rotates at an angle θ while the diffractometers rotate at an angle 2θ , as shown in Fig.3.16. Heat is applied to the filament within the sealed vacuum tube that creates the current. Higher current will accelerate the number of electrons which will hit the sample target and produce the X-rays which are directed into the powder sample and get deflected. These deflected rays are detected by diffractometers which get processed electronically to convert signals into a count rate. This technique is widely utilized to observed crystalline phases and lattice parameters that can affect the properties of the sample significantly.

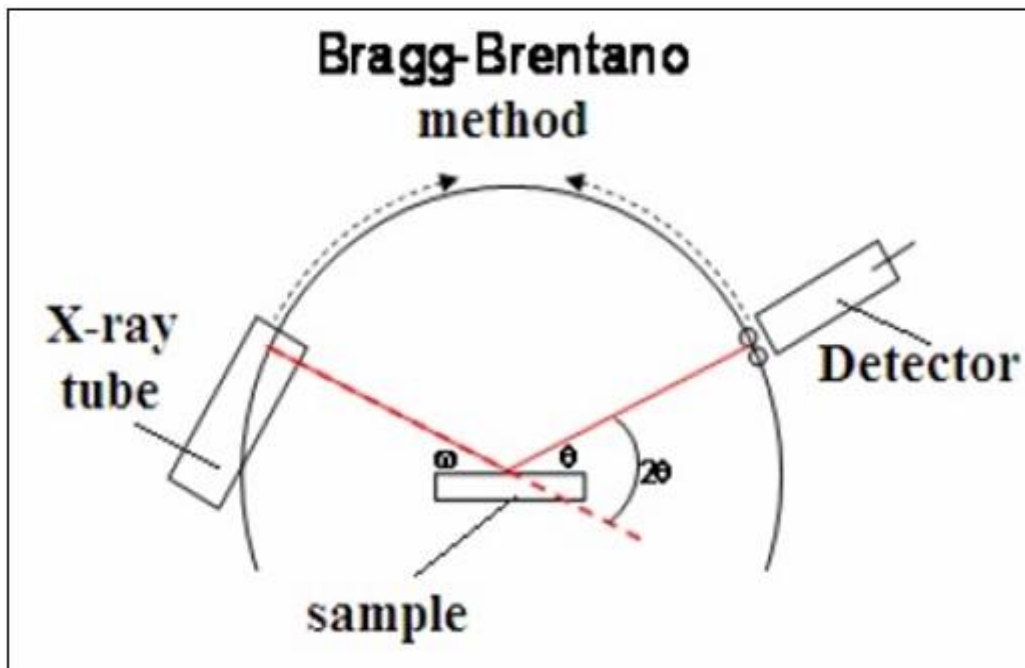


Fig.3.16: Basic layout of X-ray diffractometers (Jumate and Manea, 2011)

This technique has a wide range of utilization in the concrete specimens. It can be used to identify various crystalline phases such as ettringite, portlandite (calcium hydroxide), calcium silicate hydrates, etc. However, amorphous phases are difficult to analyze due to weak diffracted peaks. The resulted diffraction curve consists of maximum diffraction points in succession in which radiation intensity is plotted on the ordinate and angle 2θ on the abscissa. In this study, XRD analysis was carried out on fly ash and OPC materials, as shown in Fig.3.17. In addition, the analysis was also carried out on the geopolymer concrete specimens with different amount of calcium content (in the form of OPC) to determine various phases developed.



Fig.3.17: Experimental setup for XRD analysis

CHAPTER-4

RESULTS AND DISCUSSIONS

This chapter presents the results of workability properties such as slump and compaction factor, strength properties such as compressive strength and split tensile strength, and durability properties such as water absorption, porosity, sorptivity, chloride permeability and sulphuric acid resistance of low-calcium fly ash based geopolymer concrete incorporated by OPC as fly ash replacement. In addition, the results of microstructure properties such as scanning electron micrographs (SEM), energy dispersive spectroscopy (EDS) and X-Ray diffractogram (XRD) analysis are also discussed in this chapter.

4.1 WORKABILITY PROPERTIES OF GEOPOLYMER CONCRETE

Workability determines the ease with which the homogeneous concrete can be mixed, placed and finished. Homogeneity refers to the proper mixing of the ingredients that can maintain stability, mobility and compaction ability that depends on the consistency of the concrete mixture. Workability properties were determined by performing slump and compaction factor tests on fresh geopolymer concrete mixtures.

4.1.1 Slump

Slump test was performed on the fresh geopolymer concrete (GPC) mixture with different contents of OPC as partial replacement of fly ash, as well as on conventional cement concrete (CCC). The test results are presented in Fig. 4.1. The results showed that with the inclusion of OPC in the geopolymer system, the slump values decreased. The maximum value of slump was obtained for control GPC i.e. with 0% OPC. This was attributed to the fact that fly ash particles have small particle size and are spherical in shape. These small sized spherical shaped particles acted as ball bearings and increased the specific surface area which resulted in higher workability. In addition, the use of naphthalene based water reducing admixtures also increased the surface area of fly ash particles by imparting a negative charge, making the water more available to provide adequate workability. However, with the increase in OPC in GPC, a decrease in slump was observed with the minimum value of 50 mm for GPC with 30% OPC. The decrease in workability with the inclusion of OPC was also due to relatively higher particle size of OPC than fly ash. Also, it was observed from the SEM micrographs of OPC and fly ash particles, as shown in Figs. 3.2 and 3.4, that the shape of OPC is irregular in

comparison to spherically shaped fly ash particles which further decreased the surface area and hence reduced the workability.

The decrease in slump was also attributed to the quick hardening due to increased calcium content in GPC which provided extra nucleation sites for precipitation of dissolved species. A similar increase in hardening due to additional calcium content in the geopolymer system was also reported by Chindaprasirt et al. (2012); Lee and Van Deventer (2002b); Pangdaeng et al. (2014). In addition, the early and rapid hardening due to additional calcium also yielded extra heat in the geopolymer system due to its exothermic nature, which further accelerated the geopolymer mechanism (Suwan and Fan, 2014).

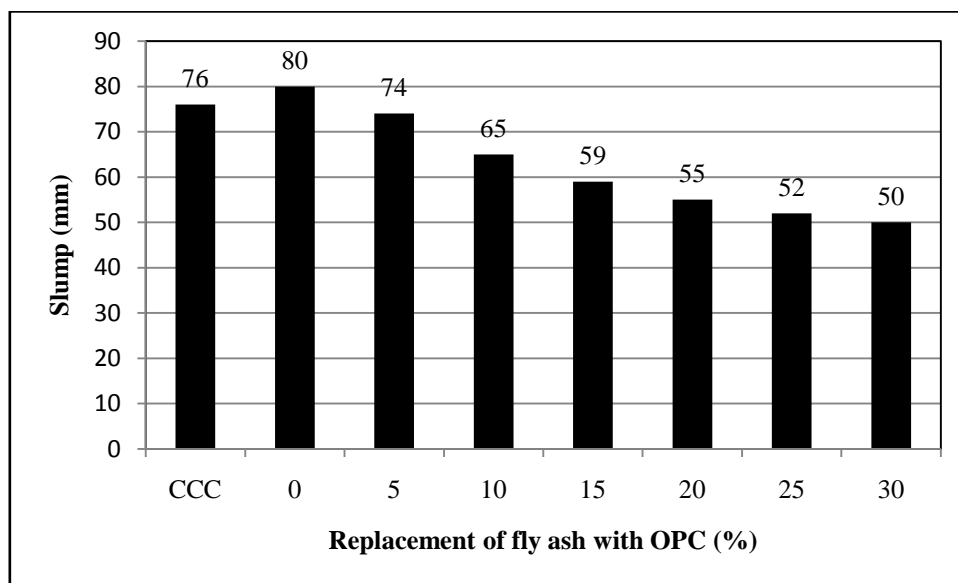


Fig.4.1: Effect of adding OPC on slump of GPC

4.1.2 Compaction Factor

The results of compaction factor are presented in Fig.4.2. It was observed that the compaction factor decreased with the increase in OPC content from 0 to 30% in GPC with the values ranging from 0.91 to 0.86, respectively. The decrease in workability in terms of compaction factor was also in agreement with the decrease in slump values. The linear curve obtained from the results of compaction factor is shown below as Eq. (1):

$$Y = -0.00157 X + 0.908 \quad \text{Eq. (1)}$$

$$R^2 = 0.986$$

Where, Y denotes the compaction factor, and X denotes the percentage replacement of fly ash by OPC up to 30%. The high value of the coefficient of determination (R^2) was obtained for the linear curve which showed good correlation between the actual results obtained in the

experimental investigation and the results obtained from the curve. The decrease in values of compaction factor was related to the increase in viscosity of the resultant matrix due to the inclusion of additional calcium in the form of OPC as also explained in section 4.1.1.

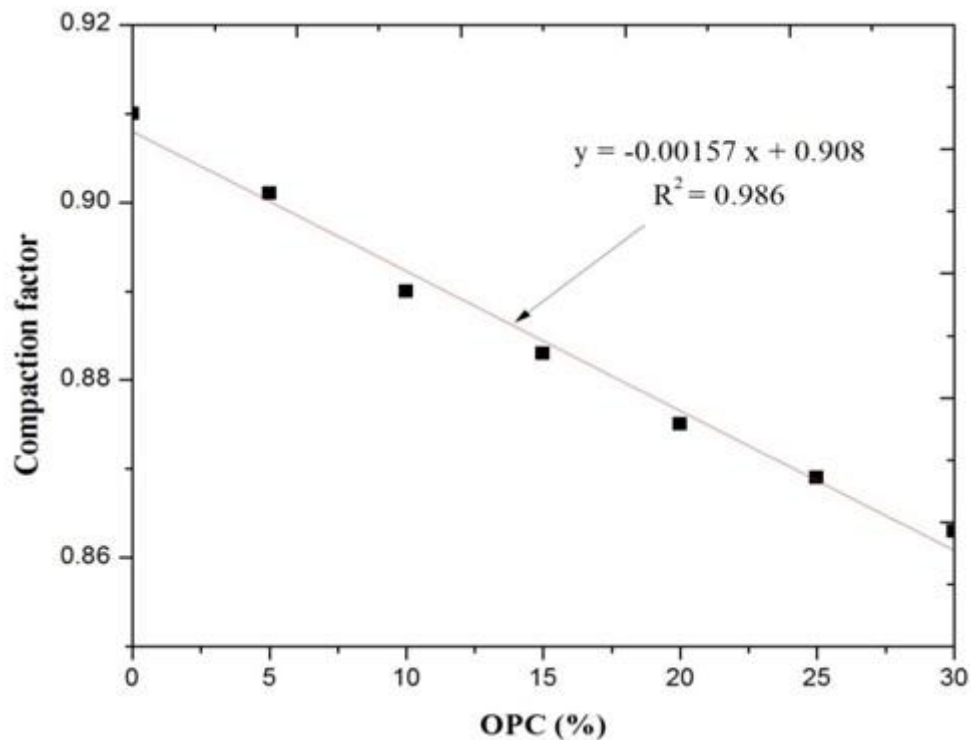


Fig.4.2: Effect of adding OPC on compaction factor of GPC

4.2 STRENGTH PROPERTIES OF GEOPOLYMER CONCRETE

The strength properties were determined by performing compressive strength and split tensile strength tests. These tests were conducted on GPC as well as CCC mixtures at 3, 7, 28, 90 and 365 days.

4.2.1 Compressive Strength

The results of compressive strength are reported as the average of three specimens for each mixture at 3, 7, 28, 90 and 365 days, as shown in Fig. 4.3 and 4.4. It was observed that the difference between the compressive strength obtained at 3 and 7 days was not significant for all GPC mixtures. At 3 days, the GPC mixtures with 0, 5, 10, 15, 20, 25 and 30% OPC achieved the compressive strength of 92.4, 93.3, 92.6, 95.3, 98.0, 96.2 and 97.8% of their 28-day compressive strength, respectively. Similarly, at 7 days, the above mixtures obtained the compressive strength of 96.7, 93.9, 95.7, 96.6, 99.1, 97.7 and 99.1% of their 28-day compressive strength, respectively. On the other hand, CCC achieved only 37.9 and 70.6% of the 28-day compressive strength at 3 and 7 days, respectively. It can be seen that high early-

age compressive strength was obtained for GPC ranging from 92-98% and 93-99% of their 28-day compressive strength at 3 and 7 days, respectively. On the other hand, the strength development after 28 days for GPC mixtures was not appreciable in comparison to CCC mixture. For instance at 90 days, the increase in compressive strength for GPC with 0, 5, 10, 15, 20, 25 and 30% OPC from their 28-day compressive strength was 2.2, 4.1, 5.6, 1.8, 1.3, 0.9 and 0.8%, respectively. Similarly, for the same mixtures at 365 days, the compressive strength was observed to be increased by 5.9, 11.9, 10.0, 6.9, 3.6, 2.1 and 2.7%, respectively. On the other hand, for CCC mixture, the increase in compressive strength was observed to be 9.7 and 15.6% at 90 and 365 days, respectively.

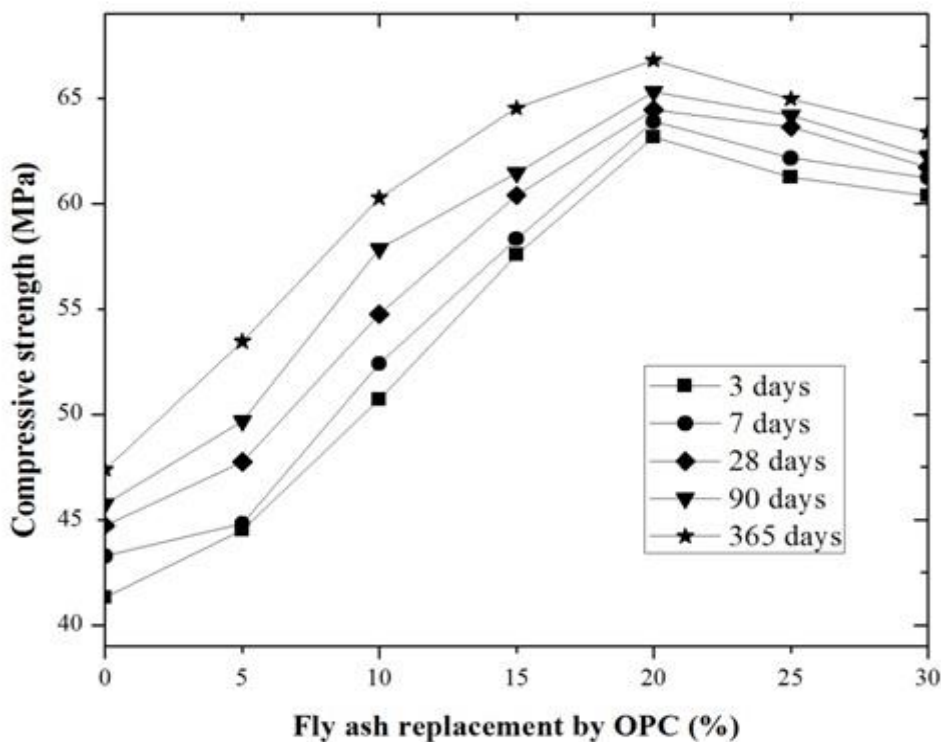


Fig.4.3: Compressive strength of GPC versus OPC content

It was concluded that GPC attained bulk of the strength at the early age and the strength development at later ages was lesser in comparison to CCC. The high early age strength was due to the Geopolymer mechanism which involves the polymerization reaction of alumina and silica obtained from the source material with the alkali-activating solutions, initiated by high-temperature curing. This polymerization reaction yielded strong Na-Al-Si bonds which contributed to high compressive strength. Once the polymerization products were formed, the homogeneity was maintained in the matrix with very slight modifications with the development of age. Similar high early-age compressive strength was also reported by the previous studies. It was reported by Hardjito et al. (2004) and Kong and Sanjayan (2008) that

no significant strength development was possible in case of geopolymers after the completion of temperature curing period as the mechanism was related to polymerization reactions. Joseph and Mathew (2012) also reported no significant development in strength beyond 7 days.

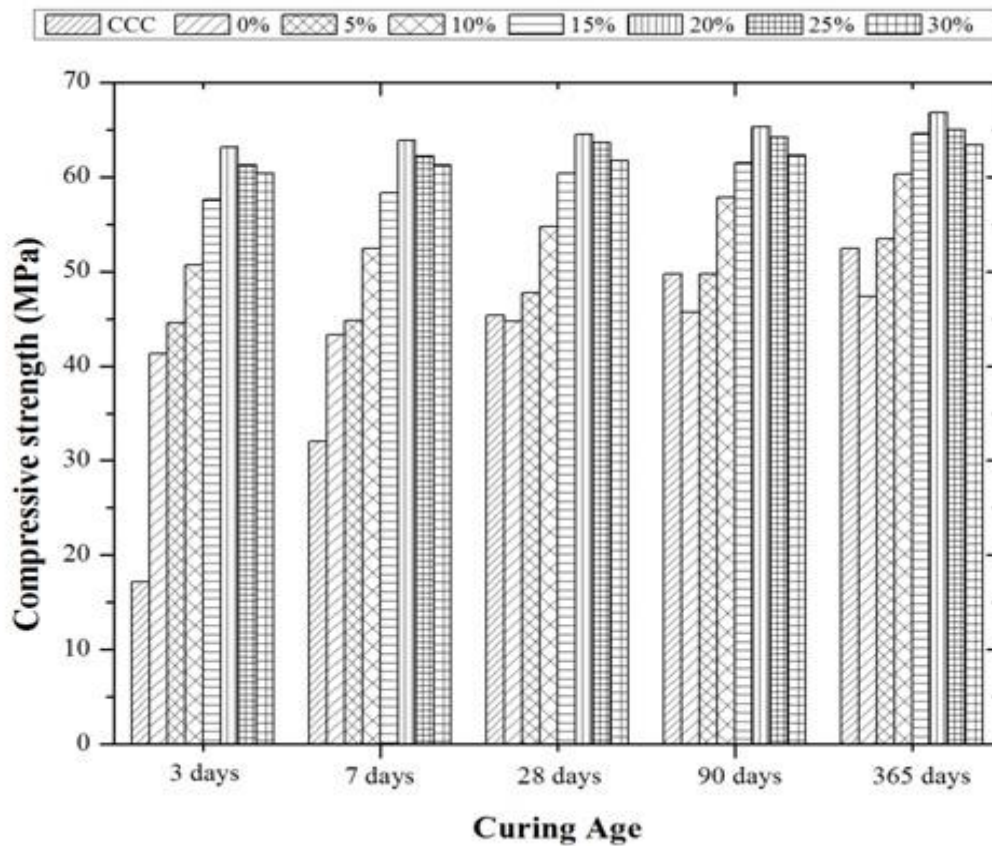


Fig.4.4: Effect of OPC inclusion on compressive strength of GPC

With the inclusion of OPC as fly ash replacement in GPC, the compressive strength increased up to 20% OPC, and beyond that it decreased. For instance at 3 days, GPC mixtures attained compressive strength of 41.32, 44.53, 50.71, 57.58, 63.16, 61.24 and 60.37 MPa with OPC at 0, 5, 10, 15, 20, 25 and 30%, respectively. A similar trend of increase and decrease beyond 20% OPC in compressive strength was also observed at all other ages as well. The maximum compressive strength of 66.81 MPa was obtained for the geopolymer concrete mixture with 20% OPC at 365 days.

For control GPC i.e. with 0% OPC, the silica and alumina were liberated from fly ash which reacted with the alkali-activating solution and form polymerization under high-temperature curing of 80 °C for 24 hours. These polymerization products consist of strong Na-Al-Si bonds which imparted strength to geopolymer concrete. These strength products were also identified from EDS analysis which showed the presence of sodium (Na), aluminium (Al) and silica

(Si), and also confirmed by the XRD analysis which showed the presence of nepheline and albite phases, as explained later in section 4.2.3. With the inclusion of OPC up to 20% in GPC, the increase in strength was due to the reaction of additional OPC with the alkalis present in the mixture which liberated large amount of heat and enhanced the geopolymer mechanism by increasing the effective curing temperature. Also, with the presence of additional calcium (due to inclusion of OPC) in GPC, hydration mechanism took place which lead to the formation of additional CASH and CSH which co-existed with the polymerization product NASH as separate phases (Nath and Sarker, 2012; Alonso and Palomo, 2001; Rovnanik, 2010). The formation of CSH was also confirmed by the XRD analysis, as explained later in section 4.2.3. The additional calcium also expected to accelerate hardening and dissolution by providing extra nucleation sites (Van Deventer et al., 2007; Lee and Van Deventer, 2002b).

On the other hand, the decrease in strength after 20% OPC was due to the reduction in alumina and silica in the geopolymer system relatively (due to lesser silica and alumina in OPC than fly ash) which reduced the polymerization product NASH. This reduction in alumina and silica was also confirmed by the EDS analysis, as explained in section 4.2.3. A similar reduction in strength values after certain calcium content was also observed in the previous studies (Yip et al., 2005; Temuujin et al., 2009; Pacheco-Torgal et al., 2008).

4.2.2 Split Tensile Strength

The tensile strength characteristics of concrete are of considerable importance and the split tensile test is a simple and reliable method of measuring the tensile strength. The cylinder specimens were tested for each mixture and the results are reported as the average of three specimens at the ages of 3, 7, 28, 90 and 365 days, as shown in Figs.4.5 and 4.6. It was observed that high early age split tensile strength was obtained for GPC mixtures as compared to CCC. At 3 days, the split tensile strength for GPC mixtures with 0, 5, 10, 15, 20, 25 and 30% OPC was 92.9, 93.4, 94.4, 93.9, 94.9, 91.2 and 92.8% of their 28-day split tensile strength, respectively as compared to 55.2% for CCC. Similarly, for the same mixtures at 7 days, the split tensile strength was determined as 93.3, 93.4, 93.6, 94.8, 95.2, 93.0 and 93.1% of their 28-day split tensile strength in comparison to 66.2% for CCC. On the other hand, split tensile strength development after 28 days was not significant for GPC mixtures, unlike CCC. At 90 days, the increase in split tensile strength for GPC mixtures with 0, 5, 10, 25, 20, 25 and 30% OPC was found to be increased by 3.1, 3.7, 4.8, 2.4, 2.8, 1.7 and 2.2% from their

28-day split tensile strength, respectively as compared to 16.8% increase for CCC. Similarly, for the same mixtures at 365 days, the increase in split tensile strength was 4.2, 6.6, 6.7, 4.9, 5.3, 4.0 and 4.3%, respectively. However, for CCC mixture at 365 days, the increase was 42.3% from its 28-day split tensile strength. It was observed that GPC mixtures attained bulk of their split tensile strength at the early age of 3 days with very less strength development at later ages. In comparison, CCC mixture showed high strength development with age but exhibited comparatively lesser early age split tensile strength. These results were also in confirmation with the compressive strength results which showed the development of strong Na-Al-Si bonds at the early ages due to polymerization.

With the inclusion of OPC in geopolymer system, an increase in split tensile strength was observed up to 20%, and beyond that it decreased at all ages. The maximum split tensile strength value of 5.35 MPa was achieved for the geopolymer concrete mixtures with 20% OPC at 365 days. The increase in strength was attributed to the fact that with the increase in OPC content, the additional calcium in the mixture reacted with the alkalis and form additional calcium based hydrated products such as CSH and CASH which coexisted with the strong geo-polymeric strength based product NASH and contributed to the early age strength development significantly. The formation of Ca-Si and Ca-Al-Si bonds in the geopolymer system with the inclusion of additional calcium can also be explained through XRD studies, as explained in section 4.2.3, which showed the existence of phases like bavenite and anorthite. Previous studies have also shown significant improvement in microstructure and strength development by adding calcium source in the geopolymer system (Suwan and Fan, 2014; Pangdaeng et al., 2014).

However, with the further increase in OPC beyond 20%, the decremented values of split tensile strength were observed at 25 and 30% OPC at all ages. The decrease in strength was attributed to the fact that with the inclusion of OPC at higher replacement level of fly ash, the increase in calcium would relatively decrease the silica and alumina content in the geopolymer system. This could make the silica and alumina less available for the geo-polymerization reaction and resulted in the lower formation of Na-Al-Si relatively. Another reason for the decremented values of split tensile strength at higher OPC content was due to the increase in effective temperature of curing. As hydration reaction is an exothermal reaction which could possibly increase the effective curing temperature too much that it resulted in substantial loss of moisture.

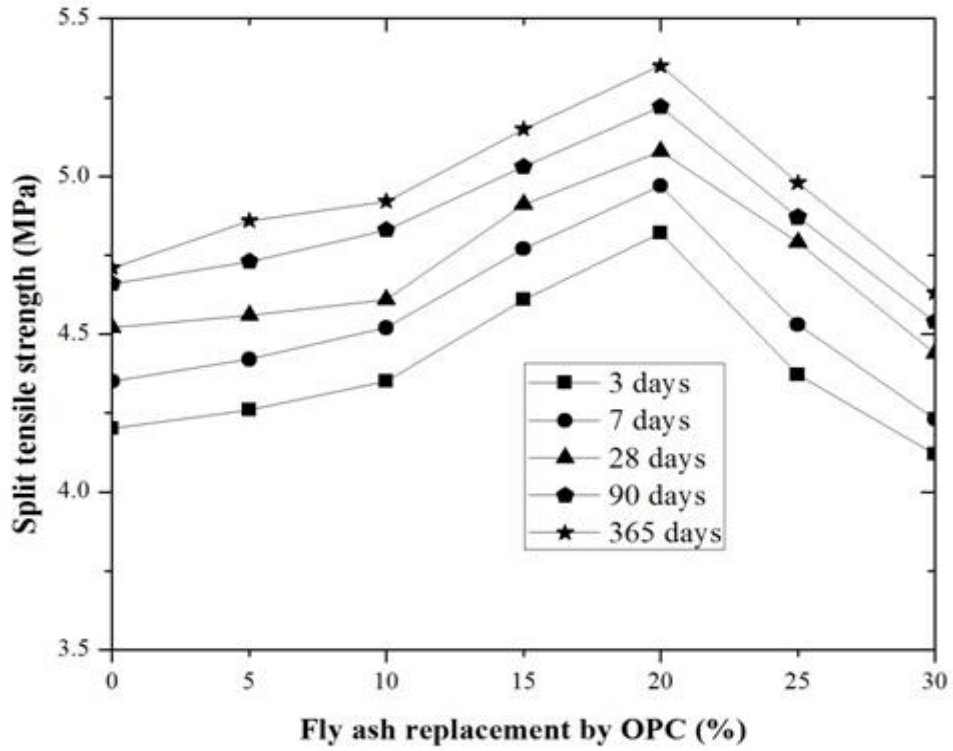


Fig.4.5: Split tensile strength of GPC versus OPC content

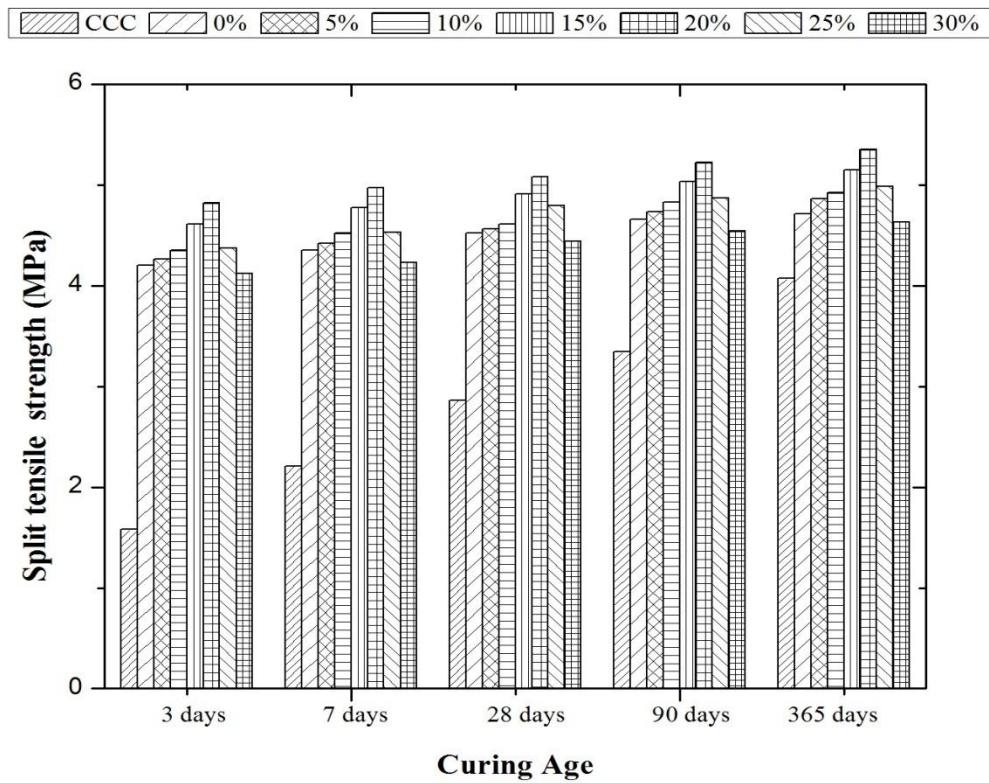


Fig.4.6: Effect of OPC inclusion on split tensile strength of GPC

The physical examination of specimens with higher OPC contents of 25 and 30% also depicted the relatively dry nature as compared to other specimens. A similar decrease in strength values with the increase in curing temperature after a certain specified limit was also observed by Chindaprasirt et al. (2006) and Bakharev (2005a) which reported the loss of moisture as the main reason for strength deterioration.

4.2.3 Microstructure Properties of Geopolymer Concrete

Having obtained the results of compressive strength and split tensile strength results, optimum content of OPC in geopolymer concrete was found to be 20% at all ages. To analyze the mechanism of geopolymer concrete with the inclusion of OPC at micro-level, microstructure properties such as scanning electron microscopy (SEM), energy dispersive spectroscopy (EDS) and X-ray diffraction (XRD) studies were performed on GPC mixtures with 0, 10, 20 and 30% OPC at 3, 7, 28, 90 and 365 days.

4.2.3.1 Geopolymer concrete mixture with 0% OPC

The results of SEM, EDS and XRD analysis for the geopolymer concrete mixture with 0% OPC at 3, 7, 28, 90 and 365 days are presented in Figs. 4.7-4.16. It was observed from the SEM micrographs of 3 and 7 days that a large number of voids and unreacted particles were present in addition to micro-cracks. The high early-age compressive strength was obtained which was associated with the strong Na-Al-Si bonds resulted from the polymerization reactions of silica and alumina with the alkali-activating solution in the presence of high temperature. However, some of the fly ash particles were observed to be unreacted in addition to voids and microcracks. These small cracks would propagate further through branching and can affect the strength characteristics of geopolymer concrete (Perera et al., 2007). The development of voids and cracks was may be due to the moisture loss caused by evaporation of water at the time of temperature curing, or caused by the induced loads at the time of compression testing. Zhao et al. (2007) also reported the presence of micropores in the geopolymer concrete caused by the mixing of geopolymer precursors. Similarly, the voids were associated with the induced air bubbles that may be introduced into the geopolymer system at the time of initial mixing, or by the spaces occupied by water which was evaporated at the time of high-temperature curing. In all the possibilities, the presence of cracks and voids resulted into degraded mechanical properties of geopolymer concrete. It was also observed from the micrographs that with the development of age, the presence of voids

and pore spaces decreased. The decrease in pore spaces confirms slightly lower values obtained for water absorption, porosity and sorptivity with the age development.

The major compounds observed in the EDS results were found to be similar at all ages. The EDS analysis was performed over the specific portion as shown in a rectangle in the micrographs. The polymerization was initiated by the high-temperature curing which resulted in the formation of strong strength based Na-Al-Si bonds. The existence of these compounds was confirmed by the presence of elements such as sodium (Na), aluminum (Al), silica (Si) and oxygen (O). Apart from these, minor peaks of elements such as potassium (K), iron (Fe), magnesium (Mg), titanium (Ti) and carbon (C) were also seen which can be considered as impurity elements. Duxson et al. (2007) also reported that the presence of impurity elements such as Fe, C, K, Ti, etc that decreases the mechanical properties of geopolymer concrete.

The XRD analysis was also carried out on the geopolymer concrete mixture with 0% OPC at the ages of 3, 7, 28, 90 and 365 days to determine the important phases. The obtained peaks were analyzed by the High score X`pert and Match software. It was observed that the major phases were similar at all ages. The results showed the presence of quartz (Q), nepheline (N) and albite (A) at all ages with slightly different intensities. As geopolymers are associated to the polymerization of particles from geological origin such as silica and alumina, the major phase obtained for the geopolymers was quartz (silica oxide). It is a mineral composed of silica and oxygen atoms which combined together to form a continuous framework of the tetrahedral SiO_4 structure.

On the other hand, nepheline is associated with the strong Na-Al-Si bonds caused by the polymerization of geopolymer precursors with the alkali-activating solution. The chemical formula of nepheline is $\text{NaAlSi}_3\text{O}_8$ with a hexagonal crystal structure and can be considered as the major product of geopolymers that impart the strength against the external loadings. Similarly, albite is also associated with the strong Na-Al-Si bonds with slightly different structural arrangements than nepheline. The chemical formula of albite is $\text{NaAlSi}_3\text{O}_8$ with the triclinic structural arrangement. This is also another important mineral in the geopolymer concrete which improves the mechanical properties of geopolymers significantly. It can be concluded here that silica and alumina get liberated by the hydroxide and silicates of sodium, which forms the polymerization products consisting of nepheline and albite in the presence of high temperature and imparted high early age strength.

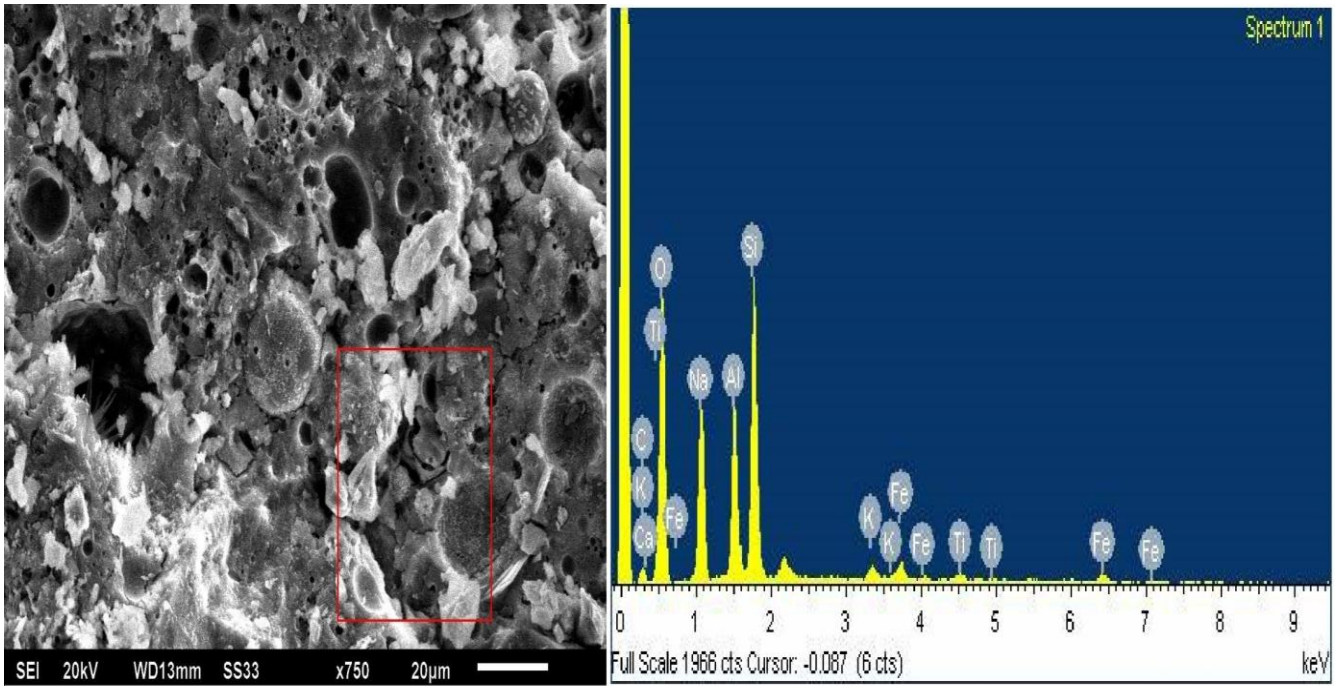


Fig.4.7: SEM/EDS analysis of GPC with 0% OPC at 3 days

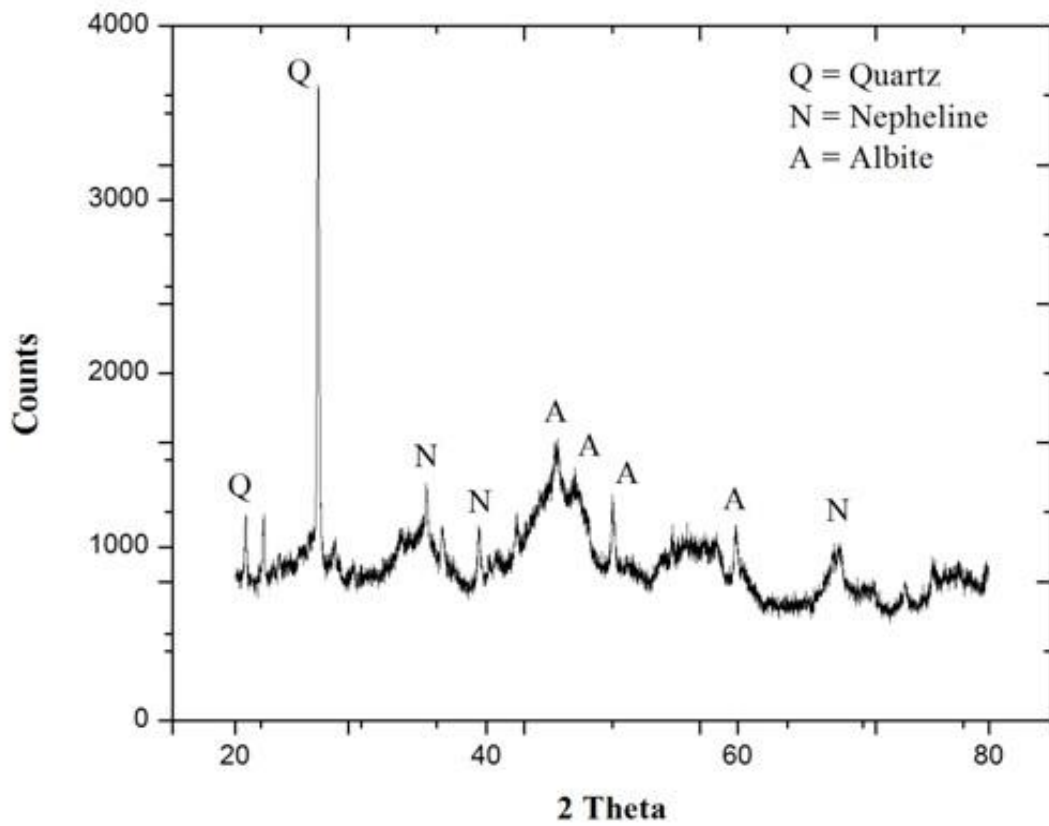


Fig.4.8: XRD analysis of GPC with 0% OPC at 3 days

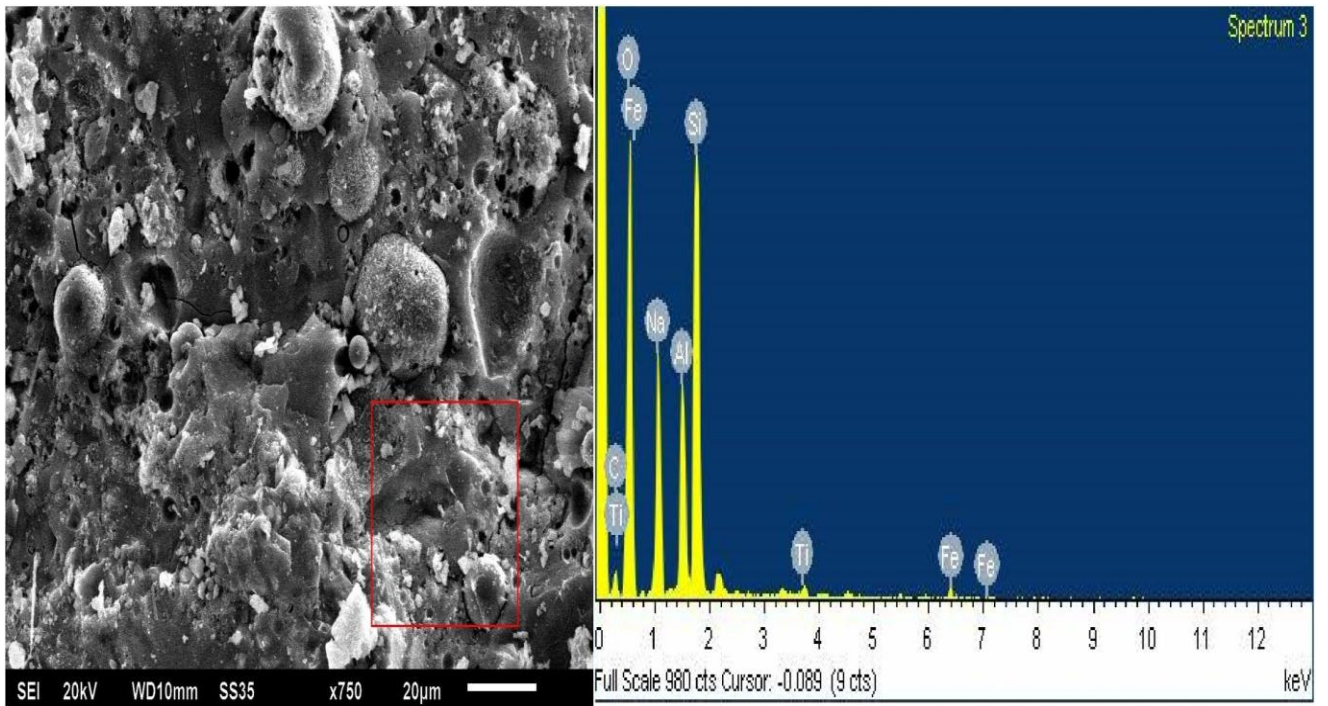


Fig.4.9: SEM/EDS analysis of GPC with 0% OPC at 7 days

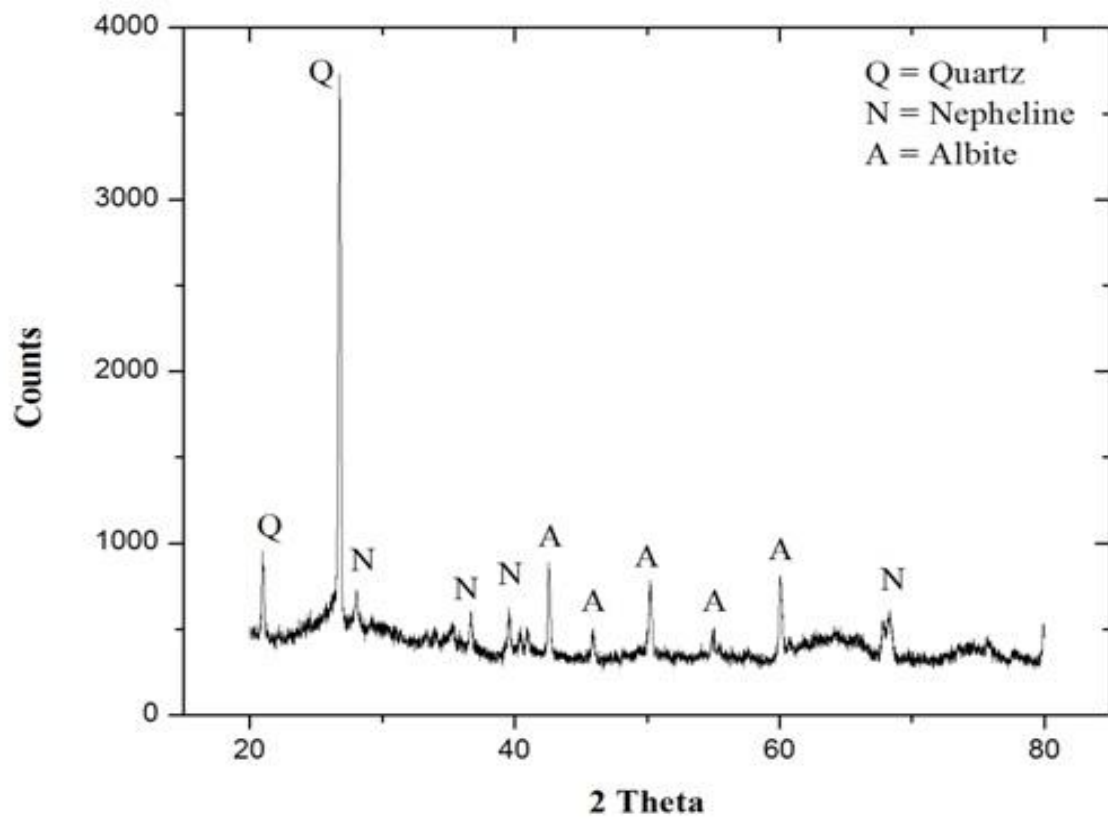


Fig.4.10: XRD analysis of GPC with 0% OPC at 7 days

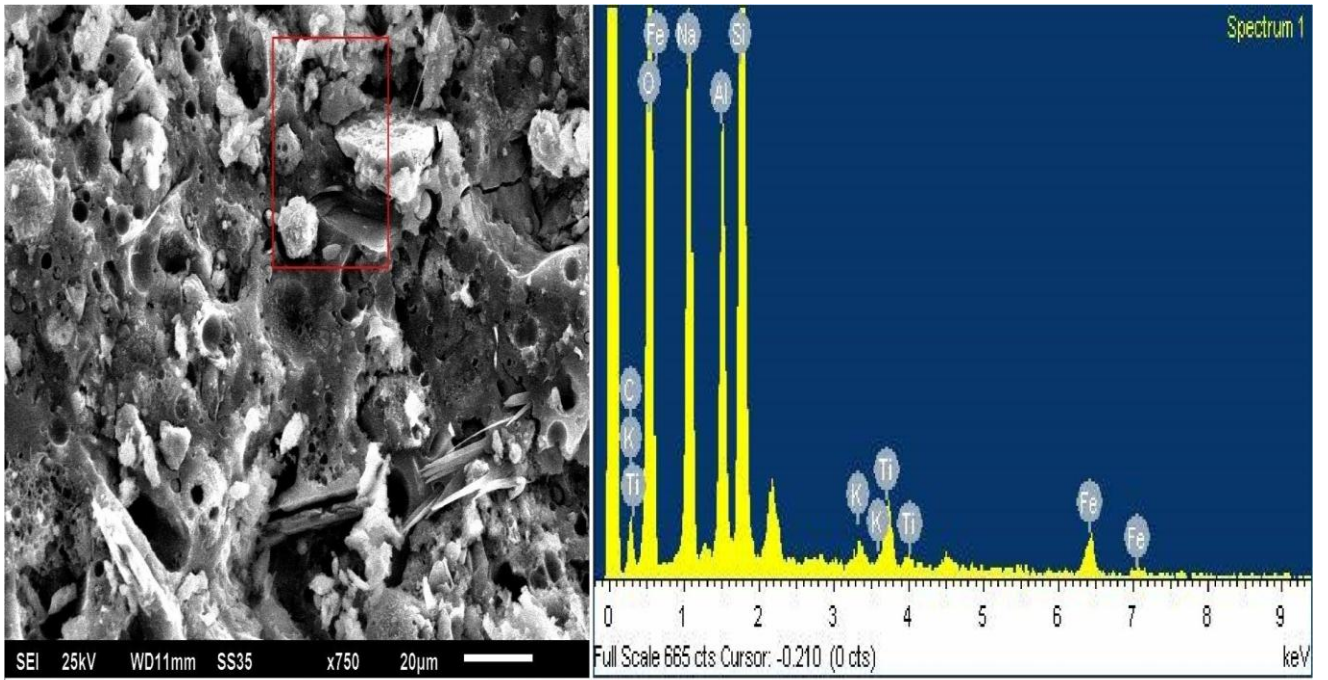


Fig.4.11: SEM/EDS analysis of GPC with 0% OPC at 28 days

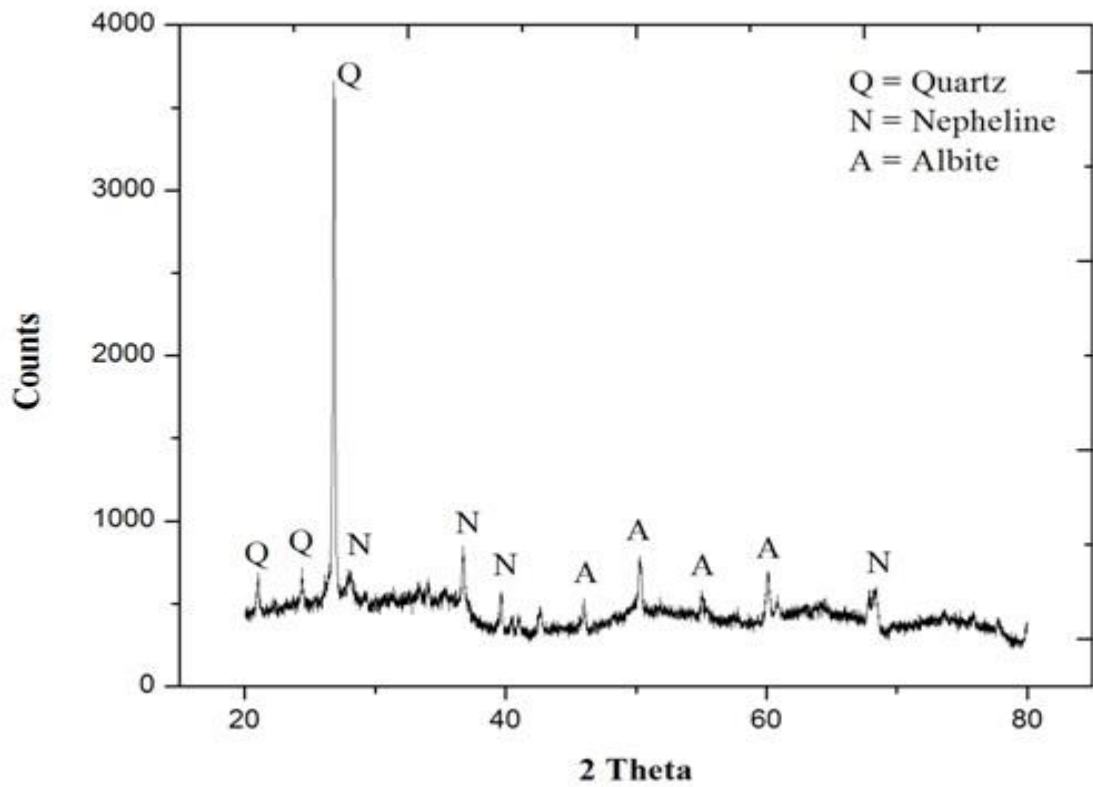


Fig.4.12: XRD analysis of GPC with 0% OPC at 28 days

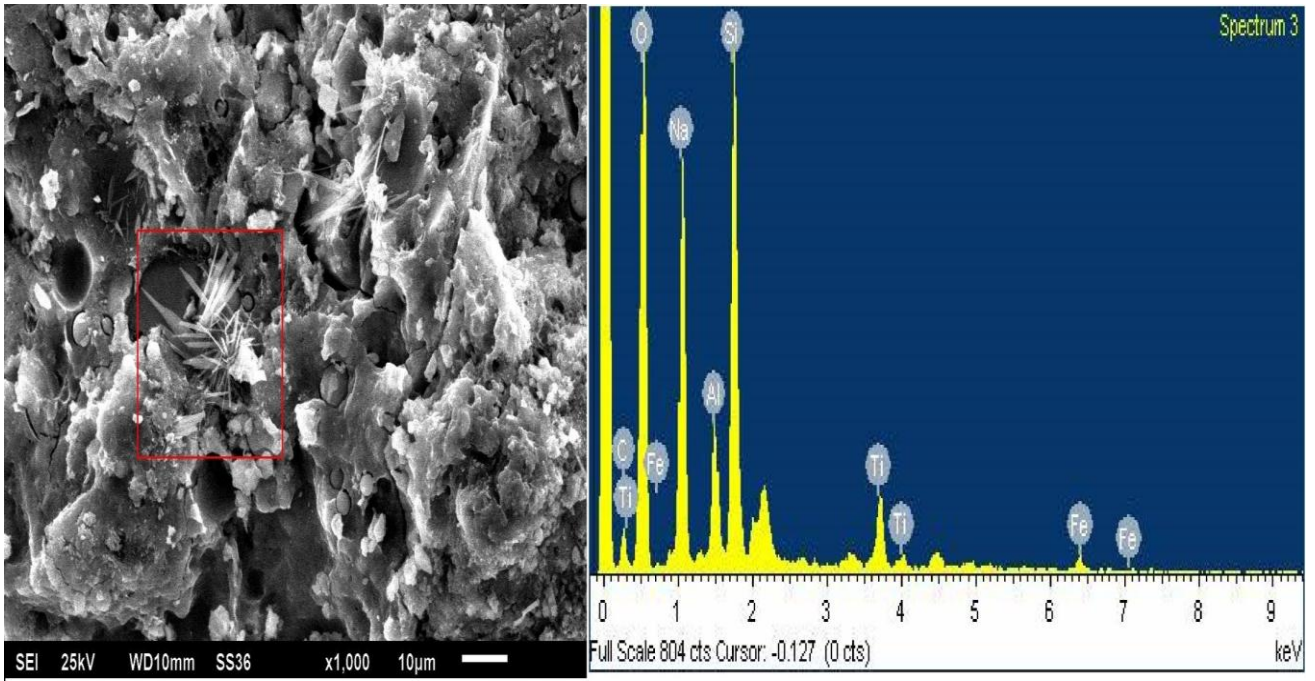


Fig.4.13: SEM/EDS analysis of GPC with 0% OPC at 90 days

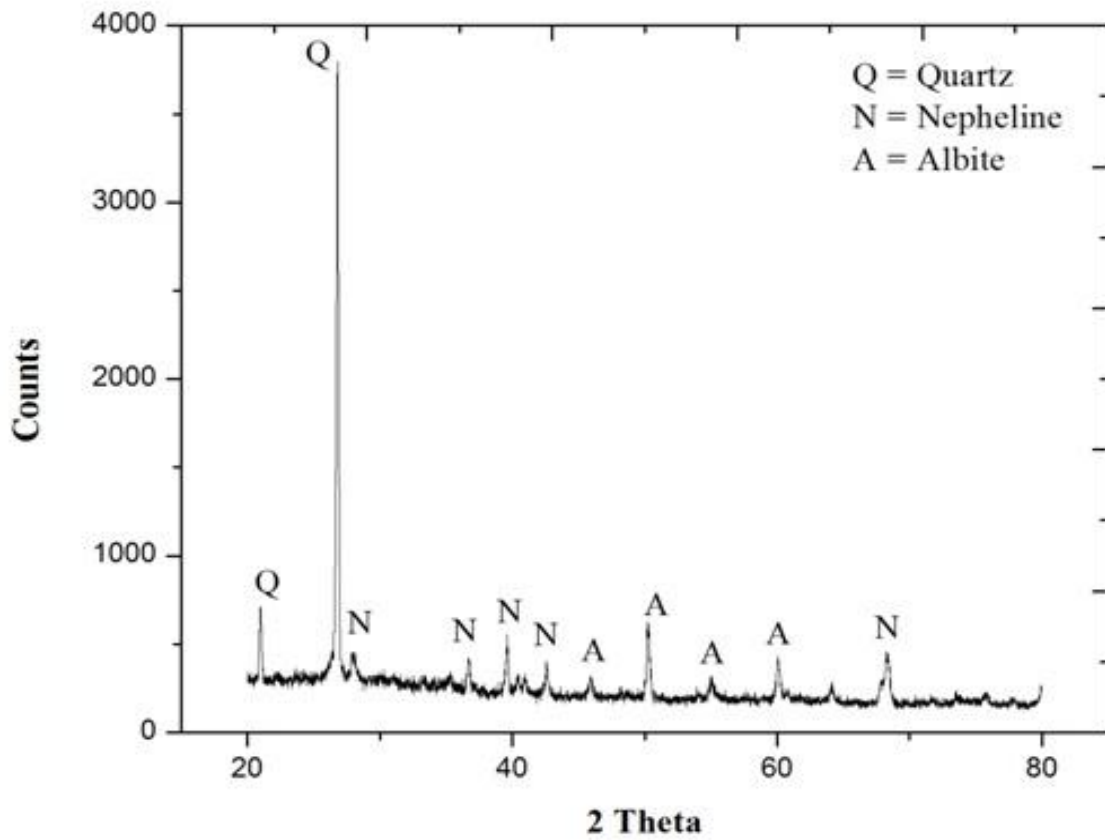


Fig.4.14: XRD analysis of GPC with 0% OPC at 90 days

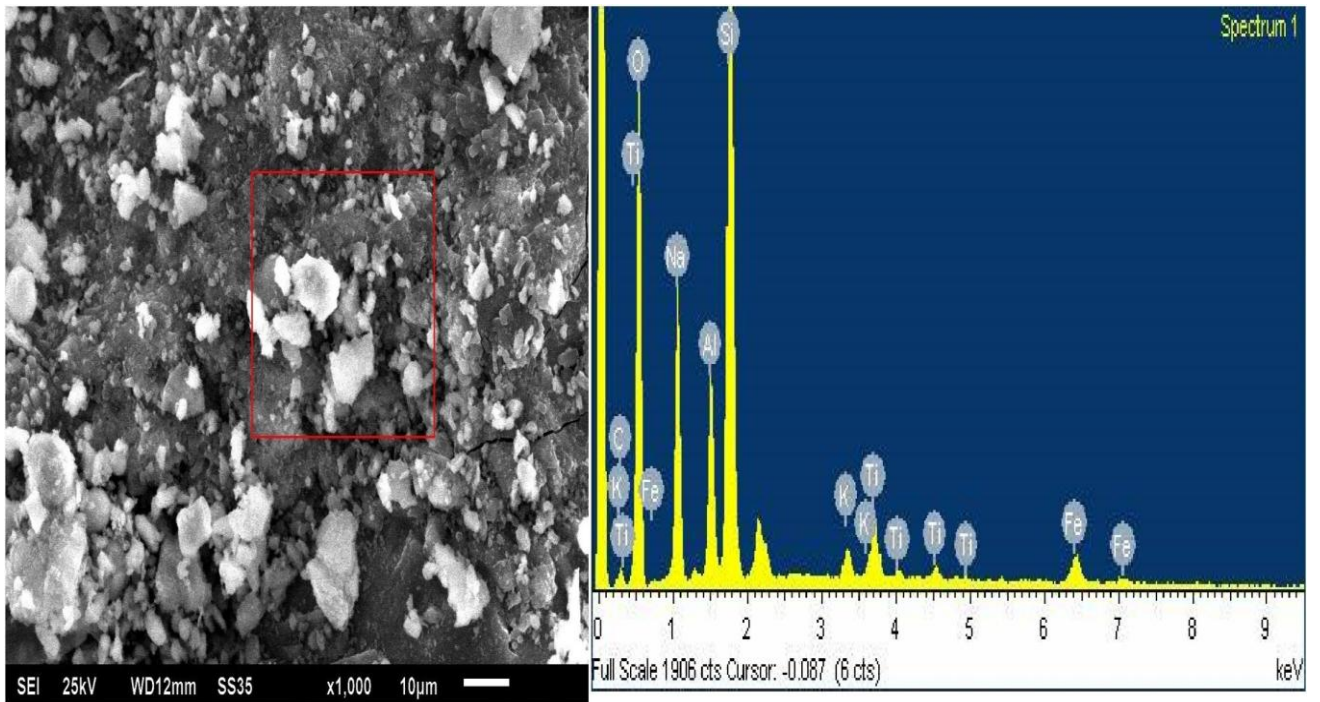


Fig.4.15: SEM/EDS analysis of GPC with 0% OPC at 365 days

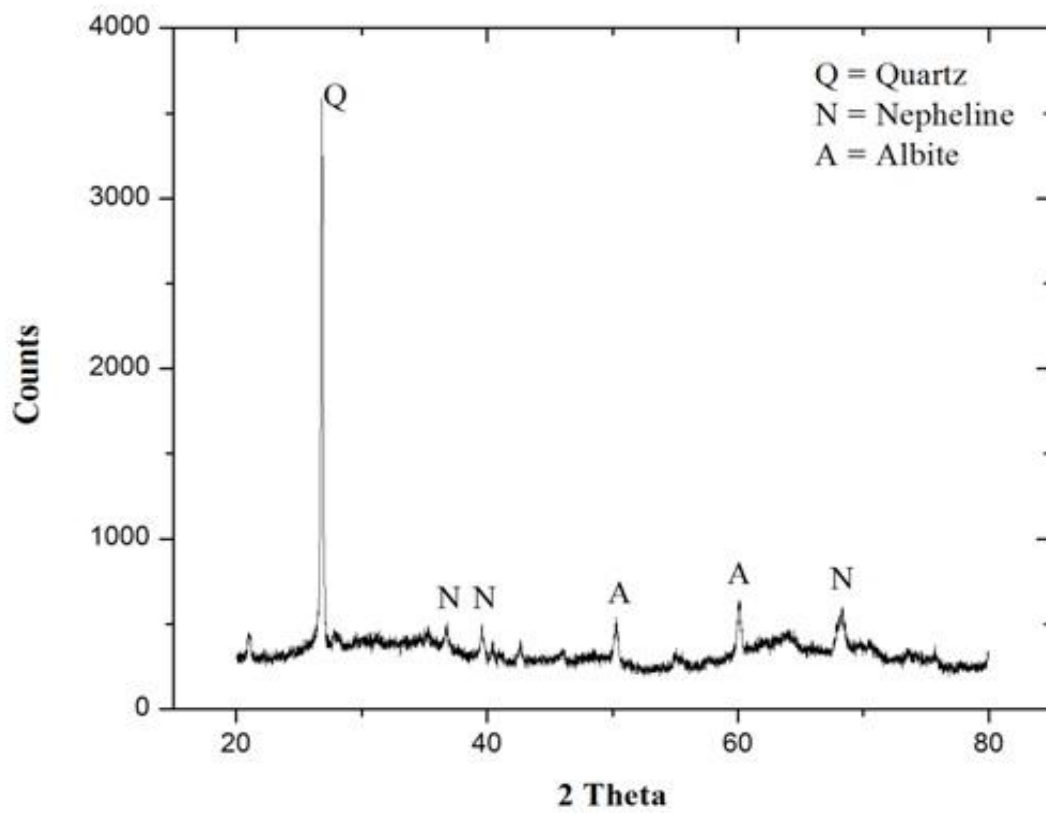


Fig.4.16: XRD analysis of GPC with 0% OPC at 365 days

4.2.3.2 Geopolymer concrete mixture with 10% OPC

SEM, EDS and XRD results of the geopolymer concrete mixtures with 10% OPC are shown in Figs. 4.17-4.26. At 3 days, the SEM micrographs showed the presence of micro-cracks and void spaces with some unreacted fly ash particles. The 7 days micrograph was observed to be similar to that of 3 days micrographs in terms of voids and pore spaces. However, at 28 days, more compact and dense matrix was seen with fewer cracks, voids and pore spaces. Similar observations were also made for the micrograph at 90 and 365 days with even more compact matrix. The improvement in microstructure was attributed to the formation of additional calcium based products that coexisted with the polymeric compounds. Also as compared to geopolymer mixture with 0% OPC, the SEM micrographs of geopolymer mixture with 10% OPC showed fewer cracks, voids and pore spaces.

The EDS analysis of the region specified as the rectangle portion in the SEM micrograph showed the presence of sodium (Na), aluminium (Al), silica (Si), oxygen (O) and calcium (Ca) as major elements and some impurity elements such as titanium (Ti), iron (Fe) and potassium (K). As compared to the geopolymer mixture with 0% OPC, calcium was observed which confirmed the presence of calcium based compounds in the geopolymer system.

This additional calcium reacted with the alkalis present in the geopolymer system and form calcium based hydrated compounds. The inclusion of OPC thus induced Ca-Si or Ca-Al-Si bonds in addition to strong Na-Al-Si polymeric bonds, which improved the microstructure and increased the load carrying capacity of GPC.

The XRD results showed the presence of quartz (Q), nepheline (N), albite (A), bavenite (B) and CSH as the major phases developed in the geopolymer concrete with the inclusion of additional calcium source i.e. OPC. Quartz is associated with oxides of silica with the maximum intensity whereas nepheline and albite are associated with the strong Na-Al-Si bonds developed by the polymerization of silica and alumina with the alkali solution.

As compared to XRD results of geopolymer mixture with 0% OPC, bavenite and CSH were determined as new phases. Bavenite is associated with calcium-based hydrated product calcium-alumino-silicate hydrate (CASH) and CSH is associated with calcium silicate hydrate, which coexisted with NASH and thus increased the mechanical properties of GPC blended with 10% OPC.

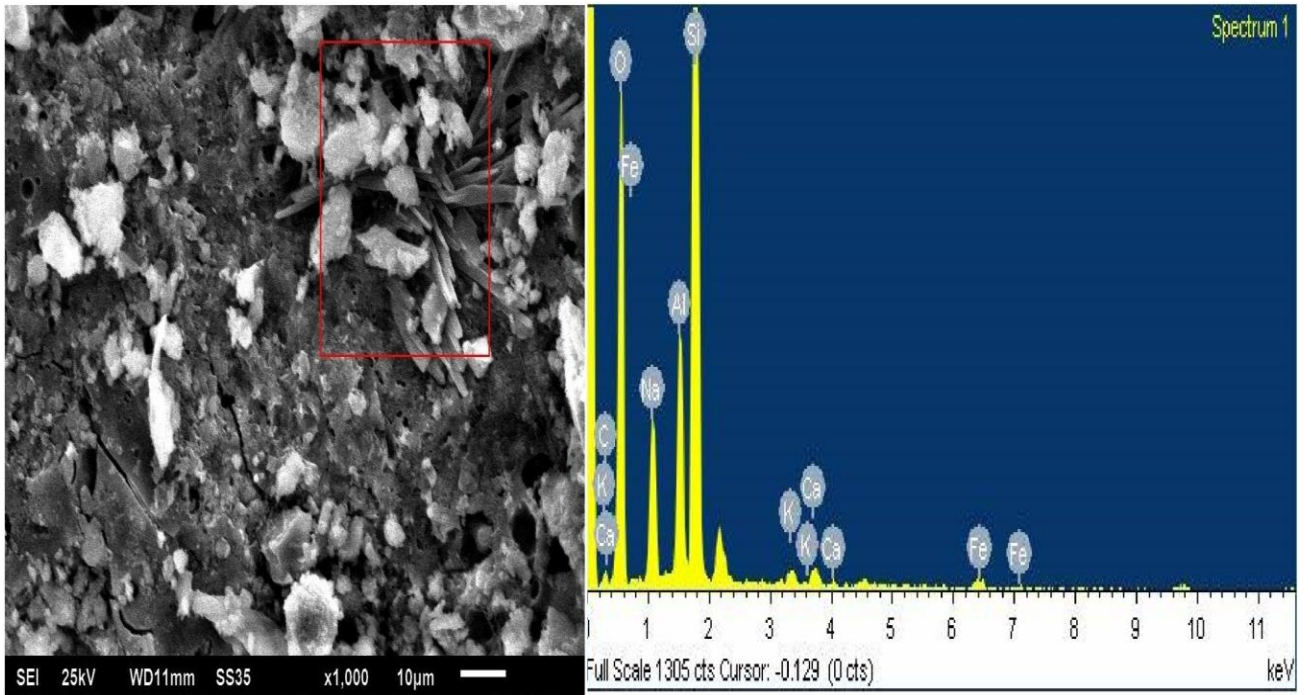


Fig.4.17: SEM/EDS analysis of GPC with 10% OPC at 3 days

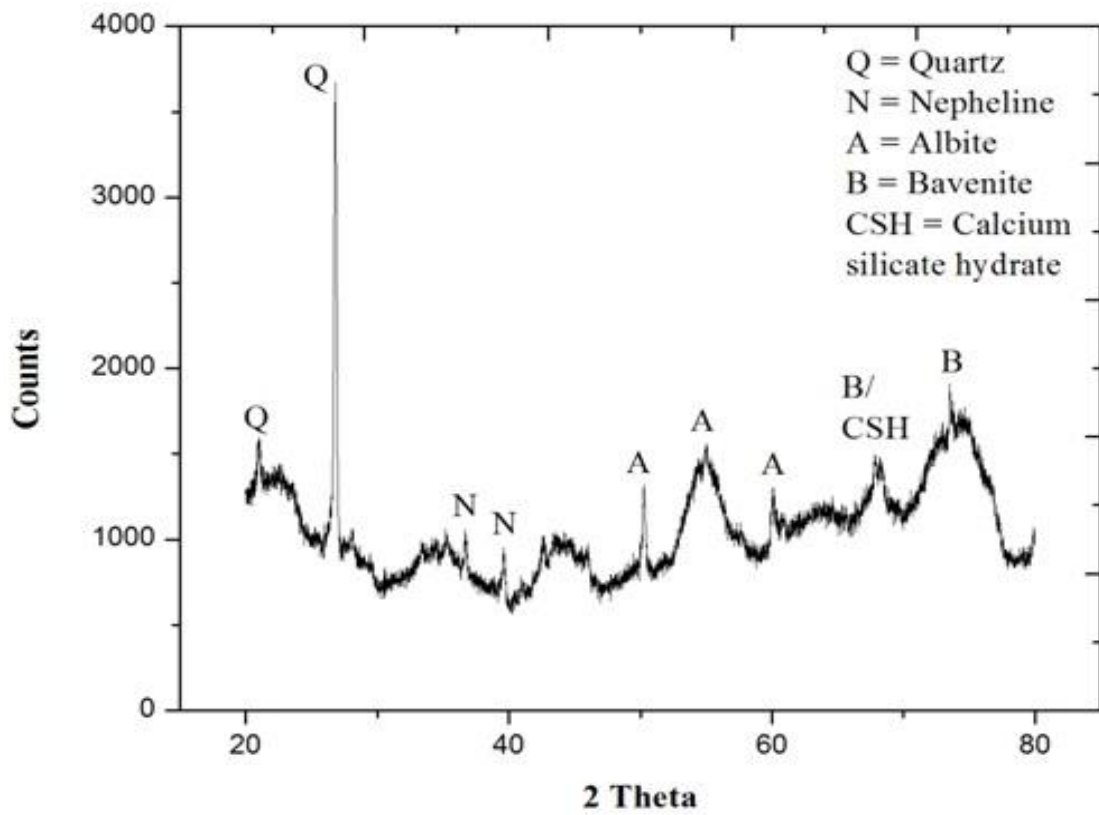


Fig.4.18: XRD analysis of GPC with 10% OPC at 3 days

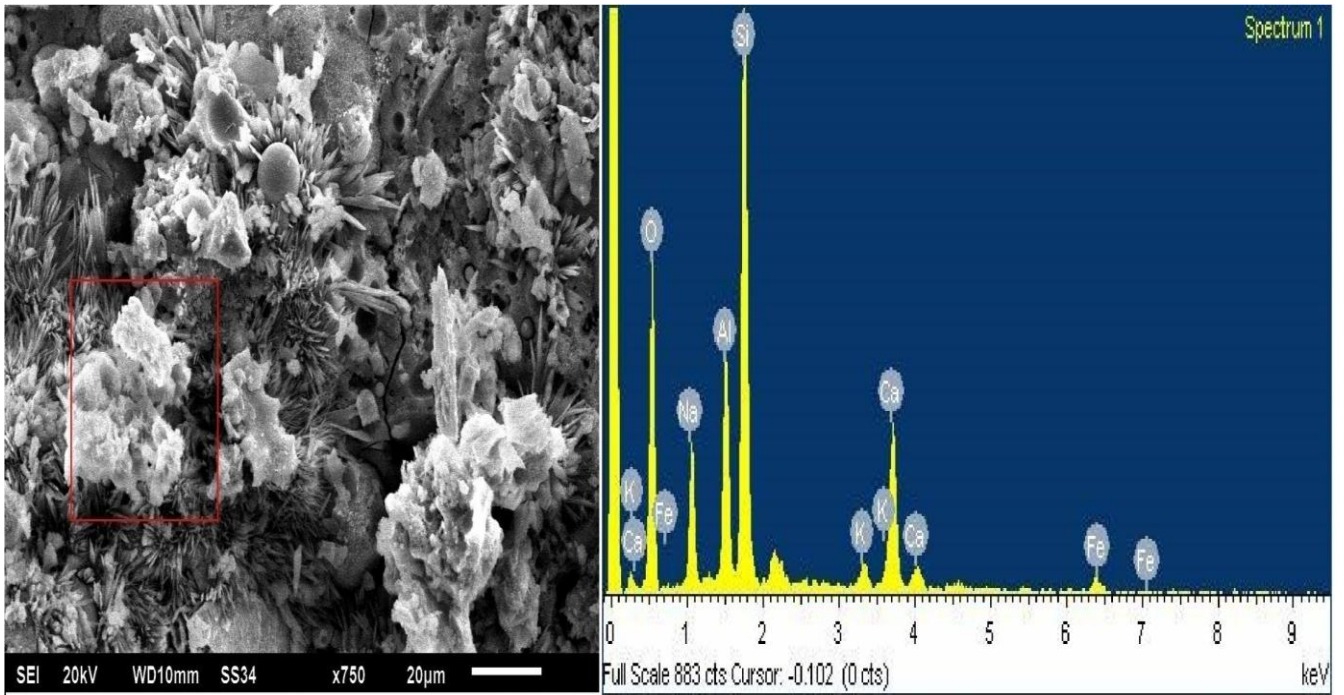


Fig.4.19: SEM/EDS analysis of GPC with 10% OPC at 7 days

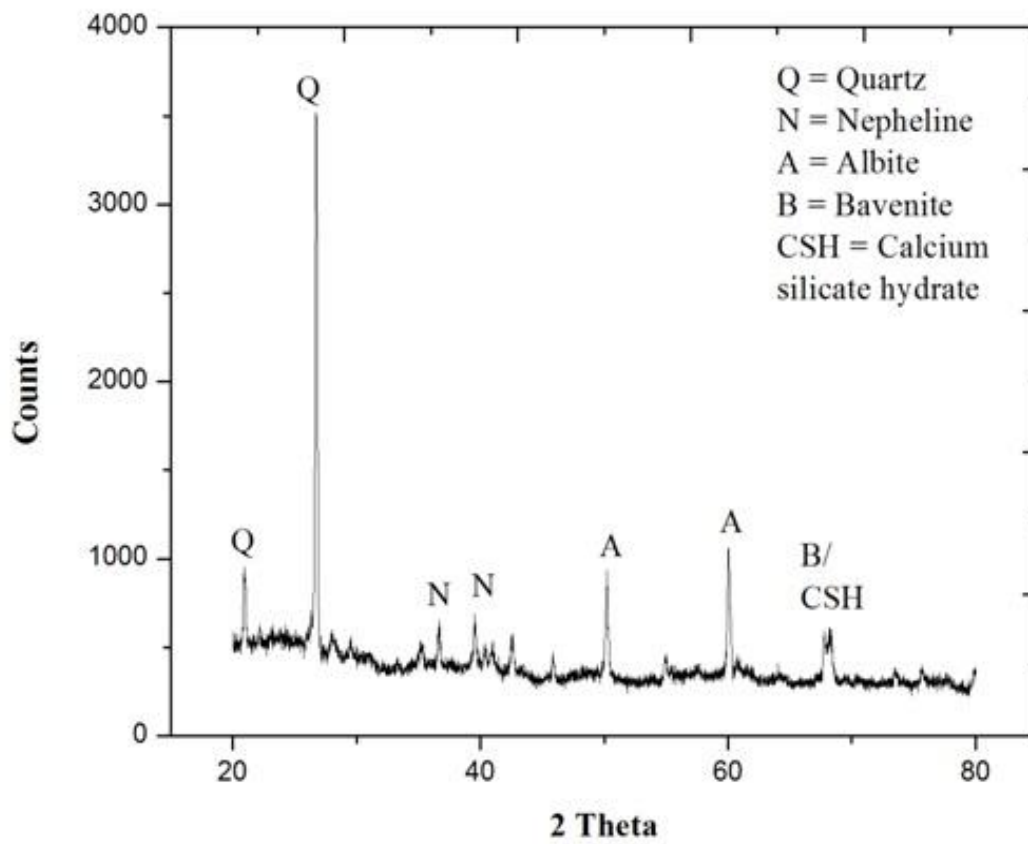


Fig.4.20: XRD analysis of GPC with 10% OPC at 7 days

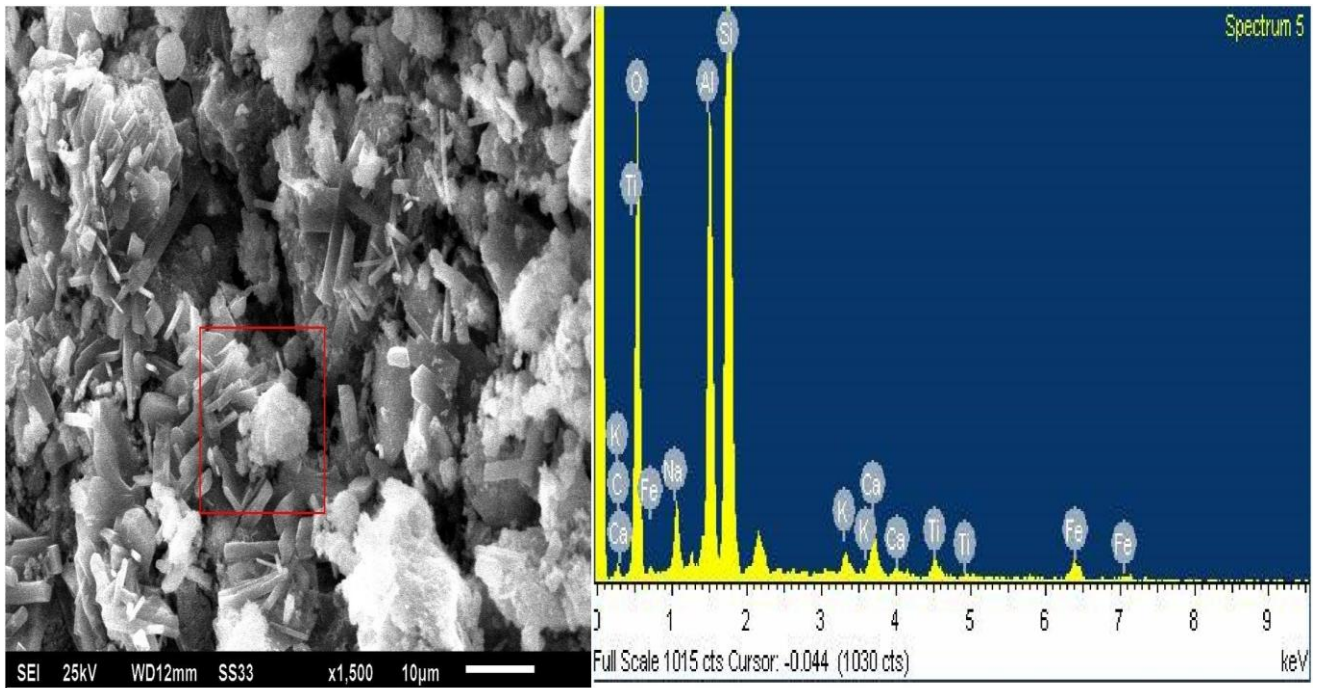


Fig.4.21: SEM/EDS analysis of GPC with 10% OPC at 28 days

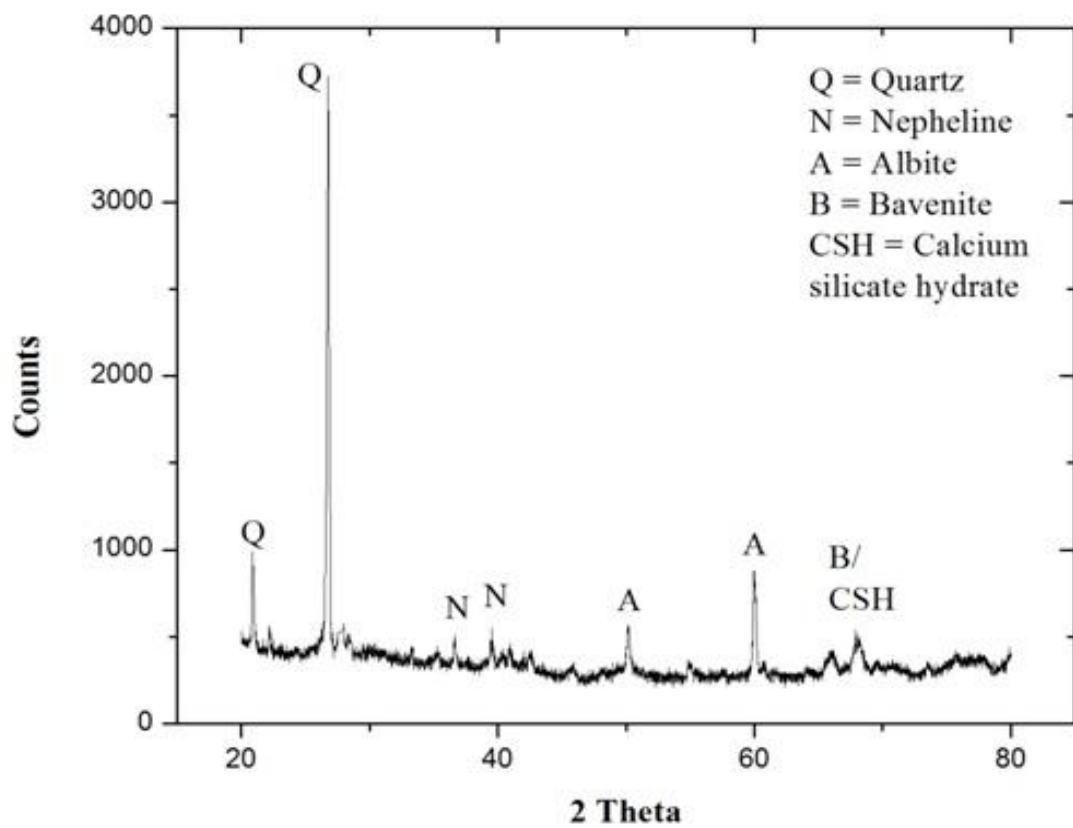


Fig.4.22: XRD analysis of GPC with 10% OPC at 28 days

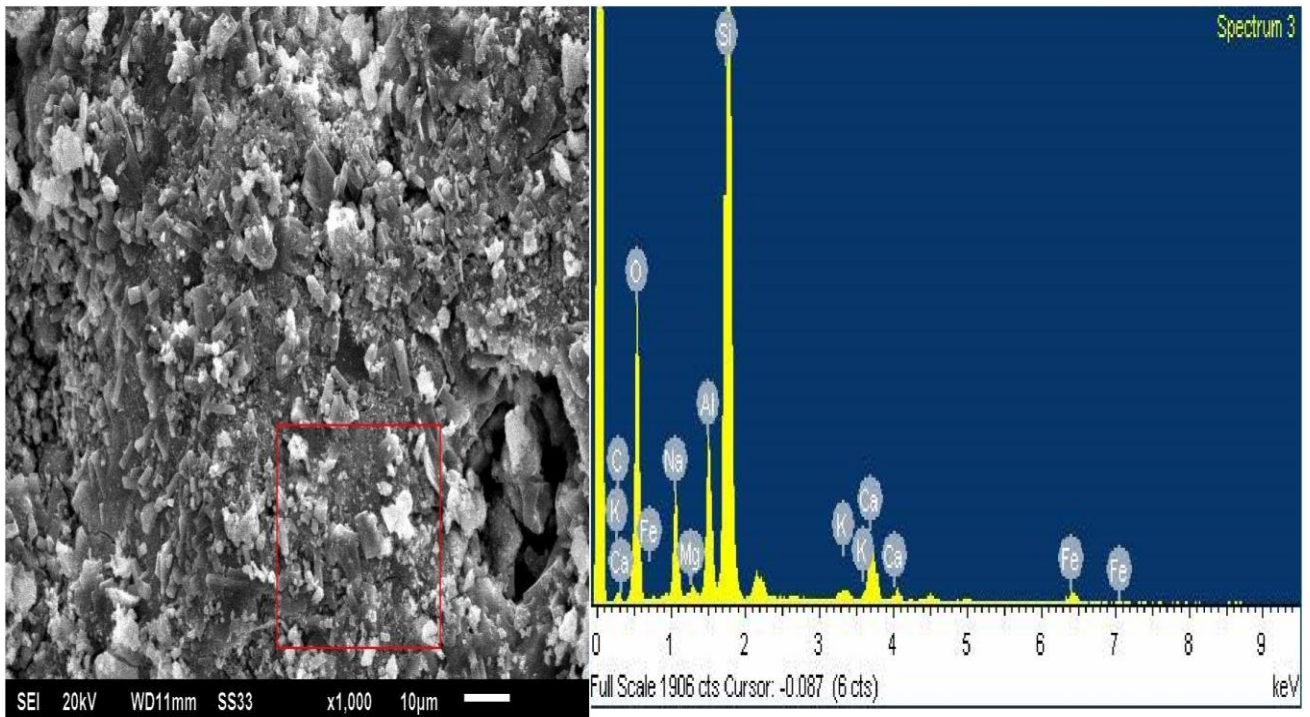


Fig.4.23: SEM/EDS analysis of GPC with 10% OPC at 90 days

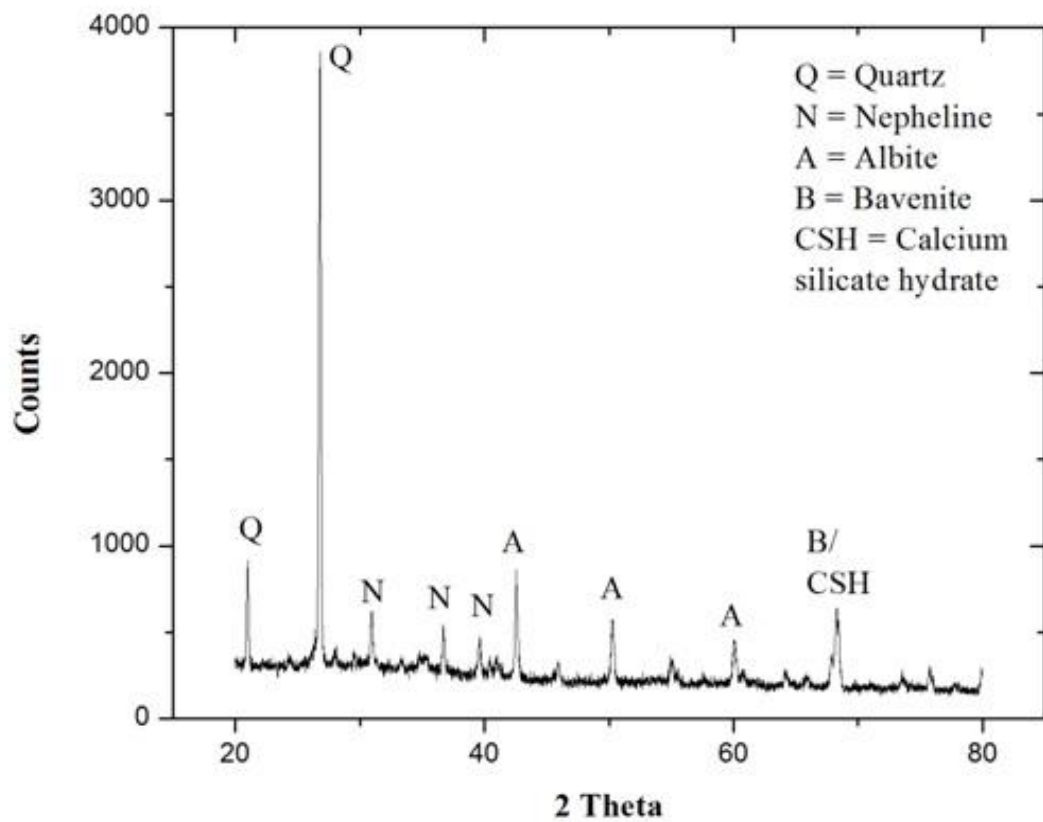


Fig.4.24: XRD analysis of GPC with 10% OPC at 90 days

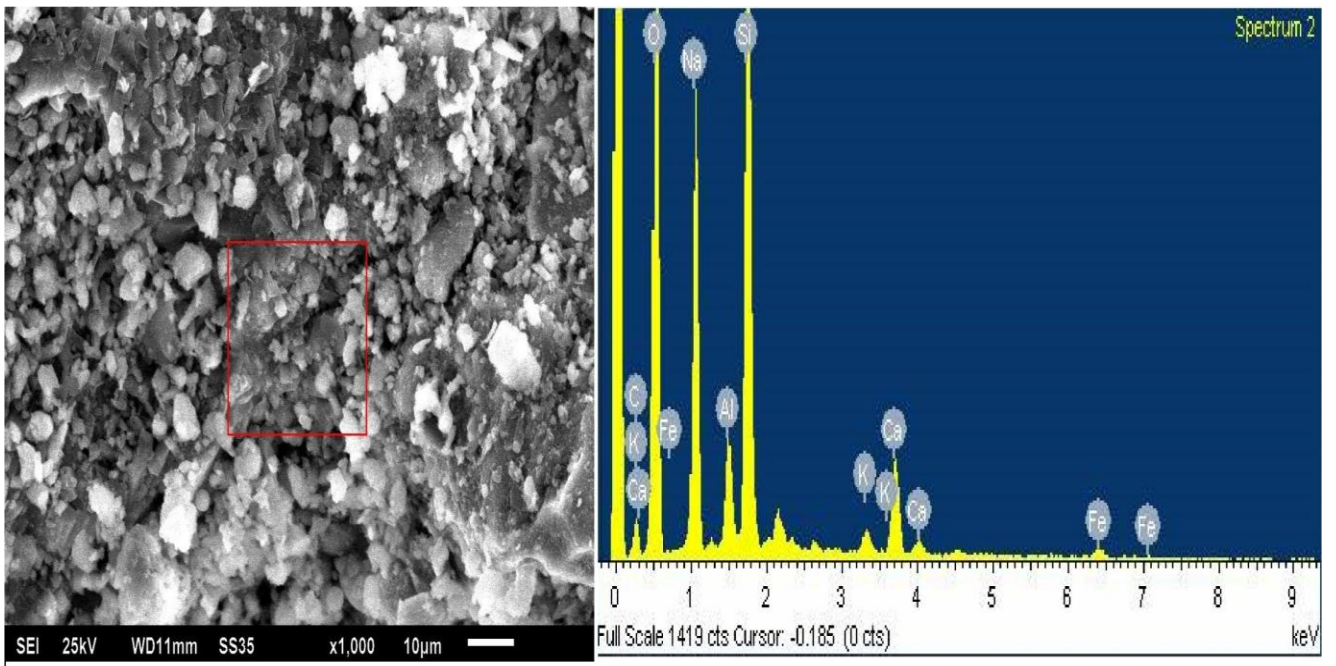


Fig.4.25: SEM/EDS analysis of GPC with 10% OPC at 365 days

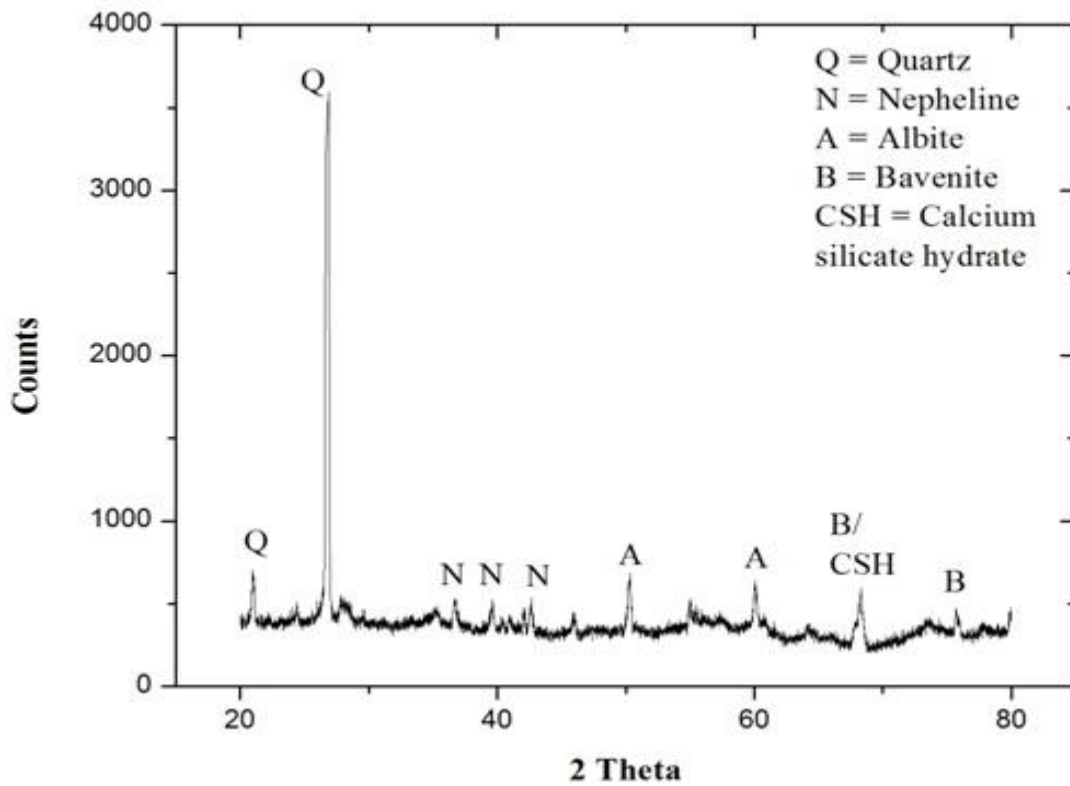


Fig.4.26: XRD analysis of GPC with 10% OPC at 365 days

4.2.3.3 Geopolymer concrete mixture with 20% OPC

The microstructure properties were evaluated for the geopolymer concrete mixture with 20% OPC by performing SEM, EDS and XRD analysis as shown in Figs. 4.27-4.36. For GPC at 3 and 7 days, almost similar SEM micrographs were obtained which showed dense and compact matrix with very few cracks, voids and pore spaces as compared to geopolymer mixtures with 0 and 10% OPC. However, with the development of age at 28, 90 and 365 days, the micrographs were appeared to be more refined with almost no cracks and pore spaces. This was attributed to the higher degree of polymerization product NASH in addition to calcium hydrated products such as CSH and CASH produced by hydration reaction of additional calcium due to OPC (Dombrowski et al., 2007). These additional CSH hydrates filled the pre-water filled pores that evaporated during temperature curing and thereby increased the mechanical strength and microstructure characteristics. The major failure of concrete is normally triggered by the presence of crack between matrix aggregate interfaces. In this case, no significant cracks were observed which indicate a proper bonding of the geopolymer matrix aggregate interface and thus enhanced the external load carrying capacity of the concrete system by blocking the crack path.

Also, almost no unreacted fly ash and OPC particles were seen in the microstructure as all the particles reacted into polymerization and hydration and resulted in the more compact matrix. In addition, due to quick solidification characteristics of calcium, its reaction with the alkaline present in OPC showed the quick formation of hydration products. The EDS analysis of geopolymer mixture with 20% OPC show the presence of sodium (Na), aluminium (Al), silica (Si), calcium (Ca) and some impurity elements such as titanium (Ti), iron (Fe), potassium (K) and carbon (C) at all ages. The significant difference in the EDS results as compared to the geopolymer mixtures with 0 and 10% OPC was the presence of calcium in a higher content, as observed from the higher peaks at all ages. The higher calcium increased the Ca/Al and Ca/Si ratio in the geopolymer system which increased the hydrated products CASH and CSH. The similar coexistence of CSH in the geopolymer system which filled the pore spaces and resulted in less permeable and compact microstructure was also reported in the previous literature (Yip et al., 2005; Buchwald et al., 2007).

The XRD results showed the presence of quartz (Q) with the highest peak and the phases like nepheline (N) and albite (A) showing the presence of geopolymer products NASH with different structural arrangements.

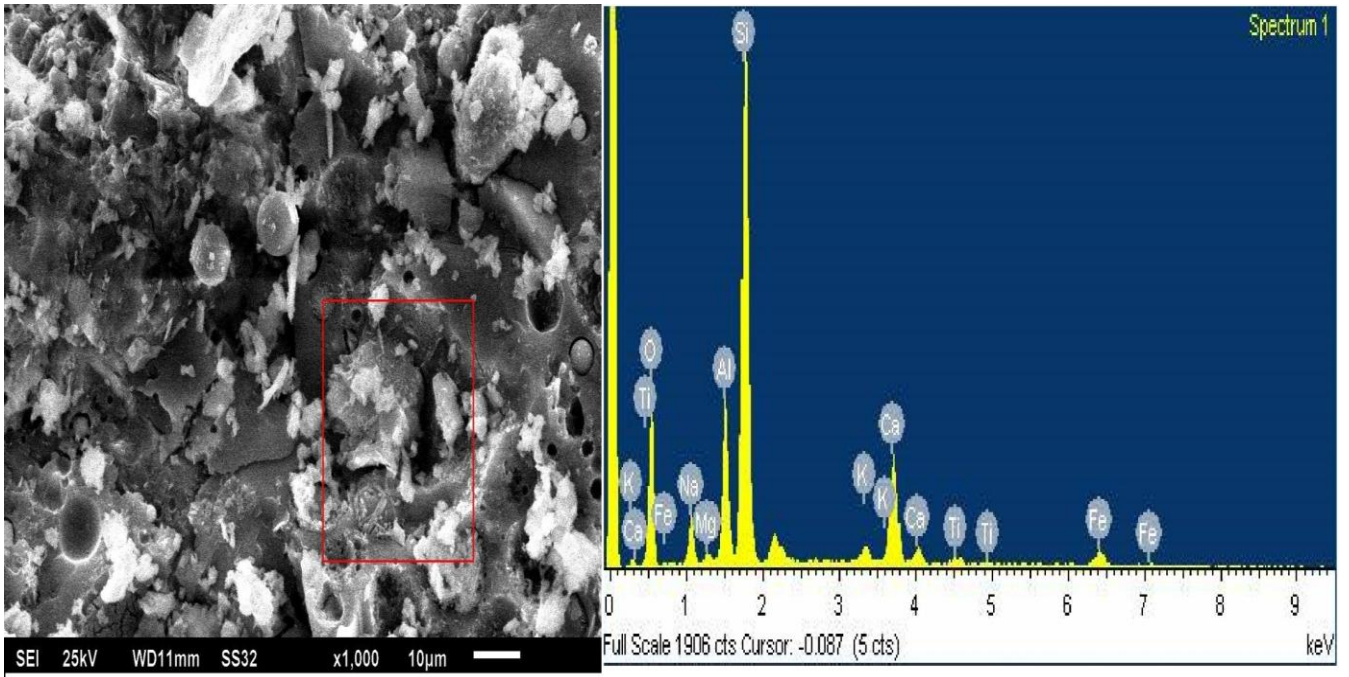


Fig.4.27: SEM/EDS analysis of GPC with 20% OPC at 3 days

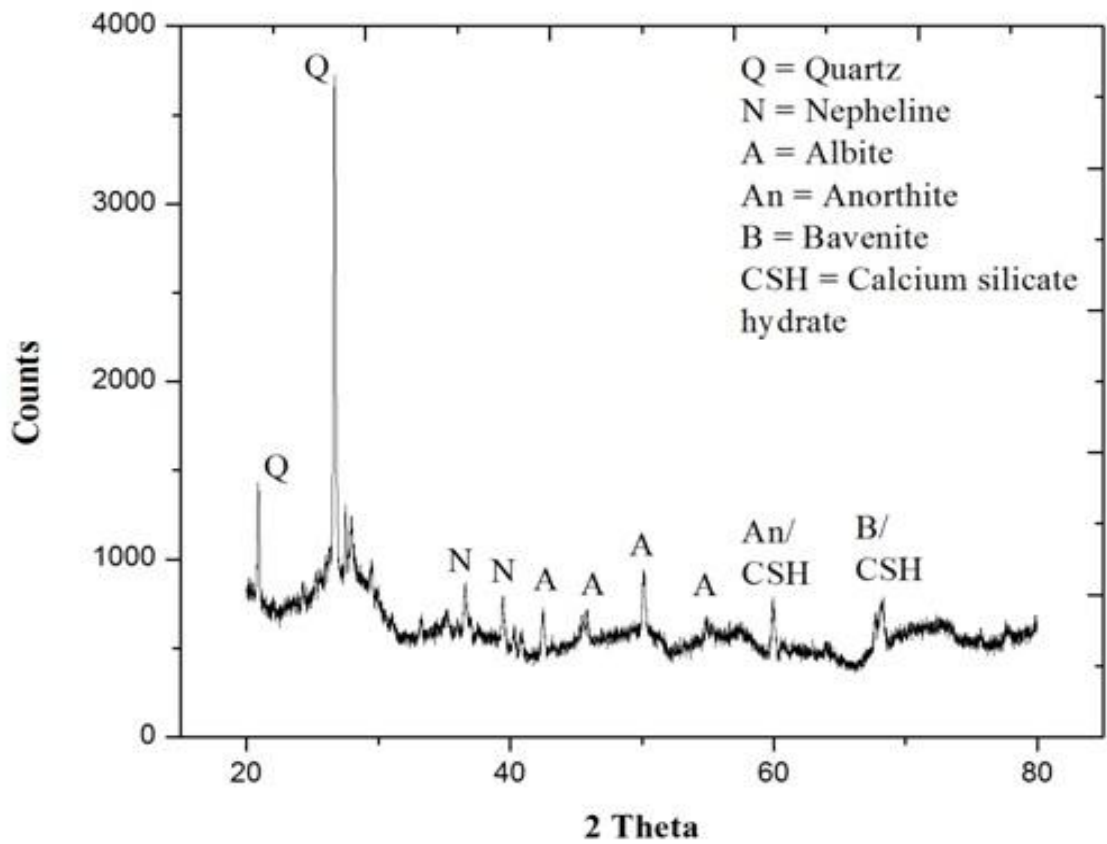


Fig.4.28: XRD analysis of GPC with 20% OPC at 3 days

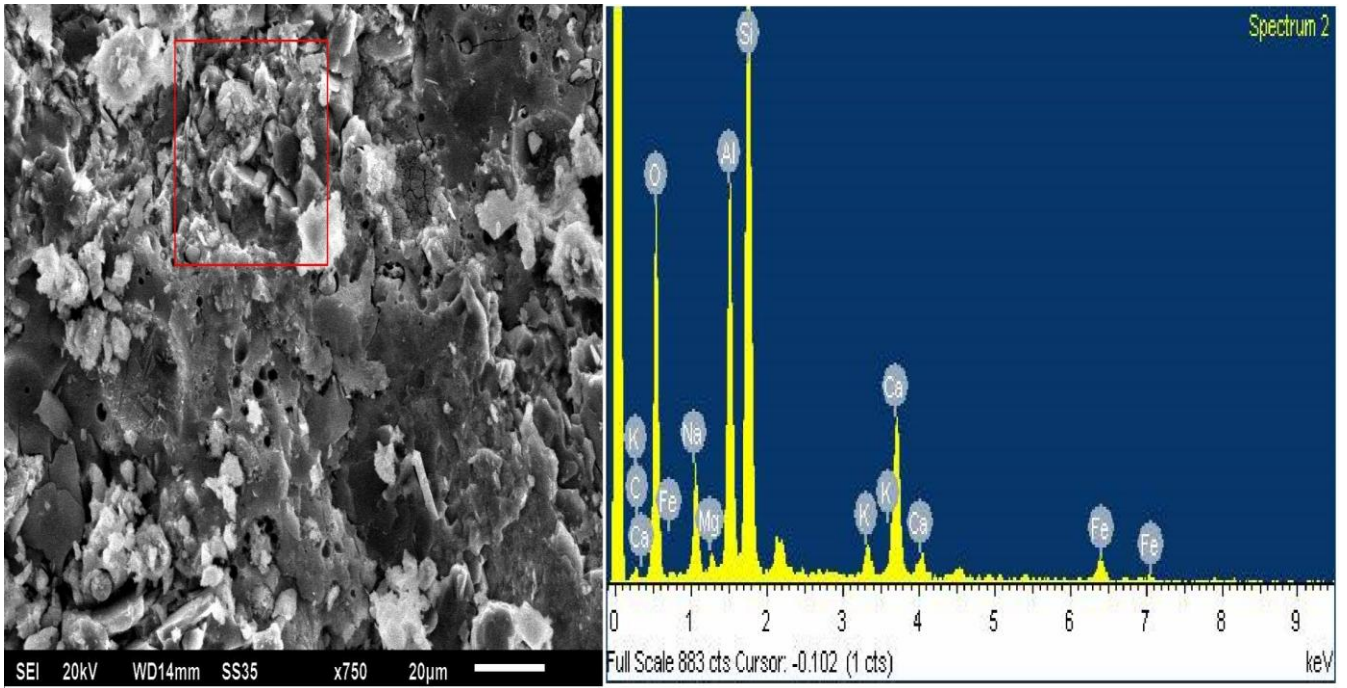


Fig.4.29: SEM/EDS analysis of GPC with 20% OPC at 7 days

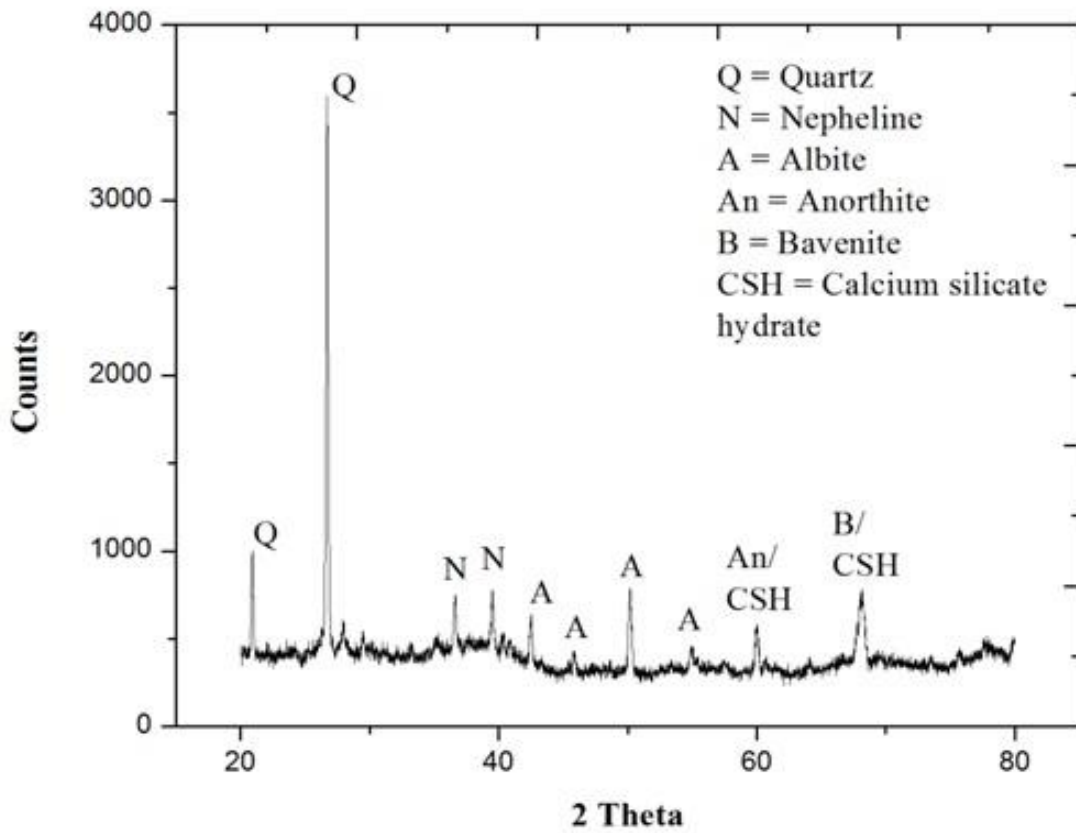


Fig.4.30: XRD analysis of GPC with 20% OPC at 7 days

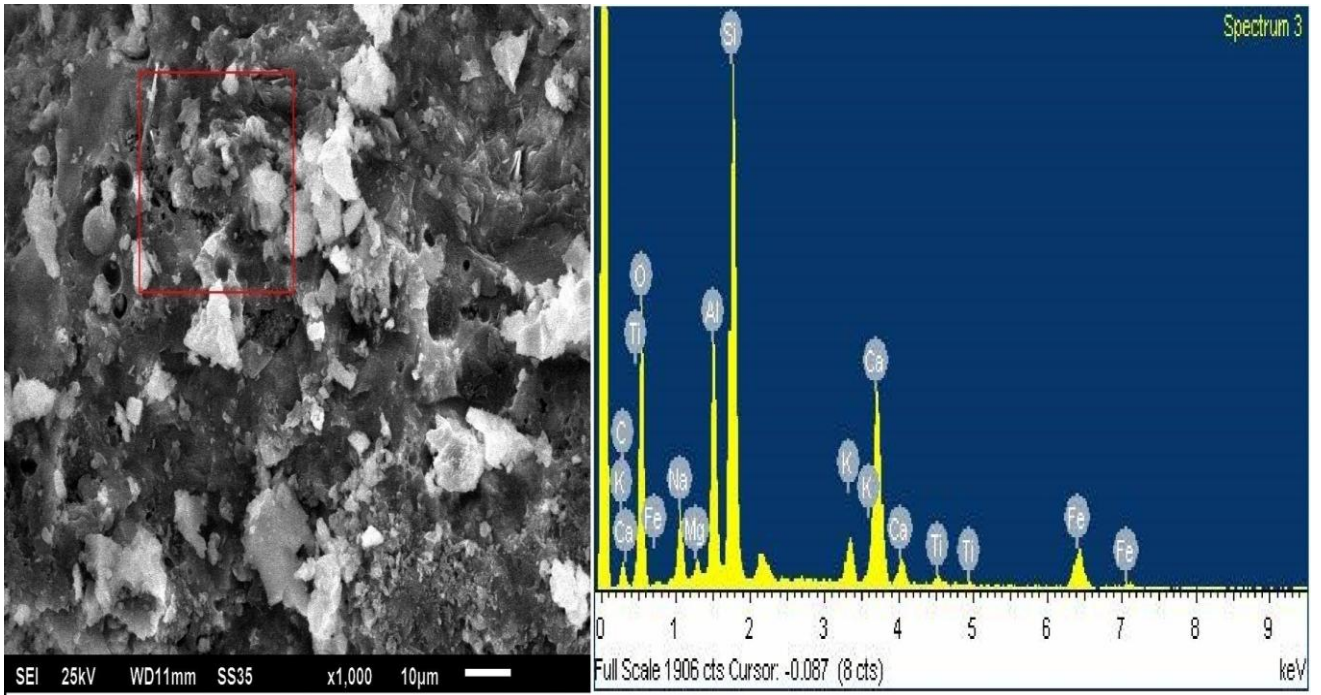


Fig.4.31: SEM/EDS analysis of GPC with 20% OPC at 28 days

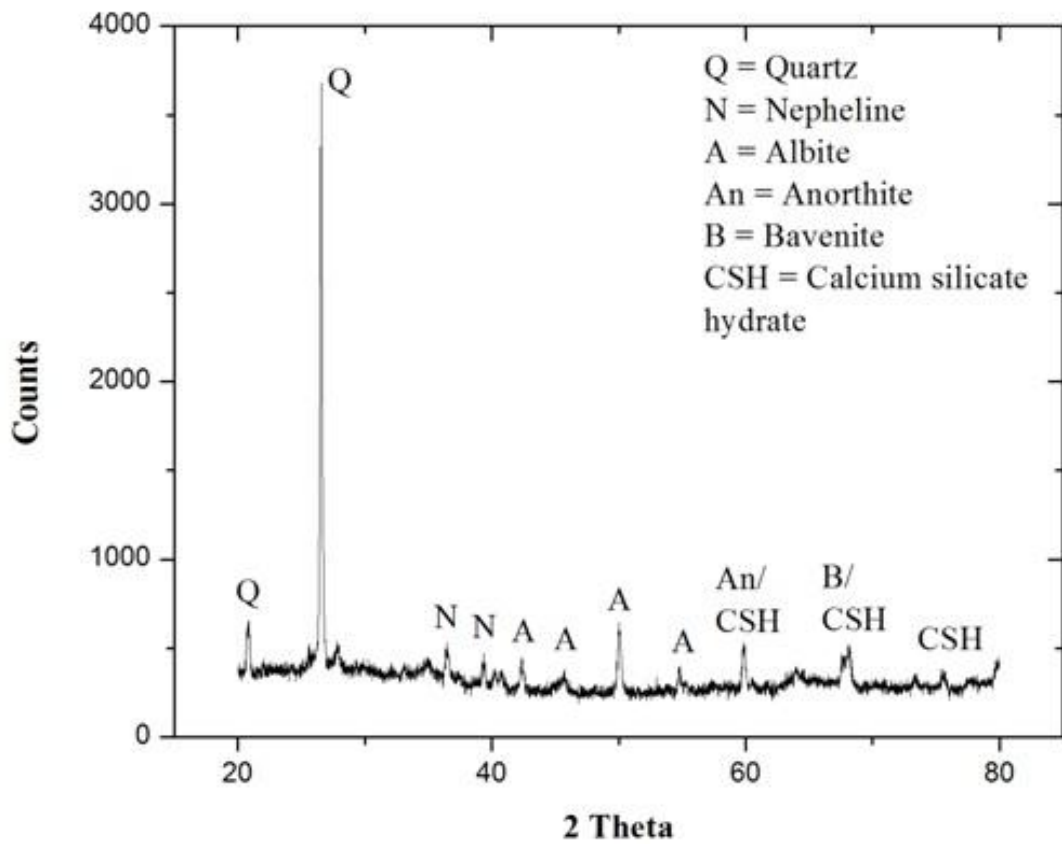


Fig.4.32: XRD analysis of GPC with 20% OPC at 28 days

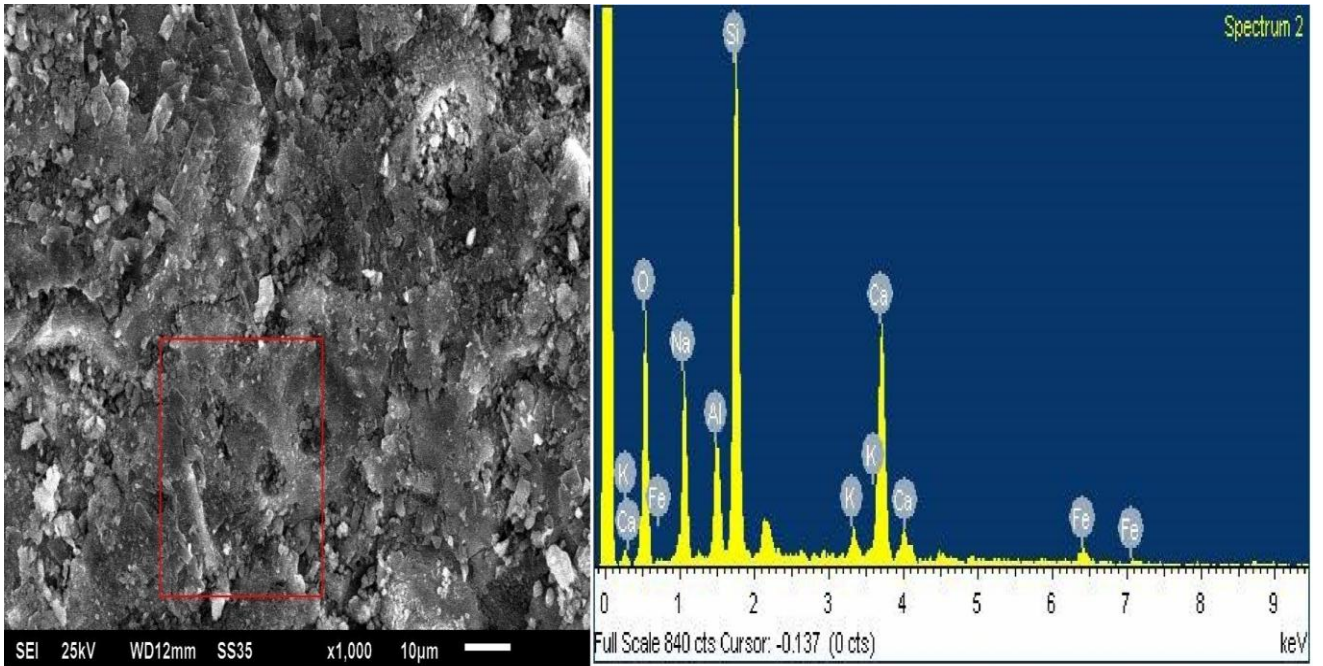


Fig.4.33: SEM/EDS analysis of GPC with 20% OPC at 90 days

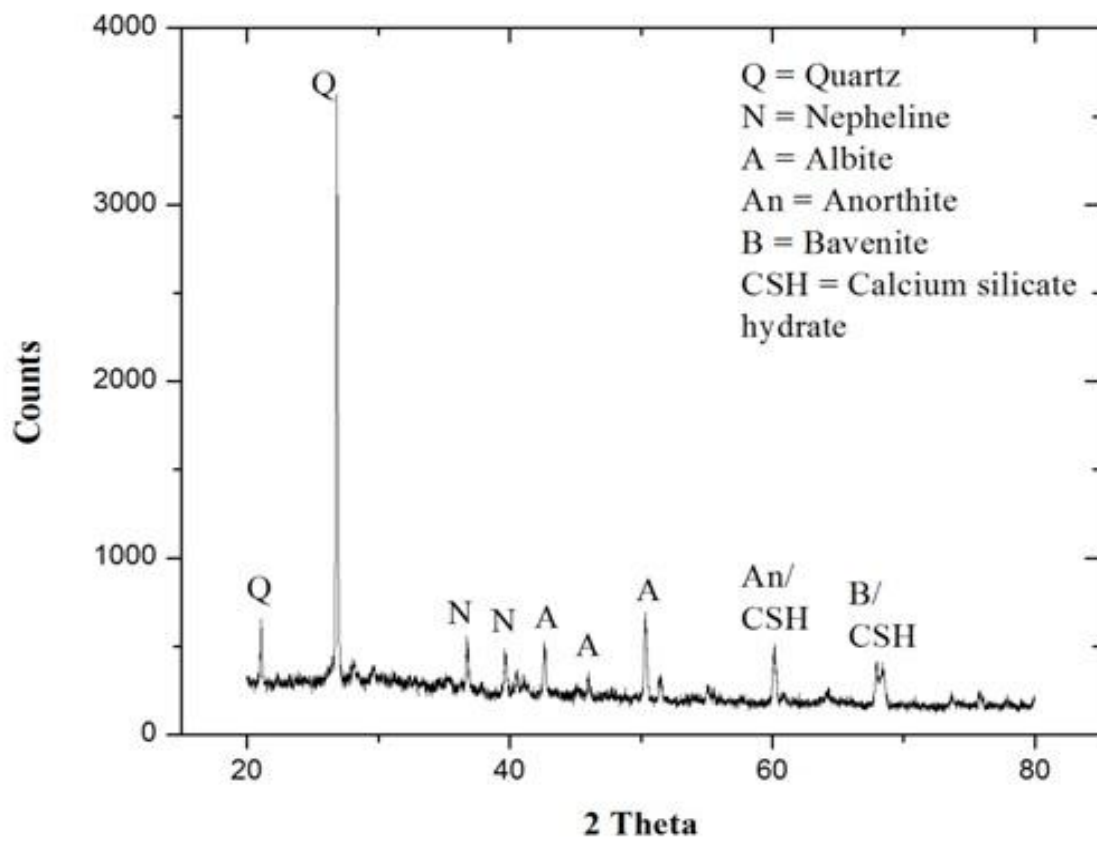


Fig.4.34: XRD analysis of GPC with 20% OPC at 90 days

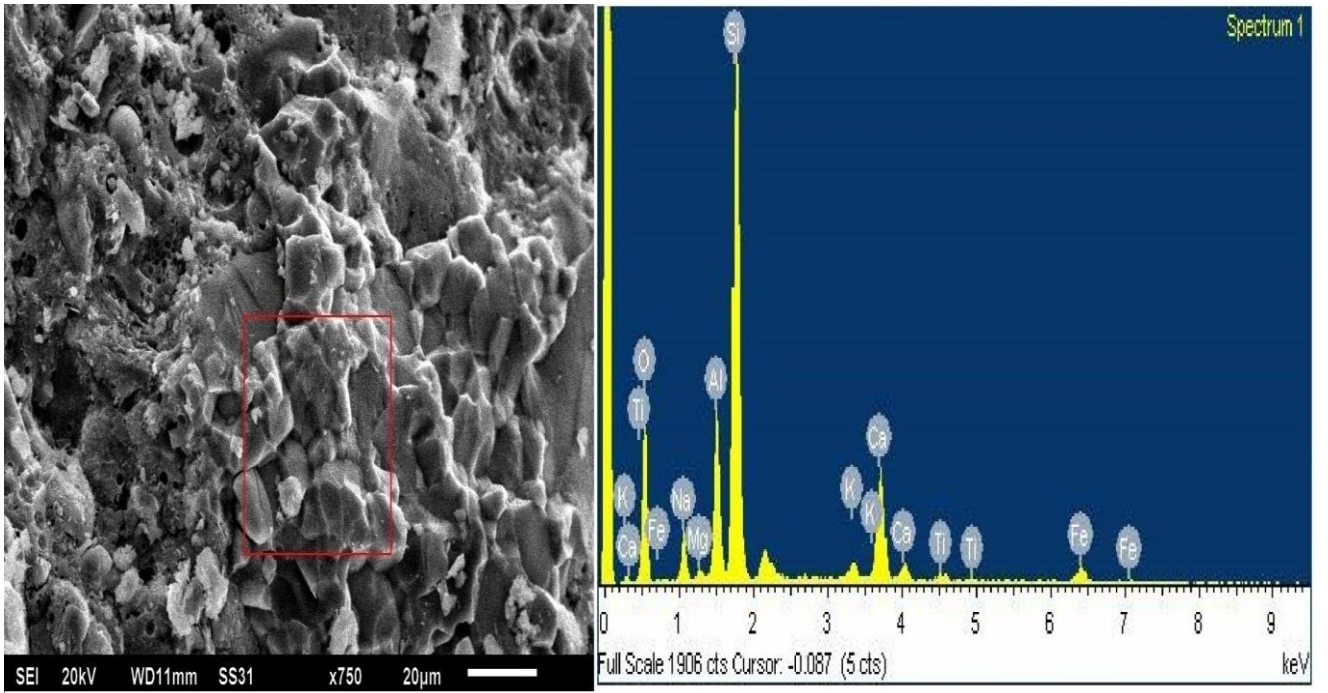


Fig.4.35: SEM/EDS analysis of GPC with 20% OPC at 365 days

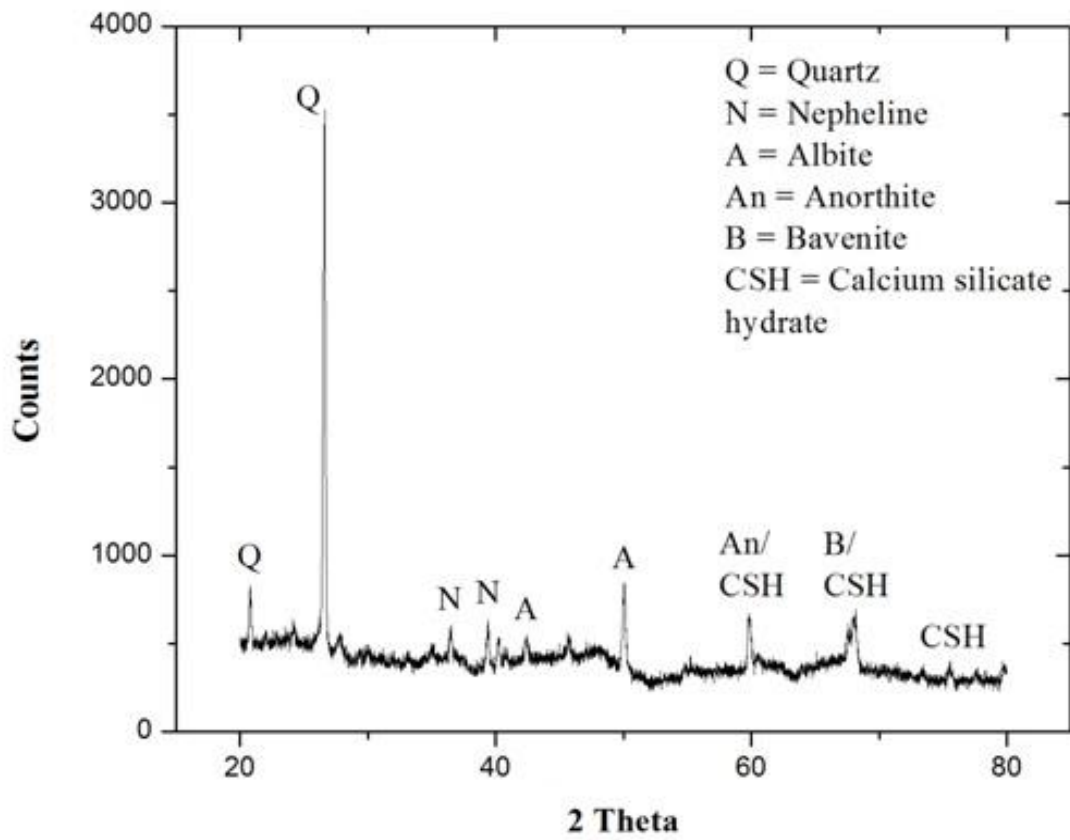


Fig.4.36: XRD analysis of GPC with 20% OPC at 365 days

These can be considered as major strength based products produced by the polymerization mechanism of alumina and silica with the alkali solution. With the addition of calcium at higher content of 20% in the geopolymer system, due to its high reactivity, additional calcium reacted with the available alkalis in the geopolymer system and forms polymeric product such as CASH and hydration product such as CSH, however, NASH bonds can be considered as stronger than calcium based CASH and CSH bonds (Suwan and Fan, 2014). The presence of CASH was confirmed by the presence of bavenite similar to geopolymer mixture with 10% OPC, however in this case, new phase such as anorthite (An) was observed. Anorthite is associated with the strong Ca-Al-Si bonds with better structural arrangement than bavenite which is responsible for imparting higher mechanical strength. CSH phase was also observed which filled the pore spaces and resulted in better strength as well as permeability characteristics. These hydration products coexisted with the polymeric products and modified the microstructure in a positive way (Oh et al., 2010; Pacheco-Torgal et al., 2008).

4.2.3.4 Geopolymer concrete mixture with 30% OPC

The SEM, EDS and XRD results of geopolymer concrete mixture with 30% OPC are presented in Figs. 4.37-4.46. The 3-day SEM micrograph showed the relatively large number of voids and pore spaces in addition to micro-cracks as compared to the micrograph of geopolymer specimens with 20% OPC. A similar increase in cracks, voids and pore spaces were also seen for GPC at 7, 28, 90 and 365 days as well. At all ages, the microstructure was observed to be lack of homogeneity as some particles were seen to be separated from the mixture. Even though the external appearance of the microstructure indicates a properly set specimen however, due to insufficient polymeric products, it had weaker matrix connectivity. Some unreacted fly ash particles surrounded by the polymeric gel was also observed which resulted in a reduction of strength properties (Dombrowski et al., 2007). It was attributed to the increase in calcium content which relatively decreased the sodium and aluminium content in the geopolymer system. This resulted in decreased polymeric product NASH and increased the calcium based products CASH and CSH, relatively. Therefore at the higher content of 30% OPC, the amount of strong Na-Al-Si bonds reduced relatively which decreased the mechanical properties of geopolymer concrete blended with a high content of OPC. Also, due to exothermic nature of hydration reactions, the formation of hydration products at high calcium content increased the effective temperature inside the geopolymer system too much that it resulted in dryness and subsequent loss of moisture through evaporation.

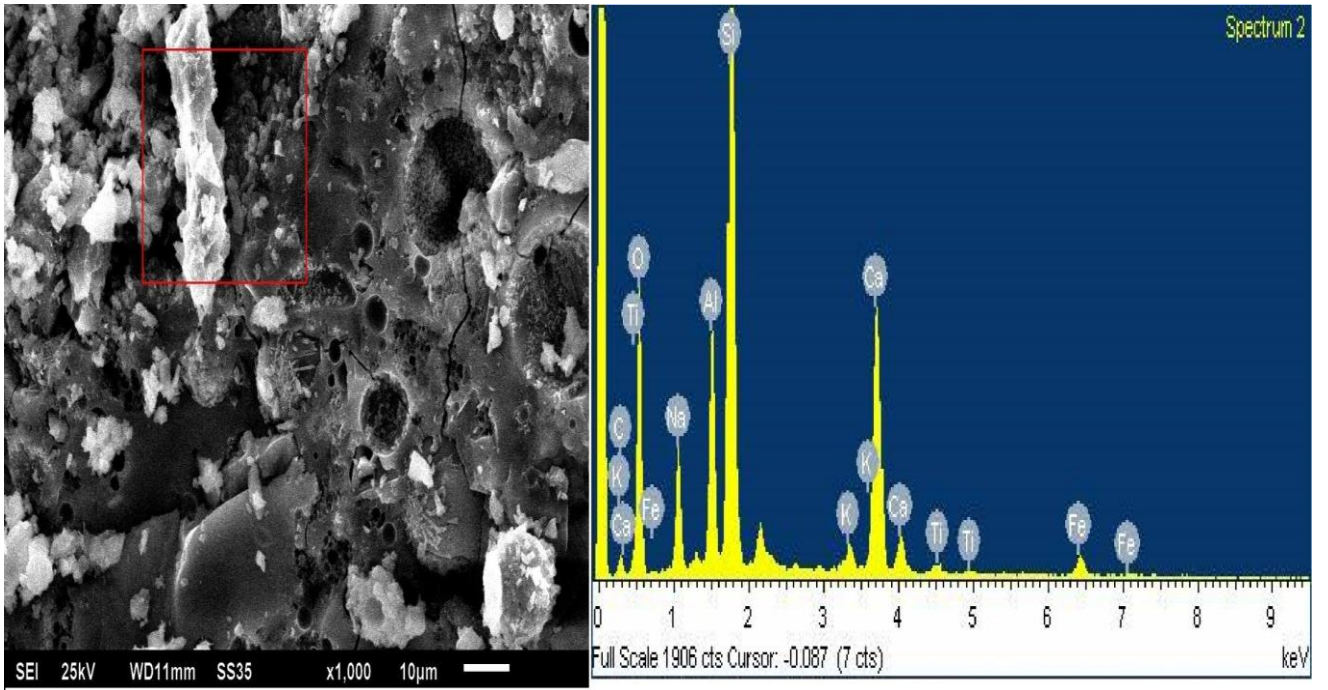


Fig.4.37: SEM/EDS analysis of GPC with 30% OPC at 3 days

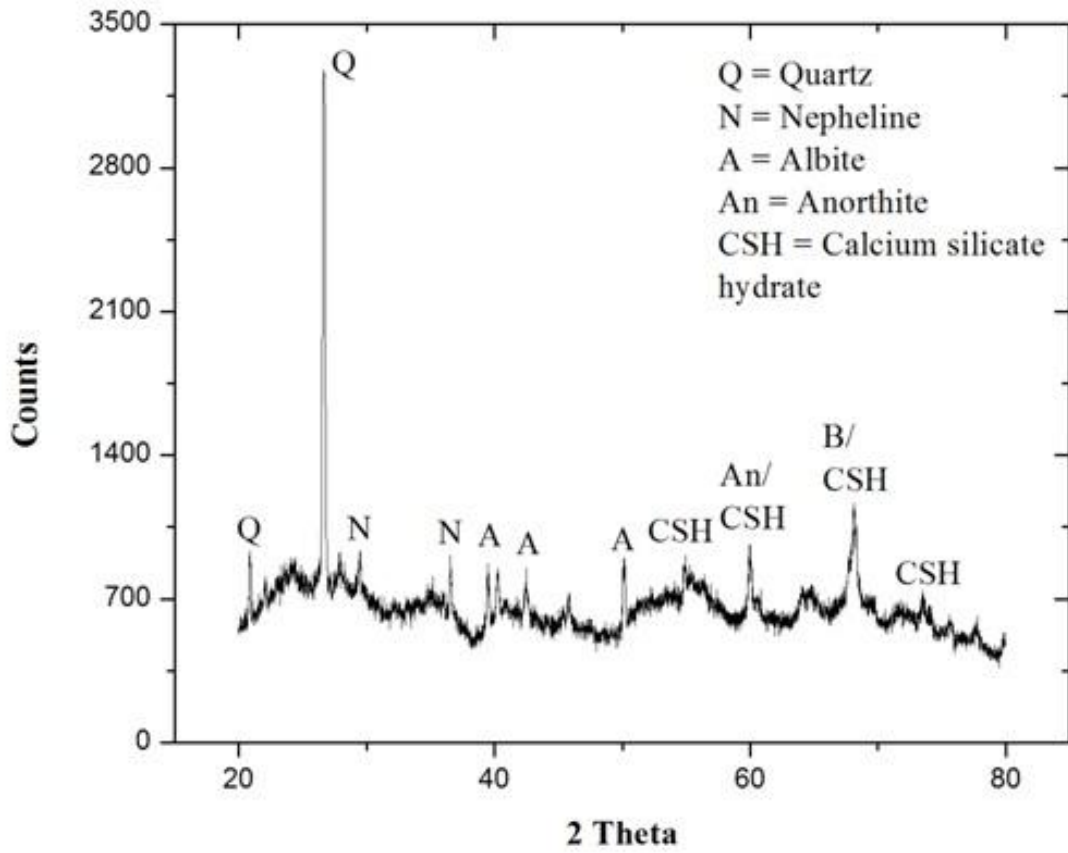


Fig.4.38: XRD analysis of GPC with 30% OPC at 3 days

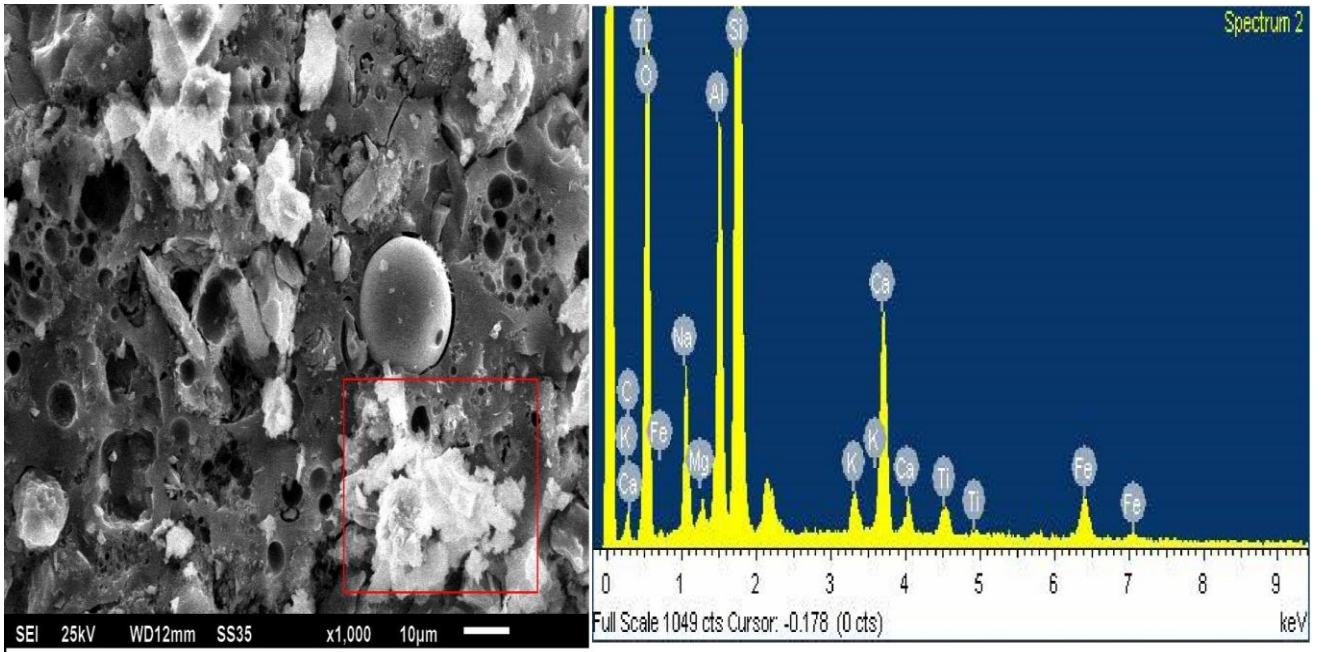


Fig.4.39: SEM/EDS analysis of GPC with 30% OPC at 7 days

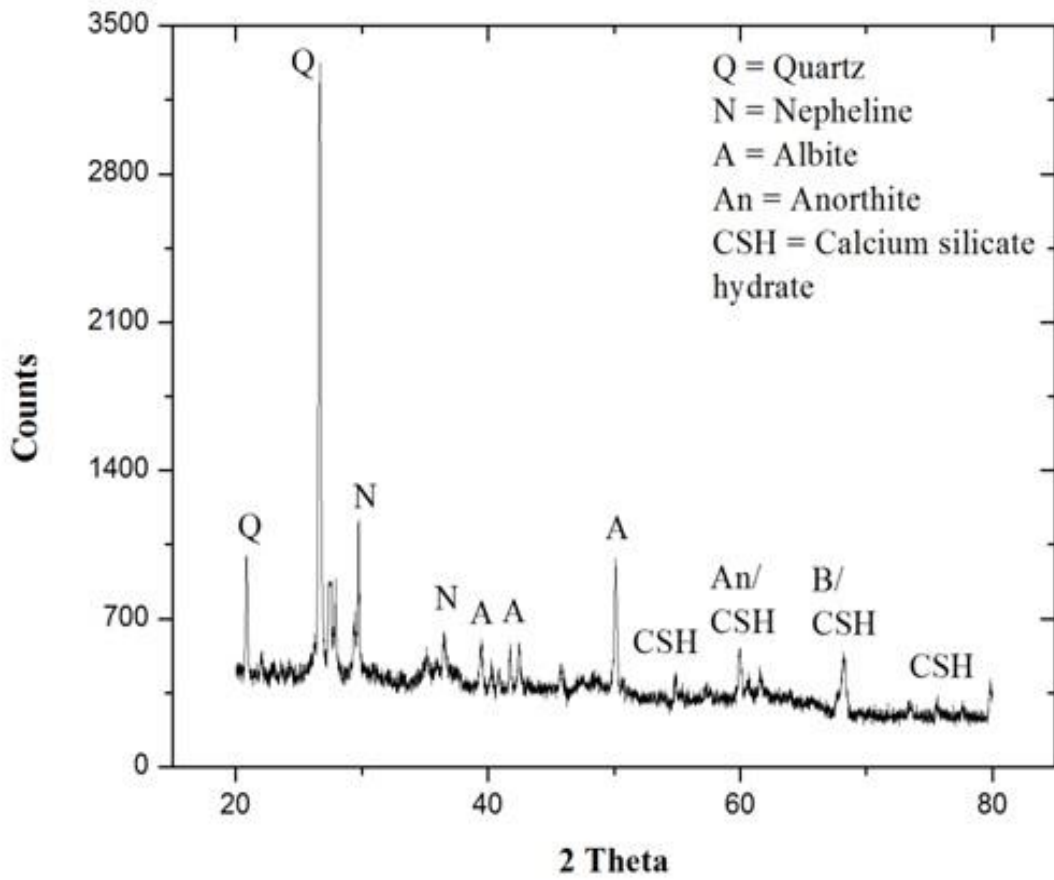


Fig.4.40: XRD analysis of GPC with 30% OPC at 7 days

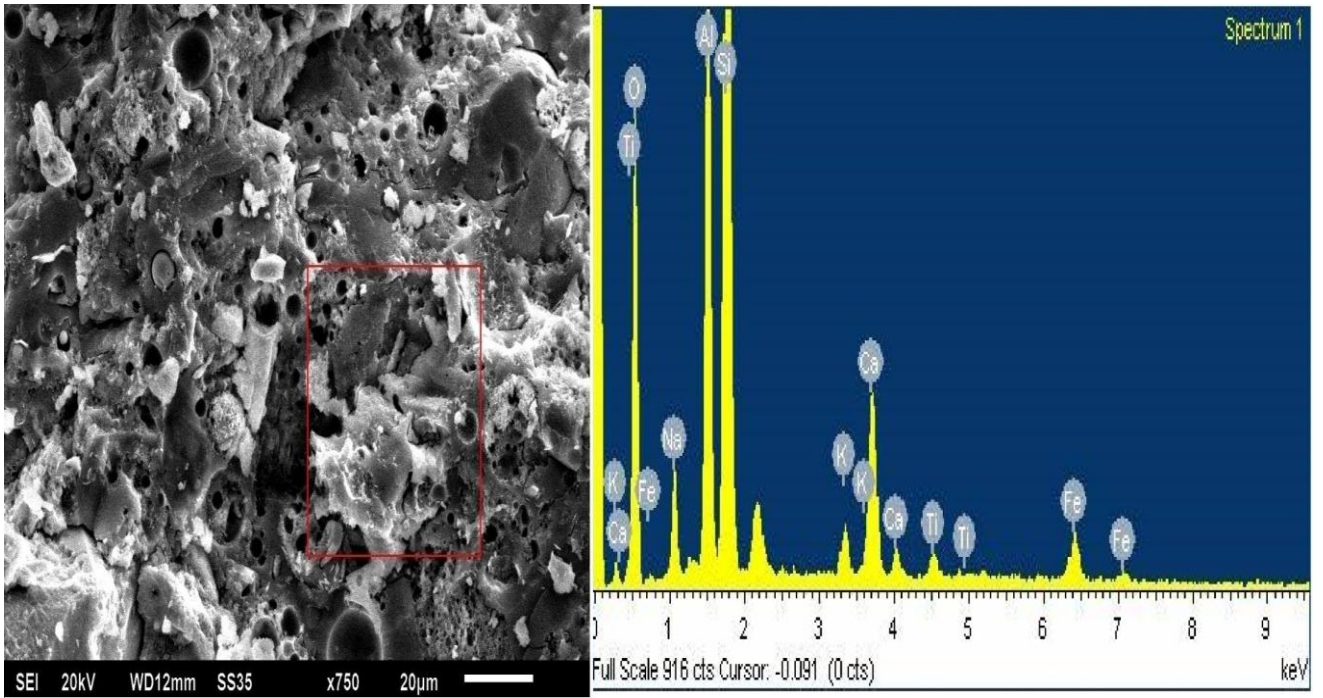


Fig.4.41: SEM/EDS analysis of GPC with 30% OPC at 28 days

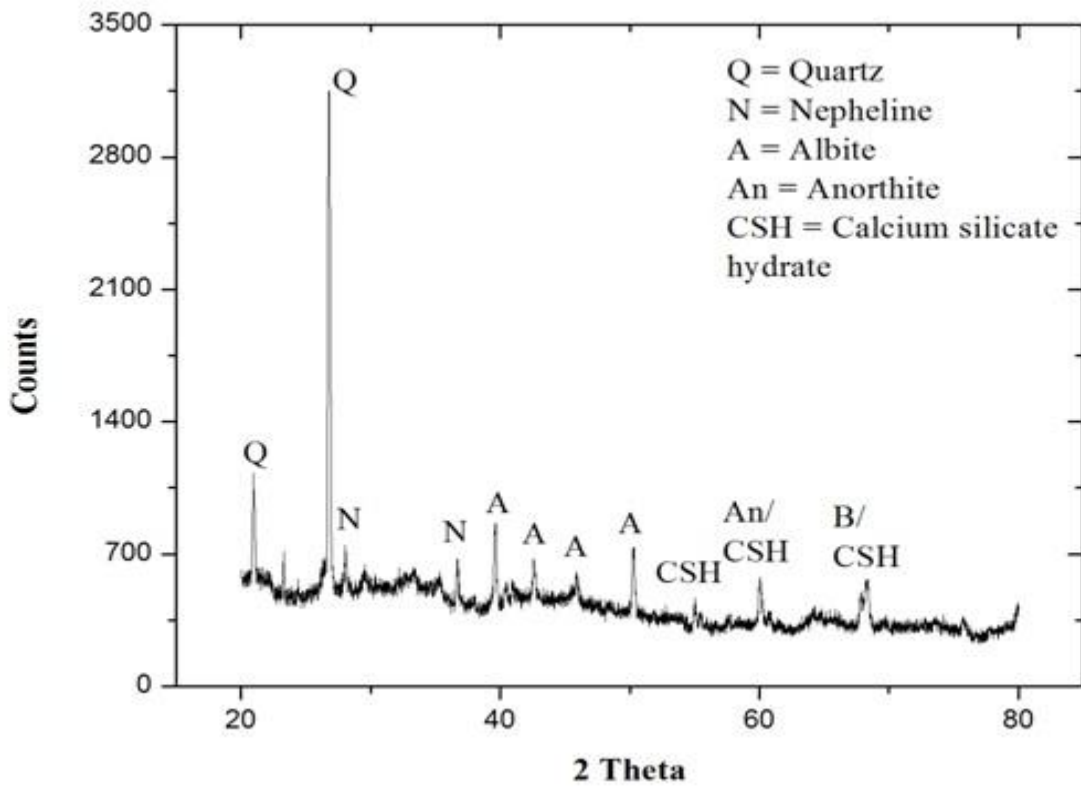


Fig.4.42: XRD analysis of GPC with 30% OPC at 28 days

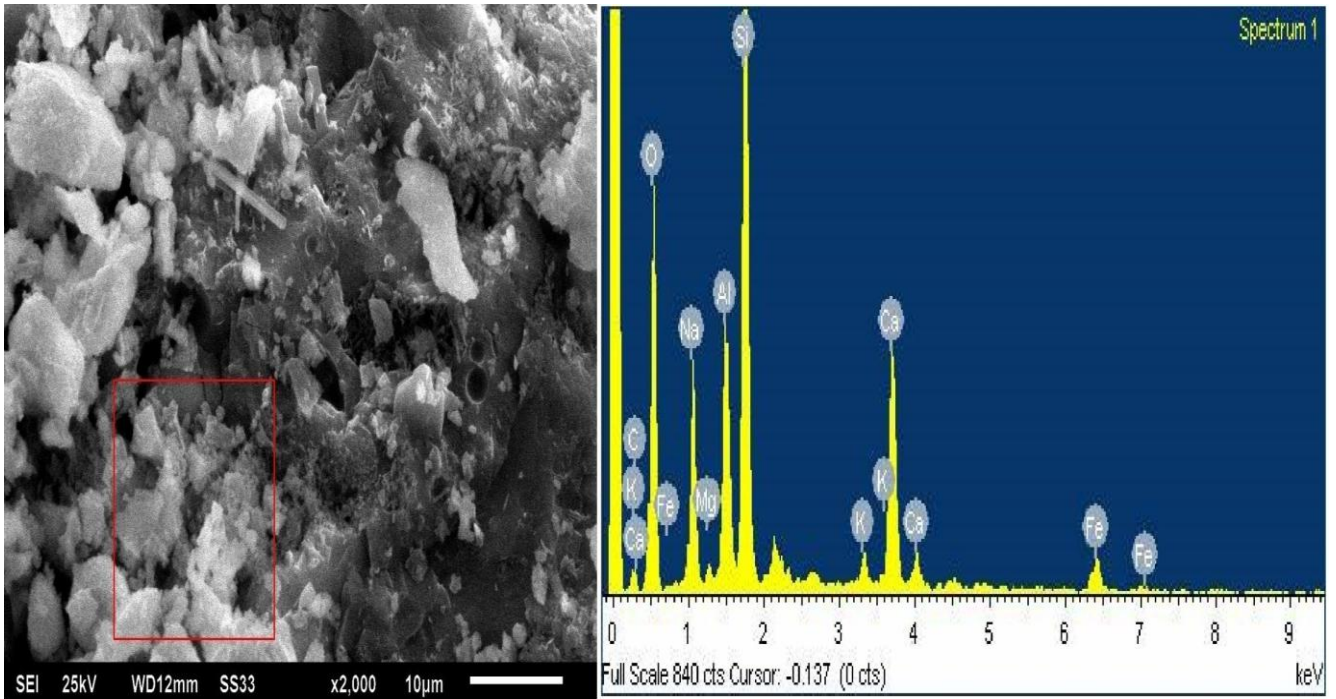


Fig.4.43: SEM/EDS analysis of GPC with 30% OPC at 90 days

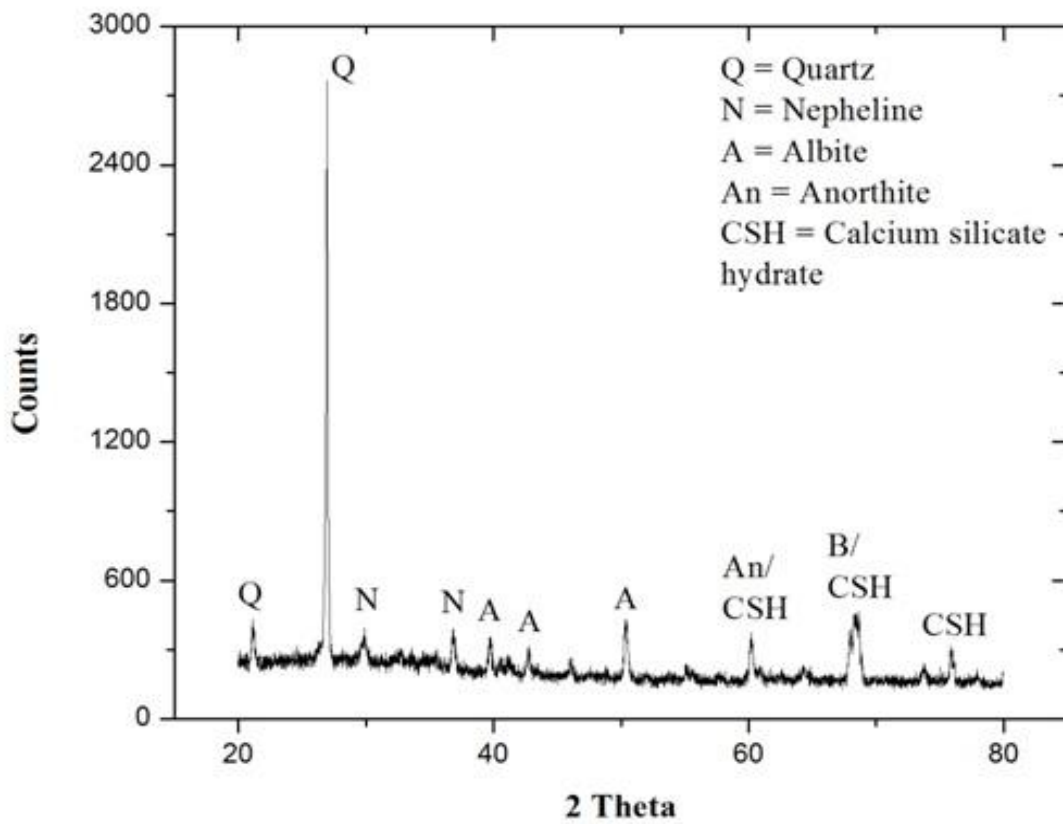


Fig.4.44: XRD analysis of GPC with 30% OPC at 90 days

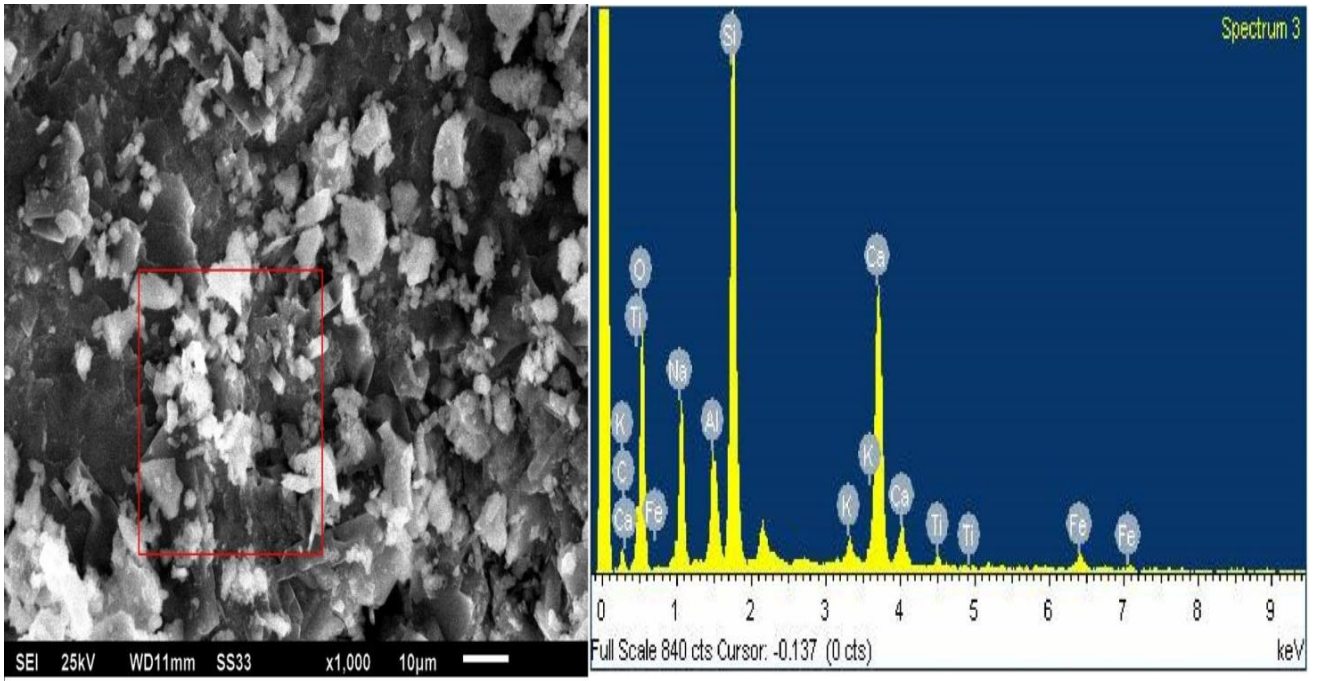


Fig.4.45: SEM/EDS analysis of GPC with 30% OPC at 365 days

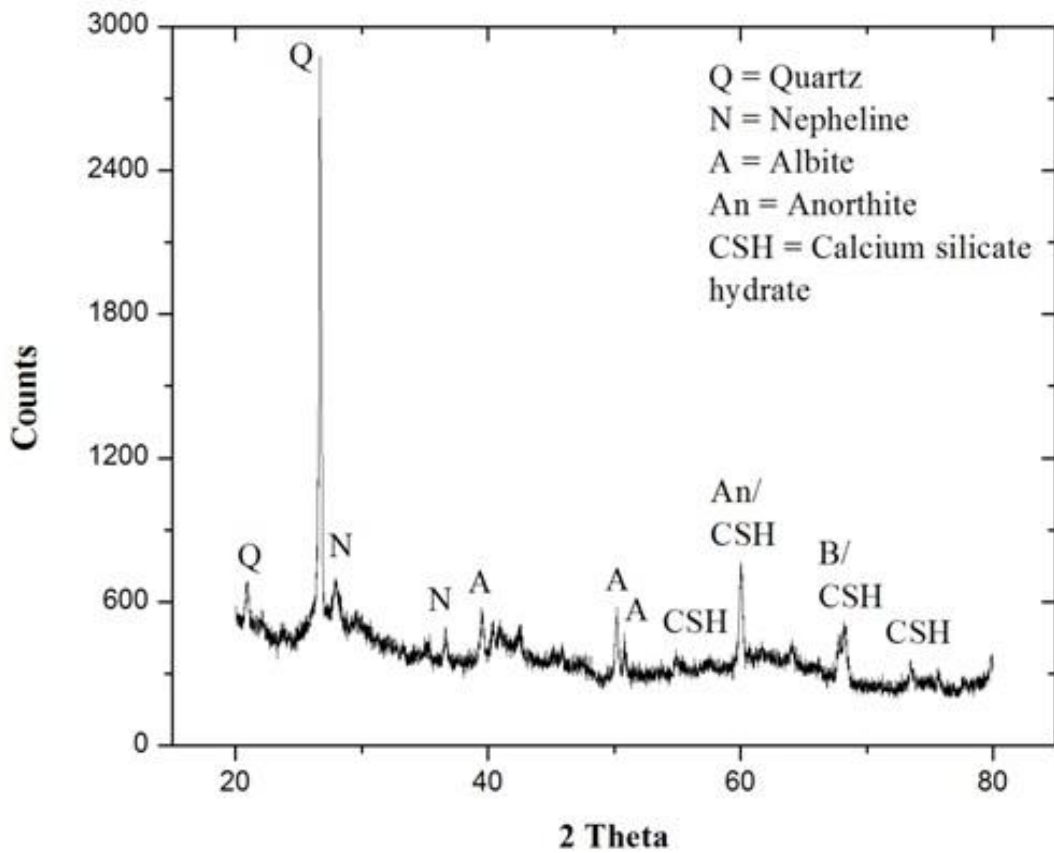


Fig.4.46: XRD analysis of GPC with 30% OPC at 365 days

This increase in effective heat in the geopolymer system resulted in more voids and extra pore spaces in its microstructure. A similar increase in voids and pore spaces with higher cracks with the increase in calcium addition after an optimum content was also reported by Temuujin et al. (2009) and Yip et al. (2005).

The results of EDS analysis for the geopolymer concrete mixture with 30% OPC showed the presence of similar elements as obtained for the mixtures with 20% OPC such as sodium (Na), aluminium (Al), silica (Si), oxygen (O), calcium (Ca) and impurity elements such as titanium (Ti), magnesium (Mg), potassium (K) and carbon (C) at all ages. However, the major difference observed was the significant increase in calcium content in the geopolymer system. This resulted in lesser Na-Al-Si and more calcium based Ca-Si and Ca-Al-Si bonds in the geopolymer system. Due to relatively stronger characteristics of Na-Al-Si bonds than Ca-Si and Ca-Al-Si bonds, the overall performance of geopolymer concrete at higher calcium is reduced in terms of mechanical and microstructure properties.

The XRD results of geopolymer mixture with 30% OPC showed the presence of similar phases as observed for the geopolymer mixture with 20% OPC at all ages. Quartz (Q), nepheline (N), albite (A), anorthite (An) and calcium silicate hydrate (CSH) were identified as major phases developed. Quartz is associated with silica oxide obtained due to high content of silica in the geopolymer system whereas; nepheline and albite are associated with the strong Na-Al-Si hydrates caused by the polymerization reactions of silica and alumina with the alkali-activating solution consisting of sodium silica and sodium hydroxide. Due to the presence of higher calcium in the geopolymer system caused by higher OPC content of 30%, due to its high reactivity and quick dissolution, it reacted with the alkalis and forms polymeric product CASH and hydration product CSH. This reduced the sodium based polymeric product NASH relatively as compared to geopolymer mixture with 20% OPC and resulted in decreased compressive strength and increased permeability values. Also, due to high curing temperature enhanced by the higher exothermic hydration reaction, the loss of moisture resulted in an increase in permeation characteristics such as water absorption, porosity and sorptivity.

4.3 DURABILITY PROPERTIES OF GEOPOLYMER CONCRETE

In the present study, the durability properties of geopolymer concrete were evaluated by performing water absorption, porosity, sorptivity, rapid chloride permeability and the resistance against sulphuric acid at the ages of 28, 90 and 365 days.

4.3.1 Water Absorption and Porosity

Water absorption at 28 days for GPC mixtures with 0, 5, 10, 15, 20, 25 and 30% OPC was found to be 4.2, 3.3, 2.1, 1.8, 1.4, 1.6 and 1.7%, respectively as shown in Figs. 4.47 and 4.48. For the same mixtures, the decrease in water absorption was observed in the range of 5-18% and 18-24% at 90 and 365 days, respectively. At 90 days, the water absorption for the geopolymer concrete mixtures with 0, 5, 10, 15, 20, 25 and 30% OPC was decreased by 17.3, 14.7, 5.4, 16.9, 17.9, 14.5 and 12.0%, respectively whereas at 365 days, water absorption was further decreased by 23.3, 22.6, 18.2, 20.8, 21.5, 22.6 and 20.1%, respectively from their 28-day water absorption. In comparison, water absorption for CCC at 28 days was determined as 4.38% and the decrease at 90 and 365 days was 21 and 43%, respectively.

With the increase in OPC content in the GPC, the values of water absorption decreased up to the OPC content of 20%, and beyond that it increased. For geopolymer concrete mixture with 0% OPC, water absorption was obtained as 4.2, 3.5 and 3.2%, whereas 10% OPC yielded the water absorption of 2.1, 2.0 and 1.7% at 28, 90 and 365 days, respectively. With the increase in OPC to 20%, water absorption further decreased to 1.4, 1.2 and 1.1% at 28, 90 and 365 days, respectively. Beyond this, the further increase in OPC content increased the water absorption. For instance, 30% OPC geopolymer mixture yielded the water absorption of 1.7, 1.5 and 1.4% at 28, 90 and 365 days, respectively. It was observed that at all ages, minimum water absorption was obtained for the geopolymer concrete mixtures with 20% OPC.

Porosity results at 28 days for GPC mixtures with 0, 5, 10, 15, 20, 25 and 30% OPC showed the values of 14.9, 11.1, 8.7, 7.5, 6.9, 7.2 and 7.9%, respectively as shown in Figs. 4.49 and 4.50. For the same mixtures, porosity decreased in the range of 2-16% and 8-25% at 90 and 365 days, respectively. At 90 days, porosity for geopolymer concrete mixtures with 0, 5, 10, 15, 20, 25 and 30% OPC was decreased by 12.7, 13, 2.5, 6.0, 10.9, 4.9 and 4.4%, respectively whereas at 365 days, it was further reduced by 24.4, 21.0, 8.6, 11.0, 12.5, 10.0 and 11.3%, respectively. For CCC, porosity was determined as 13.79% which was decreased by 20 and 35% at 90 and 365 days, respectively.

The inclusion of OPC up to 20% decreased the porosity at all ages, whereas the further increase in OPC resulted in its increase. For the geopolymer mixture with 0% OPC, the porosity was observed as 14.9, 13.0 and 11.2% at 28, 90 and 365 days, respectively. With the increase in OPC at 10%, it was determined as 8.7, 8.4 and 7.9% and with 20% OPC, it was observed to be 6.9, 6.2 and 6.1% at 28, 90 and 365 days, respectively.

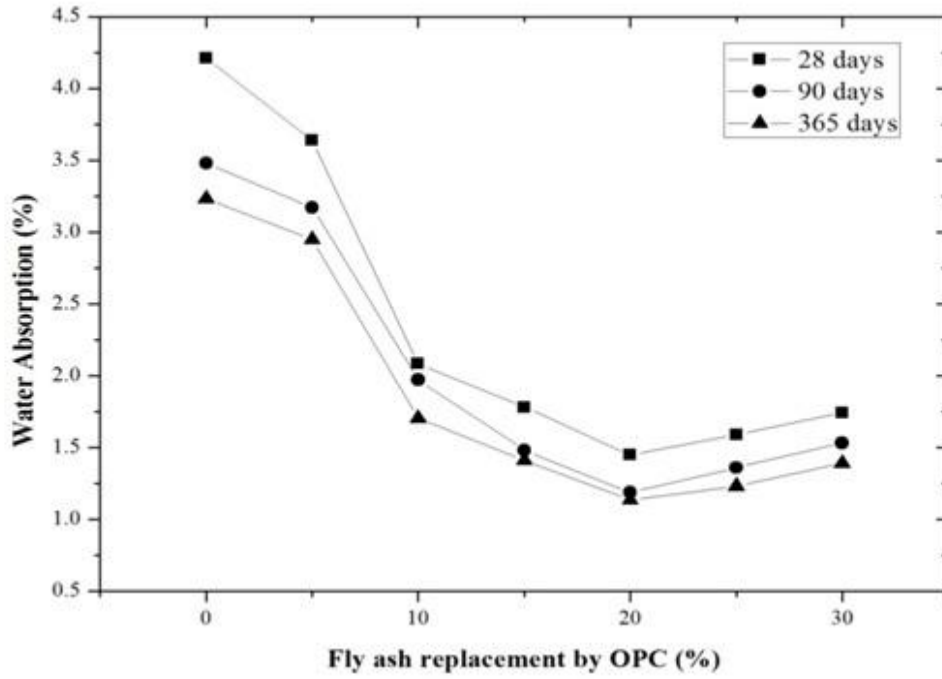


Fig.4.47: Water absorption of GPC versus OPC content

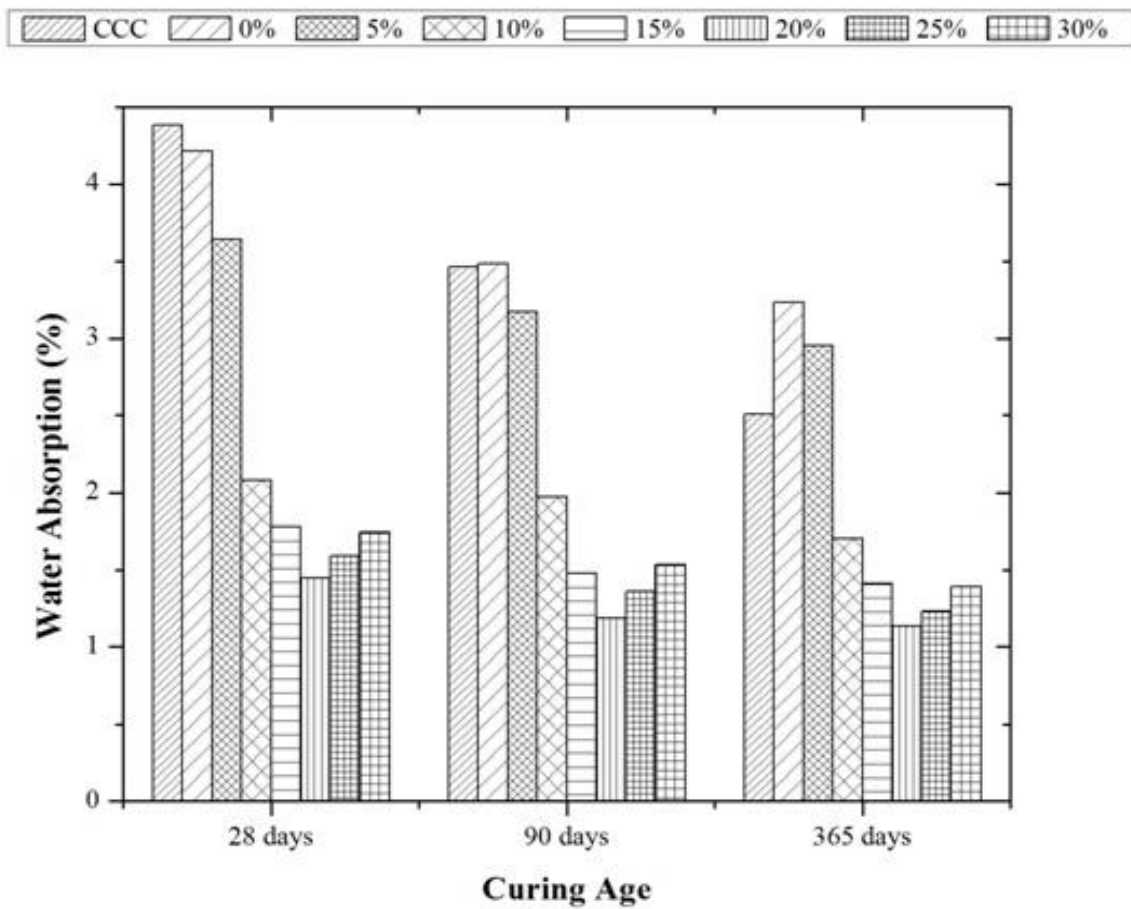


Fig.4.48: Effect of OPC inclusion on water absorption of GPC

With the further increase in OPC content beyond 20%, porosity increased. For instance, porosity obtained for GPC mixtures with 30% OPC was recorded as 7.9, 7.6 and 7.0% at the ages of 28, 90 and 365 days, respectively. In comparison, CCC mixture showed the porosity of 12.6, 10.6 and 9.0% at 28, 90 and 365 days, respectively. A similar range of porosity around 7-10% for geopolymer concrete with different fly ashes was also observed by Kupwade-Patil and Allouche (2013).

It was observed that water absorption and porosity exhibited similar trend i.e. they decreased with the increase in OPC up to 20% OPC and increased beyond that. The decrease in water absorption and porosity was attributed to the fact that the inclusion of OPC in the geopolymer system increased the calcium content in the mixture. This additional calcium reacted with the alkalis present in the mixture and formed calcium based hydrated products, CASH and CSH. In addition, due to exothermic nature of hydration reactions, the effective temperature inside the geopolymer system increased which further enhanced the polymerization products as well. These additional calcium compounds coexisted with the polymerization products and acted as micro-aggregates which increased the bonding in the matrix and filled the pore spaces within. In general, the aluminosilicate network formation by polymerization releases water which resides within the cavities of geopolymer structure.

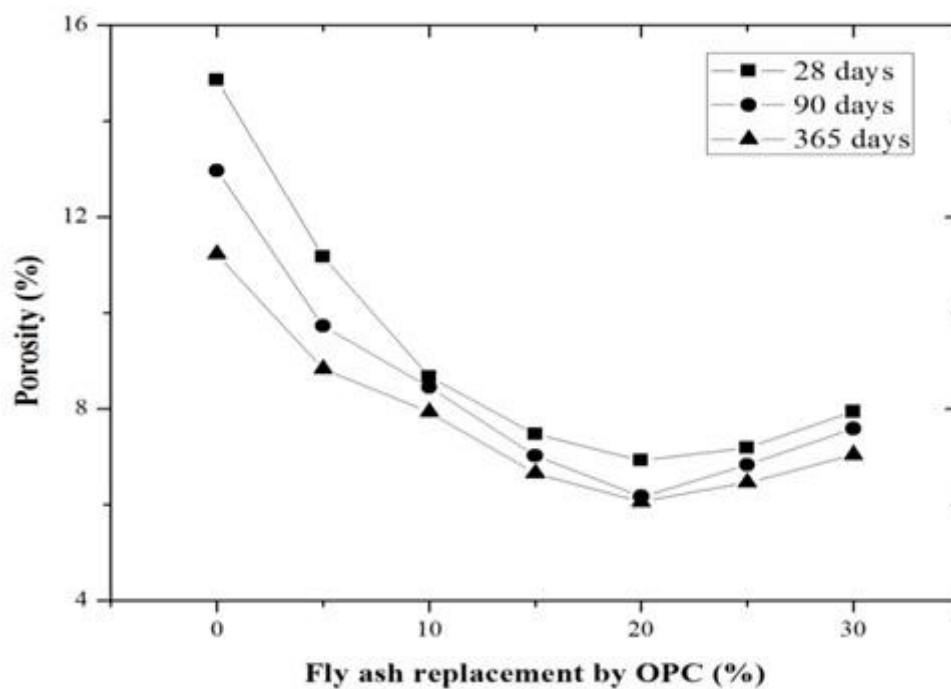


Fig.4.49: Porosity of GPC versus OPC content

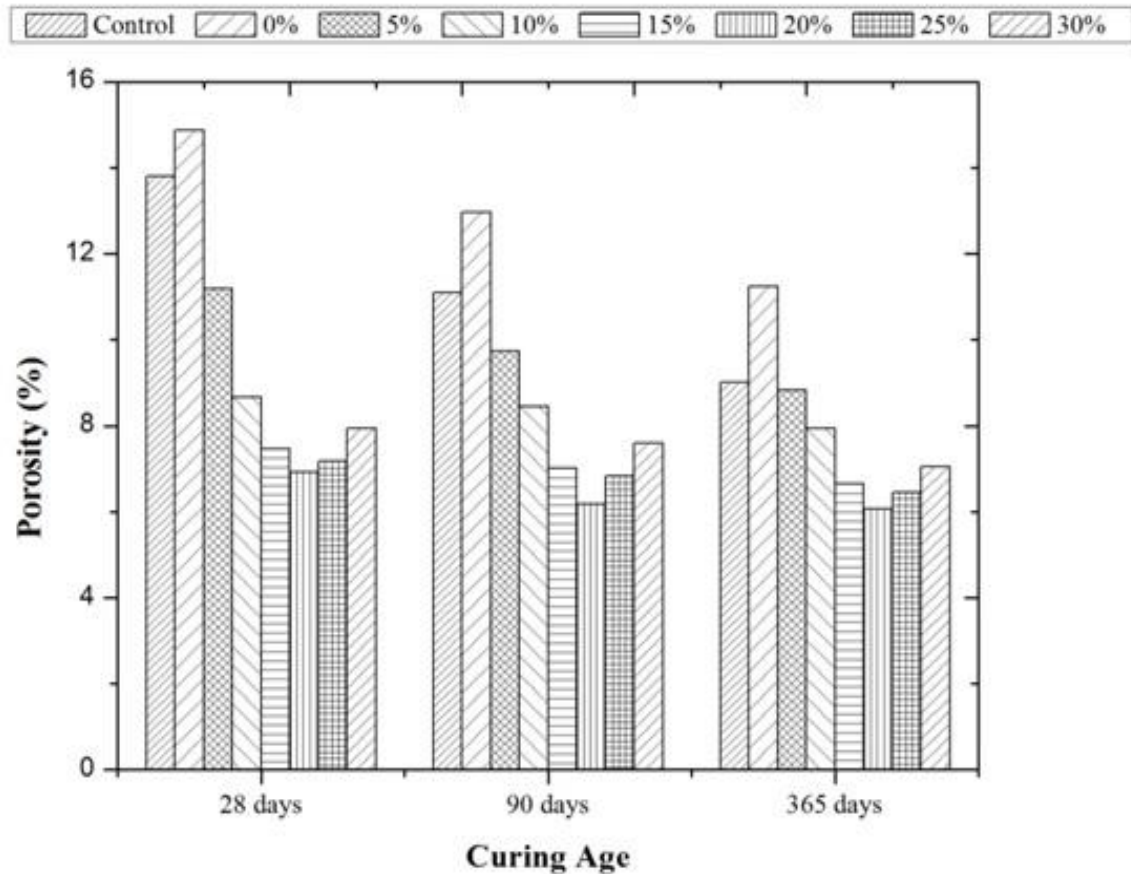


Fig.4.50: Effect of OPC inclusion on porosity of GPC

Therefore, with the further increase in OPC after 20%, the heat liberated from the hydration reaction increased the effective temperature inside the geopolymer system too much that it evaporated the moisture from water-filled pores and created the voids as well as shrinkage cracks in the matrix. Also, at higher OPC content beyond 20%, CSH and NASH competed against each other for the soluble alkalis and resulted in a binder composed of two porous phases with large pore spaces. The presence of these cracks was also observed in SEM micrographs at higher OPC content of 30% which also resulted in decreased compressive and split tensile strength.

4.3.2 Sorptivity

GPC mixtures with 0, 5, 10, 15, 20, 25 and 30% OPC obtained the sorptivity of 4.13, 3.84, 3.32, 3.18, 2.98, 3.13 and 3.26 $\mu\text{mm}/\text{s}^{1/2}$, respectively at 28 days as shown in Figs. 4.51 and 4.52. With age, the sorptivity was found to be decreased. The decrease in values was in the range of 3-10% and 6-15% at 90 and 365 days, respectively. For instance at 90 days, the sorptivity values decreased by 7.3, 6.8, 3.0, 7.9, 9.8, 8.6 and 6.7% from their 28 days

sorptivity for the geopolymer concrete mixtures with 0, 5, 10, 15, 20, 25 and 30% OPC, respectively. Similarly, for the same mixtures at 365 days, sorptivity further decreased by 12.6, 12.2, 5.7, 11.6, 14.8, 10.9 and 9.7%, respectively. A similar range of sorptivity for geopolymer concrete was also observed by Chotetanorm et al. (2013).

With the increase in OPC content in the geopolymer mixture, a decrease in sorptivity was observed up to 20% OPC and beyond that, it decreased. For geopolymer concrete mixture with 0% OPC, the sorptivity was obtained as 4.13, 3.83 and 3.61 $\mu\text{mm}/\text{s}^{1/2}$, and with the inclusion of OPC at 10%, it decreased to 3.32, 3.22 and 3.13 $\mu\text{mm}/\text{s}^{1/2}$ at 28, 90 and 365 days, respectively. Similarly, for the geopolymer concrete mixture with 20% OPC, the sorptivity further decreased to 2.98, 2.69 and 2.54 $\mu\text{mm}/\text{s}^{1/2}$ at 28, 90 and 365 days, respectively. The decrease with OPC content up to 20% was attributed to the additional calcium based hydrated compounds that acted as micro-aggregates, which coexisted with the geo-polymeric compounds and resulted in the strong and dense microstructure. This restrained the water ingress from the capillary action.

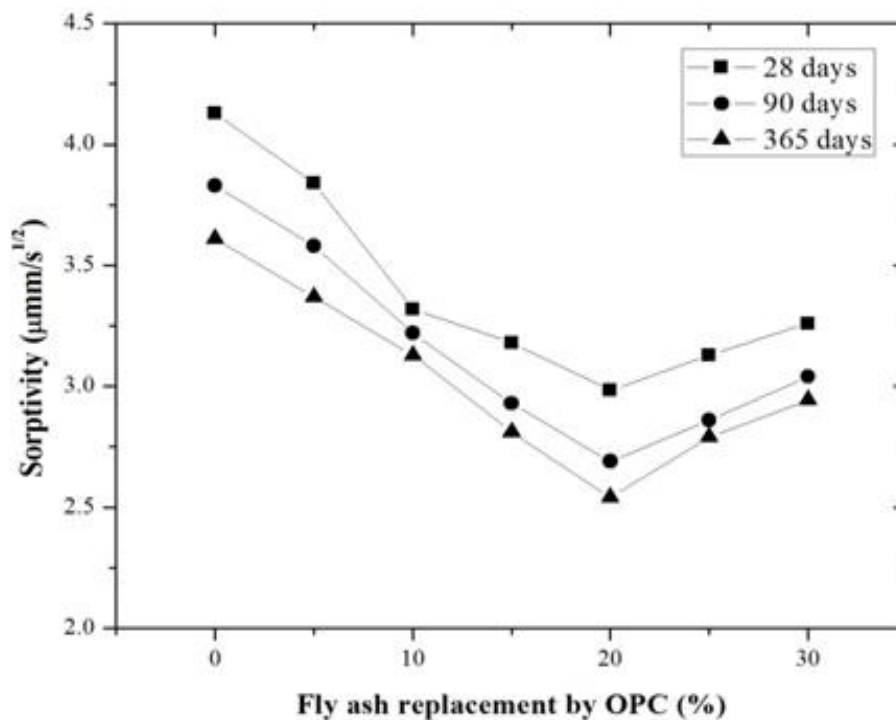


Fig.4.51: Sorptivity of GPC versus OPC content

However, with the further increase in OPC content beyond 20%, sorptivity increased. For instance, the geopolymer concrete mixture with 30% OPC exhibited the sorptivity of 3.26, 3.04 and 2.94 $\mu\text{mm}/\text{s}^{1/2}$ at 28, 90 and 365 days, respectively. The increase in sorptivity values

after 20% OPC was due to the additional pore and void spaces developed due to the evaporation of moisture from the matrix which also created micro-cracks. These pore spaces increased the sorptivity by the ingress of water through these additional pores. In comparison, the sorptivity obtained for the CCC was 4.09, 3.57 and 3.16 $\mu\text{mm/s}^{1/2}$ at 28, 90 and 365 days, respectively.

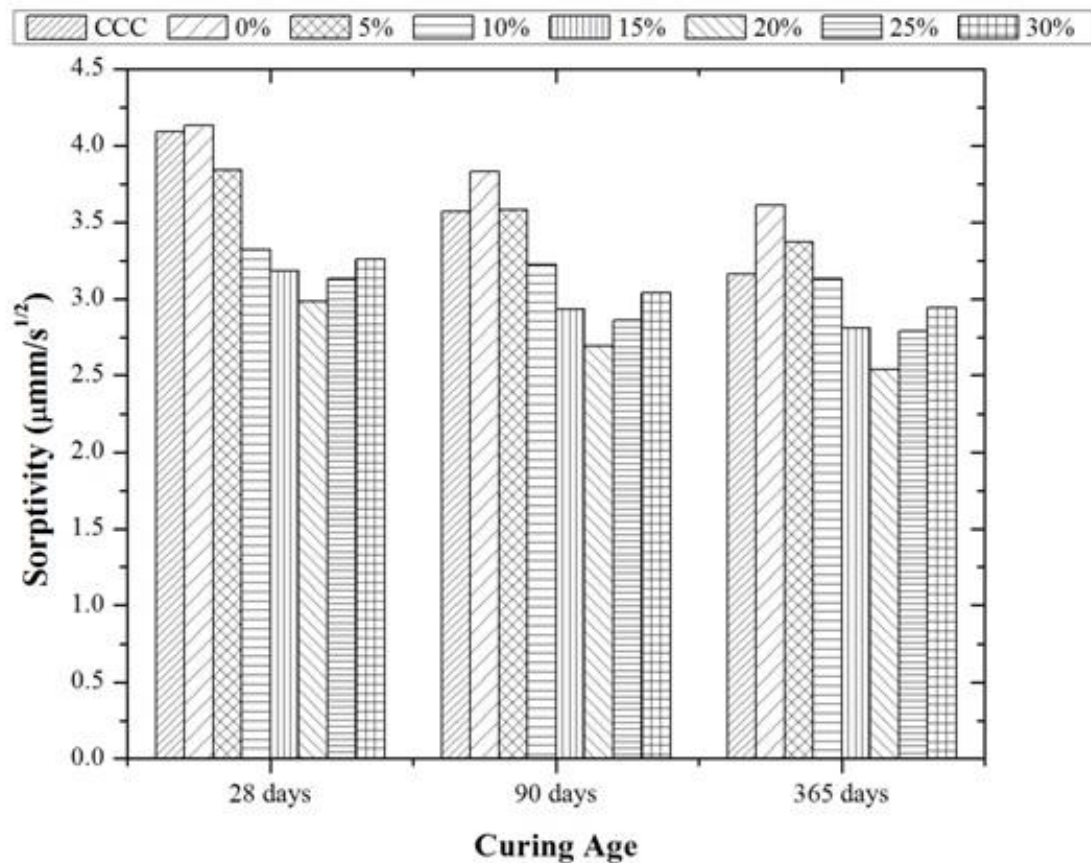


Fig.4.52: Effect of OPC inclusion on sorptivity of GPC

4.3.3 Rapid Chloride Permeability

Tests were conducted in accordance with ASTM C1202 to evaluate the chloride permeability of GPC mixtures with OPC inclusion and CCC at the ages of 28, 90 and 365 days. The results are presented in Table 4.1 and Fig. 4.53. In general, the resistance against chloride ion penetration depends largely on the volume and size of interconnected capillary voids in the concrete and microcracks present in the paste and at the aggregate-paste interface. It was observed from the results that in terms of total charge passed, CCC of similar compressive strength showed almost similar chloride permeability to fly ash based GPC with 0% OPC at all ages.

The values of total charge passed obtained for geopolymer concrete with 0% OPC were 2899, 2456 and 2165 at 28, 90 and 365 days, respectively. With the inclusion of OPC in the geopolymer concrete, the chloride permeability in terms of total charge passed was reduced at all ages up to the content of 20% and beyond that, it increased slightly. For instance, total charge passed for geopolymer concrete mixtures; with 5% OPC was 2184, 1192 and 1087, and with 10% OPC was 977, 992 and 851 at 28, 90 and 365 days, respectively. Similarly, geopolymer concrete mixtures; with 15% OPC showed the total charge passed values of 638, 405 and 369, and with 20% OPC, was 404, 186 and 165 at the age of 28, 90 and 365 days, respectively. However, with the further increase of OPC in geopolymer concrete beyond 20%, an increase in chloride permeability was observed. For instance, the total charge passed for the geopolymer concrete mixtures; with 25% OPC was 445, 246 and 219 and for 30% OPC, it was 669, 526 and 446 at the age of 28, 90 and 365 days, respectively. In comparison, for CCC the values of total charge passed were observed as 2864, 2341 and 1885 at 28, 90 and 365 days, respectively.

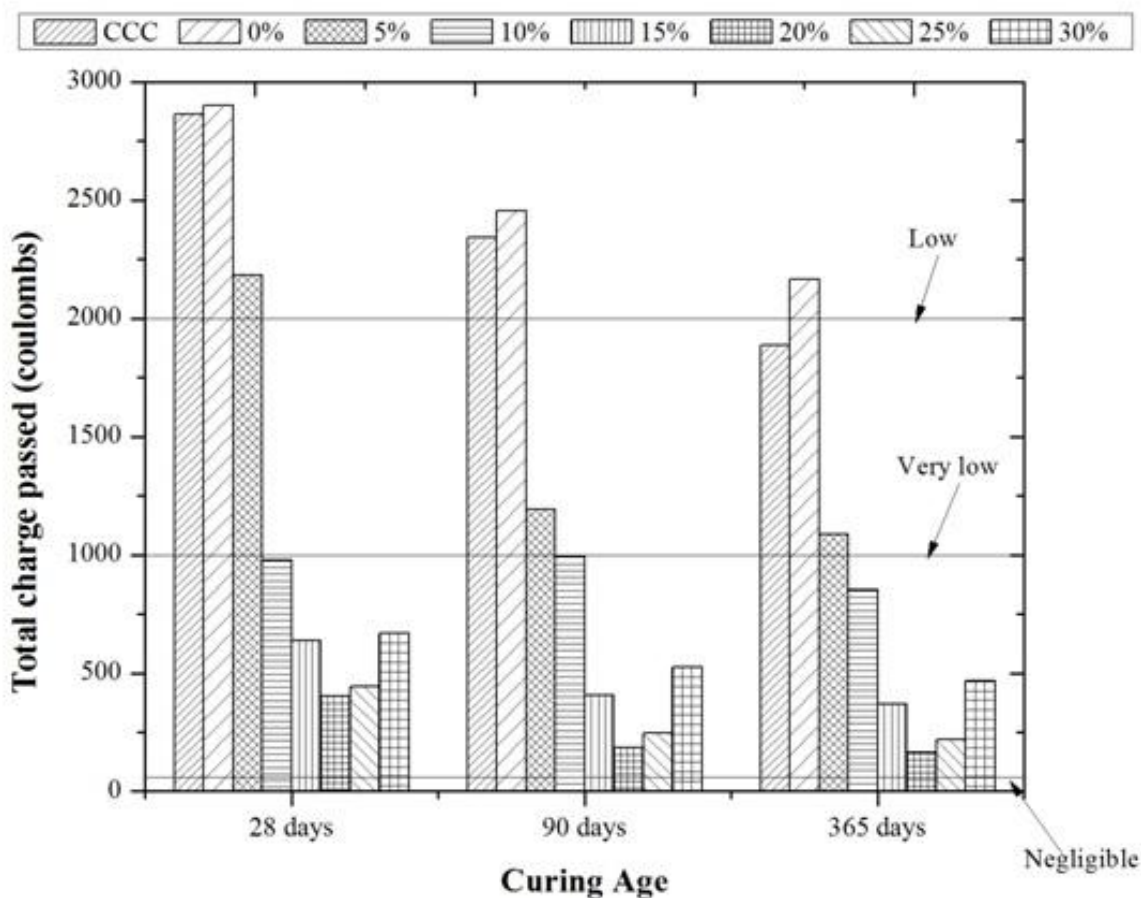


Fig.4.53: Effect of OPC on chloride ion penetration in GPC

Table 4.1: Permeability category of GPC as per ASTM C1202

Mixture	OPC (%)	Permeability category (ASTM C1202) (days)		
		28	90	365
CCC	-	Moderate	Moderate	Low
F100C0	0	Moderate	Moderate	Moderate
F95C05	5	Moderate	Low	Low
F90C10	10	Very low	Very low	Very low
F85C15	15	Very low	Very low	Very low
F80C20	20	Very low	Very low	Very low
F75C25	25	Very low	Very low	Very low
F30C30	30	Very low	Very low	Very low

With reference to the chloride permeability range as specified in ASTM C1202, it was observed that for CCC as well as for control GPC with 0% OPC, the chloride permeability was “moderate” at all ages. With the inclusion of OPC at 5%, chloride permeability was “moderate” at 28 days, however, at 90 and 365 days, it was improved to “low” category. On the other hand, with the further increase in OPC from 10-30%, the chloride permeability further reduced to “very low” at all the ages. Any concrete falling under “very low” category can be considered as highly resistant against the external chloride attack. It can be concluded from the results that even though the chloride ion permeability in terms of total charge passed increased after 20%, but the increase in values was not significant and almost comparable to those obtained for GPC with 20% OPC. An another important observation can be made here that even though the optimum value of OPC content for the maximum chloride ion resistance was 20%, but beyond this OPC content, the chloride ion resistance was still better than mixture with 0% OPC i.e. the addition of OPC at all the content up to 30% improved the resistance against the chloride attack.

4.3.4 Sulphuric Acid Resistance of Geopolymer Concrete

In the present study, fly ash based GPC mixtures were prepared with the inclusion of OPC as fly ash replacement and their resistance to sulphuric acid was examined. The reason for choosing sulphuric acid over any other acid is due to its practical utilization as concrete members are often subjected to sulphuric acid in various applications like mining, sewage and food processing industries. OPC was included in GPC at 0, 5, 10, 15, 20 and 30% and its effect on sulphuric acid resistance was examined at 28, 90 and 365 days. The parameters such as change in mass and change in compressive strength were used to observe the deterioration. In addition, to examine the microstructure of deteriorated specimens, scanning electron microscopy (SEM), energy dispersive X-ray spectroscopy (EDS) and X-ray diffraction

(XRD) tests were carried out on the sulphuric acid exposed specimens at maximum exposure of 365 days for the geopolymer concrete mixtures with 0, 10, 20 and 30% OPC.

4.3.4.1 Change in Mass

The results of the change in mass for the CCC and GPC mixtures are presented in Fig. 4.54 at 28, 90 and 365 days. At 28 days, the mass gained by 1.6, 1.8, 2.3, 2.6, 2.9, 3.5 and 4.3% for geopolymer concrete mixtures with 0, 5, 10, 15, 20, 25 and 30% OPC, respectively. This was attributed to the fact that geopolymer concrete was subjected to oven curing for 24 hours at 80 °C which created the extra pores in the concrete matrix due to moisture evaporation. When they were exposed to sulphuric acid solution, these pores absorbed the solution and therefore, increased the resultant mass at 28 days. Similar results of mass gain at early ages were also reported by Attiogbe and Rizkalla (1988) and Thokchom (2014). Also previous study (Soroka, 1979) reported the increase in volume due to the absorbed solution, and mentioned as major cause for increasing the mass of geopolymer concrete specimens at early age.

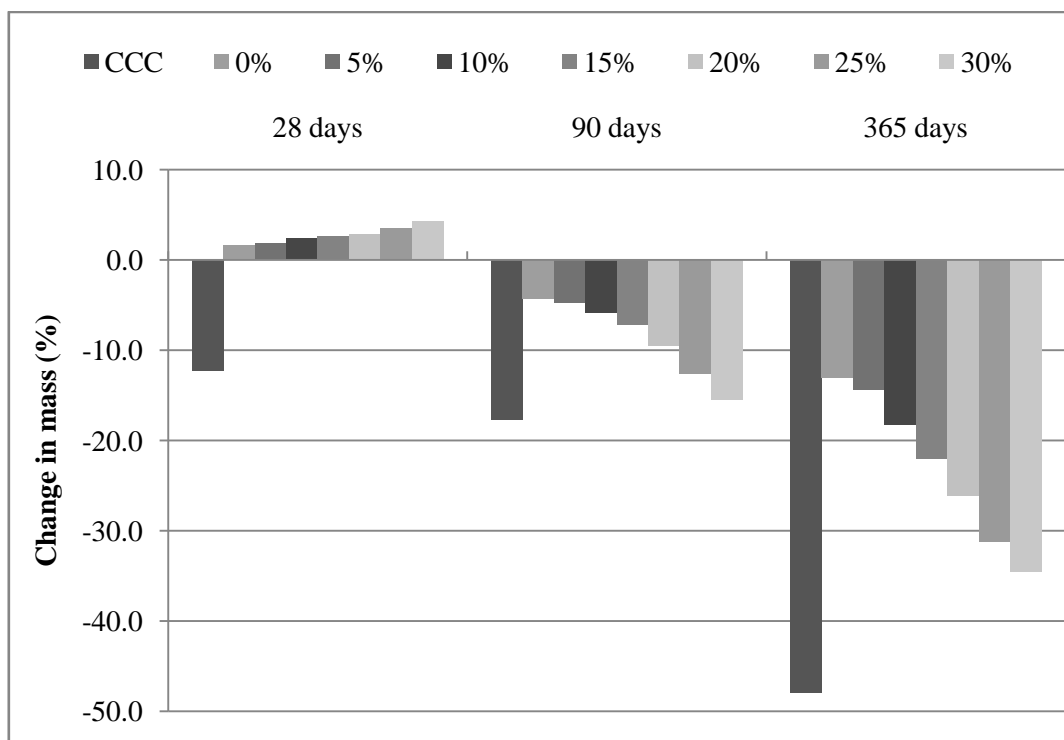


Fig.4.54: Change in mass of sulphuric acid exposed GPC

However, with the increase in exposure period at 90 days, the mass loss of 4.3, 4.7, 5.8, 7.2, 9.5, 12.6 and 15.5% was observed for the GPC mixtures with 0, 5, 10, 15, 20, 25 and 30% OPC, respectively. Similarly, at 365 days, mass loss for the above mixtures was increased to 13.0, 14.4, 18.3, 21.9, 26.1, 31.2 and 34.6%, respectively. This was attributed to the

development of calcium sulphates in GPC caused by the reaction of calcium compounds with sulphuric acid at higher exposure. The calcium based compounds are generally weaker than geopolymer compounds and get easily attacked by sulphuric acid to form calcium sulphates. Therefore, with the increase in calcium content in geopolymer concrete mixtures, additional calcium resulted in the formation of high calcium sulphate which was deposited on the surface as a weak layer (Rajamane et al., 2012). In comparison, loss in mass was observed for CCC by 12.3, 17.7 and 47.9% at 28, 90 and 365 days, respectively.

4.3.4.2 Change in Compressive Strength

The deterioration in terms of change in compressive strength was also evaluated for GPC with 0-30% OPC at 28, 90 and 365 days as shown in Fig. 4.55. At 28 days, the loss in compressive strength was observed as 18.3, 16.4, 15.7, 17.7, 22.1, 25.3 and 28.4% for GPC mixtures with 0, 5, 10, 15, 20, 25 and 30% OPC, respectively. Similarly, for the above mixtures at 90 days, the compressive strength decreased to 21.5, 18.6, 17.8, 21.3, 31.4, 32.2 and 34.2%, respectively. Whereas, at the maximum exposure of 365 days, the compressive strength further decreased to 39.0, 33.8, 29.3, 35.7, 47.6, 51.2 and 56.6% for GPC mixtures with 0, 5, 10, 15, 20, 25 and 30% OPC, respectively. The results showed that with the increase in OPC content in geopolymer concrete, the sulphuric acid resistance increased up to 10% OPC, and beyond that it decreased. In other words, the least values of decrease in compressive strength were obtained for geopolymer concrete mixture with 10% OPC at all ages. This was attributed to the positive effects of additional calcium based products which acted as micro-aggregates and resulted in dense microstructure with reduced permeability. However, the decrease in resistance beyond 10% OPC was due to the adverse effects of additional calcium based CASH and CSH products which created extra nucleation sites for the acid attack in the geopolymer concrete and form additional calcium sulphates, as calcium products are more susceptible to acid attack. Similar deterioration caused by the breakage of calcium based bonds such as CSH and CASH was also reported in the previous study (Mehta and Monteiro, 2005).

It was also observed that geopolymer concrete showed better resistance in comparison to conventional cement concrete against sulphuric acid with OPC content ranging from 0-30% at all ages. For CCC, the compressive strength decreased by 41.4, 52.1 and 72.3% at 28, 90 and 365 days sulphuric acid exposure, respectively. This indicated the better resistance of GPC mixtures as compared to CCC in terms of reduction in compressive strength at all ages.

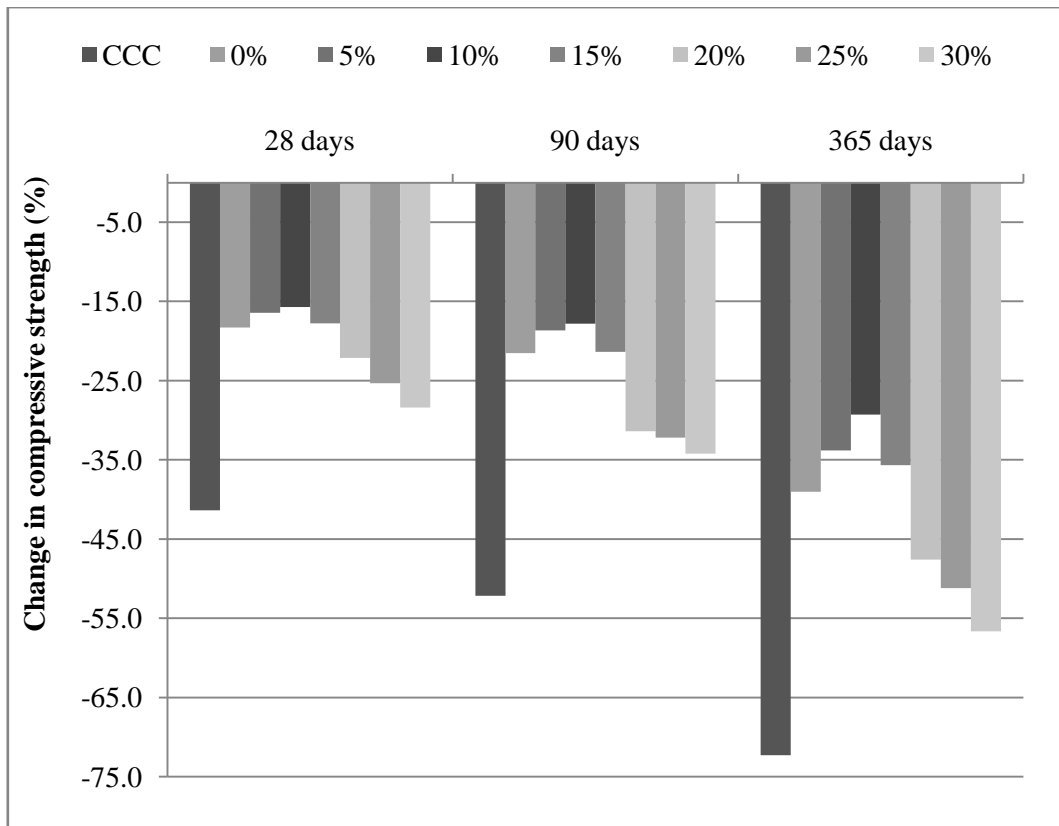


Fig.4.55: Change in compressive strength of sulphuric acid exposed GPC

The mechanism of GPC results in polymerization products of strong sodium-alumino-silicate bonds which do not get easily affected by the acid exposure, therefore, in comparison to CCC, they showed better results. A previous study (Gourley and Johnson, 2005) also reported better acid resistance for geopolymer concrete in comparison to conventional concrete. Song et al. (2005) reported a similar reduction in strength in the range of 32 to 37% for the geopolymer concrete specimens immersed in 10% sulphuric acid solution. Bakharev (2005a) also reported the strength reduction due to the formation of zeolites and depolymerization of geo-polymeric products.

4.3.4.3 Microstructure properties of sulphuric acid exposed geopolymer concrete

To evaluate the microstructure of geopolymer concrete specimens exposed to sulphuric acid, the fractured pieces of compressive strength tests were subjected to SEM, EDS and XRD tests. As observed from the results of change in mass and change in compressive strength, maximum deterioration occurred at the exposure of 365 days, therefore, SEM, EDS and XRD tests were conducted on the geopolymer concrete mixtures with 0, 10, 20 and 30% OPC at the age of 365 days.

- **SEM/EDS Analysis**

The GPC mixtures were found to be deteriorated significantly in terms of change in compressive strength as obtained from the experimental results. The SEM micrographs of GPC exposed to sulphuric acid for 365 days with 0, 10, 20 and 30% OPC are presented in Figs. 4.56-4.59. Previous study (Attiogbe and Rizkalla, 1988) reported that the acid attack on concrete is a surface phenomenon i.e. deterioration starts at the surface and further elongates inward; therefore, it becomes necessary to study the micrographs of exposed surface. The SEM micrographs of unexposed geopolymer concrete are already explained in section 4.2.3. The micrograph of unexposed geopolymer concrete with 0% OPC was associated with the strong polymerization products formed by the reaction between silica and alumina with the alkali-solution in presence of high temperature. The major strength imparting product in geopolymer concrete was NASH as also observed by the XRD results of unexposed specimen which yielded nepheline as its major phases. It had very strong Na-Al-Si bond characteristic which is difficult to break by the external acid at their surface. For the exposed geopolymer concrete with 0% OPC, due to large voids and pore spaces as observed in the SEM micrograph of unexposed specimen, the acid solution was percolated into the matrix and caused deterioration. As observed in the SEM micrograph of exposed specimen, shown in Fig. 4.56, void spaces were found to be fully covered by the acid solution.

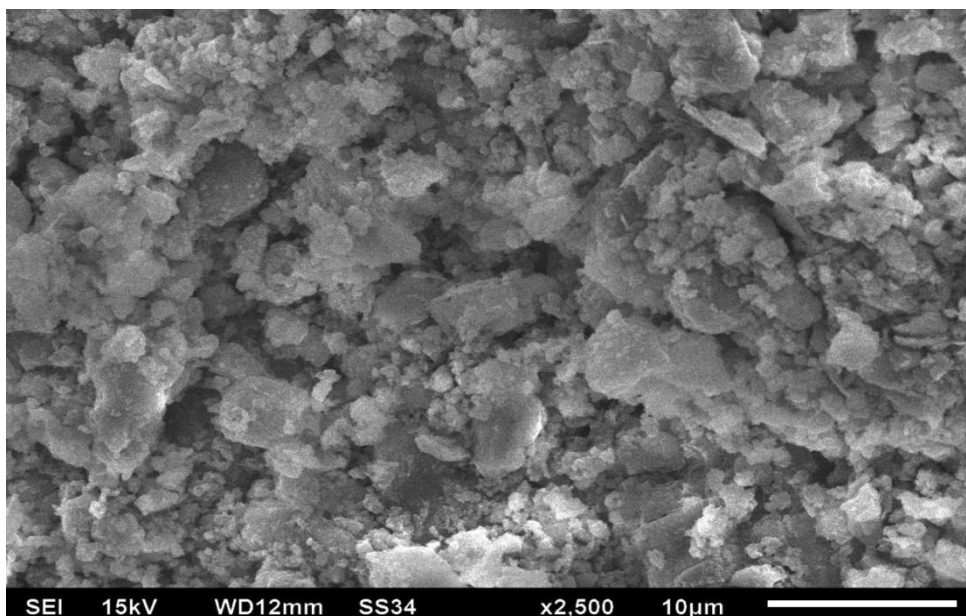


Fig.4.56: SEM micrograph of sulphuric acid exposed GPC with 0% OPC at 365 days

It was also reported in previous study (Ariffin et al., 2013) that at high concentration of acids, the nepheline gets decomposed with a separation of gelatinous silica and cubes of salt. This

transforms the otherwise clear crystals of nepheline into cloudy when exposed to sulphuric acid. In the present study also SEM micrograph showed cloud like formation which was identified as sulphates by EDS analysis and can be considered as major cause of deterioration. The EDS results of the exposed GPC with 0% OPC showed high content of sodium (Na), aluminium (Al), silica (Si) and sulphur (S) with oxygen (O), iron (Fe) and very small content of calcium (Ca) as shown in Fig. 4.60.

For geopolymer concrete with 10% OPC exposed to sulphuric acid for 365 days, the SEM micrograph as shown in Fig. 4.57, was observed to be more compact and dense. Also, the unexposed geopolymer concrete specimens with 10% OPC showed better compact micrograph in terms of lesser voids, pore spaces and micro cracks. It can be explained that even though the addition of calcium in GPC at 10% induced the calcium based hydrated compounds on the surface, which also increased the extra sites for the acid attack due to weaker CSH than NASH, but on the other hand it also decreased the permeability of matrix which didn't allow the acidic ions to penetrate inside the surface easily. Therefore, even though the sulphates were deposited and weakened the outside surface but due to lower permeability, the acid solution was not able to percolate inside the matrix easily and therefore, more strength was retained in comparison to GPC with 0% OPC. The EDS results as shown in Fig. 4.60 showed similar contents of sodium (Na), aluminium (Al) and silica (Si) with relatively higher contents of calcium (Ca) and sulphur (S) compounds in the matrix. The presence of similar strength based compounds in addition with more compact and dense microstructure imparted better compressive strength retained after acid exposure of 365 days as compared to geopolymer specimens with 0% OPC. For GPC with high OPC contents of 20 and 30%, the SEM micrographs are shown in Figs. 4.58 and 4.59, respectively. The SEM micrographs show highly deteriorated surfaces with the further addition of OPC beyond 10%. The formation of calcium compounds trounced over the improvement in microstructure and reacted with sulphuric acid to form calcium sulphates which were adhered to the outer surface too much that they enhanced the deterioration process. The formation of calcium sulphates in higher amount with the increase in OPC was also confirmed by the EDS results. For both the specimens with 20 and 30% OPC, the strength based compounds such as sodium (Na), aluminium (Al) and silica (Si) were found to be decreased significantly whereas the deterioration enhancing compounds such as calcium (Ca) and sulphur (S) were found to be in relatively much higher content. These sulphur based products can be considered as

responsible for decrease in retained strength for the geopolymer concrete specimens with OPC exposed to the sulphuric acid solution.

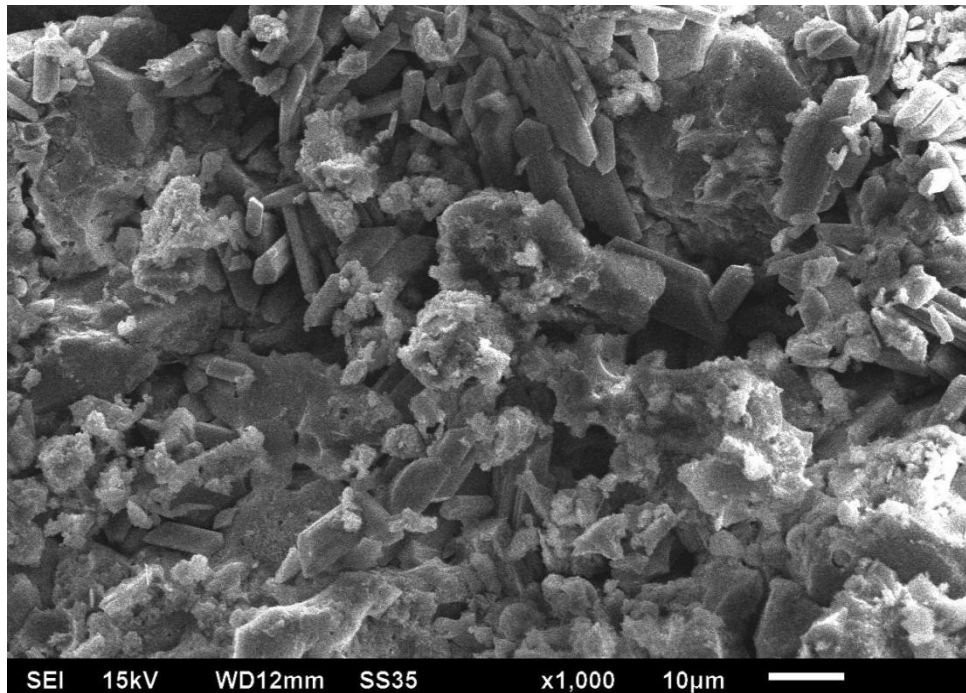


Fig.4.57: SEM micrograph of sulphuric acid exposed GPC with 10% OPC at 365 days

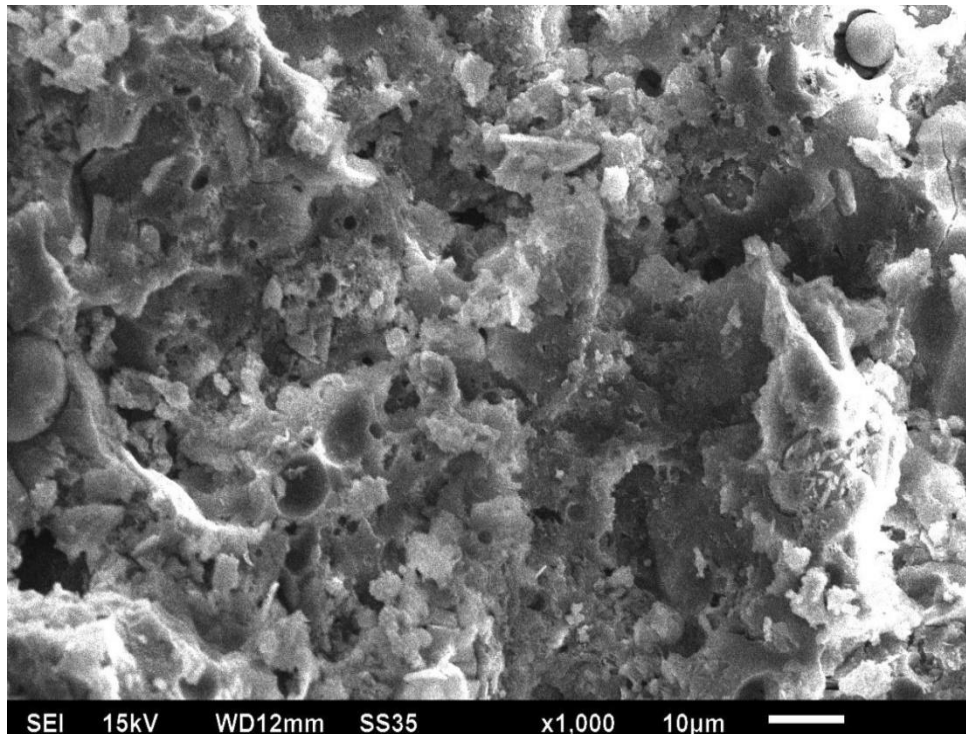


Fig.4.58: SEM micrograph of sulphuric acid exposed GPC with 20% OPC at 365 days

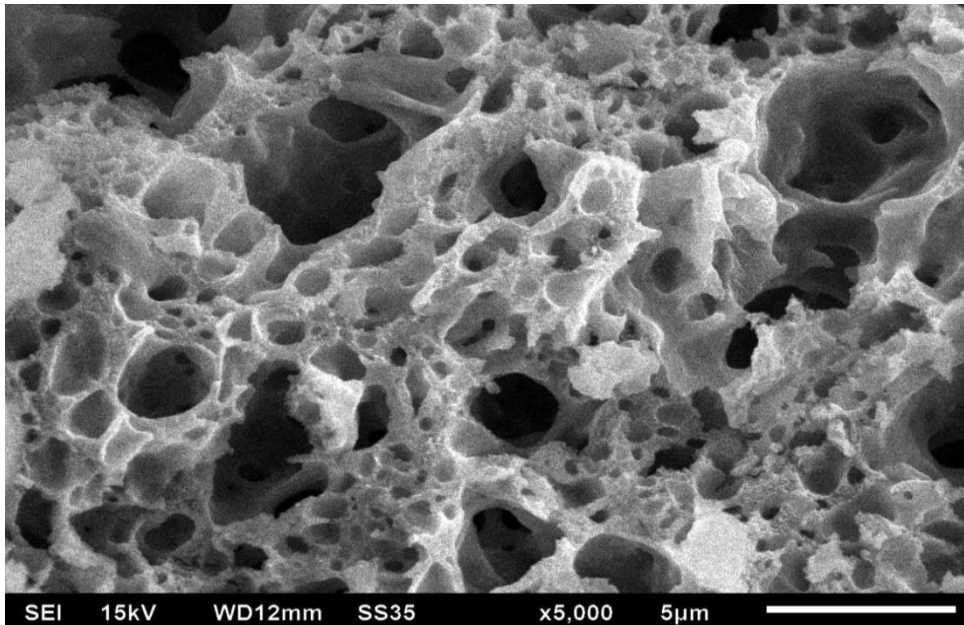


Fig.4.59: SEM micrograph of sulphuric acid exposed GPC with 30% OPC at 365 days

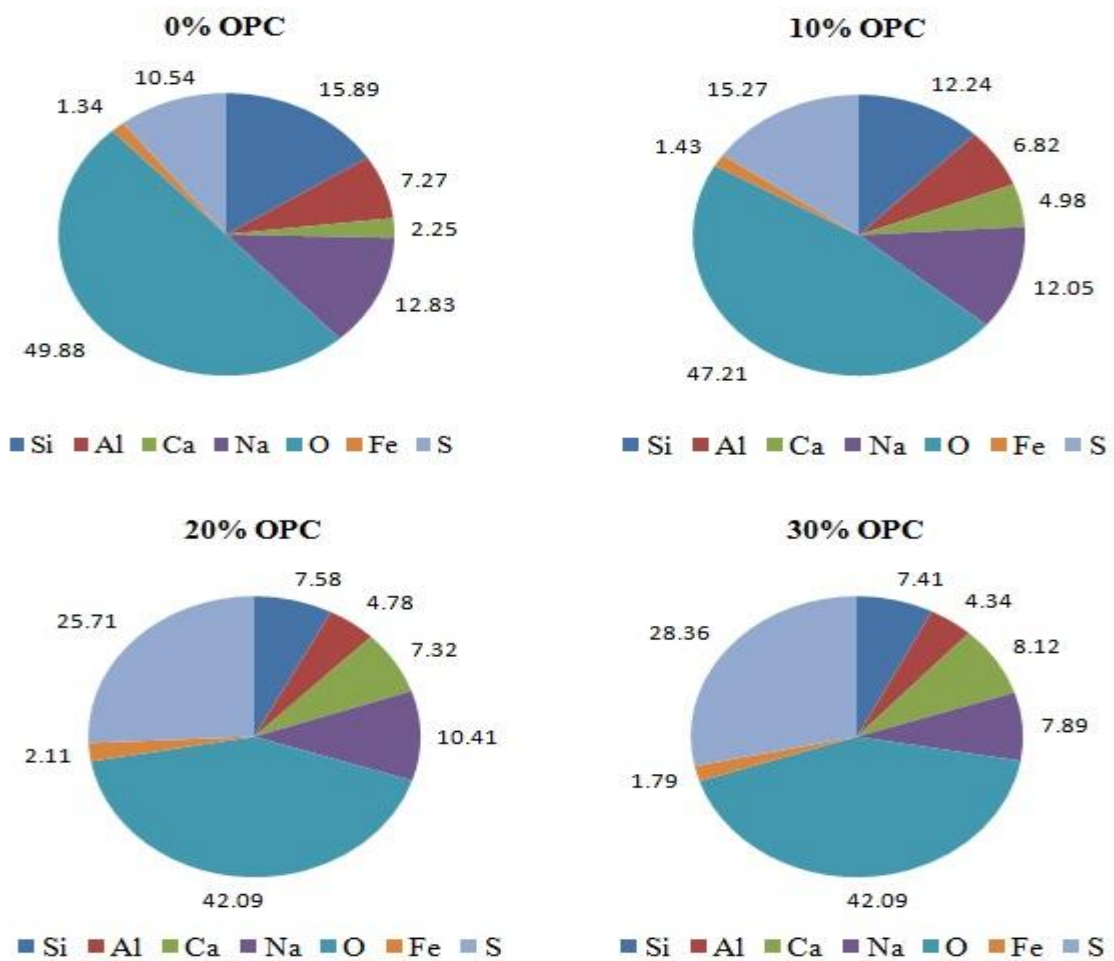


Fig.4.60: EDS results of sulphuric acid exposed GPC with 0, 10, 20 & 30% OPC at 365 days

- **XRD Analysis**

XRD tests were performed on GPC mixtures exposed to sulphuric acid for 365 days. The results for exposed GPC with 0, 10, 20 and 30% OPC are presented in Figs. 4.61-4.64. It was observed that for GPC with 0% OPC, major peaks were identified as quartz, albite, nepheline and tamarugite. The polymerization products such as NASH, as indicated by the presence of nepheline and albite, are very strong bonds of Na-Al-Si which are very difficult to break in comparison to calcium-based CSH and CASH compounds. However, due to the presence of large voids and pore spaces, as observed from SEM micrographs of unexposed specimens, the acid solution gets percolated inside the matrix and absorbed within. The mechanism of geopolymers involves the polymerization reactions with the formation of strong Na-Al-Si bonds, however, when they were exposed to sulphuric acid for a longer duration, depolymerisation of aluminosilicate polymers took place which leads to its deterioration as indicated by the presence of tamarugite phase which is associated with sodium-alumino sulphates.

With the inclusion of OPC in geopolymer concrete at 10%, due to the presence of relatively more calcium in the geopolymer system, additional CASH and CSH were formed as observed by bavenite phase in unexposed geopolymer concrete with 10% OPC. These additional calcium based products filled the pre-existing pores and resulted in dense matrix comparatively. When these specimens were exposed to sulphuric acid, due to lower permeability, acid solution was not able to percolate easily but higher exposure depolymerises NASH and formed sodium-alumino sulphates (as indicated by phase tamarugite). Also, as calcium compounds are more susceptible to acid attack, they reacted with sulphuric acid and formed calcium sulphates as indicated by a new phase anhydrite. It corresponds to calcium sulphate which tends to develop in the OPC-blended geopolymer system due to the reaction between sulphuric acid and the calcium based hydrated products.

With the further inclusion of OPC at 20 and 30% in geopolymer concrete, even though the permeability was further decreased, however, more calcium based CASH and CSH were also formed which further reacted with sulphuric acid to form calcium sulphates in addition to sodium-alumino sulphates. These calcium and sodium-alumino sulphates further reacted to form gypsum compounds, as observed by higher intensities of tamarugite and anhydrite.

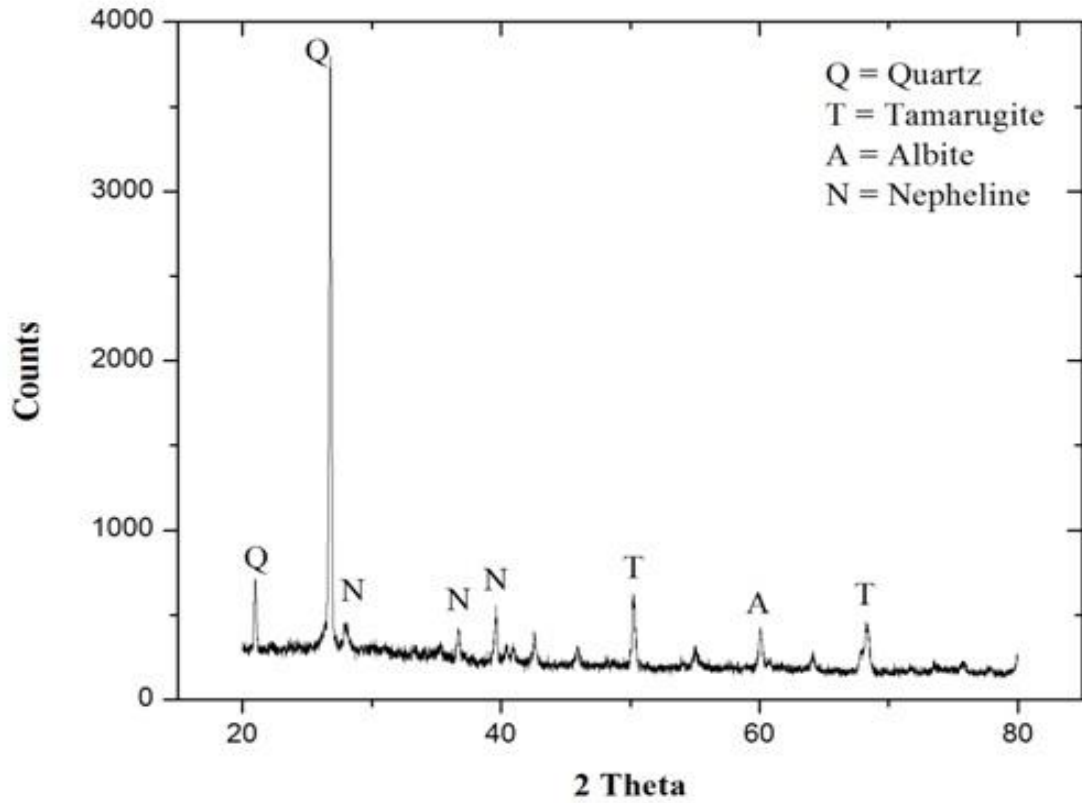


Fig.4.61: XRD analysis of GPC with 0% OPC exposed to sulphuric acid for 365 days

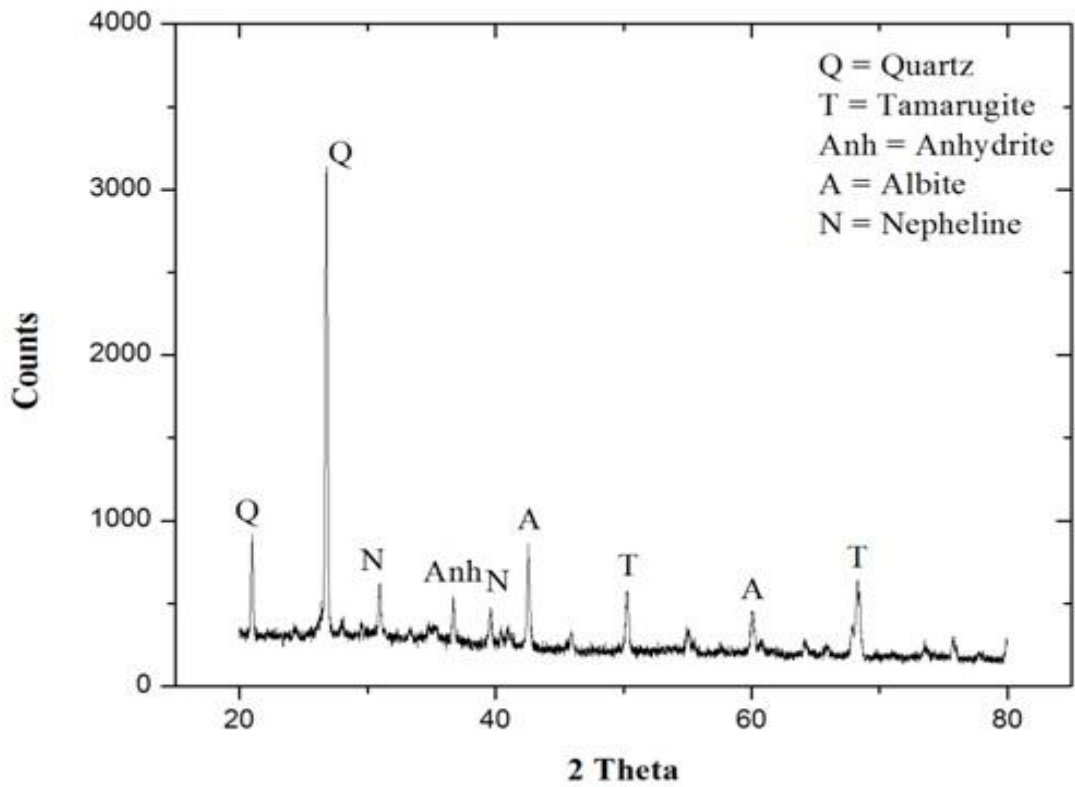


Fig.4.62: XRD analysis of GPC with 10% OPC exposed to sulphuric acid for 365 days

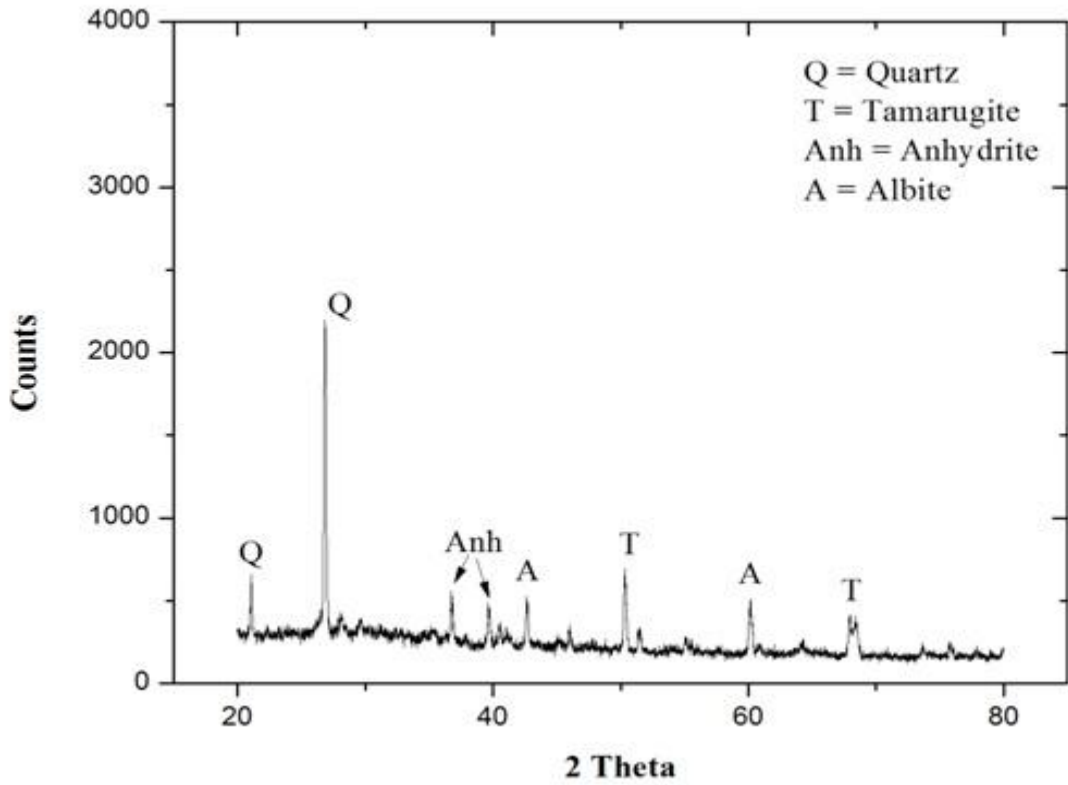


Fig 4.63: XRD analysis of GPC with 20% OPC exposed to sulphuric acid for 365 days

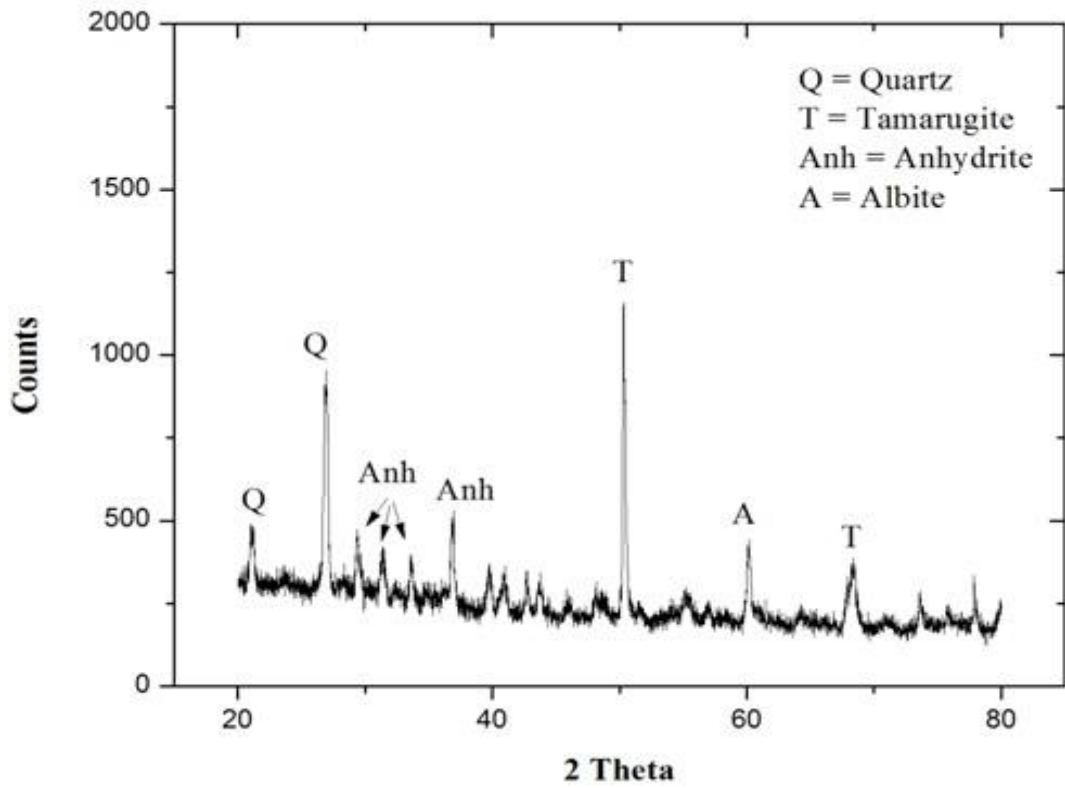


Fig.4.64: XRD analysis of GPC with 30% OPC exposed to sulphuric acid for 365 days

The formation of calcium sulphate had a negative impact on the compressive strength of exposed specimens and can be considered as a significant factor for the concrete deterioration (Attiogbe and Rizkalla, 1988). This calcium sulphate either reacted further to form gypsum or deposited as a weak layer on the concrete surface which decreases its density and softens the matrix. Therefore, the application of external load results in quicker failure of concrete and causes its deterioration. Similar deterioration due to calcium sulphate layer deposition was also reported in previous studies (Chang et al., 2005; Bassuoni and Nehdi, 2007). On similar grounds, it can be explained that CCC was deteriorated more severely than geopolymer concrete due to high calcium compounds which resulted in more calcium sulphates and gypsum formation. Previous studies (Arrifin et al., 2013; Thokchom, 2014) have also reported better acid resistance of geopolymer concrete in comparison to conventional concrete.

4.4 COST-BENEFIT ANALYSIS

The production cost of control GPC and GPC with 20% OPC were compared with the conventional cement concrete CCC of similar 28-day compressive strengths of around 40 and 60 MPa, respectively. The conventional cement concrete of M60 grade was not in the scope of present work, therefore for the cost comparison, the mixture design of M60 concrete was adopted from the previous literature (Muthupriya et al., 2011) as shown in Table 4.2. The costs of materials are confirmed from the available sources and corresponding to their proportion, production cost per cubic meter is calculated as shown in Table 4.3 and Table 4.4.

Table 4.2: Design mixture adopted for the present study

<i>Mixture</i>	<i>Fly ash (kg/m³)</i>	<i>OPC (kg/m³)</i>	<i>Silica fume (kg/m³)</i>	<i>Alkali- activatin g solution (kg/m³)</i>	<i>Coarse aggregates (kg/m³)</i>	<i>Fine aggregates (kg/m³)</i>	<i>Water (kg/m³)</i>	<i>Super plasticizer (kg/m³)</i>
F100C0	310	0	-	171	1204	649	0	6.2
F80C20	248	62.0	-	171	1204	649	0	6.2
CCC	0	410	-	0	1191	667	164	4.1
CCC (60) (Muthupriya et al., 2011)	0	528.7	42.87	0	1171.8	594.58	172	9.23

Table 4.3: Cost comparison of F100C0 and CCC

Material	Cost (Rs./kg)	Quantity (kg/m ³)		Cost (Rs.)	
		F100C0	CCC	F100C0	CCC
Fly Ash	0.5	310	0	155	0
OPC	6.4	0	410	0	2624
Sodium hydroxide	32	48	0	1536	0
Sodium silicate	6	123	0	738	0
Coarse aggregates	2	1204	1191	2408	2382
Fine aggregates	2.15	649	667	1395.35	1434.05
Superplasticizer	52	6.2	4.1	322.4	213.2
<i>Total (Rs./m³)</i>				6554.75	6653.25

It was observed that the production cost of M40 fly ash based geopolymer concrete was found to be around Rs. 100 per cubic meter lesser in comparison to conventional cement concrete. Similarly, fly ash based geopolymer concrete was found to Rs. 1594 per cubic meter cheaper than conventional concrete of M60 grade concrete. The important conclusion can be made here that the inclusion of OPC at 20% optimum content not only exhibit high compressive strength but is also around 23% more economical than conventional concrete.

Table 4.4: Cost comparison of F80C20 and CCC (60)

Material	Cost (Rs./kg)	Quantity (kg/m ³)		Cost (Rs.)	
		F80C20	CCC (60)	F80C20	CCC (60)
Fly Ash	0.5	248	0	124	0
OPC	6.4	62	528.7	396.8	3383.68
Silica Fume	24	-	42.87	-	1028.88
Sodium hydroxide	32	48	0	1536	0
Sodium silicate	6	123	0	738	0
Coarse aggregates	2	1204	1171.8	2408	2343.6
Fine aggregates	2.15	649	594.58	1395.35	1278.347
Superplasticizer	52	6.2	9.23	322.4	479.96
<i>Total (Rs./m³)</i>				6920.55	8514.467

4.5 QUALITY CONTROL REQUIREMENTS FOR FIELD APPLICATIONS

Quality control in concrete construction can be divided into three stages:

- Quality control before concreting

This stage includes the testing of materials used in concreting. The general materials used in the production of geopolymer concrete are source material, alkali-activating solution, admixture and aggregates. The physical and chemical characteristics of source materials should be checked and trial mixtures should be performed to determine the values of certain parameters such as alkali solution to fly ash ratio, sodium silicate to sodium hydroxide ratio, total aggregate content, concentration of sodium hydroxide, fine aggregates to total aggregates ratio, curing temperature, etc. Depending on the target compressive strength, trial mixtures would yield the optimum values of these parameters from which mixture design can be finalized. During the entire construction, it must be ensured that same values of parameters are adopted. Another important quality control parameter is the quality of source materials. In general, source materials used in the production of geopolymer concrete are industrial by-products. These industrial by-products generally do not possess similar chemical compositions obtained from different sources. Therefore, it must be ensured that source material should be obtained from similar source or in case of change of source; the entire mixture design should be performed again.

In addition, temperature curing is an important parameter for geopolymer concrete to attain target compressive strength. Therefore, the curing chambers should be checked carefully for the leakage and constant temperature should be maintained for the entire curing duration.

Other materials such as coarse and fine aggregates should be tested accordingly confirming to BIS 383-1970. In general, the quality of concrete is affected by different physical and mechanical properties of aggregate, i.e. shape, grading, durability, specific gravity and water absorption, etc. which should be tested before using it for concrete production.

- Quality control during concreting

Careful supervision during concrete manufacture is necessary for all concreting operations such as batching, mixing, transporting, laying, compacting and curing. During mixing the mixer should be charged to its full capacity. The materials should be fed in proper sequence. The speed of the mixer should be range from 15 to 20 revolutions per minute. The mixing time should not be less than 2 minutes in any case. Segregation should be avoided while unloading the concrete from the mixer. Workability of concrete is an important property of

concrete while concrete is in its fresh state. Therefore slump test or compaction factor test should be performed to check the workability of concrete.

Vibrators should be used for compacting concrete. The insertion spacing of internal vibrators should not be more than 0.6 m. It should be drawn out slowly so that no holes remain in the concrete. The frequency of vibrators should not be less than 7000 cycles/minutes.

- Quality control after concreting

Once the concrete is laid and compacted, compression tests should be made on the cubes made out of this concrete. The hardened concrete should be checked for trueness in dimensions, shape and sizes as per design specification. General surface appearance of geopolymer concrete should also be checked. Reinforcement should have adequate concrete cover and if the reinforcement is visible in part of a structure, the part should be rejected or necessary actions should be taken accordingly.

Concrete strength is normally to be ascertained from cube or cylinder samples tested at 28 days. In case the strength obtained is less than the specific minimum, one or more of following steps may be taken:

- a) Load test and measurement of deflection and / or strain (the quality of the structure can then be ascertained by calculating back the concrete strength).
- b) Cutting cores from the structures and testing them for strength.
- c) Non-destructive tests like Rebound hammer or Ultrasonic pulse velocity test. These tests give only a very rough idea and are primarily used to ascertain the uniformity of construction.
- d) Chemical analysis of hardened concrete.

CHAPTER-5

CONCLUSIONS

The novelty of present work was to determine the optimized values of various parameters such as ratio of alkali solution-to-fly ash, ratio of sodium silicate-to-sodium hydroxide, molarity of sodium hydroxide, total aggregate content, ratio of fine aggregates-to-total aggregates and curing temperature to develop fly ash based Geopolymer concrete and to study the effect of additional calcium source on fresh, strength and durability properties of low-calcium fly ash based Geopolymer concrete.

The properties of geopolymer concrete studied include workability properties such as slump and compaction factor, strength properties such as compressive strength and split tensile strength, and durability properties such as water absorption, porosity, sorptivity, rapid chloride permeability and sulphuric acid resistance. The microstructure and XRD analysis have also been carried out in this work. Based on the results obtained, the important conclusions are presented in this chapter.

5.1 DEVELOPMENT OF GEOPOLYMER CONCRETE

Various parameters were considered for the development of low-calcium fly ash based geopolymer concrete such as ratio of alkali solution-to-fly ash (0.45-0.75), ratio of sodium silicate-to-sodium hydroxide (2.0-2.75), molarity of sodium hydroxide (5-20M), total aggregate content (60-75%), ratio of fine aggregates-to-total aggregates (0.30-0.45), and curing temperature (60-90 °C for constant duration of 24 hours). Trial mixtures, designed by Taguchi method, were grouped into 3 groups of mixtures, and optimum values were obtained based on maximum 3-day compressive strength.

- Control geopolymer concrete with 3-day compressive strength of 41.3MPa was developed with fly ash content of 310 kg/m³, alkali-solution-to-fly ash ratio of 0.55, sodium silicate-to-sodium hydroxide ratio of 2.5, total aggregate content of 70%, molarity of sodium hydroxide as 10M, fine aggregates-to-total aggregates ratio of 0.35, and temperature curing at 80 °C for 24 hours. Further, additional geopolymer concretes were made by partially replacing fly ash with Ordinary Portland cement (5-30%).

5.2 WORKABILITY PROPERTIES OF GEOPOLYMER CONCRETE

Workability properties were evaluated by slump and compaction factor tests performed on fresh geopolymer concrete mixtures with 0, 5, 10, 15, 20, 25 and 30% OPC and conventional cement concrete. Following conclusions were drawn:

5.2.1 Slump

- Slump for control geopolymer concrete was found to be comparable to the conventional cement concrete of similar 28-day compressive strength.
- It decreased with the increase in fly ash replacement by OPC due to its large irregular sized particles and rapid hardening characteristics.
- Minimum slump of 50 mm was obtained for geopolymer concrete mixture with 30% OPC.

5.2.2 Compaction Factor

- The compaction factor for geopolymer concrete decreased with the increase in OPC content as partial replacement of fly ash.
- The values of compaction factor ranged from 0.91 to 0.86 with OPC content from 0 to 30%, respectively.
- High value of coefficient of determination was obtained which suggested the linear dependency of compaction factor values with OPC content.

5.3 STRENGTH PROPERTIES OF GEOPOLYMER CONCRETE

Strength properties were evaluated on geopolymer concrete with 0, 5, 10, 15, 20, 25 and 30% OPC (as fly ash replacement) and conventional cement concrete. The compressive strength and split tensile strength tests were performed at 3, 7, 28, 90 and 365 days. Following conclusions were drawn:

5.3.1 Compressive Strength

- The compressive strength of fly ash based geopolymer concrete increased with the increase in OPC content up to 20%, and beyond that it decreased. The increase in strength was due to additional CASH and CSH caused by calcium hydration which coexisted with NASH, whereas decrease after 20% was due to the relatively lesser availability of silica and alumina for polymerization.

- The maximum compressive strength of 66.81MPa was obtained for geopolymer concrete with 20% OPC at 365 days.
- High early age compressive strength of 92-98% of its 28-day strength was achieved at 3 days for geopolymer concrete with inclusion of OPC from 0-30%, in comparison to 38% for conventional cement concrete.

5.3.2 Split Tensile Strength

- With the increase in percentage replacement of fly ash by OPC, split tensile strength of geopolymer concrete increased up to an optimum content of 20%, and beyond that it decreased.
- The maximum split tensile strength of 5.35MPa was achieved for geopolymer concrete with 20% OPC at 365 days.
- High early age split tensile strength of 91-95% of its 28-day strength was achieved at 3 days for geopolymer concrete with inclusion of OPC from 0-30% in comparison to 55% for conventional cement concrete as mechanism of geopolymer concrete involves polymerization reaction which took place in the initial curing period of 24 hours.

5.3.3 Microstructure

- The SEM micrographs of control geopolymer concrete with 0% OPC showed lesser bonding with unreacted fly ash particles in addition to voids and pores spaces.
- The best micrograph was observed for geopolymer concrete mixture with 20% OPC in terms of lesser voids, fewer cracks and dense matrix.
- The EDS and XRD analysis of geopolymer concrete mixture with higher OPC content of 30% exhibited more calcium based products CSH and CASH and lesser polymerization product NASH as compared to geopolymer mixtures with 20% OPC which resulted in decremented strength values.

5.4 DURABILITY PROPERTIES OF GEOPOLYMER CONCRETE

Durability properties of geopolymer concrete were evaluated by performing water absorption, porosity, sorptivity, rapid chloride permeability and sulphuric acid resistance tests at the age of 28, 90 and 365 days. Following conclusions were drawn:

5.4.1 Water Absorption and Porosity

- Water absorption, porosity, and sorptivity of fly ash based geopolymer concrete decreased with the increase in OPC up to 20%, and beyond that the values increased.
- The initial decrease was due to additional calcium based products which acted as micro-aggregates and filled the pores, whereas increase after 20% was due to moisture evaporation caused by an enhancement in the effective heat for curing due to hydration reaction.
- For geopolymer concrete, the decrease in water absorption after 28 days was in the range of 5-17% and 18-24% at 90 and 365 days, respectively as compared to 21 and 43% for conventional cement concrete.
- The decrease in porosity after 28 days was in the range of 2-16% and 8-25% at 90 and 365 days, respectively for geopolymer concrete as compared to 16 and 29% for control concrete.

5.4.2 Sorptivity

- Sorptivity was found to decrease with the increase in OPC up to 20%, and beyond that it increased.
- With the age development after 28 days, the sorptivity of geopolymer concrete decreased in the range of 3-10% and 6-15% at 90 and 365 days, respectively in comparison to 13 and 23% for control concrete.

5.4.3 Rapid Chloride Permeability

- The chloride permeability of control geopolymer concrete with 0% OPC was found to be comparable to that of conventional cement concrete at all ages.
- With the inclusion of OPC in geopolymer concrete, the chloride permeability in terms of total charge passed reduced up to 20% OPC, and beyond that the charge values increased slightly. The decrease in permeability was attributed to the pore spaces filled by additional CSH, whereas increase beyond 20% was due to increase in pore spaces caused by evaporation of water from water-filled pores.
- With reference to permeability range specified in ASTM C1202, geopolymer concrete with OPC content from 10-30% exhibited the chloride permeability under “very low” category at all ages.

5.4.4 Sulphuric Acid Resistance

- The geopolymer concrete mixtures with OPC ranging from 0-30% showed better resistance against sulphuric acid as compared to conventional cement concrete at all ages.
- The loss in compressive strength for sulphuric acid exposed geopolymer concrete decreased with the increase in OPC content up to 10%, and beyond that it increased i.e. maximum strength was retained by geopolymer concrete with 10% OPC.
- The decrease in resistance after 10% was due to the adverse effect of additional calcium compounds which reacted with sulphuric acid to form a weak layer of calcium sulphate and gypsum.

5.5 RECOMMENDATIONS

The optimized values of various parameters such as alkali solution to fly ash ratio of 0.55, sodium silicate to sodium hydroxide ratio of 2.5, total aggregate content of 70%, molarity of sodium hydroxide as 10M, fine aggregates to total aggregates ratio of 0.35, and temperature curing at 80°C for 24 hours obtained in this study can be used as reference for the future investigations using materials with similar properties as used in this study. In this way the present work addresses the limitation of not having any reference values of parameters that have a significant effect on properties of geopolymer concrete.

Based on the results obtained in the present study, the present work can be recommended to the pre-cast construction applications where provision can be made for high temperature curing. This can be done by installing a thermally insulated large chamber depending on the size of pre-cast elements. The temperature inside the chamber can be monitored and maintained accordingly. Also, from the cost-benefit analysis of M60 grade of concrete, production cost of fly ash based geopolymer concrete with optimum OPC content found to be cheaper than conventional cement concrete with an extra benefit of achieving around 95% of its 28-day compressive strength at 3 days. Therefore, this research work can be recommended for high strength economic construction applications.

5.6 SUGGESTIONS FOR FUTURE STUDY

The present work has reported the results of an experimental investigation on properties of low-calcium fly ash based geopolymer concrete by incorporating OPC as partial replacement of fly ash. However, due to time constraints the objectives of this study had to be limited and

there are few areas still left which require investigations. The following are the scope of future investigations:

- Investigation of geopolymer concrete with additional OPC should be further expanded to flexural strength and other durability properties such as shrinkage, creep, carbonation, etc.
- The present study was conducted with plain geopolymer concrete. The behaviour of reinforced geopolymer concrete should also be studied subjected to static and dynamic loadings.
- Fire resistance of geopolymer concrete should also be investigated.
- On the basis of optimum OPC content obtained in this study, future study should be more emphasized on the development of self-cured geopolymer concrete.
- Alternate aggregates like quarry dust, copper slag, recycled aggregates, etc should be tried which can make geopolymer technology even more sustainable.
- The cost comparison made in this research is very elementary and gives only a rough estimate of geopolymer and conventional concrete production. A detailed cost analysis can be conducted including the operation cost as well.
- The optimum OPC content should also be evaluated for high-calcium fly ash based geopolymer concrete in future studies which can be used as reference for obtaining a standard mixture design of geopolymer concrete depending on chemical composition of fly ash.

REFERENCES

- Abdulkareem, O.A., Mustafa Al Bakri, A.M., Kamarudin, H., Nizar, K., and Saif, A.A. (2014), "Effects of elevated temperatures on the thermal behavior and mechanical performance of fly ash geopolymer paste, mortar and lightweight concrete." *Construction and Building Materials*; 50: 377-387.
- Adak, D., Sarkar, M., and Mandal, S. (2014), "Effect of nano-silica on strength and durability of fly ash based geopolymer mortar." *Construction and Building Materials*; 70: 453-459
- Aggarwal, P., Aggarwal, Y., and Gupta, S.M. (2007). "Effect of bottom ash as replacement of fine Aggregates in concrete." *Asian journal of civil engineering (Building and Housing)*; 8(1): 49-62.
- Aguilar, A.R., Diaz, O.B., and Escalante-Garcia, J.I. (2010), "Lightweight concretes of activated metakaolin-fly ash binders, with blast furnace slag aggregates." *Construction and Building Materials*; 24: 1166-1175.
- Ahmari, S., and Zhang, L. (2012), "Production of eco-friendly bricks from copper mine tailings through geopolymerization." *Construction and Building Materials*; 29: 323-331.
- Ahmari, S., and Zhang, L. (2013), "Utilization of cement kiln dust (CKD) to enhance mine tailings-based geopolymer bricks." *Construction and Building Materials*; 40: 1002-1011.
- Ahmari, S., Zhang, L., and Zhang, J. (2012), "Effects of activator type/concentration and curing temperature on alkali-activated binder based on copper mine tailings." *Journal of Material Science*; 12: 6497-6499.
- Ahn, T.H., and Kishi, T. (2010), "Crack self-healing behavior of cementitious composites incorporating various mineral admixtures." *Journal of Advanced Concrete Technology*; 8(2): 171-186.
- Aldred, J., and Day, J. (2012), "Is geopolymer concrete a suitable alternative to traditional concrete?" 37th Conference on Our World in Concrete & Structures, Singapore, 29-31 August 2012.
- Alonso, S., and Palomo, A. (2001), "Alkaline activation of metakaolin and calcium hydroxide mixtures: influence of temperature, activator concentration and solids ratio." *Materials Letters*; 47: 55-62.

- Ariffin, M.A.M., Bhutta, M.A.R., Hussin, M.W., and Mohd-Tahir, M. (2013), "Sulfuric acid resistance of blended ash geopolymer concrete." *Construction and Building Materials*; 43: 80-86.
- ASTM C 1202-10, "Standard test methods for Electrical Indication of Concrete's Ability to Resist Chloride Ion Penetration." ASTM International, West Conshohocken, USA.
- ASTM C 1585-04, "Standard test methods for Measurement of Rate of Absorption of Water by Hydraulic - Cement Concretes." ASTM International, West Conshohocken, USA.
- ASTM C 642-97, "Standard test method for density, absorption, and voids in hardened concrete." ASTM International, West Conshohocken, USA.
- Attiogbe, E.K., and Rizkalla, S.H. (1988), "Response of Concrete to Sulfuric Acid Attack." *ACI Material Journal*; November-December.
- Bakharev, T. (2005a), "Resistance of geopolymer materials to acid attack." *Cement and Concrete Research*; 35 (4): 658-670.
- Bakharev, T., (2005b), "Durability of geopolymer materials in sodium and magnesium sulfate solutions." *Cement and Concrete Research*; 35(6): 1233-1246.
- Balaguru, P., Kurtz, S., and Rudolph, J. (1997), "Geopolymer for repair and rehabilitation of reinforced concrete beams." The Geopolymer Institute, www.geopolymer.org.
- Barbosa, V.F., MacKenzie, K.D., and Thaumaturgo, C. (2000), "Synthesis and characterisation of materials based on inorganic polymers of alumina and silica: sodium polysialate polymers." *International Journal of Inorganic Materials*; 2(4): 309-317.
- Bassuoni, M.T., and Nehdi, M.L. (2007), "Resistance of self-consolidating concrete to sulfuric acid attack with consecutive pH reduction." *Cement and Concrete Research*; 37(7): 1070-1084.
- Bernal, S.A., Mejia de Gutierrez, R., and Provis, J.L. (2012), "Engineering and durability properties of concretes based on alkali-activated granulated blast furnace slag/metakaolin blends." *Construction and Building Materials*; 33: 99-108.

- Bhargava, P., Sharma, U.K., and Kaushik, S.K. (2006), "Compressive Stress-Strain Behavior of Small Scale Steel Fibre Reinforced High Strength Concrete Cylinders." *Journal of Advanced Concrete Technology*; 4(1): 109-121.
- BIS: 10262-2009, "Recommended guidelines for concrete mix design." Bureau of Indian Standards, New Delhi, India.
- BIS: 2386 (Part-I)-1997, "Methods of tests for aggregates for concrete-particle size and shape." Bureau of Indian Standards, New Delhi, India.
- BIS: 2386 (Part-III)-1997, "Methods of tests for aggregates for concrete-specific gravity, density, voids, absorption and bulking." Bureau of Indian Standards, New Delhi, India.
- BIS: 3812-2003, "Specifications for Pulverized fuel ash." Bureau of Indian Standards, New Delhi, India.
- BIS: 383-1970, "Indian standard Specification for coarse and fine aggregates from natural sources for concrete." Bureau of Indian Standards, New Delhi, India.
- BIS: 4031 (Part-IV)-1988, "Methods of physical tests for hydraulic cement-determination of consistency of standard cement paste." Bureau of Indian Standards, New Delhi, India.
- BIS: 4031 (Part-V)-1988, "Methods of physical tests for hydraulic cement-determination of initial and final setting times." Bureau of Indian Standards, New Delhi, India.
- BIS: 4031 (Part-VI)-1988, "Methods of physical tests for hydraulic cement-determination of compressive strength of hydraulic cement other than masonry cement." Bureau of Indian Standards, New Delhi, India.
- BIS: 516-1959, "Indian standard methods of test for strength of concrete." Bureau of Indian Standards, New Delhi, India.
- BIS: 5816-1999, "Indian standard Splitting tensile strength of concrete- Test method." Bureau of Indian Standards, New Delhi, India.
- BIS: 8112-1989, "Indian standard 43 Grade ordinary Portland cement-specification." Bureau of Indian Standards, New Delhi, India.
- BIS: 9103-1999, "Concrete admixtures-specifications." Bureau of Indian Standards, New Delhi, India.

- Bondar, D., Lynsdale, C.J., Milestone, N.B., Hassani, N., and Ramezani pour, A.A. (2011), "Effect of type, form, and dosage of activators on strength of alkali-activated natural pozzolans." *Cement and Concrete Composites*; 33(2): 251-260.
- Buchwald, A., Hilbig, H., and Kaps, C.H. (2007), "Alkali-activated metakaolin-slag blends performance and structure in dependence of their composition." *Journal of Materials Science*; 42(9): 3024-3032.
- Bui, D.D., Hu, J., and Stroeven, P. (2005), "Particle size effect on the strength of rice husk ash blended gap-graded Portland cement concrete." *Cement and Concrete Composites*; 27: 357-366.
- Cachim, P., Velosa, A.L., and Rocha, F. (2010), "Effect of Portuguese metakaolin on hydraulic lime concrete using different curing conditions." *Construction and Building Materials*; 24: 71-78.
- Castel, A., and Foster, S.J. (2015), "Bond strength between blended slag and Class F fly ash geopolymer concrete with steel reinforcement." *Cement and Concrete Research*; 72: 48-53.
- Cembureau (2007), "Cement in cembureau countries statistics 2005-2007." Cembureau, <http://www.cembureau.be/Documents/KeyFacts/STATISTICS/Cementpercent20inpercent20CEMBpercent20countries.pdf>.
- Chalee, W., Ausapanit, P., and Jaturapitakkul, C. (2010), "Utilization of fly ash concrete in marine environment for long term design life analysis." *Materials and Design*; 3: 1242-1249.
- Chang, Z.T., Song, X.J., Munn, R., and Marosszeky, M. (2005), "Using limestone aggregates and different cements for enhancing resistance of concrete to sulfuric acid attack." *Cement and Concrete Research*; 35(8): 1486-1494.
- Chindaprasirt, P., Chareerat, T., and Sirivivatnanon, V. (2007), "Workability and strength of coarse high calcium fly ash geopolymer." *Cement and Concrete Composites*; 29: 224-229.
- Chindaprasirt, P., Chareerat, T., Hatanaka, S., and Cao, T. (2011), "High-strength geopolymer using fine high-calcium fly ash." *Journal of Materials in Civil Engineering*; 23: 264-270.

- Chindaprasirt, P., Silva, P., Sagoe-Crentsil, K., and Hanjitsuwan, S. (2012), "Effect of SiO₂ and Al₂O₃ on the setting and hardening of high calcium fly ash-based geopolymer systems." *Journal of Materials and Science*; 47: 4876-4883.
- Chotetanorm, C., Chindaprasirt, P., Sata, V., Rukzon, S., and Sathonsaowaphak, A. (2013), "High-calcium bottom ash geopolymer: sorptivity, pore size, and resistance to sodium sulfate attack." *Journal of Materials in Civil Engineering*; 25: 105-111.
- Collins, F.G., and Sanjayan, J.G. (1999), "Workability and mechanical properties of alkali activated slag concrete." *Cement and Concrete Research*; 29(3), 455-458.
- Comrie, D. C., Paterson, J. H., and Ritchey, D. J. (1988), "Geopolymer technologies in toxic waste management." *First European Conference on Soft Mineralurgy, Compiègne, France, 1988.*
- Cwirzen, A., Provis, J.L., Penttala, V., and Habermehl-Cwirzen, K. (2014), "The effect of limestone on sodium hydroxide-activated metakaolin-based geopolymers." *Construction and Building Materials*; 66: 53-62.
- Cyr, M., Trinh, M., Husson, B., and Casaux-Ginestet, G. (2014), "Effect of cement type on metakaolin efficiency." *Cement and Concrete Research*; 64: 63-72.
- Davidovits, J. (1991), "Geopolymer: inorganic polymer new materials." *Journal of Thermal Analysis*; 37(8): 1633-1656.
- Davidovits, J. (1994a), "High-alkali cements for 21st century concretes." *Proceedings of V. Mohan Malhotra Symposium, ACI SP*; 144: 383-397.
- Davidovits, J. (1994b), "Global warming impact on the cement and aggregates industries." *World Resource Review*; 6(2): 263-278.
- Davidovits, J. (1994c), "Properties of geopolymer cements." *First International Conference on Alkaline Cements and Concrete, SRIBMK State Technical University, 1994.*
- Davidovits, J. (2002), "30 years of successes and failures in geopolymer applications." *Proceedings of the Geopolymer 2002 Turning potential into profit Third International Conference, Melbourne, Australia, 2002.*

- Demie, S., Nuruddin, M.F., and Shafiq, N. (2013), "Effects of micro-structure characteristics of interfacial transition zone on the compressive strength of self-compacting geopolymer concrete." *Construction and Building Materials*; 41: 91-98.
- Dombrowski, K., Buchwald, A., and Well, M. (2006), "The influence of calcium content on the structure and thermal performance of fly ash based geopolymers." *Journal of Materials Science*; 42(9): 3033-3043.
- Duxson, P., Fernandez-Jimenez, A., Provis, J.L., Lukey, Palomo, G.C.A., and Van Deventer, J.S.J. (2007), "Geopolymer technology: the current state of the art." *Journal of Materials Science*; 42: 2917-2933.
- Feng, Q., Yamamichi, H., Shoya, M., and Sugita, S. (2004), "Study on the pozzolanic properties of rice husk ash by hydrochloric acid pretreatment." *Cement and Concrete Research*; 34: 521-526.
- Fernandez-Jimenez, A., and Palomo, A. (2003), "Characterisation of fly ash: potential reactivity as alkaline cements." *Fuel*; 82: 2259-2265.
- Ferraz, E., Andrejkovicova, S., Velosa, A.L., Silva, A.S., and Rocha, F. (2014), "Synthetic zeolite pellets incorporated to air lime-metakaolin mortars: Mechanical properties." *Construction and Building Materials*; 69: 243-252.
- Fletcher, R.A., Mackenzie, K.J.D., Nicholson, C.L., and Shimada, S. (2005), "The composition range of aluminosilicate geopolymers." *European Ceramic Society*; 25: 1471-1477.
- Gartner, E. (2004), "Industrially interesting approaches to low-CO₂ cements." *Cement and Concrete Research*; 34(9): 1489-1498.
- Gayarre, F.L., Perez, C.L.C., Lopez, M.A.S., and Cabo, A.D. (2014), "The effect of curing conditions on the compressive strength of recycled aggregate concrete." *Construction and Building Materials*; 53: 260-266.
- Glukhovskiy, V.D. (1959), *Soil silicates (Gruntosilikaty)*, USSR Kiev. Budivelnik Publisher, 1959.
- Gourley, J.T., and Johnson, G.B. (2005), "Developments in geopolymer precast concrete." *International Workshop on Geopolymers and Geopolymer Concrete*, Perth, Australia, 2005.

- Guo, X.L., Shi, H.S., and Dick, W.A. (2010), "Compressive strength and microstructural characteristics of class C fly ash geopolymer." *Cement and Concrete Composites*; 32(2): 142-147.
- Haq, E.U., Padmanabhan, S.K., and Licciulli, A. (2014), "Synthesis and characteristics of fly ash and bottom ash based geopolymers—A comparative study." *Ceramics International*; 40: 2965-2971.
- Hardjito, D., Wallah, S.E., Sumajouw, D.M.J., and Rangan, B.V. (2004), "On the development of fly ash based geopolymer concrete." *ACI Material Journal*; 101(6): 467-472.
- Hardjito, D., Cheak, C.C., and Ing, C.H.L. (2008), "Strength and setting times of low calcium fly ash based geopolymer mortar." *Modern Applications of Science*; 2(4): 3-11.
- He, J., Zhang, G., Hou, S.A., and Cai, C.S. (2011), "Geopolymer-based smart adhesives for infrastructure health monitoring: concept and feasibility." *Journal of Materials in Civil Engineering*; 23(2), 100-109.
- He, J., Zhang, J., Yu, Y., and Zhang, G. (2012), "The strength and microstructure of two geopolymers derived from metakaolin and red mud-fly ash admixture: A comparative study." *Construction and Building Materials*; 30: 80-91.
- He, J., Jie, Y., Zhang, J., Yu, Y., and Zhang, G. (2013), "Synthesis and characterization of red mud and rice husk ash-based geopolymer composites." *Cement & Concrete Composites*; 37(3): 108-118.
- Hwang, C.L., and Wu, D.S. (1989), "Properties of cement paste containing rice husk ash." *American Concrete Institute SP*; 114: 733-765.
- IPCC (2007), "Climate change 2007: Working group III: Mitigation of climate change, emission trends (global and regional)." IPCC, [http:// www.ipcc.ch/publications and data /ar4/wg3/en/tssts-ts-7-2-emission-trends.html](http://www.ipcc.ch/publications_and_data/ar4/wg3/en/tssts-ts-7-2-emission-trends.html).
- Joseph, B., and Mathew, G. (2012), "Influence of aggregate content on the behavior of fly ash based geopolymer concrete." *ScientiaIranica, Transactions A: Civil Engineering*; 19: 1188-1194.
- Jumate, E., and Manea, D.L. (2011), "X-Ray diffraction study of hydration processes in the Portland cement." *Journal of Applied Engineering Sciences*; 1(14): 79-86.

- Junaid, M.T., Kayali, O., Khennane, A., and Black, J.(2015), "A mix design procedure for low calcium alkali activated fly ash-based Concretes." *Construction and Building Materials*; 79: 301-310.
- Khater, H.M., El-Sabbagh, B.A., and Fanny, M. (2012), "Effect of nano-silica on alkali activated water-cooled slag geopolymer." *ARPN Journal of Science and Technology*; 2(3): 170-176.
- Khatib, J.M., Negim, E.M., Yeligbayeva, G.Z.H., and Mun, G.A. (2014), "Strength characteristics of mortar containing high volume metakaolin as cement replacement." *Research and Reviews in Materials Science and Chemistry*; 3(1): 85-95.
- Koehler, E.P., and Fowler, D.W. (2003), "Summary of concrete workability test methods." ICAR, Austin, 2003.
- Kong, D.L.Y., Sanjayan, J.G., and Sagoe-Crentsil, K. (2007), "Comparative performance of geopolymers made with metakaolin and fly ash after exposure to elevated temperatures." *Cement and Concrete Research*; 37(12): 1583-1589.
- Kong, D.L.Y., and Sanjayan, J.G. (2008), "Damage behavior of geopolymer composites exposed to elevated temperatures." *Cement and Concrete Composites*; 30(10): 986-991.
- Kong, D.L.Y., and Sanjayan, J.G. (2010), "Effect of elevated temperatures on geopolymer paste, mortar and concrete." *Cement and Concrete Research*; 40(2): 334-339.
- Kouamo, H.T., Elimbi, A., Mbey, J.A., Ngally, S.C.J., and Njopwouo, D. (2012), "The effect of adding alumina-oxide to metakaolin and volcanic ash on geopolymer products: A comparative study." *Construction and Building Materials*; 35: 960-969.
- Kourti, I., Rani, D.A., Boccaccini, A.R., and Cheeseman, C.R. (2011), "Geopolymers from DC plasma treated APC residues, metakaolin and GGBFS." *Journal of Materials in Civil Engineering*; 23(6): 735-740.
- Krammart, P., and Tangtermsirikul, S. (2004), "Properties of cement made by partially replacing cement raw materials with municipal solid waste ashes and calcium carbide waste." *Construction and Building Materials*; 18: 579-583.

- Kroehong, W., Sinsiri, T., Jaturapitakkul, C., and Chindaprasirt, P. (2011), "Effect of palm oil fuel ash fineness on the microstructure of blended cement paste." *Construction and Building Materials*; 25: 4095-4104.
- Kusbiantoro, A., Nuruddin, M.F., Shafiq, N., and Qazi, S.A. (2012), "The effect of microwave incinerated rice husk ash on the compressive and bond strength of fly ash based geopolymer concrete." *Construction and Building Materials*; 36: 695-703.
- Lee, W.K.W., and Van Deventer, J.S.J. (2002a), "The effects of inorganic salt contamination on the strength and durability of geopolymers." *Colloids and Surfaces A*; 211: 115-126.
- Lee, W.K.W., and Van Deventer, J.S.J. (2002b), "The effect of ionic contaminants on the early age properties of alkali-activated fly ash based cements." *Cement and Concrete Research*; 32: 577-584.
- Lee, W.K.W., and Van Deventer, J.S.J. (2007), "Chemical interactions between siliceous aggregates and low-Ca alkali-activated cements." *Cement and Concrete Research*; 37(6): 844-855.
- Li, Z.J., and Liu, S.F. (2007), "Influence of slag as additive on compressive strength of fly ash based geopolymer." *Journal of Materials in Civil Engineering*; 19(6): 470-474.
- Liu, Z., Deng, D., Schutter G.D., and Yu, Z. (2012), "Chemical sulfate attack performance of partially exposed cement and cement + fly ash paste." *Construction and Building Materials*; 28: 230-237.
- Madan, S.K., Kumar, G.R., and Singh, S.P. (2007), "Steel fibers as replacement of web reinforcement for RCC deep beams in shear." *Asian Journal of Civil Engineering (Building and Housing)*; 8(5): 479-489.
- McCaffrey, R. (2002), "Climate change and the cement industry." *Global Cement and Lime Magazine (Environmental Special Issue)*; 15-19.
- Mehta, P.K. (1992), "Rice husk ash-a unique supplementary cementing material." *Proceedings of the International Symposium on Advances in Concrete Technology, Athens, Greece, 1992*, 407-430.
- Mehta, P.K. (2002), "Greening of the concrete industry for sustainable development", *ACI Concrete International*; 24(7): 23-28.

- Mehta, P.K., and Monteiro, P.J.M. (2005), "Concrete: Microstructure, Properties and Materials." Tata Mc-Graw Hill, New York (3rd edition), 2005.
- Milicevic, I., Bjegovic, D., and Siddique, R. (2015), "Experimental research of concrete floor blocks with crushed bricks and tiles aggregate." *Construction and Building Materials*; 94: 775-783.
- Mishra, S., Yamamoto, A., Tsutsumi, T., and Motohashi, K. (1994), "Application of rapid chloride permeability test to quality control of concrete." *Special publication American Concrete Institute*; 145: 487-502.
- Mobili, A., Belli, A., Giosue, C., Bellezze, T., and Tittarelli, F. (2016), "Metakaolin and fly ash alkali-activated mortars compared with cementitious mortars at the same strength class." *Cement and Concrete Research*; 88: 198-210.
- Motorwala, A., Shah, V., Kammula, R., Nannapaneni, P., and Raijiwala, D.B. (2013), "Alkali activated fly-ash based geopolymer concrete." *International Journal of Emerging Technology and Advanced Engineering*; 3(1): 159-166.
- Muthupriya, P., Subramanian, K., and Vishnuram, B.G. (2011), "Experimental investigation on high performance reinforced concrete column with silica fume and fly ash as admixtures." *Asian Journal of Civil Engineering (Building and Housing)*; 12(5): 597-618.
- Nagendra, V., Sashidhar, C., Prasanna, S.M.K., and Ramana, N.V. (2016), "Particle Size Effect of Ground Granulated Blast Furnace Slag (GGBS) in Cement Concrete." *International Journal of Recent Trends in Engineering & Research (IJRTER)*; 2(8): 6-10.
- Nath, P., and Sarker, P.K. (2012), "Geopolymer concrete for ambient curing condition." *The Australasian Structural Engineering Conference, Perth, Western Australia, 2012.*
- Nath, P., and Sarker, P.K. (2014), "Effect of GGBFS on setting, workability and early strength properties of fly ash geopolymer concrete cured in ambient condition." *Construction and Building Materials*; 66: 163-171.
- Nath, S.K., and Kumar, S. (2013), "Influence of iron making slags on strength and microstructure of fly ash geopolymer." *Construction and Building Materials*; 38: 924-930.

- Nazari, A., and Sanjayan, J.G. (2015), "Synthesis of geopolymer from industrial wastes." *Journal of Cleaner Production*; 3(3): 1-8.
- Netinger, I., Rukavina, M.J., and Mladenovic, A. (2013), "Improvement of post-fire properties of concrete with steel slag aggregate." *The 9th Asia-Oceania Symposium on Fire Science and Technology - Procedia Engineering*; 62: 745-753.
- Ng, S., Jelle, B.P., Sandberg, L.I.C, Gao, T., and Wallevik, O.H. (2015), "Experimental investigations of aerogel-incorporated ultra-high performance concrete." *Construction and Building Materials*; 77: 307-316.
- Oh, J.E., Monteiro, P.J.M., Jun, S.S., Choi, S., and Clark, S.M. (2010), "The evolution of strength and crystalline phases for alkali-activated ground blast furnace slag and fly ash based geopolymers." *Cement and Concrete Research*; 40: 189-196.
- Olivia, M., and Nikraz, H.R. (2011), "Strength and water penetrability of fly ash geopolymer concrete." *Journal of Engineering and Applied Sciences*; 6(7): 70-78.
- Pacheco-Torgal, F., Castro-Gomes, J., and Jalali, S. (2008), "Investigations of tungsten mine waste geopolymeric binder: Strength and microstructure." *Construction and Building Materials*; 22 (11): 2212-2219.
- Pacheco-Torgal, F., Moura, D., Ding, Y., and Jalali, S. (2011), "Composition, strength and workability of alkali-activated metakaolin based mortars." *Construction and Building Materials*; 25: 3732-3745.
- Palomo, A., Grutzeck, M.W., and Blanco, M.T. (1999), "Alkali activated fly ashes: A cement for the future." *Cement and Concrete Research*; 29(8): 1323-1329.
- Pan, Z., and Sanjayan, J.G. (2010), "Stress-strain behaviour and abrupt loss of stiffness of geopolymer at elevated temperatures." *Cement and Concrete Composites*; 32(9): 657-664.
- Pan, Z., Sanjayan, J.G., and Rangan B.V. (2009), "An investigation of the mechanisms for strength gain or loss of geopolymer mortar after exposure to elevated temperature." *Journal of Materials Science*; 44(7): 873-1880.

- Pangdaeng, S., Phoo-ngernkham, T., Sata, V., and Chindaprasirt, P. (2014), "Influence of curing conditions on properties of high calcium fly ash geopolymer containing Portland cement as additive." *Materials and Design*; 53: 269-274.
- Patil, K.K., and Allouche, E.N. (2013), "Impact of alkali silica reaction on fly ash-based geopolymer concrete." *Journal of Materials in Civil Engineering*; 25: 131-139.
- Perera, D.S., Uchida, O., Vance, E.R., and Finnie, K.S. (2007), "Influence of curing schedule on the integrity of geopolymers." *Journal of Material Science*; 42 (9): 3099-3106.
- Pietersen, H.S., Fraay, A.L.A., and Bijen, J.M. (1989), "Reactivity of fly ash at high pH." *MRS Proceeding*; 178: 139-157.
- Prince, M.J.B., and Singh, B. (2014), "Bond behaviour between recycled aggregate concrete and deformed steel bars." *Materials and Structures*; 47: 503-516.
- Puertas, F., and Fernandez-Jimenez, A. (2003), "Mineralogical and micro structural characterisation of alkali-activated fly ash/slag pastes." *Cement and Concrete Composites*; 25(3): 287-292.
- Puertas, F., and Torres-Carrasco, M. (2014), "Use of glass waste as an activator in the preparation of alkali-activated slag cements: Mechanical strength and paste characterization." *Cement and Concrete Research*; 57: 95-104.
- Rahul, P.C., and Mundhada, A.R. (2012), "Effect of fire on flexural strength of reinforced concrete beam." *International Journal of Engineering Research & Technology*; 1(3): 1-6.
- Rajamane, N.P., Nataraja, M.C., Lakshmanan, N., Datatreya, J.K., and Sabitha, D. (2012), "Sulphuric acid resistant ecofriendly concrete from geopolymerization of blast furnace slag." *Indian Journal of Engineering and Material Science*; 19: 357-367.
- Rao, A., Jha, K.N., and Mishra, S. (2007), "Use of aggregates from recycled construction and demolition waste in concrete." *Resources, Conservation and Recycling*; 50: 71-81.
- Rattanasak, U., Chindaprasirt, P., and Suwanvitaya, P. (2010), "Development of high volume rice husk ash alumino silicate composites." *International Journal of Minerals, Metallurgy, and Materials*; 17(5): 654-659.

- Reddy, D.V., Edouard, J.B., and Sobhan, K. (2013), "Durability of fly ash-based geopolymer structural concrete in the marine environment." *Journal of Materials in Civil Engineering*; 25: 781-787.
- Rees, C.A., Provis, J.L., Lukey, G.C., and Van Deventer, J.S.J. (2007), "Attenuated total reflectance fourier transform infrared analysis of fly ash geopolymer gel aging." *Langmuir*; 23(15): 8170-8179.
- Rovnanik, P. (2010), "Effect of curing temperature on the development of hard structure of metakaolin-based geopolymer." *Construction and Building Materials*; 24: 1176-1183.
- Ryu, G.S., Lee, Y.B., Koh, K.T., and Chung, Y.S. (2013), "The mechanical properties of fly ash-based geopolymer concrete with alkaline activators." *Construction and Building Materials*; 47: 409-418.
- Sachan, A.K., and Sahu, A.K. (2013), "Effect of aggressive chemical environment on setting characteristics of plain and blended cement." *International Journal of Structural and Civil Engineering Research*; 2(2): 77-83.
- Sagawa, Y., Yamamoto, D., and Henzan, Y. (2011), "Properties of concrete with GGBS and its Applications for Bridge Superstructures." *Third International conference on sustainable construction materials and technologies, Japan, 2011.*
- Sata, V., Sathonsaowaphak, A., and Chindaprasirt, P. (2012), "Resistance of lignite bottom ash geopolymer mortar to sulfate and sulphuric acid attack." *Cement and Concrete Composites*; 34: 700-708.
- Sathonsaowaphak, A., Chindaprasirt, P., and Pimraksa, K. (2009), "Workability and strength of lignite bottom ash geopolymer mortar." *Journal of Hazardous Materials*; 168(1): 44-50.
- Shi, C., Jimenez, F., and Palomo, A. (2011), "New cements for the 21st century: The pursuit of an alternative to Portland cement." *Cement and Concrete Research*; 41(7): 750-763.
- Silva, P.D., Sagoe-Crenstil, K., and Sirivivatnanon, V. (2007), "Kinetics of geopolymerization: Role of Al_2O_3 and SiO_2 ." *Cement and Concrete Research*; 37(4): 512-518.
- Singh, G. (2012), "Strength and durability studies of concrete containing waste foundry sand." *Ph.D Thesis-Department of Civil Engineering, Thapar University, India.*

- Skavara, F., Jilek, T., and Kopecky, L. (2005), "Geopolymer materials based on fly ash." *Ceramic Silikaty*; 49(3): 195-204.
- Smarzewski, P., and Barnat-Hunek, D. (2016), "Mechanical and durability related properties of high performance concrete made with coal cinder and waste foundry sand." *Construction and Building Materials*; 121: 9-17.
- Song X.J., Marosszeky, Brungs, M.M., and Munn, R. (2005), "Durability of fly ash-based Geopolymer concrete against sulphuric acid attack." *International Conference on Durability of Building Materials and Components*, Lyon, France, 2005.
- Soroka, I. (1979), "Portland Cement Paste and Concrete." *Macmillan Press*; 151-152: London (1979).
- Spannagle, M. (2002), "Environmental drivers-geopolymers and greenhouse geopolymers." *Turn Potential into Profit (ISBN: 0975024205)*; 46: 193.
- Suwan, T., and Fan, M. (2014), "Influence of OPC replacement and manufacturing procedures on the properties of self-cured geopolymer." *Construction and Building Materials*; 73: 551-561.
- Swanepoel, J.C., and Strydom, C.A. (2002), "Utilisation of fly ash in a geopolymeric material." *Applied Geochemistry*; 17(8): 1143-1148.
- Tasong, W.A., Wild, S., and Tilley, R.J.D. (1999), "Mechanism by which ground granulated blast furnace slag prevents sulfate attack of lime stabilized kaolinite." *Cement and Concrete Research*; 29: 975-982.
- Teixeira-Pinto, A., Fernandes, P., and Jalali, S. (2002), "Geopolymer manufacture and application - main problems when using concrete technology." *Geopolymers International Conference*, 2002.
- Temuujin, J., Van Riessen, A., and MacKenzie, K.J.D. (2010), "Preparation and characterisation of fly ash based geopolymer mortars." *Construction and Building Materials*; 24: 1906-1910.
- Temuujin, J., Van Riessen, A., and Williams, R. (2009), "Influence of calcium compounds on the mechanical properties of fly ash geopolymer pastes." *Journal of Hazardous Materials*; 167: 82-88.

- Thakur, I.C., Kisku, N., Singh, J.P., and Kumar, S. (2016), "Properties of concrete incorporated with ggbs." *International Journal of Research in Engineering and Technology*; 5(8): 275-281.
- Thokchom, S. (2014), "Fly Ash Geopolymer Pastes in Sulphuric Acid." *International Journal of Engineering Innovation and Research*; 3 (6): 943-947.
- Topcu, I.B., Toprak, M.U., and Uygunoglu, T. (2014), "Durability and microstructure characteristics of alkali activated coal bottom ash geopolymer cement." *Journal of Cleaner Production*; 81: 211-214.
- Torres-Carrasco, M., and Puertas, F. (2015), "Waste glass in the geopolymer preparation: Mechanical and microstructural characterisation." *Journal of Cleaner Production*; 90: 397-408.
- Tripathy, D.K., and Barai, S.V. (2005), "Partial replacement using crushed stone dust." *Divisional Journal of Civil Engineering*; 87: 44-46.
- Van Deventer, J.S.J, Provis, J.L., Duxson, P., and Luckey, G.C. (2007), "Reaction mechanisms in the geopolymeric conversion of inorganic waste to useful products." *Journal of Hazardous Materials A*; 139: 506-513.
- Van Jaarsveld, J.G.S., Van Deventer, J.S.J., and Lukey, G.C. (2003), "The characterisation of source materials in fly ash-based geopolymers", *Materials Letters*; 57(7), 1272-1280.
- Van Jaarsveld, J.G.S., Van Deventer, J.S.J., and Lukey, G.C. (2002), "The effect of composition and temperature on the properties of fly ash and kaolinite based geopolymers." *Chemical Engineering Journal*; 89(1-3): 63-73.
- Wang, W.C., Wang, H.Y., and Lo, M.H. (2014), "The engineering properties of alkali activated slag pastes exposed to high temperatures." *Construction and Building Materials*; 68: 409-415.
- Weng, L., and Sagoe-Crentsil, K. (2007), "Dissolution processes, hydrolysis and condensation reactions during geopolymer synthesis: Part I-low Si/Al ratio systems." *Journal of Material Science*; 42(9): 2997-3006.

- Winnefeld, F., Leemann, A., Lucuk, M., Svoboda, P., and Neuroth, M. (2010), "Assessment of phase formation in alkali activated low and high calcium fly ashes in building materials." *Construction and Building Materials*; 24(6): 1086-1093.
- Wongpa, J., Kiattikomol, K., Jaturapitakkul, C., and Chindaprasirt, P. (2010), "Compressive strength, modulus of elasticity, and water permeability of inorganic polymer concrete." *Materials and Design*; 31(10): 4748-4754.
- Xu, H., and Van Deventer, J.S.J. (2000), "The geopolymerisation of aluminosilicate minerals." *International Journal of Mineral Process*; 59(3): 247-266.
- Yang, K., Hwang, H., and Lee, S. (2010), "Effects of water-binder ratio and fine Aggregate-total aggregate ratio on the properties of hwangtoh-based alkali-activated concrete." *Journal of Materials in Civil Engineering*; 22(9): 887-897.
- Yeoh, A.K., Bidin, R., Chong, C.N., and Tay, C.Y. (1979), "The relationship between temperature and duration of burning of rice-husk in the development of amorphous rice-husk ash silica." *Proceedings of UNIDO/ESCAP/ RCTT, AlorSetar, Malaysia, 1979.*
- Yip, C.K., Lukey, G.C., and Van Deventer, J.S.J. (2005), "The coexistence of geopolymeric gel and calcium silicate hydrate at the early stage of alkaline activation." *Cement and Concrete Research*; 35: 1688-1697.
- Yip, C.K., Provis, J.L., Lukey, G.C., and Van Deventer, J.S.J. (2008), "Carbonate mineral addition to metakaolin-based geopolymers." *Cement and Concrete Composites*; 30: 979-985.
- Yuksel, I., Siddique, R., and Ozkan, O. (2011), "Influence of high temperature on the properties of concretes made with industrial by-products as fine aggregate replacement." *Construction and Building Materials*; 25: 967-972.
- Yusuf, M.O., Johari, M.A.M., Ahmad, Z.A., and Maslehuddin, M. (2014), "Influence of curing methods and concentration of NaOH on strength of the synthesized alkaline activated ground slag-ultrafine palm oil fuel ash mortar/concrete." *Construction and Building Materials*; 66: 541-548.
- Zhang, G., He, J., and Gambrell, R.P. (2010), "Synthesis, characterization, and mechanical properties of red mud-based geopolymers." *Transportation Research Record*; 2167: 1-9.

Zhang, L., Ahmari, S., and Zhang, J. (2011), "Synthesis and characterization of fly ash modified mine tailings-based geopolymers." *Construction and Building Materials*; 25(9): 3773-3781.

Zhao, Q., Nair, B., Rahimian, T., and Balaguru, P. (2007), "Novel geopolymer based composites with enhanced ductility." *Journal of Material Science*; 42 (9): 3131-3137.